SUPRASPINAL LOCOMOTOR NETWORK DERANGEMENTS: A MULTIMODAL APPROACH

STÖRUNGEN DES SUPRASPINALEN LOKOMOTORISCHEN NETZWERKS: EIN MULTIMODALER ANSATZ

Doctoral thesis for a Joint doctoral degree in Bioengineering and Neuroscience
at the Politecnico di Milano and the Graduate School of Life Sciences,
Julius-Maximilians-Universität Würzburg

submitted by

Chiara Palmisano

from

Milano, Italia

Würzburg 2021

Submitted on: ……

Office stamp

Members of the Thesis Committee

Chairperson: Prof. Dr. Christian Wegener

Primary Supervisor: Prof. Dr. Ioannis Ugo Isaias

Supervisor (Second): Prof. Carlo Albino Frigo

Supervisor (Third): Prof Anna Maria Bianchi

Supervisor (Fourth): Prof. Dr. Andrea Kübler

Date of Public Defence: ……

Date of Receipt of Certificates: ……

Affidavit

I hereby confirm that my thesis entitled SUPRASPINAL LOCOMOTOR NETWORK DERANGEMENTS: A MULTIMODAL APPROACH is the result of my own work. I did not receive any help or support from commercial consultants. All sources and / or materials applied are listed and specified in the thesis.

Furthermore, I confirm that this thesis has not yet been submitted as part of another examination process neither in identical nor in similar form.

Place, Date Signature

Eidesstattliche Erklärung

Hiermit erkläre ich an Eides statt, die Dissertation STÖRUNGEN DES SUPRASPINALEN LOKOMOTORISCHEN NETZWERKS: EIN MULTIMODALER ANSATZ eigenständig, d.h. insbesondere selbständig und ohne Hilfe eines kommerziellen Promotionsberaters, angefertigt und keine anderen als die von mir angegebenen Quellen und Hilfsmittel verwendet zu haben.

Ich erkläre außerdem, dass die Dissertation weder in gleicher noch in ähnlicher Form bereits in einem anderen Prüfungsverfahren vorgelegen hat.

Ort, Datum Unterschrift

Table of contents

1. Abstract

Parkinson's Disease (PD) constitutes a major healthcare burden in Europe. Accounting for aging alone, ~700,000 PD cases are predicted by 2040. This represents an approximately 56% increase in the PD population between 2005 and 2040, with a consequent rise in annual disease-related medical costs. Gait and balance disorders are a major problem for patients with PD and their caregivers, mainly because to their correlation with falls. Falls occur as a result of a complex interaction of risk factors. Among them, *Freezing of Gait* (FoG) is a peculiar gait derangement characterized by a sudden and episodic inability to produce effective stepping, causing falls, mobility restrictions, poor quality of life, and increased morbidity and mortality. Between 50–70% of PD patients have FoG and/or falls after a disease duration of 10 years, only partially and inconsistently improved by dopaminergic treatment and Deep Brain Stimulation (DBS). Treatment-induced worsening has been also observed under certain conditions. Effective treatments for gait disturbances in PD are lacking, probably because of the still poor understanding of the supraspinal locomotor network.

In my thesis, I wanted to expand our knowledge of the supraspinal locomotor network and in particular the contribution of the basal ganglia to the control of locomotion. I believe this is a key step towards new preventive and personalized therapies for postural and gait problems in patients with PD and related disorders. In addition to patients with PD, my studies also included people affected by Progressive Supranuclear Palsy (PSP). PSP is a rare primary progressive parkinsonism characterized at a very early disease stage by poor balance control and frequent backwards falls, thus providing an in vivo model of dysfunctional locomotor control.

I focused my attention on one of the most common motor transitions in daily living, the initiation of gait (GI). GI is an interesting motor task and a relevant paradigm to address balance and gait impairments in patients with movement disorders, as it is associated with FoG and high risk of falls. It combines a preparatory (i.e., the Anticipatory Postural Adjustments [APA]) and execution phase (the stepping) and allows the study of movement scaling and timing as an expression of muscular synergies, which follow precise and online feedback information processing and integration into established feedforward patterns of motor control.

By applying a multimodal approach that combines biomechanical assessments and neuroimaging investigations, my work unveiled the fundamental contribution of striatal dopamine to GI in patients with PD. Results in patients with PSP further supported the fundamental role of the striatum in GI execution, revealing correlations between the metabolic intake of the left caudate nucleus with diverse GI measurements. This study also unveiled the interplay of additional brain areas in the motor control of GI, namely the Thalamus, the Supplementary Motor Area (SMA), and the Cingulate cortex. Involvement of cortical areas was also suggested by the analysis of GI in patients with PD and FoG. Indeed, I found major alterations in the preparatory phase of GI in these patients, possibly resulting from FoG-related deficits of the SMA. Alterations of the weight shifting preceding the stepping phase were also particularly important in PD patients with FoG, thus suggesting specific difficulties in the integration of somatosensory information at a cortical level. Of note, all patients with PD showed preserved movement timing of GI, possibly suggesting preserved and compensatory activity of the cerebellum. Postural abnormalities (i.e., increased trunk and thigh flexion) showed no relationship with GI, ruling out an adaptation of the motor

pattern to the altered postural condition. In a group of PD patients implanted with DBS, I further explored the pathophysiological functioning of the locomotor network by analysing the timely activity of the Subthalamic Nucleus (STN) during static and dynamic balance control (i.e., standing and walking). For this study, I used novel DBS devices capable of delivering stimulation and simultaneously recording Local Field Potentials (LFP) of the implanted nucleus months and years after surgery. I showed a gait-related frequency shift in the STN activity of PD patients, possibly conveying cortical (feedforward) and cerebellar (feedback) information to mesencephalic locomotor areas. Based on this result, I identified for each patient a Maximally Informative Frequency (MIF) whose power changes can reliably classify standing and walking conditions. The MIF is a promising input signal for new DBS devices that can monitor LFP power modulations to timely adjust the stimulation delivery based on the ongoing motor task (e.g., gait) performed by the patient (adaptive DBS).

Altogether my achievements allowed to define the role of different cortical and subcortical brain areas in locomotor control, paving the way for a better understanding of the pathophysiological dynamics of the supraspinal locomotor network and the development of tailored therapies for gait disturbances and falls prevention in PD and related disorders.

2. Zusammenfassung

Die Parkinson-Krankheit (PD) stellt in Europa eine große Belastung für das Gesundheitswesen dar. Allein unter Berücksichtigung der Alterung werden bis zum Jahr 2040 etwa 700 000 Fälle von Parkinson prognostiziert. Dies entspricht einer Zunahme der Parkinson-Population um etwa 56 % zwischen 2005 und 2040, was zu einem Anstieg der jährlichen krankheitsbedingten medizinischen Kosten führt. Gang- und Gleichgewichtsstörungen sind ein großes Problem für Morbus-Parkinson-Patienten und ihre Betreuer, vor allem, weil sie mit Stürzen zusammenhängen. Stürze sind das Ergebnis einer komplexen Interaktion von Risikofaktoren. Zu diesen Faktoren gehört das Freezing of Gait (FoG), eine besondere Gangstörung, die durch eine plötzliche und episodische Unfähigkeit gekennzeichnet ist, einen effektiven Schritt zu machen, was zu Stürzen, Mobilitätseinschränkungen, schlechter Lebensqualität und erhöhter Morbidität und Mortalität führt. Zwischen 50 und 70 % der Morbus-Parkinson-Patienten haben nach einer Krankheitsdauer von 10 Jahren FoG und/oder Stürze, die sich durch dopaminerge Behandlung und Tiefe Hirnstimulation (DBS) nur teilweise und uneinheitlich verbessern. Unter bestimmten Bedingungen wurde auch eine behandlungsbedingte Verschlechterung beobachtet. Es gibt keine wirksamen Behandlungen für Gangstörungen bei Morbus Parkinson, was wahrscheinlich auf das noch immer unzureichende Verständnis des supraspinalen lokomotorischen Netzwerks zurückzuführen ist.

In meiner Dissertation wollte ich unser Wissen über das supraspinale Bewegungsnetzwerk und insbesondere den Beitrag der Basalganglien zur Steuerung der Fortbewegung erweitern. Ich glaube, dass dies ein wichtiger Schritt auf dem Weg zu neuen präventiven und personalisierten Therapien für Haltungs- und Gangprobleme bei Patienten mit Parkinson und verwandten Erkrankungen ist. Neben Morbus-Parkinson-Patienten wurden in meine Studien auch Menschen mit progressiver supranukleärer Lähmung (PSP) einbezogen. PSP ist ein seltener primär progressiver Parkinsonismus, der in einem sehr frühen Krankheitsstadium durch eine schlechte Gleichgewichtskontrolle und häufige Rückwärtsstürze gekennzeichnet ist und somit ein In-vivo-Modell für eine gestörte Bewegungskontrolle darstellt.

Ich habe mich auf einen der häufigsten motorischen Übergänge im täglichen Leben konzentriert, die Initiierung des Gangs (GI). GI ist eine interessante motorische Aufgabe und ein relevantes Paradigma zur Untersuchung von Gleichgewichts- und Gangstörungen bei Patienten mit Bewegungsstörungen, da sie mit FoG und einem hohen Sturzrisiko verbunden ist. Sie kombiniert eine Vorbereitungsphase (d. h. die antizipatorischen posturalen Anpassungen [APA]) und eine Ausführungsphase (den Schritt) und ermöglicht die Untersuchung der Bewegungsskalierung und des Timings als Ausdruck muskulärer Synergien, die einer präzisen und online erfolgenden Verarbeitung von Feedback-Informationen und der Integration in etablierte Feedforward-Muster der motorischen Kontrolle folgen.

Durch Anwendung eines multimodalen Ansatzes, der biomechanische Bewertungen und bildgebende Untersuchungen kombiniert, hat meine Arbeit den grundlegenden Einfluss des striatalen Dopamins auf GI bei Patienten mit Parkinson enthüllt. Die Ergebnisse bei Patienten mit PSP untermauerten die grundlegende Rolle des Striatums bei der Ausführung von GI, indem sie Korrelationen zwischen der metabolischen Aufnahme des linken Nucleus caudatus und verschiedenen GI-Parametern aufzeigten. Diese Studie enthüllte auch das Zusammenspiel

weiterer Hirnareale bei der motorischen Kontrolle von GI, nämlich des Thalamus, der Supplementary Motor Area (SMA) und des Cingulum-Kortex. Die Beteiligung kortikaler Areale wurde auch durch die Analyse der GI bei Patienten mit Parkinson und FoG nahegelegt. In der Tat fand ich bei diesen Patienten erhebliche Veränderungen in der Vorbereitungsphase des GI, die möglicherweise auf FoG-bedingte Defizite der SMA zurückzuführen sind. Veränderungen der Gewichtsverlagerung, die der Schrittphase vorausgeht, waren bei Morbus-Parkinson-Patienten mit FoG ebenfalls besonders ausgeprägt, was auf spezifische Schwierigkeiten bei der Integration somatosensorischer Informationen auf kortikaler Ebene schließen lässt. Bemerkenswert ist, dass alle Morbus-Parkinson-Patienten ein gut erhaltenes Bewegungs-Timing von GI aufwiesen, was möglicherweise auf eine ebenfalls gut erhaltene und kompensatorische Aktivität des Kleinhirns hindeutet. Haltungsanomalien (d. h. verstärkte Rumpf- und Oberschenkelflexion) standen in keinem Zusammenhang mit GI, was eine Anpassung des motorischen Musters an die veränderten Haltungsbedingungen ausschließt. Bei einer Gruppe von Morbus-Parkinson-Patienten, denen eine DBS implantiert wurde, untersuchte ich die pathophysiologische Funktionsweise des lokomotorischen Netzwerks weiter, indem ich die rechtzeitige Aktivität des subthalamischen Nucleus (STN) während der statischen und dynamischen Gleichgewichtskontrolle (d. h. Stehen und Gehen) analysierte. Für diese Studie habe ich neuartige DBS-Geräte verwendet, die in der Lage sind, Stimulationen abzugeben und gleichzeitig lokale Feldpotentiale (LFP) des implantierten Nucleus Monate und Jahre nach der Operation aufzuzeichnen. Ich konnte eine gehbezogene Frequenzverschiebung in der STN-Aktivität von Morbus-Parkinson-Patienten nachweisen, die möglicherweise kortikale (feedforward) und zerebelläre (feedback) Informationen an mesenzephale Bewegungsbereiche weiterleitet. Auf der Grundlage dieses Ergebnisses habe ich für jeden Patienten eine maximal informative Frequenz (MIF) identifiziert, deren Leistungsänderungen eine zuverlässige Klassifizierung von Steh- und Gehzuständen ermöglichen. Die MIF ist ein vielversprechendes Eingangssignal für neue DBS-Geräte, die LFP-Leistungsmodulationen überwachen können, um die Stimulationsabgabe zeitnah an die laufende motorische Aufgabe (z. B. Gehen) des Patienten anzupassen (adaptive DBS).

Insgesamt ist es mir gelungen, die Rolle verschiedener kortikaler und subkortikaler Hirnareale bei der Bewegungskontrolle zu definieren. Dies ebnet den Weg für ein besseres Verständnis der pathophysiologischen Dynamik des supraspinalen Bewegungsnetzwerks und die Entwicklung maßgeschneiderter Therapien für Gangstörungen und Sturzprävention bei Morbus Parkinson und verwandten Erkrankungen.

3. Introduction

The overarching goal of my research activities was to investigate the pathophysiological alterations of the supraspinal locomotor network at gait initiation (GI) in subjects with Parkinson's Disease (PD) and related disorders.

I specifically focused on GI as it is a critical transition task that is highly demanding in terms of balance maintenance. Additionally, specific neurological symptoms in PD and other parkinsonisms are related to GI, e.g., *Freezing of Gait* (FoG) at GI (*start hesitation*) [1]–[3]. FoG is among the most disabling problems for parkinsonian patients and their caregivers, causing falls, mobility restrictions, poor quality of life, and increased morbidity and mortality leading to a high economic burden [1], [2], [11]–[13], [3]–[10].

Despite several studies aimed at identifying the biomechanical alterations of GI in PD, [14]–[22] results are controversial. In PD patients suffering from *freezing of gait*, clinical evidence points towards specific alterations of GI [23]–[25], but previous studies failed to prove consistent *freezing*-related alterations of GI [26]–[28]. The pathological mechanisms underlying FoG at GI remain indeed still elusive [25] and require further investigations. The influence of confounding factors (i.e., anthropometric measurements, initial stance condition, medication condition and cues) on motor performance has consistently been neglected and may constitute the grounds for the poor agreement on the topic in the scientific literature. A better understanding of PD- and *freezing*-related biomechanical alterations at GI may offer an insight into the underlying pathophysiological mechanism, promoting the development of tailored and effective therapies.

Neuroimaging investigations may help greatly in this regard. Indeed, the supraspinal areas related to alterations at GI in patients with PD and related disorders are still largely unknown. Specifically, the contribution of striatal dopamine in the execution of the task has not been fully unveiled yet [29]–[36]. Elucidating the role of striatal dopamine in GI and identifying the brain areas related to postural alterations would assist in deepening our knowledge of motor networks specifically responsible for balance maintenance and their pathophysiological functioning.

Of relevance, GI represents an interesting paradigm to study a centrally-mediated motion achieved in a structured, controlled manner, including *feedforward* signals, such as Anticipatory postural adjustments (APA) [37], [38]. Studying specific neural derangements related to APA production and execution may elucidate the top-down functioning of the supraspinal locomotor network. Additionally, this would facilitate the identification of new gait-related biomarkers to be used as input signals for a timely adaptation of DBS paradigms. *Feedforward* motor control is a perfect candidate as a biomarker for adaptive DBS protocols, as intervening at the earliest stage of the movement, when *feedback*-based corrections are still not possible [9], [39]–[41], thus allowing a prompt adaptation of the stimulation to the upcoming motor activity in a predictive manner. As a first step towards the identification of a neural biomarker for GI, I characterized the STN activity during standing and forthcoming linear steady-state walking. The few studies available on the topic showed several limitations and conflicting results [42]–[50] and the neural dynamics of deep brain structures underlying locomotor control remained still poorly understood. The limitations of the deep brain recording device available at the time of this study (i.e., PC+S, Medtronic PLC) combined with the short duration of the GI transition (in the investigated populations of about 0.4s) prevented the acquisition of a sufficient numbers of GI

trials to reliably identify the neural dynamics related to this task. Newly available devices (i.e., Percept PC [Medtronic PLC] [51] or AlphaDBS [Newronika S.r.l.] [52], [53]) may allow the recordings of deep brain structures also during GI trial. The biomarkers of standing and walking, here identified, provided relevant preliminary data for future studies investigating the neural dynamics underlying GI and modulation of locomotion.

4. State of the Art

4.1. Biomechanics of gait initiation

GI is the transient state between standing and walking [33]. GI is of fundamental importance during daily life activities, as it allows a switch from a static to a dynamic condition. It is one of the first voluntary destabilizing motor tasks observed along the development of the locomotor pattern [54] as it allows the interaction of the subject with the surroundings [55]. During GI the Centre of Mass (CoM), the barycenter of the subject, is intentionally dislocated from a large to a narrow Base of Support (BoS) to propel forward movement [38], [56], [57].
GI is a highly challenging task for the balance control system and it has been extensively studied as a paradigm of balance control in healthy young subjects [37], [58]–[64], elderly people [4], [17], [54], [65]–[70], and subjects with varying neurological disorders [71]–[75], especially PD [1], [13], [65], [71], [76], [16], [18], [30], [32], [33], [35], [38], [56].

The stepping phase of the GI is preceded by stereotyped muscular activities called APA [37], [59], [62], [63], [77], aiming to destabilize the antigravitary postural set via misalignment between the Centre of Pressure (CoP) and the CoM to generate a gravitational moment favoring CoM forward acceleration [62]–[64]. The action mechanism of APA can be described with the inverted pendulum model for human posture [78]. Disregarding the action of inertia, during upright posture the only external forces exerted to the body are the Body Weight (BW) and the Ground Reaction Force (GRF), applied to the CoM and the CoP, respectively (**Figure 1**). These two forces have the same module but opposite orientation and act mainly towards the vertical direction. Accordingly, a standing subject can be modelled with an inverted pendulum with a mass equal to the mass of the whole body, concentrated in a unique point corresponding to the position of the CoM, and supported by a rigid rod without any mass. Only the sagittal plane only is considered, as during standing and GI the forces act mostly along the anterior-posterior (AP) and vertical directions. The rod is free to rotate clockwise or counterclockwise around the flexion-extension axis of a hinge, representing both ankle joints (**Figure 1**). Of relevance, during upright standing the GRF is anterior to the ankle joints, thus provoking a dorsiflexor moment acting on the foot. This moment is counteracted by the action of the plantarflexor muscles (i.e., soleus and gastrocnemius), which generate an equal and opposite moment on the foot and in turn a moment on the leg equal to the external one. In the inverted pendulum model, the action of the plantarflexor muscles can be represented by a rotational actuator placed coaxially with the hinge and providing a moment equal to the one of the GRF to the rod (**Figure 1**).

The inverted pendulum model represents an intrinsically unstable equilibrium, as the only condition for achieving balance is a perfect alignment of the BW on the vertical axis of the pendulum, and even small shifts of the mass from the vertical line generates a forward/backward acceleration of the body [79].During quiet standing, small movements due to respiration, heartbeat, blood flow etc. perturbate continuously the position of the CoM over time, thus provoking a constant misalignment between the lines of action of the BW and GRF [79]. By applying the condition for dynamic rotational equilibrium in an instant in which the pendulum is moving, the variables result to be related as follows:

$$-GRF \cdot p + m \cdot (g + \ddot{y}) \cdot L \cdot sin(\alpha) - m \cdot \ddot{x} \cdot L \cdot cos(\alpha) = 0$$

where p is the AP distance between the ankle rotation and the application point of the GRF, m the mass of the subject, g the gravitational acceleration, $\ddot{y}$ the vertical acceleration of the mass of the pendulum, L the length of the pendulum, α the angle of inclination of the pendulum and $\ddot{x}$

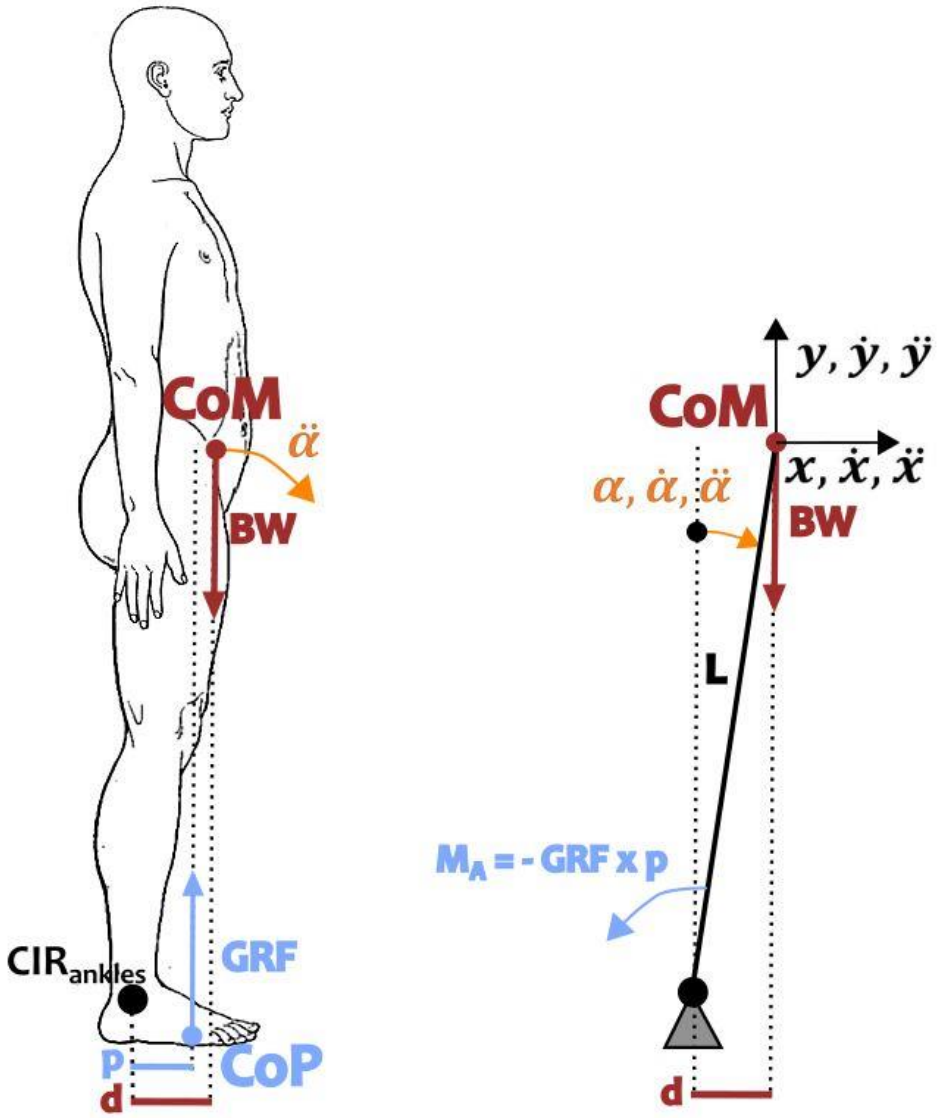

Figure 1: The inverted pendulum model for upright posture. During standing, the main forces acting on the body are the BW and the GRF. Accordingly, the human body can be modelled as a point mass equal to the mass of the subject and concentrated at CoM location, supported by a rod of length L, approximately equal to the limb length, free to rotate around a hinge clockwise or counterclockwise. A small shift of the mass from the vertical direction causes a forward/backward acceleration of the mass, proportional to the angle α of deviation of the rod with respect to the vertical. A rotational actuator coaxial to the hinge represents the moment applied by the plantarflexor muscles on the leg, equal to the external moment generated by the GRF.
Abbreviations: $\alpha, \dot{\alpha}, \ddot{\alpha}$: inclination of the rod with respect to the vertical line, angular velocity and acceleration of the rod; BW: Body Weight; CIR: Centre of Instantaneous Rotation; CoM: centre of mass; CoP: centre of pressure; d: anterior-posterior distance between ankle join centre and CoM projection; GRF: Ground Reaction Force; p: anterior-posterior distance between ankle join centre and CoP; L: length of the pendulum; M_A: moment generated by the actuator; $x, \dot{x}, \ddot{x}$: horizontal position, velocity, and acceleration of the CoM; $y, \dot{y}, \ddot{y}$: vertical position, velocity, and acceleration of the CoM.

the horizontal acceleration of the CoM (**Figure 1**). BW was expressed as the product between the mass *m* and the gravitational acceleration *g*.

It is possible to relate the vertical and horizontal position, velocity, and acceleration of the mass to the angle of rotation α of the pendulum as follows:

$$\begin{aligned} y = L\,cos(\alpha); \quad \dot{y} = -L\,\dot{\alpha}\,\sin(\alpha); \quad \ddot{y} = -L\,\ddot{\alpha}\,\sin(\alpha) - L\,\dot{\alpha}^2\cos(\alpha) \\ x = L\,sin(\alpha); \quad \dot{x} = L\,\dot{\alpha}\,\cos(\alpha); \quad \ddot{x} = L\,\ddot{\alpha}\,\cos(\alpha) - L\,\dot{\alpha}^2\sin(\alpha) \end{aligned}$$

By inserting these relations in the condition for rotational equilibrium, the expression can be simplified as follows [79]:

$$m \cdot g \cdot d - GRF \cdot p = m \cdot L^2 \cdot \ddot{\alpha}$$

where *d* is the moment arm of the *BW (mg)*, corresponding to the AP distance between the CoM and the ankle joint center, mL^2 is the moment of inertia *I* of the concentrated body mass about the ankle joint, and $\ddot{\alpha}$ the angular acceleration of the inverted pendulum. Specifically, disregarding the vertical component of the inertial force (the vertical acceleration is negligible in the present conditions) we can assume GRF equal to BW, so that:

$$mg(d - p) = I\ddot{\alpha}$$

It appears that the shift between the position of the CoM and CoP generates a proportional angular acceleration of the rod , which in turn corresponds to AP acceleration of the CoM [78]. The angular acceleration of the CoM can be approximated as $\ddot{\alpha} = \frac{\ddot{x}}{L}$, thus leading to the following equation:

$$d - p = \frac{I}{mgL}\ddot{x}$$

$$d - p = K\ddot{x}$$

where *K* is a constant feature of the pendulum and equal to $\frac{I}{mgL}$, which can be expressed as $\frac{L}{g}$. This equation underlines the proportionality relationship between the forward acceleration of the CoM and the distance between CoM and CoP (*d-p*), a key variable for the postural control. To maintain balance over time, the central postural command is able to shift the position (p) of the CoP, constantly adapting it to timely counteract the movements of the CoM and the consequently applied torque to the CoM [78]–[83]. If d is higher than p, the body experiences a clockwise angular acceleration α (**Figure 2, panel B**) [78]. As the corresponding clockwise angular velocity $\dot{\alpha}$ increases, the subject counteracts the perturbation by shifting the CoP anterior to the CoM projection (**Figure 2, panel C**). As a result, d becomes lower than p, thus changing the sign of α and decreasing ω till its reversal. In this way, the body starts experiencing a backward acceleration. The postural control reacts by shifting the CoP backward, posterior to the CoM projection (**Figure 2, panel D**). The angular acceleration α is now reversed and $\dot{\alpha}$ consequently decreases till changing sign and a clockwise rotation is again experienced. In this continuous

process, the movements of the CoP constrain the CoM projection always inside the BoS and balance is dynamically maintained (**Figure 3**).

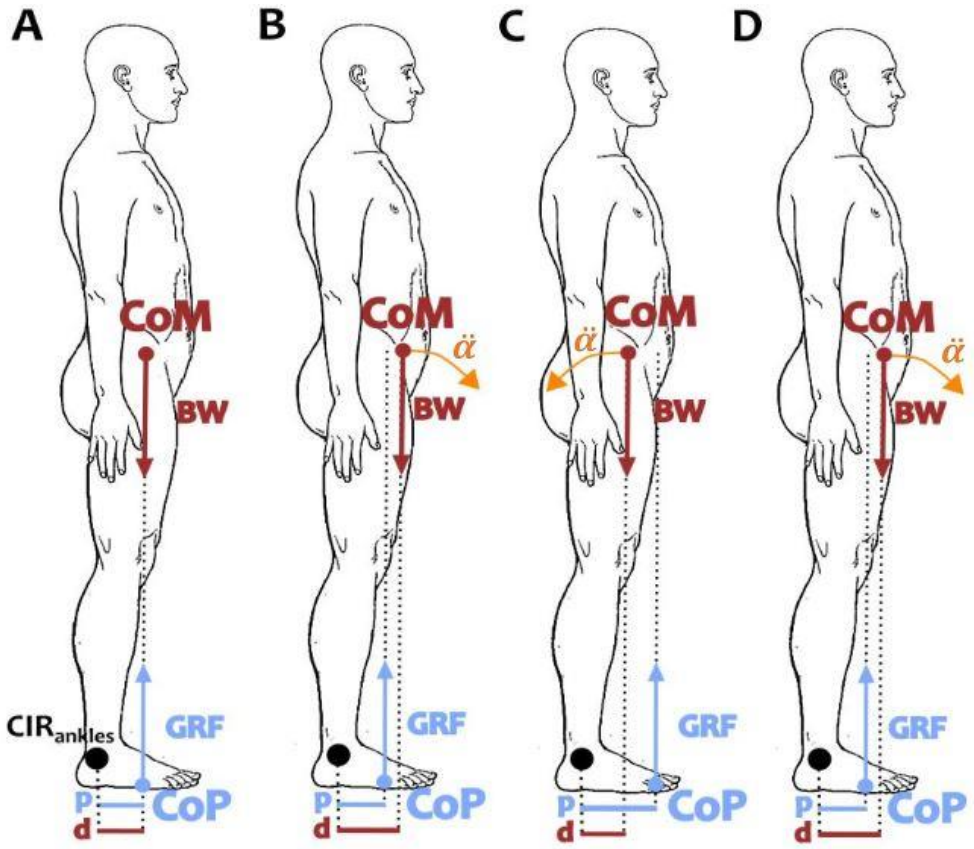

Figure 2: A) Schematic representation of the inverted pendulum model in static condition. BW and GRF are equal and contrary, and the net applied momentum is zero. B) When the CoM projection is anterior to the CoP, a net momentum and a consequent angular acceleration α is applied to the body in the clockwise direction, and the CoM accelerates forward. Consequently, the body gains an angular velocity $\dot{\alpha}$ in the same direction. C) The central postural control responds to the forward CoM displacement by shifting the CoP anterior to the CoM projection. In this way, a counterclockwise angular acceleration α is applied to the body, which decreases the angular velocity $\dot{\alpha}$ D) When the angular velocity $\dot{\alpha}$ changes sign, the postural control acts by displacing again the CoP backwards, to restore the initial condition (B). The process is continuous along the maintenance of the standing posture.
Abbreviations: α: angular acceleration of the body; $\dot{\alpha}$: angular velocty of the body; BW: Body Weight; CIR: Centre of Instantaneous Rotation; CoM: centre of mass; CoP: centre of pressure; d: anterior-posterior distance between ankle joint centre and CoM projection; GRF: Ground Reaction Force; p: anterior-posterior distance between ankle join centre and CoP.

Therefore, even if the instant position of CoP and CoM do not correspond, their average value over time is the same, thus ensuring stability. CoP displacement during upright standing is measurable by means of dynamometric force plates (**Figure 3**), which are able to detect with high spatial and temporal resolution CoP position over time and the GRF exchanged with the floor by the subject (see paragraph 6.3.1). Balance control is regulated by central postural commands by means of two main strategies: the "ankle strategy" and the "hip strategy". These two paradigms primarily rely on the activity of the muscles acting on the ankle joints and on trunk rotation around the hips, respectively. During quiet physiological standing, there is evidence for a predominance of the "ankle strategy" in the modulation of the CoP displacement, while the "hip strategy"

seems more involved in the response to large and fast perturbations (e.g., displacement of the support). Specifically, during upright posture the movement of the CoP in the AP direction is mainly modulated by the activity of the triceps surae (gastrocnemius and soleus muscles), whose increment/decrement provokes a forward/backward shift of the CoP [80].

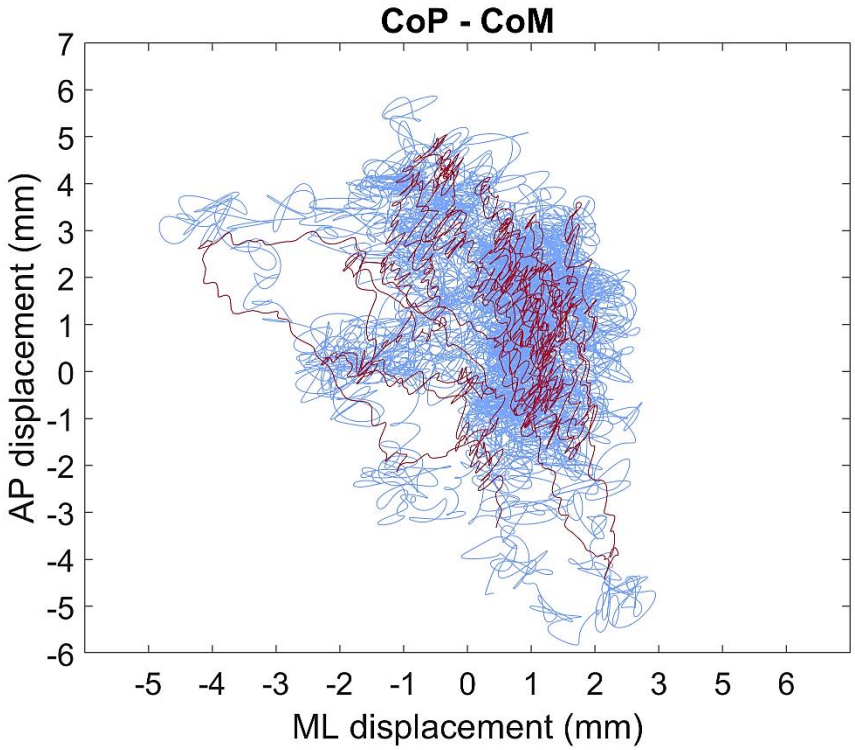

Figure 3: CoP and CoM oscillation in the transversal plane during quiet upright standing of a healthy subject (blue and red line, respectively). The shown CoP track was acquired with dynamometric force plates, while CoM movements were detected with a motion capture system. See paragraph 6.36.4.1 for further details. The sway of the CoP confines the CoM projection inside a very small area included in the BoS, avoiding balance loss. For ensuring balance maintenance, CoP dynamic range must be wider with respect to the CoM displacement. Of interest, the main direction of oscillation is the anterior-posterior, but medio-lateral oscillations are also present.
Abbreviations: AP: anterior-posterior; BoS: Base of Support; CoM: centre of mass; CoP: centre of pressure; ML: medio-lateral.

The projection of the CoM during standing always falls anterior to the ankle joint, at an average distance equal to the 24±5% of the foot length [81]. Accordingly, during upright posture the gastrocnemius shows a tonic activity, which maintain the CoP average position in the mid/forefoot area, in correspondence to the CoM projection. Gatev and colleagues showed that the activity of the lateral gastrocnemius correlates with the sway of both CoP and CoM [80]. Of interest, the gastrocnemius muscle activates when the CoM is anterior to the CoP, in correspondence to a forward momentum and consequent muscle loading, and relaxes when the CoM is posterior to the CoP, when the ankle dorsiflexor muscles are unloaded [80]. This data agrees with the "climbing hill" model, which assumes that "a muscle contracts when loaded and stays contracted until unloaded" [80], [82]. Of relevance, the sway of CoP and CoM showed to be maximally correlated at a phase shift of zero degrees, while the modulation of the activity of the gastrocnemius was correlated to both CoP and CoM excursion in a predictive manner (with a phase shift ranging from 300 to 100 ms) [80], [83]. These findings suggest the presence of

feedforward mechanisms for postural control, adopted in combination with *feedback* loops [80], [84].

The "hip mechanism" becomes of fundamental relevance when extending the inverted pendulum model to the frontal plane. Indeed, while in the sagittal plane it is possible to represent the action of the two ankles as a unique moment, in the frontal plane it is necessary to consider the action of the two limbs separately, each having its own interaction with the ground (**Figure 4)** [78], [79]. With regards to the "hip strategy", hip muscles are mainly responsible for the loading/unloading process of the two limbs during upright standing. Specifically, the lateral shift of the CoM towards one limb can be obtained by the contraction of the ipsilateral hip abductor muscles or contralateral hip adductor muscles. The action mechanism of the hip muscles causes a dynamic variation over time of weight distribution between the two limbs. In particular, the loading of each foot is in antiphase with respect to the other one: when the load on one foot is increased, the other foot will be unloaded of the same amount. The CoP_{net} resultant from the separate action of the two limbs can be calculated by applying the condition for rotational equilibrium with respect to a reference point to the system (**Figure 4**) [78], [79]:

$$CoP_{net}(t)GRF(t) = CoP_L(t)GRF_L(t) + CoP_R(t)GRF_R(t)$$

where GRF_L and GRF_R are the *GRF* under the left and right foot, respectively, and GRF_L and GRF_R their point of application with respect to the reference point considered. As $GRF = GRF_L + GRF_R$, we can rephrase the equation as follows:

$$CoP_{net}(t) = CoP_L(t)\frac{GRF_L(t)}{GRF_L(t) + GRF_R(t)} + CoP_R(t)\frac{GRF_R(t)}{GRF_L(t) + GRF_R(t)}$$

The CoP_{net} is therefore the result of the combined action of four different time-dependent variables, each of them controlled by a different set of muscles. Specifically, while the *GRF* are controlled by the hip muscles, the CoP_L and CoP_R are regulated by the activity of the eversion/inversion ankle muscles [79]. To disentangle the contribution of the ankle and hip muscles on the determination of the CoP_{net} position, it can be hypothesized that in the presence of a perfectly symmetric load distribution between the two legs, its position will be determined only by the action of the ankle muscles:

$$CoP_{ankle}(t) = CoP_L(t)0.5 + CoP_R(t)0.5$$

As the CoP_{net} is the sum between the separate actions of the ankle and hip muscles, the contribution of the loading/unloading mechanisms acted by the hip abduction/adduction can be estimated by subtracting from the recorded CoP_{net} position the contribution given by the ankle muscles [78], [79]:

$$CoP_{hip}(t) = CoP_{net}(t) - CoP_{ankle}(t)$$

Of relevance, the action of the left and right ankle muscles is highly synchronized in the AP direction, as demonstrated by the zero-phase lag between the CoP_L and CoP_R AP displacement.

The CoP_{net} position in the AP direction lies in between the CoP_L and CoP_R tracks, thus showing that the "ankle strategy" plays a major role in the regulation of the CoP AP position. Conversely, the mechanism of loading/unloading acted by the hip muscles are majorly responsible for CoP movement in the ML direction [78], [79].

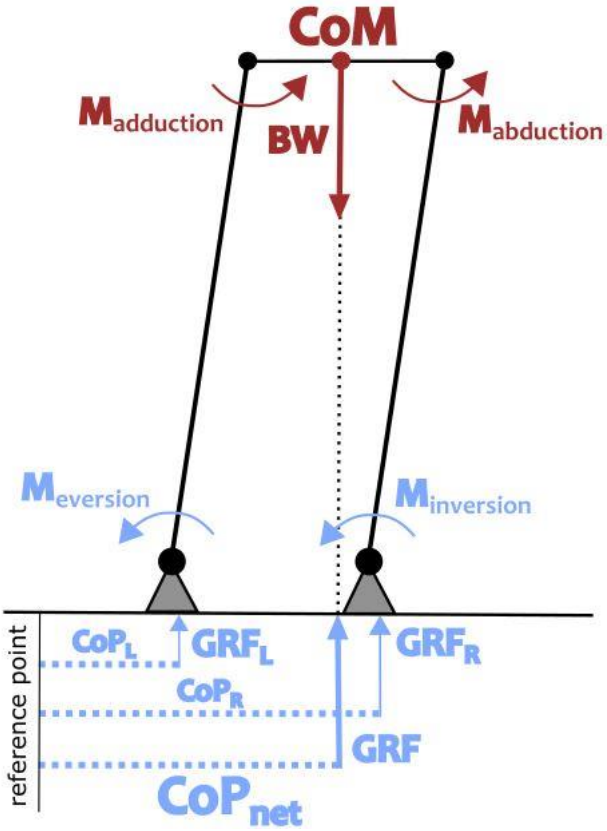

Figure 4: Inverted pendulum model in the frontal plane. The two ankles are represented as separated hinges providing their own moments to the two rods modelling the lower limbs. The total CoP (CoP_{net}) is the weighted sum of the CoP of the two feet. The position of the CoM in the ML direction and the resulting GRF are regulated by the action adduction/abduction hip muscles.
Abbreviations: BW: Body Weight; CoM: Centre of Mass; CoP_{net}: Centre of Pressure; CoP_L: Centre of Pressure under the left foot; CoP_R: Centre of Pressure under the right foot; GRF: Ground Reaction Force; GRF_L: Ground Reaction Force under the left foot; GRF_R: Ground Reaction Force under the right foot; M: Moment; ML: medio-lateral.

Control of the CoP displacement is not only essential for balance maintenance during standing, but also for gait propulsion [78], [79]. Specifically, GI is characterized by a stereotyped muscular activity (APA) causing specific CoP movements aimed at promoting the forward acceleration of the CoM and unloading the swing foot (i.e. the foot which is going to execute the first step) while efficiently maintaining balance [66]. As the increment of the GRF is obtained by a displacement of the CoP rather than by moving the CoM, the central nervous system is able to deal with an intrinsically unstable transition with a controlled and efficient mechanism [66]. From their first description by Carlsöö in 1966 [85], physiological APA at GI have been widely characterized in literature in terms of muscular, dynamic and kinematic resultants (**Table 1**). With regards to the electromyographic (EMG) activity, the earliest researches on APA at GI aimed at describing the patterns of the muscles of the lower limbs [85]–[89]. These authors described the fundamental role of the muscles acting on the ankle joints for the plantarflexion and dorsiflexion of the foot (i.e. soleus, gastrocnemius and tibialis anterior) in driving the CoP movements at GI, also

confirmed by later studies [10], [62], [66], [69], [81], [90]. However, a synchronized activity was recorded also in more proximal muscles the rectus femoris, the biceps femoris, and the gluteus [69], [81]. During quiet stance, the soleus, the gastrocnemius, and, to a lesser degree, the biceps femoris are tonically active [62], [66], [81], [90].

APA starts with a bilateral silencing of the soleus and gastrocnemius (**Figure 5**) [62], [66], [81], [90] [62], [66], [81], [90], the latter more visible and less variable in the stance leg, as the gastrocnemius and soleus of the swing limb frequently continue to fire also after the onset of the APA [81]. The biceps femoris is bilaterally inhibited synchronously with the soleus and gastrocnemius [81]. The silencing of the soleus is tightly coupled with the subsequent bilateral activation of the tibialis muscles (**Figure 5**) after a temporally invariant interval of about 100-150ms [62], [81]. The rectus femoris mimics the activity of the tibialis, starting to fire just a few milliseconds after its activation [81]. The muscular synergy, including the silencing of the soleus/gastrocnemius and the re-activation of the tibialis anterior, generates a backward displacement of the CoP directed towards the swing foot (**Figure 5**) [62]. This first phase characterizing the APA is called imbalance (IMB, **Figure 6**) and is able to generate a controlled forward falling by providing the CoM the forward momentum needed to progress. It also allows the CoM to accelerate towards the stance foot, thus leading to the unloading of the swing limb [81]. The gastrocnemius and soleus of the swing leg are then activated again (**Figure 5**), at about 200ms after the activation of the tibialis anterior. This second burst of activity of the plantarflexor muscles is responsible for the subsequent CoP displacement towards the stance foot, called unloading (UNL) phase (**Figure 6**) [81]. Last, the soleus and gastrocnemius of the stance limb are activated as well to provide a push off and prepare the leg for leaving the ground [81].

The stereotyped displacement of the CoP during APA at GI (**Figure 6**) is a hallmark of the GI motor task, and one of the most studied measurements in the assessment of this motor task (**Table 1**). In the transversal plane it is possible to identify the IMB phase as the first displacement of the CoP, from the onset of the APA to the maximum ML displacement towards the swing foot, which roughly corresponds to the heel off of the swing foot (**Figure 6**) [19], [38], [90]. The subsequent movement of the CoP towards the stance foot represents the UNL phase, which goes from the heel off of the swing limb to the instant of change of direction of the CoP under the stance foot from mainly lateral to mainly anterior motion. It approximately corresponds to the swing toe off and the beginning of the single support phase (**Figure 6**) [19], [38], [90]. After APA execution, it is possible to identify the stepping phase as the period in which the CoP trave ls under the stance foot from the swing to the stance toe off, identified as the end of GI (**Figure 6**) [19], [38], [90]. The movement of the CoP during APA has been characterized in terms of displacement, average and maximum velocity during the IMB and UNL phases. Specifically, the CoP movement during the IMB phase has received particular attention as expressions of the integrity of *feedforward* motor control [37].

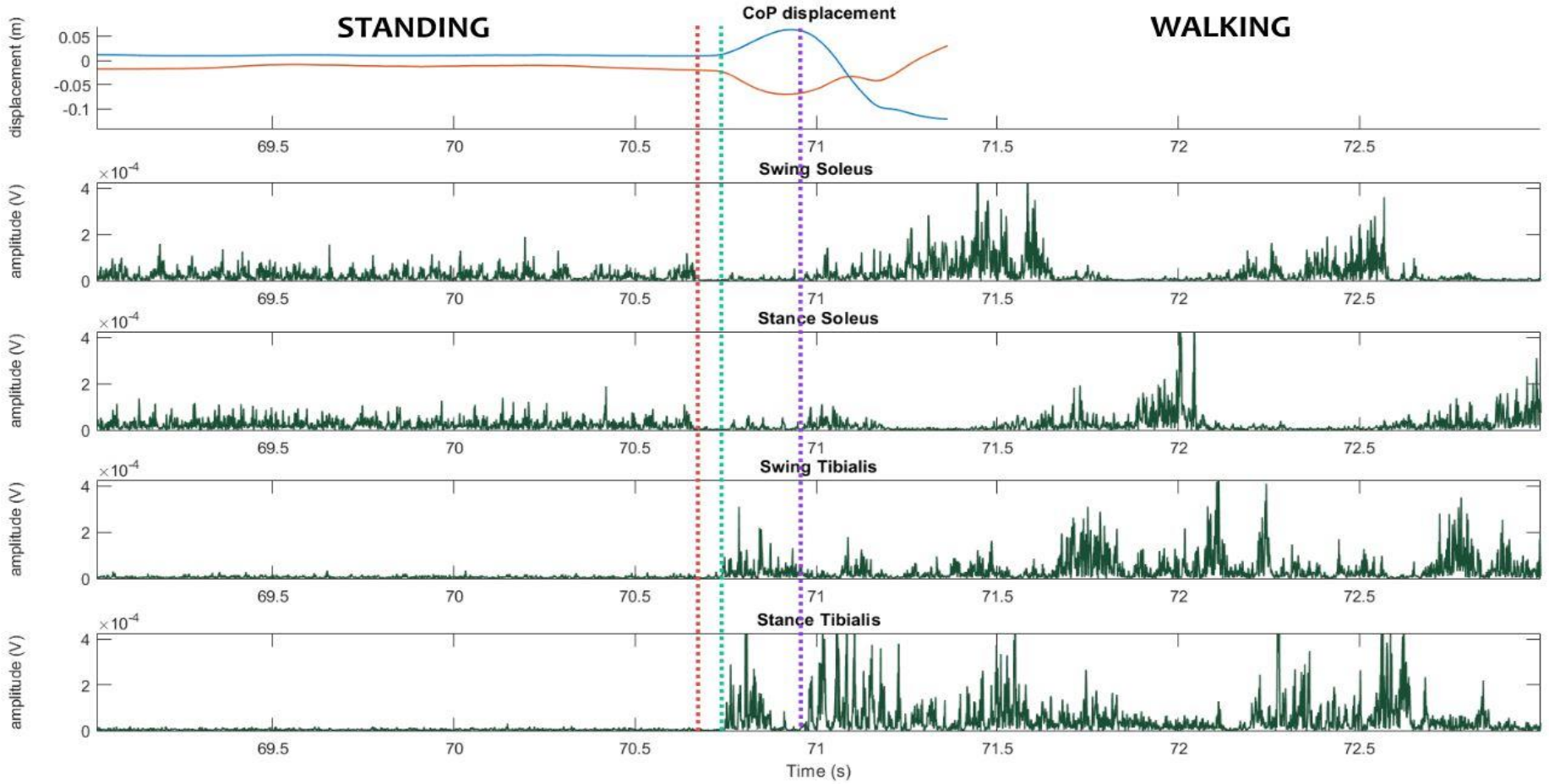

Figure 5*:* CoP displacement in the ML and AP directions (red and blue line in the top panel) and rectified muscular activity of swing and stance soleus and tibialis during GI. In the top panel, positive values correspond to movements backwards and towards the stance foot. The standing phase is characterized by a tonic activity of the soleus muscles, while the tibialis muscles are bilaterally silent. APA start at the silencing of the soleus of both swing and stance limbs (red dashed line) followed by a subsequent activation of the tibialis muscles (green dashed line). These two synergic actions lead to a displacement of the CoP backward and toward the swing limb (IMB phase). The re-activation of the soleus (purple dashed line) and gastrocnemius (not shown in the figure) allows to stop the backward progression of the CoP and to start the UNL phase. After the GI, it is possible to observe the alternate activation pattern of the two limbs typical of gait.
Abbreviations: APA: anticipatory postural adjustment; AP: anterior-posterior; CoP: centre of pressure; ML: medio-lateral; GI: gait initiation; IMB: imbalance; UNL: unloading.

The kinematic outcomes of GI were thoughtfully characterized as well, first with electrogoniometers (EG) applied at the ankles, knees, and hips [86], [87], [91], [92], accelerometers [93], [94], and later with motion capture systems [62], [69], [101]–[110], [81], [88], [95]–[100]. Even in the absence of direct kinematic measurements, several studies estimated the movement of the CoM, the most relevant kinematic resultant of GI, with force plate data [60], [61], [116]–[121], [63], [93], [94], [111]–[115] by applying the Euler's scheme, described first by Philips and colleagues [122]. The CoM was characterized by its position, velocity, and acceleration at the end of APA, as well as its relationship with the displacement of the CoP. The interplay between the CoP and the CoM is indeed fundamental for effective balance control, especially during dynamic transitions [123]. The length, velocity, and acceleration of the first step have also been extensively monitored and quantified as main outcomes of GI and indexes of the motor performance [69], [98], [120], [121], [124]–[129], [99], [102], [103], [106]–[109], [113]. **Table 1** summarizes the main studies conducted on GI of healthy subjects from the first description of APA [85] to the current year, describing the techniques and main outcome measurements adopted in each study for the investigation of this task.

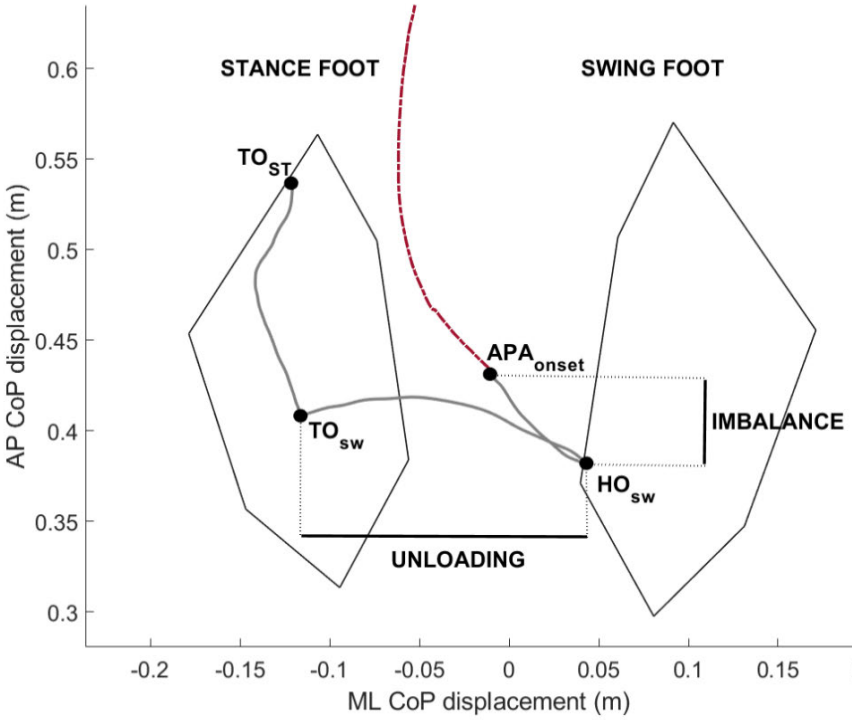

Figure 6: The typical displacement of the CoP (grey line) and the resultant movement of the CoM (red dashed line) during a GI trial of a healthy subject. In this trial, the left is the swing foot, i.e., the foot adopted to perform the first step. At GI, the CoP moves first backwards and towards the swing foot (IMB). The IMB phase ends when the CoP reaches its most ML position towards the swing foot and corresponds approximately to the heel off of the swing limb (HOSW). The first displacement of the CoP generates a moment arm able to accelerate the CoM forward and towards the stance limb. After the HOSW, the CoP starts moving towards the stance foot, thus allowing the swing foot to leave the ground (UNL). The IMB and UNL phases constitute the APA at GI. The UNL phase terminates with the swing foot toe off (TOSW), when the CoP changes its direction and proceeds along the stance foot till the last frame of contact of the foot with the force plate, i.e., the toe off of the stance foot (TOST).
Abbreviations: APA: anticipatory postural adjustments; AP: anterior-posterior; CoM: centre of Mass; CoP: centre of pressure; GI: gait initiation; HO: heel off; IMB: imbalance; ML: medio-lateral; ST: stance; SW: swing; UNL: unloading.

First Author	Year	EMG	DYN	KIN	Task	HC
Carlsöö	1966	10 channels for onset and cessation	two force plates; GRF and COP changes	no	GI from upright position	8 (21-38)
Herman	1973	9 channels for onset and cessation	two force plates; events from force plates signal changes	EG on the hips, knees, ankles	GI from upright position with tibial nerve suppression and with an ankle foot orthosis	17 (18-28)
Cook	1976	5 channels for onset and cessation	one force plate; events from force plate signal changes	EG on the hips, knees, ankles; velocity tachometer to approximate the CoM	GI from upright position	10 (23-52)
Yamashita	1976	no	one force plate; GRF changes	foot switches	GI from upright position	4 (23-34)
Mann	1979	8 channels for onset and cessation	one force plate; GRF and COP changes	3D kinematics of the hips, knees, ankles	GI from upright position	10 (19-43)
Brenière	1981	15 channels for timing postural responses	one force plate; GRF changes	no	GI from upright position	7 (NA-NA)
Do	1982	no	one force plate; GRF changes	no	GI from upright position; from 5° and 35° trunk inclination	8 (NA-NA)
Brenière	1986	no	one force plate; CoP displacement	CoM estimation from force plate measurements	GI from upright position at three speeds	6 (25-35)
Brenière	1987	no	one force plate; GRF and COP changes	CoM estimation from force plate measurements	GI from upright position at three speeds	5 (25-35)

Brenière	1988	no	one force plate; CoP displacement	CoM estimation from force plate and five accelerometers	GI from upright position at three speeds	1 (NA)
Nissan	1990	no	two force plates; GRF changes	3D lower limbs kinematics	GI from upright position	15 (22-62)
Brenière	1991	no	one force plate; CoP displacement	CoM estimation from force plate measurements	GI from upright position with three step lengths	6 (25-35)
Brunt	1991	2 channels for onset and cessation	one force plate; GRF changes	3D pelvis kinematics	GI from upright position at three speeds	9 (18-40)
Crenna	1991	2 channels for onset and cessation	one force plate; GRF and COP changes	3D full body kinematics	GI from upright position, rising on toes, sit to stand, throw, catch, and forward bend of trunk events	6 (22.5±1.5)
Brenière	1992	no	one force plate; CoP displacement	accelerometers at the hips and shoulders; CoM estimation from force plate measurements	GI from upright position	5 (NA-NA)
Gormley	1993	no	no	EG at the knees	GI from upright position	8 (19.2±1.4)
Jian	1993	no	three force plates; CoP displacement; moment at ankle, knee, and hip	3D full body kinematics; CoM estimation	GI from upright position	4 (25-31)
Patla	1993	no	one force plate and pressure-sensitive mats; GRF changes	no	GI with a step forward, backward, and lateral	23 (63-79) 12 (17-21)

Elble	1994	4 channels for onset and cessation	two force plates; CoP displacement	3D full body kinematics; CoM estimation	GI from upright position	12 (20-82)
Lepers	1995	2 channels for onset and cessation	one force plate; calculation of the ankle and gravitational moments	CoM estimation from force plate measurements	GI from upright position at three speeds	5 (26±3)
Miller	1996	no	two force plates; GRF for steps identification	3D unilateral full body kinematics; CoM estimation for the calculation of energy and work	GI from upright position	7 (23.6±2.3)
Brunt	1999	2 channels for onset and cessation	two force plates; GRF changes for phases identification	2D foot clearance estimation and foot switches	GI from upright position over a ruler and an obstacle	10 (21-34)
Brunt	2000	2 channels for onset and cessation	two force plates; GRF changes	foot switches	GI from upright position at fast velocity hitting different targets with the foot	10 (21-34)
Couillandre	2000	no	one force plate; CoP displacement	CoM estimation from force plate measurements	GI from upright position at three different speeds and with heels slightly off the ground	6 (NA-NA)
Rogers	2001	no	two force plates; CoP displacement	no	GI from upright position with a light, sound, or a cutaneous cue	15 (23-47) 35 (64-86)
Patchay	2003	no	two force plates; GRF and COP changes	3D right limb kinematics	GI from upright position and with asymmetric loading of the limbs	10 (38.1±8.4)

Hass	2004	no	one force plate; CoP displacement	no	GI from upright position before and after Tai Chi training	50 (79.6±5.8)
Mickelborough	2004	3 channels for onset and cessation	one force plate; CoP displacement	3D foot kinematics	GI from upright position	21 (65.8-75.8)
Brunt	2005	3 channels for onset and cessation	two force plates; GRF changes	no	GI from upright position and with various obstacles	9 (62-82) 9 (63-84)
Henriksson	2005	2 channels for onset and cessation	four force plates; GRF changes	3D foot kinematics	GI from upright position with self-chosen and imposed swing limb	28 (23-40) 29 (65-79)
Gélat	2006	no	one force plate; CoP displacement	CoM estimation from force plate measurements accelerometer on the swing foot	GI from upright position and stepping to a new level	8 (23-33)
Hiraoka	2007	2 channels for onset and cessation	no	EG on the swing ankle	GI from upright position as fast as possible	7 (20-30)
Park	2009	5 channels for onset and cessation	four force plates; CoP displacement	3D lower limb kinematics; CoM estimation; hips, knees and ankles joint angles	GI from upright position	20 (21-28)
Chastan	2010	2 channels for onset and cessation	one force plate; CoP displacement	CoM estimation from force plate measurements	GI from upright position with different sensory inputs and with gait termination after the first and second step	22 (37.9±12.2)

Queralt	2010	5 channels for onset and cessation	no	foot switches	GI from upright position with various cues	8 (23-50)
Dessery	2011	2 channels for onset and cessation	two force plates; CoP displacement	3D full body kinematics; CoM estimation; evaluation of the first step and trunk inclination	GI from upright position with the dominant and non-dominant limb	24 (25.3)
Gélat	2011	no	one force plate; CoP displacement	CoM estimation from force plate measurements	GI from upright position with pleasant and unpleasant images	15 (20-32)
Martin	2011	no	one force plate; CoP displacement	no	GI from upright position with and without a cognitive interference task	128 (60-86)
Delval	2012	3 channels for auditory reflex, visual reflex and movement onset	two force plate; CoP displacement	3D swing foot kinematics	GI from upright position with different acoustic and visual signals	15 (22-27) (1^{st}-3^{rd} quartile)
Caderby	2013	no	two force plates; CoP displacement; first step	CoM estimation from force plate measurements	GI from upright position with changes in body weight distribution	15 (21±2)
Leteneur	2013	no	two force plates; GRF and CoP changes; moment at ankle, knee, hip, and L5 vertebra; impulse	3D full body kinematics; CoM estimation; trunk inclination	GI from upright position with different trunk inclinations	25 (26.5±6.0)
Caderby	2014	no	two force plates; CoP displacement; impulse; first step	CoM estimation from force plate measurements	GI from upright position with an additional load	19 (20.3±9.1)

Hiraoka	2014	no	one force transducer; CoP displacement	no	GI from upright position with preferred and externally selected swing limb	11 (31±2.0)
Mille	2014	6 channels for onset and cessation and responses to perturbations	two force plates; CoP displacement	3D full body kinematics; CoM estimation; first step	GI from upright position as fast as possible with postural perturbations	11 (21-29)
Muir	2014	no	no	3D lower limb kinematics; characterizatio n of the first four steps	GI from upright position	19 (20–25) 11 (65–79) 18 (80–91)
Hiraoka	2015	no	one force transducer; CoP displacement	no	GI from upright position with different acoustic signals	12 (27.0 ± 2.6)
Khanmohammadi	2015	8 channels for onset and cessation	one force plate; CoP displacement	no	GI from upright position after an acoustic stimulus	16 (26.12±3.1) 15 (71.03±2.7)
Khanmohammadi	2016	8 channels for onset and cessation	one force plate; CoP displacement	no	GI from upright position as soon as possible after an acoustic stimulus	16 (26.12±3.1) 15 (71.03±3.7)
Caderby	2017	no	two force plates; CoP displacement; first step	CoM estimation from force plate measurements ; margin of stability	GI from upright position at three different speeds	13 (27±6)
Lu	2017	no	sensorized mat; CoP displacement	no	GI from upright position	157 (20-79)
Mizusawa	2017	no	one force plate; CoP displacement	no	GI from upright position with visual signals cueing the swing leg	10 (29.7±1.7)

Delafontaine	2017	2 channels for onset and cessation	one force plate; CoP displacement	CoM estimation from force plate measurements	GI from upright position with and without a rigid ankle-foot orthosis	19 (30.3±4.4)
Fawver	2018	no	one force plate; CoP displacement	3D full body kinematics; characterizatio n of the first four steps	GI from upright position with different degrees of forward voluntary lean	29 (21±1)
Stansfield	2018	no	no	3D right lower limbs kinematics	GI from upright position at different speeds	20 (22-44)
Lee	2019	6 channels for onset and cessation and responses to perturbations	one force plate; CoP displacement	accelerometer on the pelvis for movement onset detection	GI from upright position with postural perturbations	11 (28.09±4.3)
Artico	2020	no	one force plate; CoP displacement	3D right foot kinematics; CoM estimation from force plate measurements	GI from upright position with obstacle clearance	13 (28.7±1.5)
Hiraoka	2020	no	one force plate; CoP displacement	accelerometer for first heel contact	GI from upright position with different acoustic signals	11 (31.1±10.8)
Laudani	2021	2 channels for onset and cessation and responses to perturbations	three force plates; GRF and COP changes	3D full body kinematics; CoM estimation; characterizatio n of the first step; ankle plantar flexion	GI from upright position with postural perturbations	10 (25±2) 10 (73±5)
Rum	2021	2 channels for onset and cessation and responses to perturbations	two force plates; GRF and COP changes	3D full body kinematics; angular displacement of the trunk	GI from upright position with postural perturbations	10 (25 2) 10 (73±5)

Vieira	2021	no	two force plates; CoP displacement	3D malleoli kinematics; CoM estimation from force plate measurements	GI from upright position with different additional loads	68 (23.65±3.21)

Table 1: List of papers on GI of healthy subjects (HC) from 1966 till 2021. Papers were identified by means of a search of Google Scholar using the following key word combination: [gait initiation] and [healthy]. All abstracts were inspected to exclude papers including children and/or patients. For each identified paper, the table reports the devices and main outcome variables used to explore gait initiation in terms of muscular activity (EMG), dynamometric measurements (DYN), and kinematic aspects (KIN). Last column specifies the number of healthy subjects investigated in the studies and their age. Age is expressed as (min-max) or (mean± std) -unless otherwise specified- according to the information found in the paper.
Abbreviations: CoM: centre of mass; CoP: centre of pressure; EG: electrogoniometers; GI: Gait Initiation; GRF: ground reaction force; NA: not available.

4.2. The supraspinal locomotor network in healthy subjects

4.2.1. Methodological considerations

Gait movements are strongly driven by rhythms generating networks in the spinal cord and brainstem crucially embedded in more widely distributed networks comprising cortical regions.

Only few non-invasive devices allow studying gait-related supraspinal locomotor network activity: (1) Electroencephalography (EEG), (2) cortical (ECoG) and subcortical invasive recordings by means of implantable leads, (3) functional near-infrared spectroscopy (fNIRS), and (4) positron emission tomography (PET) or single-photon emission computed tomography (SPECT).

The strengths of the EEG are the possibility of a direct assessment of neural activity with a high temporal resolution, its portability and compact size, and the relatively low cost. Drawbacks are related to the low spatial resolution and the lack of information of subcortical brain structures. This can be improved by high-density EEG systems and new electrode configurations (e.g., tripolar concentric ring electrodes) combined with precise information of the head anatomy and source localization algorithms [130], [131]. Of note, movement-related artefacts are known to contaminate EEG signals. The subdural placement of ECoG electrodes is an emerging approach to measure cortical activity with high temporal and spatial resolution, while eliminating the possibility of correlated EMG contamination [132]. Similarly, intracerebral recordings of local field potentials in patients chronically implanted for deep brain stimulation (DBS) are an extraordinary new aid to explore the contribution of deep brain structures to human locomotion. However, being invasive, brain investigation with these techniques is only applicable in patients for which the ECoG/DBS is clinically prescribed and provides effective benefit (e.g., epileptic and patients with PD). At the opposite end, PET or SPECT measurements of brain metabolism of receptor and transporter availability occur minutes after the injection of the radioactive compound and can therefore provide only a global evaluation change of brain activity during locomotion. Still, these measurements have higher spatial resolution than EEG and provide fundamental biochemical correlates with the investigated motor task [133], [134].

fNIRS positions itself between the other methods, comprising however most of the disadvantages rather than positive features of the other techniques, including low spatial resolution, limited penetration depth, motion artefacts, and the difficulty of performing whole-brain imaging due to probe size and extracerebral contamination from superficial tissues (i.e., cutaneous or skull perfusion) of the recordings [135].

4.2.2. Gait

Gait is strongly driven by rhythms generating circuits in the spinal cord (central pattern generators, CPGs) and brainstem [136]–[138]. These circuits are integrated into more widely distributed networks involving the entire neuraxis. This is a crucial aspect to enable dynamic involvement of multiple sensory domains (sensory-motor *feedback*) and *feedforward* postural adjustments in gait control and modulation, underscoring a trade-off between manoeuvrability and stability.

Several studies described activation within the frontal cortices during gait, and a specific role of the primary motor cortex (M1), the supplementary motor area (SMA), the pre-SMA, the dorso-lateral prefrontal cortex (DLPFC).

Direct recordings of M1 with ECoG showed a generalized gamma band (40–200Hz) synchronization during treadmill walking, as well as periodic gamma band changes within each stride (regardless of walking speeds) [132]. These results corroborated previous EEG findings that showed increased high gamma amplitudes (70–90Hz) in central sensorimotor areas during walking [139], [140]. Of interest, high gamma amplitudes coupled conversely to low gamma (24–40Hz) amplitudes, both modulated during the gait cycle [140], directly contributed to muscular activity [141]–[144]. These findings, combined with a suppression (desynchronization) of mu and beta bands during walking relative to a non-movement reference [145]–[148] are suggestive for a combined amplitude and frequency modulation of the locomotor network in relation to the gait cycle.

While M1 is thought to directly drive muscular activity for steady-state walking [139], [149]–[153] other frontal areas play an active role during postural control under challenging conditions [154]–[156]. Preliminary evidence shows a key role of the SMA in gait control and modulation [9], [134], including gait initiation [20] and arm swing [157]. The major role of the SMA in planning and adaptation of gait patterns needs to be incorporated into a more diffuse cortico-cortical network, with additional distant brain areas involved in the control of postural movements. Preliminary evidence suggests a frequency specific modulation of visuo-parieto-frontal cortical interplay is needed for proper postural control under challenging conditions and for modification of gait trajectory [158]. The posterior parietal cortex must be engaged to register and store the temporospatial relationship between discrete body parts and the environment for a proper pre-programming of motor task and for the integration and timing of movement intentions with ongoing movements [159]–[165].

The cerebellum plays a fundamental, complementary role in providing motor pattern adaptability. This brain region processes sensory inputs and makes immediate alterations to ongoing movement patterns [166], [167], by modulating motor responses in a reactive or feedback manner based on sensory perturbations. Alternatively, the cerebellum is hypothesized to alter movement patterns in a predictive manner using trial-and-error practice [168]. This predictive, or *feedforward*, adjustment in human locomotion critically involves also the basal ganglia dopaminergic systems (see WP-1, paragraph 7.1). Using PET and 2-β-carbomethoxy-3β-(4-fluorophenyl) tropane, a radioligand binding to the dopamine reuptake transporters (DAT), Ouchi and colleagues showed an increased dopamine release in the putamen during unperturbed walking in healthy subjects and parkinsonian patients [133].

The mesencephalic locomotor region (MLR) and the subthalamic locomotor region (SLR) further play a relevant role in modulating the spinal locomotor networks. The MLR was originally defined functionally as a mesencephalic region in which continuous electrical stimulation evoked persistent locomotion [169]. This brain area in mammals encompasses the pedunculopontine nucleus (PPN), the cuneiform nucleus (CN) and the mesencephalic reticular nucleus (MRN), and interconnecting fibres. The interplay between these areas finely tunes postural muscle tone that encodes speeds of locomotion (rhythm generation and coordination) [170]. The level of postural muscle tone is further regulated by the reticulospinal, the vestibulospinal and the rubrospinal tract and monoaminergic descending pathways, such as the coerulo- and raphespinal tracts [136].

The role of the SLR and subthalamic nucleus (STN) in human gait is largely obscure and derives mainly from indirect evidence of clinical studies in parkinsonian patients with DBS of the STN.

Only in the past few years, new devices capable of recording local field potentials (LFP) with chronic implanted electrodes, allowed the direct recording of the STN during active human locomotion. These findings support the hypothesis of a "clutch-control" activity of the STN in human locomotion by activating or inhibiting top-down *feedforward* information flow to the MLR via direct glutamatergic projection or basal ganglia GABAergic output. The STN is indeed a cornerstone of the supraspinal locomotor network, receiving direct afferences from the SMA and projecting to both the MLR and the basal ganglia output nuclei (i.e., the globus pallidus internus [GPi] and the substantia nigra pars reticulata [SNr]), which also project to the MLR [171].

4.2.3. Gait initiation

The GI task is a crucial motor activity for everyday life and a highly challenging task for the balance control system. Surprisingly, despite being widely investigated with kinematic analyses, few studies have deepened our understanding of the supraspinal control of this motor task.

Very few studies made use of electrophysiological techniques to investigate GI. One of the few that did, Varghese and coll., combined a kinematic analysis with EEG recordings and showed a desynchronization of sensorimotor rhythms (alpha and beta bands) related to sensorimotor cortex activation during lateral stepping [172]. Additionally, Delval and coll. showed extended event-related desynchronization (ERD) in the beta band over the sensorimotor cortex, and more pronounced event-related synchronization (ERS) in the alpha band in trials with erroneous APA preceding a forward stepping after presentation of the visual target (a screen presenting an arrow pointing to the right or to the left foot) [173].

Using fNIRS, Coelho and coll. showed an additional contribution of the SMA and the DLPFC during a GI task under cognitive conflict to select the foot to step (congruent and incongruent conditions) [174].

Of relevance, molecular imaging techniques have never been previously used to study this motor task (see WP-1 and WP-3, paragraphs 7.1 and 7.3), and the role of deep brain structures in the control of this motor transition remains elusive.

4.3. Parkinson's Disease

4.3.1. Prevalence and etiopathogenesis

PD is the second most common neurodegenerative disorder after Alzheimer's disease. Its yearly prevalence is estimated between 108 to 257 cases and its incidence between 11 to 19 cases per 100˙000 persons [175]. The prevalence of PD significantly increases when considering subjects older than 60 years, reaching values between 1280 to 1500 per 100˙000 persons [176]. This is of great relevance considering the continuing increase in the percentage of the population aged over 65 years. By 2040, the number of people with PD is projected to exceed 12 million [177].

The causes of PD are still elusive. Ageing is the only certain single risk factor for PD. Some genetic factors have been identified but only in 5–10% of the patients [178]. Environmental factors (e.g., exposure to pesticides [179]) are associated with increased risk of PD, but only in specific cases.

Despite recent research and postmortem and genetic studies highlighted several factors involved in the neurodegenerative process (i.e., deficits in mitochondrial function, oxidative and nitrosative stress, the accumulation of aberrant or misfolded proteins, and ubiquitin-proteasome system dysfunction) [178] the etiopathogenesis of PD remains largely unknown.

The pathological hallmark of PD is the aberrant aggregation and accumulation of alpha-synuclein in the form of Lewy bodies and Lewy neurites. The exact pathophysiological contribution of the Lewy bodies in the neurodegenerative process of PD remains unclear [180]. Still, this is associated with the dysfunctionality and degeneration of dopaminergic neurons at the level of the substantia nigra pars compacta (SNc), leading to low levels of dopamine at a striatal level [181].

At the appearance of the motor symptoms (e.g., bradykinesia and rigidity) leading to the clinical diagnosis, over 50% of the SNc cells are usually lost and the nigro-striatal dopaminergic projects are reduced by 80% [182], [183]. This evidence emphasizes the presence of compensatory mechanisms able to counteract the dopaminergic loss at early stages of the disease. Along with disease progression, Lewy pathology propagates to cortical areas [182], adding new motor and non-motor symptoms to the clinical spectrum of PD [184].

4.3.2. Clinical spectrum

In parkinsonian patients, the SNc degeneration causes complex and interlinked brain network alterations leading to multiple motor and non-motor [185] symptoms (e.g., fatigue, anxiety, pain, etc.). Non-motor symptoms are unrelated to the specific research of this thesis and therefore are not discussed further.

The clinical diagnosis of PD demands bradykinesia and one of the following additional symptoms: muscular rigidity (plastic hypertonus), rest tremor and postural instability [186]. Balance and gait disturbances usually appear along with disease progression (Hoehn and Yahr stage 2-3, see later) and represent a major problem in parkinsonian patients [187]–[189].

The parkinsonian gait is characterized by short, shuffling, slow steps, often combined with enhanced knee and trunk flexion [190]. Additionally, advanced PD patients might suffer from specific gait disturbances, such as FoG, a transient inability to generate effective stepping. Patients experiencing FoG describe it as having their feet glued to the floor [191], thus impeding the forward stepping. FoG is generally triggered by a transition of motor behavior [25], [28], [192],

mostly occurring at gait initiation, but also during turning, or when adapting the walking speed or trajectory to pass an obstacle (e.g., a door).
Gait disturbances and FoG are major concerns for subjects with PD and their caregivers, as they expose patients to a high fall risk [6], [11], [193]. Up to 68-70% of patients fall at least once a year, and up to two thirds of them fall recurrently [11], [193]. Multiple falls produce a vicious circle beginning with a fear of falling which leads to poor and loss of mobility and independence as well as a protective gait, causing subjects to fall again [12], [194]–[200]. Consequences of falls are often dramatic for these patients, leading to injuries, fractures, and in turn decreased quality and quantity of life [193], [201]. Not only do recurrent falls effect the patients, they also have a large impact on the disease-related economic and social [11], [193], [202], [203].

In the clinical workup, the severity of motor symptoms is assessed with the Unified Parkinson's Disease Rating scale (UPDRS-III) [204], a clinical scale first proposed in the '80s by Stanley Fahn and colleagues [204] that is now the standard for scoring motor symptoms in PD [205]. The clinician asks the patient to perform specific motor tasks to assess speech, facial expression, bradykinesia, muscular rigidity, tremor, gait and postural instability. For each task, the clinician assigns a score from 0 to 4, where 0 is the absence of the symptom and 4 is the most sever clinical manifestation or the impossibility to perform the task. The disease stage is instead assessed with the Hoehn & Yahr (H&Y) scale [187], which identifies five stages according to the level of disability of the subject [204]:

0. Asymptomatic
1. Unilateral distribution of the symptoms
2. Bilateral involvement without impairment of balance
3. Mild to moderate disease with balance impairment
4. Severe disability but able to walk and stand unassisted
5. Wheelchair bound or bedridden unless aided

These clinical scales are standard practice to clinically evaluate parkinsonian patients, in terms of disease severity and response to medications. Their diffusion and easy administration make these scales a valuable tool in clinical practice. However, it is important to underline that they provide just a qualitative evaluation of the motor condition and suffer from inter-rater and intra-rater variability [205]–[208].

4.3.3. Dopaminergic brain imaging

PD is characterized by a loss of pigmented cells in the SNc, which in turn leads to a reduction of dopaminergic afferents mainly to the striatum [209]–[212]. Intense brain imaging research aimed at directly assesses the SNc cell loss with still debatable results [213], [214]. Conventional structural imaging (i.e., magnetic resonance imaging [MRI] [215]) remains normal in PD. More useful and robust results were obtained with nuclear medicine techniques targeting the dopaminergic nigrostriatal pathway. Several radioligands are now available for routine clinical measurements of dopaminergic innervation or functionality [216]. A first approach to determining the integrity of the presynaptic dopaminergic terminal is to study the DAT. For this use, the most widely used radioactive compound is the [123I]-N-ω-fluoropropyl-2β-carbomethoxy-3-(4-iodophenyl)nortropane (FP-CIT) (DaTSCAN®; GE Healthcare, London, U.K.)

and SPECT. PD patients consistently show low FP-CIT binding values in the putamen and, along with disease progression, also in the caudate nucleus [181], [212], [217]–[219]. Low FP-CIT binding values correlate with disease severity and distribution in mild-to-moderate cases [220]–[222].

FP-CIT and SPECT provides a significant aid in the clinical management of patients [181], [223], [224]. FP-CIT and SPECT is a valuable aid in support of the clinical diagnosis of PD, especially for uncertain cases, such as early-onset PD [225], [226], or in the differential diagnosis with Essential or Dystonic Tremor [227]–[232]. FP-CIT and SPECT also provides some utility in the differential diagnosis of atypical parkinsonism, especially when differentiating dementia with Lewy bodies from Alzheimer's disease or other dementias [233].

A second approach to assess the functionality of the presynaptic dopaminergic terminals is to study the vesicular monoamine transporter type 2 (VMAT2). VMAT2 is an integral membrane protein that transports monoamines into their synaptic vesicles. At a striatal level, more than 90% of VMAT2 binds to dopamine nerve terminals making this radioligand particularly interesting to study the integrity of the dopaminergic system in parkinsonian patients [234], [235]. However, VMAT2 binding is typically studied with [11C]dihydrotetrabenazine (DTBZ) which is not widely available and only in use for research purposes in a few centers.

Another possibility for studying striatal dopaminergic functioning is 6-[18F]-fluoro-L-dopa (F-Dopa). This compound is the immediate precursor of dopamine. It is carried into the brain by the large neutral amino acid transport system, taken up by monoaminergic neurons, decarboxylated to (fluoro)dopamine, and then stored in intraneuronal vesicles, from which it is released when the nerve cell fires. This positron-emitting compound is clinically used to assess the decarboxylating enzyme of the dopaminergic pathway and the storage capacity of dopamine [236], [237]. Despite being as accurate as FP-CIT SPECT and reasonably correlating with motor scores and disease duration in PD [238], [239], this compound is not often used in the clinical setting because of the need for a cyclotron-based radiopharmacy and the relative complexity of the synthesis [240].

Finally, several PET ligands are available to study the density and activity of dopamine receptors at the striatal level. Most of these ligands bind to the dopamine D2/D3 receptor subtype (D2/D3-R), but more ligands are becoming available also for the dopamine receptors of the D1/D4/D5 family, particularly dopamine D1-receptor (D1-R) [241]. The two receptor families have opposite effects of dopaminergic signaling [242] , which are balanced by the distribution of D1-R predominantly on cells providing output via the direct nigrostriatal pathway and D2/D3-R on cells of the indirect pathway [243].

4.3.4. Pathophysiology: lesson learned from locomotor brain network derangements

The pathophysiology of PD is not yet fully clarified. The loss of SNc neurons in PD would result in a decreased excitatory activity of the direct pathway from GABAergic striatal neurons to the internal segment of the GPi and SNr, and an increased inhibitory drive of the indirect pathway, involving particularly the external segment of the globus pallidus (GPe) and STN. As a consequence, the activity of the basal ganglia output structures (GPi and SNr) is disrupted, causing, in turn, alterations of the activity of brainstem motor areas (including MLR) and the thalamocortical motor system, leading to the manifestation of bradykinesia and rigidity [244].

Novel insights into the supraspinal locomotor derangements in parkinsonian patients provided preliminary evidence that many of the symptoms, especially the symptoms with a more transient and episodic nature (such as FoG), may arise as a consequence of disordered activity in neural circuits following, but not correlating with, striatal dopaminergic denervation [245]. Indeed, cortical-subthalamic decoupling in a low frequency band (4–13 Hz) was recently associated to the transition from normal walking into gait *freezing*. This was present in the brain hemisphere displaying less striatal dopaminergic innervation, but it did not correlate with the striatal DAT binding values measured with FP-CIT and SPECT. This is among the first evidence in humans of a symptom-specific derangement of the networked processing of locomotion in PD and suggests that FoG is indeed a "circuitopathy" related to a dysfunctional cortical-subcortical communication. This study was in line with the results of Tard and coll. who nicely showed an impairment of interaction between dorsal and ventral cortical locomotor pathways in PD patients suffering from FoG [246]. More recent evidence also supports oscillation derangements for other cardinal symptoms of PD (e.g., rest and action tremor, [247], [248], whereas bradykinesia and rigidity seem to be associated with increased cortical and subthalamic beta oscillations [249].

4.3.5. Therapeutic strategies

Pharmacological treatment

The main therapeutic approach for motor symptoms in PD relies on dopamine replacement drugs, which aim at restoring the physiological dopamine level. Although several dopamine-agonist compounds have been introduced in the therapeutic workup of PD, the most valid medication remains L-dopa, a precursor of dopamine [244], [250]. Indeed, bradykinesia and rigidity remarkably ameliorate with levodopa intake, even at late stages of the disease [251], [252]. Tremor is also reduced by Levodopa [252], but with a more variable response than akinetic-rigid signs [253]. However, dopaminergic medications are poorly effective on balance and gait disturbances [254]–[256], making the treatment of these symptoms particularly troublesome. In some cases, dopaminergic drugs can even increase fall risk, as they improve mobility without ameliorating balance [12], [257]. Furthermore, specific gait problems of parkinsonian patients, such as festination and FoG, might be worsened or caused in some cases by levodopa (e.g., "*on freezing*") [258], [259]. Levodopa also has long-term adverse effects that further increase the complexity of the treatment. Specifically, patients might suffer from levodopa-induced dyskinesias [251], [260], [261], defined as "Involuntary, nonrhythmic choreic or choreo-dystonic movements most often related to peak dopamine levels" [262], "off phases", i.e. periods with suboptimal medication effect, or motor fluctuations, when alternating dyskinesia and "off phases" along the day [260], [262].

Electrical neuromodulation

An alternative therapeutic option for late stages of PD – when levodopa-related motor fluctuations usually appear – is DBS. DBS is a neuromodulatory technique which allows the delivery of electrical impulses to specific brain targets by means of implanted electrodes connected to an internal pulse generator (IPG) [263]. DBS originated from the ablative stereotaxic procedures, such as pallidotomies and thalamotomies. In the pre-levodopa-era, they were the ultimate solution for the treatment of resistant and disabling motor symptoms, such as

dystonia [264] and tremor [265], [266]. Despite some effective results, dramatic and irreversible adverse effects such as dysarthria or hemiparesis were often encountered, especially in case of bilateral procedures [266]. Surgeons continued searching for more effective targets for ablation, and in the process, created an increasing knowledge base on the effects of stimulation of different brain areas. In patients with motor disorders, it was noted that lower frequency stimulation of particular areas could exacerbate symptoms, while higher frequencies could reduce symptoms [267]. Noting the therapeutic effect of higher frequency stimulation, some surgeons carried out chronic stimulation on their patients [263], [267]–[269]. In contrast to the ablative surgery, DBS showed to be a safer procedure, especially when performed bilaterally. Also, it had the great advantage to be reversible, as it did not lesion the brain tissue. Moreover, it is possible to modify the stimulation parameters in the post-operative phase to improve its efficacy, allowing for a tailored therapy that better fits the needs of the patients and their individual disease progression [263].

For all these reasons, from its first description by Cooper in 1980 [268], and especially thanks to the pioneering work of Benabid and colleagues [269], the use of DBS has rapidly spread into clinical practice, in terms of types of application and number of patients treated [270]. Main targeted areas for PD are the STN and GPi, for akinetic-rigid syndrome, and the ventralis intermediate nucleus (VIM) of the thalamus for tremor-dominant PD patients. Particularly, STN-DBS showed to consistently provide a significant improvement to the general motor condition of the implanted patients (UPDRS-III score amelioration pre/post-surgery of 38.1-67.0%), comparable to the benefit given by the Levodopa intake in the pre-operative phase (UPDRS-III score amelioration pre/post Levodopa intake of 38.1-67.0) [263], also at long-term use [252], [271]. Of relevance, DBS allows to remarkably decrease levodopa intake and consequently reduce levodopa-related adverse events (dyskinesia amelioration pre/post-surgery of 30%-92%) [263]. It is important to notice that DBS carries, additional to the surgical-related risks, possible adverse

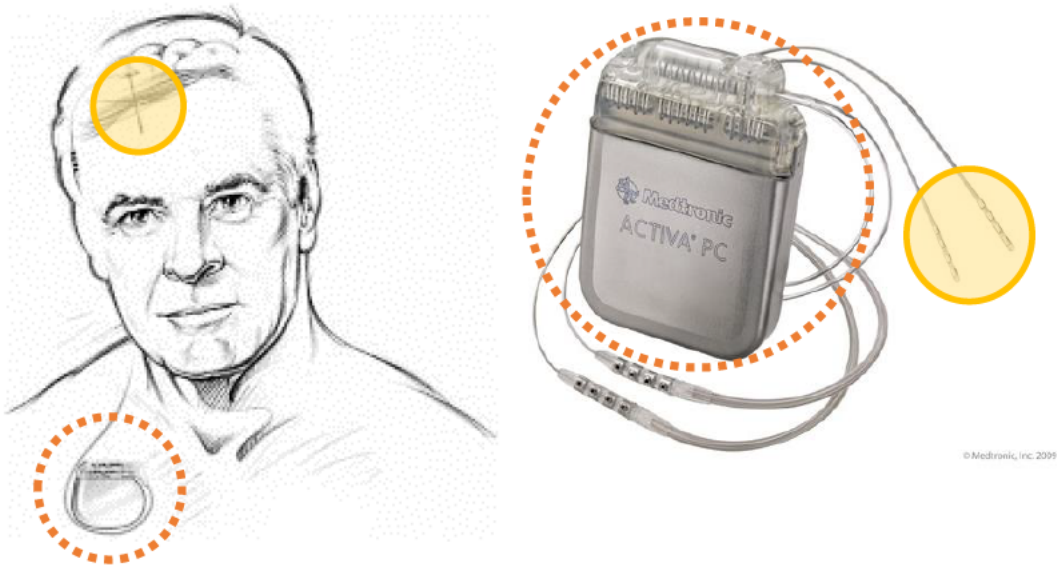

Figure 7: Unilateral DBS implant in a parkinsonian patient. An internal pulse generator (IPG), generally located in the chest area and connected to the electrodes by means of extensions, delivers the current as specified by the stimulation parameters. Stimulation settings can be tuned with an external device which communicates with the IPG via transcutaneous transmission. Figure adapted from www.medtronic.com. Abbreviations: DBS: Deep Brain Stimulation.

consequences such as stimulated-induced motor (e.g., gait and balance problems) and non-motor side effects (i.e., depression and cognitive impairment) [272]. In some cases, these symptoms are reversible by modifying the stimulation parameters [263], [273] may be difficult to balance the benefit and the adverse events of DBS.

DBS is not only an effective therapeutic device, but also a powerful tool to explore the brain network dynamics. Indeed, DBS devices provide the unique opportunity to directly record deep brain areas in humans and to directly interact with their activity [270]. This is of fundamental importance as the circuital derangements underlying motor symptoms in PD and movement disorders are largely unknown [45], [274]. The lack of understanding of the pathophysiological mechanisms of the locomotor network in motor disorders has till now limited the development of more effective neuromodulation therapies.

Deep brain recordings in patients with PD were initially performed during or immediately after the surgical procedure by means of externalized electrodes [275]–[279]. Despite the unquestionable importance of these studies, it is worth mentioning that immediate post-operative recordings might suffer from the so-called "stunning" effect. The surgical procedure produces a lesion to the implanted area, which directly impacts motor symptoms, similar to what happens with a pallidotomy or thalamotomy. This has been shown by the immediate improvement of the patients motor condition just after electrode placement [280]–[282]. Since the lesional effect might take some time (up to three months) to fade away, the post-operative recordings may be biased by this transitory condition, and not reflect the actual activity of the recorded brain area [44], [52], [283]. Additionally, the safety and technical limitations (e.g., short, externalized electrodes) of the experimental setup limited these recordings to resting or simple motor actions, such as upper-limb movement. Gait and full-body motor tasks were never explored. Only recently, the development of fully implantable DBS prototypes capable of not only stimulating but recording the activity of the implanted nucleus has allowed the evaluation of more complex motor tasks (i.e., gait) and motor symptoms (i.e., FoG) months and years after implantation [44], [45], [284]–[286].

These devices fostered the search of new and more reliable electrophysiological biomarkers related to specific motor tasks (e.g., gait, standing, resting) and symptoms (e.g., FoG). They have paved the way for the development of closed-loop stimulation protocols, able to adapt to the stimulation delivery to ongoing neural activity (adaptive DBS [aDBS]). This new DBS modality relies on the online recording of an input signal (generally the neural activity of the implanted brain area) for a timely and automatic adjustment of the stimulation delivery according to the actual needs of the patients. First applications of aDBS paradigms showed promising results in the treatment of motor symptoms in PD [52], [276], [287]–[289], making the novel aDBS almost ready for clinical applications. The identification of more specific and robust biomarkers is now a first and urgent step to foster the introduction and application of these promising protocols in clinical practice.

4.4. Progressive Supranuclear Palsy

4.4.1. Prevalence and etiopathogenesis

Progressive Supranuclear Palsy (PSP) is the second most common form of parkinsonism after idiopathic PD [290]. This is a rare and dramatic neurological disorder with a crude prevalence and incidence between 1.0 to 5.82 and 1.14 to 5.3 cases per 100˙000 persons, respectively [291]–[295]. There is a rapid increase of PSP incidence with age, ranging from 1.7 cases per 100˙000 at 50 to 59 years to 14.7 per 100˙000 persons at 80 to 99 years [292]. Accordingly, the risk of developing PSP is minimal before 50 years and increases with age [292]. The average age at onset is 63 years [296], [297] usually with a rapid progression of the neurodegenerative process which leads to a short median survival time after the diagnosis (5.6 years, range 2-16.6 years) [298]. The tentative identification of other risk factors other than age has so far not been successful [297], [299]–[301].

The pathogenesis of PSP is still unknown. PSP is characterized by the presence of neurofibrillary tangles, neuropil threads, and fibrillary gliosis, resulting from the aggregation of hyperphosphorylated tau-protein filaments [290], thereby causing PSP to be considered a "tauopathy". Tau proteins are normally distributed mainly in axons and modulate the assembly, dynamic behaviour, and spatial organisation of axonal microtubules. In PSP, conformational changes in tau-protein and its subsequent accumulation may directly contribute to cellular death [297], [302]. Specifically, tau-protein aggregates and neuropil threads were found in the globus pallidus (GP), STN, red nucleus, substantia nigra (SN), pontine tegmentum, striatum, oculomotor nucleus, medulla and dentate nucleus [297], [298], [303], [304].

4.4.2. Clinical spectrum

The most common form of PSP is the Steele-Richardson-Olszewski syndrome (PSP-RS) [290], [305]. The definitive diagnostic feature is vertical supranuclear gaze palsy, but several other symptoms may occur, including unsteady gait and unprovoked backward falls, bradykinesia, apathy, disinhibition, executive dysfunction and bradyphenia, speech disturbances (slow, ataxic, spastic and hypophonic) and dysphagia [294], [303], [305].

Several variants of PSP syndromes have been described and named according to their predominant clinical features, and include PSP with predominant parkinsonism (PSP-P), PSP with progressive gait freezing (PSP-PGF), corticobasal syndrome (PSP-CBS), PSP with predominant speech or language disorder [PSP-SL]), PSP with predominant frontal presentation (PSP-F) and PSP with predominant cerebellar ataxia (PSP-C) [305].

Clinical criteria for a PSP diagnosis require the age at onset to be after 40 years, a progressive course, and the presence of bradykinesia and supranuclear gaze palsy. In addition, at least three of the following symptoms/conditions should apply: frequent falls or gait disturbance early in disease course, axial rigidity greater than limb rigidity, neck in extension, tremor minimal or absent, pyramidal tract signs, dysarthria or dysphagia [291]. Despite having a well-defined clinical picture [298], [306], the diagnosis of PSP can be challenging as the spectrum of its clinical manifestation is particularly broad [305]–[307]. Additional PD-like symptoms might indeed be present (i.e., bradykinesia, rigidity, and postural instability) [306], [307] which often lead to underdiagnoses and misdiagnoses of PSP as PD [308]. Nevertheless, some differences between PSP and other bradykinetic rigid syndromes can help with the differential diagnosis. First, postural

instability and falls are present in PSP also at early stages of the disease, while in PD they are generally related to later stages of disease. In addition, in PD patients falls usually occur forward, whereas PSP falls usually happen backward, unprovoked, and with high morbidity [309]. Indeed, the median latency from disease onset to the first fall is much shorter in PSP (12 months) than in PD patients (108 months) [310]. Second, in PSP patients axial rigidity is more evident than limb rigidity [297]. Third, motor symptoms are generally more symmetric, and tremor rarely appears. Last, Levodopa response is usually poor and transient in PSP patients but not in PD [307], [311], [312].

Falls are among the most dramatic symptoms in PSP patients. Conversely to PD patients [313], the vast majority of patients with PSP falls backwards [297], [298], [303], thus exposing them to a high risk of severe injuries, as they are less likely able to protect themselves leading to considerable morbidity [314] and even mortality. Indeed, fractures of the skull, ribs, and vertebrae were reported to be more frequent in PSP than in any other bradykinetic rigid syndromes [310]. The incidence of falls increases along disease progression, as gait disturbances and postural impairment get more severe: during the first year, the 58% of the screened patients reported falls, while after two years falls were observed in all patients [298]. Interestingly, preliminary data suggest that the number of falls reduces at advanced stages of the disease, possibly due to lack of mobility, as by this stage patients are generally wheelchair bound or bedridden [315].

In clinical practice, patients with PSP are assessed mainly by qualitative scales specifically created for these patients and focusing on particular symptoms/aspects:

- The PSP-Quality of Life Scale (PSP-QoL) is related to quality of life as perceived by patients and composed of 46 items [316]. It is disease-specific, but longitudinal data are lacking [317].
- The Progressive Supranuclear Palsy Rating Scale (PSPRS) is a clinical scale for the assessment of disease severity [318] and the only one prospectively evaluated [317]. It is composed of six areas (History, Mentation, Bulbar, Ocular motor, Limb motor, Gait and midline) attempting to include all significant aspects of clinical impairment in PSP [318]. In particular, the last area addresses motor symptoms and mobility, evaluating neck rigidity or dystonia, arising from the chair, gait, postural stability, and sitting down. Scores range from zero (absence of the symptom) to four, the most severe clinical manifestation of the motor symptom. Number of falls are counted in the *history* area, ranging from absence of falls, corresponding to the score zero, to 30 per month, rated with the maximum score of four.
- The Progressive Supranuclear Palsy Clinical Deficits Scale (PSPCDS) is a very rapid clinical scale addressing seven clinical areas (Akinesia-rigidity, Bradyphrenia, Communication, Dysphagia, Eye movements, Finger dexterity, and Gait & balance), with scores ranging from zero to three (absent, mild, moderate, or severe impairment) [317]. It was developed to speed up the evaluation process and overcome some limitations of the PSPRS, which was designed on PSP-RS and underestimated symptoms specific to other variants of PSP [317]. Preliminary applications of this scale are promising but its diffusion is still limited.

Despite the clinical utility of these scales to assess disease severity and progression and longitudinal response to treatment [319], the data on the inter-rater variability and test-retest

stability are lacking for the first two scales and have been calculated only on a small cohort of patients (164) for the latter (0.96 and 0.99, respectively) [317].

4.4.3. Brain imaging

In early disease stages, the clinical diagnosis of PSP only shows limited sensitivity and moderate specificity as revealed by recent autopsy studies [320].

MRI measurements, particularly of brainstem structures (e.g., the ratio of the midsagittal areas of the midbrain and pons), may provide a useful aid to distinguish patients with PSP from those with PD and healthy subjects on an individual basis [321]–[323]. However, different expertise of manual raters evaluating these brain structures and the phenotypic variability of PSP create a high percentage of conflicting and inconclusive results. For these reasons, MRI studies only provide poor and indirect pathophysiological information in PSP.

Previous studies also demonstrated that FP-CIT and SPECT is not helpful for diagnosing degenerative atypical parkinsonism [233] and retains poor utility in differentiating PD from these syndromes [324]–[326]. Patients with PSP may only show a more symmetric and profound loss (including the caudate head) of presynaptic DAT density at an early disease stage [327], [328]. Similar findings apply to PET ligands for DAT [329] and F-Dopa PET [330], [331]. One study [332] reported significantly reduced VMAT2 density in the caudate nucleus, putamen, and SNc, consistent with degeneration of dopaminergic nigrostriatal projection neurons in PSP. PET tracer that binds to striatal post-synaptic receptors (e.g., 11C-raclopride) showed reduced D2/D3-R in PSP patients versus controls [333]. Usually, untreated PD patients show normal or up regulated D2/D3-R binding potentials [334], [335].

While PET Imaging of alpha-synuclein is still an unmet need for PD, new radioligands for tau pathology have been tested in small cohorts of patients with PSP [336]–[339]. Unfortunately, two recent anatomopathological studies showed poor correlation of PET findings with neuronal and glial inclusions of straight tau filaments in tauopathy brains [338], [340].

The differential diagnosis and workup of parkinsonian syndromes greatly benefit, instead, from the assessment of cerebral metabolism, which is commonly studied with 18F-labelled fluorodeoxyglucose (FDG). The application of a spatial covariance analysis on FDG and PET imaging led to the identification of distinctive disease-related metabolic patterns [341], [342]. These patterns have proven to be useful in the differential diagnosis and disease progression monitoring as well as for the assessment of clinical treatment, including dopaminergic therapy [343], STN DBS [344]–[346], and gene therapy [343]. In PD, the major feature of this spatial covariance pattern is relative metabolic increases in the pallidum, thalamus, pons and cerebellum, and concurrent hypometabolism in the premotor and posterior parietal-occipital areas [342]. Tang and coll. also reported elevated putamen metabolism in the initially presymptomatic hemisphere of PD patients, suggesting marked ongoing compensatory mechanisms in the early stages of PD [347]. Patients with PSP usually present metabolic reduction in the basal ganglia (caudate nucleus), thalamus, midbrain, anterior cingulate cortex, frontal lobe and primary motor cortex [341].

4.4.4.Pathophysiology: on the origin of postural imbalance and falls in PSP

The motor and neurobehavioral findings seen in patients with PSP reflect the marked and widespread neuronal degeneration. Despite intense ongoing research in PSP, a correlation between alterations of specific brain areas and motor and non-motor symptoms is lacking.

In particular, the pathophysiological mechanisms underlying postural instability, the distinctive clinical trait of PSP-RS, are still poorly understood [315]. Falls in PSP-RS are not related to environmental hazards, loss of consciousness, or cardiovascular causes [315]. Besides my study [75], only Zwergal and coll. investigated pathologic mechanisms in the supraspinal locomotor network of PSP patients by correlating a kinematic assessment of the gait performance and brain metabolic changes. In a first study, they showed a positive correlation between gait velocity and step length with increased FDG uptake in the prefrontal cortex and subthalamic nucleus and decreased in the precentral gyrus and superior vermis [348]. The authors also found a strong correlation between the CoP sway path during standing with FDG uptake of the precentral gyrus and the thalamus, the latter being also influenced by modulation of sensory input [349].

4.4.5.Therapeutic strategies

Unfortunately, treatment for PSP is only symptomatic, overall poorly effective and with no impact on disease progression [305], [350]. As neurodegeneration in PSP is related to tau pathology, some clinical trials exploited the utility of tau- or mitochondrial-directed therapeutic strategies but with poor results [305], [351]. The knowledge gap between molecular alterations and pathophysiological mechanisms underlying PSP is a main limiting factor for the design and implementation of prevention and therapeutic trials in this disease [305], [352]. The only clinical evaluation of the patients in such trials represents an additional limiting factor preventing a clear identification of the specific PSP variants most responsive towards experimental treatments. A first step to overcome this limitation was done in a recent study [353] assessing PSP-RS patients with a combined imaging and kinematic evaluation before and after the intra-arterially administration of autologous mesenchymal stromal cells.

With regards to available symptomatic treatments, patients with PSP and particularly with PSP-RS may have a transient benefit from Levodopa, especially at an early stage of disease [305], [350]. Poor response to Levodopa remains one criteria for the differential diagnosis between PSP and PD [307], [312], [350]. Physiotherapy strategies are probably the most effective treatments to improve motor condition and balance in patients with PSP [305], [315], [354]. Specifically, preliminary results suggested that aerobic, multidisciplinary, intensive, motor-cognitive and goal-based rehabilitation approaches with a treadmill [354], [355] or biofeedback training [356] are particularly effective in some patients, but results should be confirmed in larger cohorts [315].

DBS of the PPN alone [352], [357]–[360] or in combination with the stimulation of the GPi [358] or STN [360], was also explored as a possible therapeutic strategy specifically addressing balance instability and falls [361]. Findings are controversial, but the clinical efficacy is in general poor, not consistent and limited in time. The lack of positive results possibly derives from to the complex and multisite impairment of the locomotor network of which PPN is just one node [315]. Even if proven to be effective, DBS may have a limited application in patients with PSP as clinical manifestations often include cognitive and psychiatric disorders, that are set exclusion criteria for DBS-surgery eligibility [315], [360].

Given the higher prevalence of PD and the common traits between PD and PSP, researches and medical therapies in patients with PD have till now guided the development of new strategies for PSP treatment and care [315]. However, despite sharing some similarities with PD, PSP constitutes two very different neurological disorders [312] and should be therefore specifically addressed. It is of fundamental relevance to further expand our knowledge of the peculiar pathophysiological mechanism underlying PSP and to start developing therapeutic options tailored for these patients [352].

5. Aims

The overarching goal of my research activities was to investigate the pathophysiological alterations of the supraspinal locomotor network at GI in subjects with PD and related disorders.

With this aim, I developed my research activities into four work packages (WP), each responding to a specific question:

- **WP-1: What is the role of striatal dopamine in APA production at GI in PD?**

This study showed the contribution of striatal dopamine to APA production at GI in patients with PD, by describing the effect of levodopa intake and the correlations of biomechanical measurements with putaminal dopaminergic innervation. Of relevance, the experimental setup and analysis pipeline were designed and developed to assess and minimize the influence of confounding factors on the GI outcome variables. This was then adopted in WP-2 and WP-3.

Palmisano, C, Brandt, G, Vissani, M, [...], Frigo, C A, Isaias, I U, Frontiers in Bioengineering and Biotechnology, 2020, 8:137 [38]

- **WP-2: Is *feedforward* motor control at GI specifically altered in patients with PD and *freezing of gait?***

In this study, I identified alterations of GI execution specific for patients with PD and *freezing of gait*. The distinct influence of postural alterations on APA and motor performance was also assessed and described.

Palmisano, C, Beccaria, L, Haufe, S, Pezzoli, G, Isaias, I U, under review at Frontiers in Bioengineering and Biotechnology [362]

- **WP-3: Which brain areas are responsible for poor balance control during GI?**

I correlated the biomechanical features of APA and GI execution with brain metabolic alterations in patients with PSP-RS, identifying brain areas related to poor postural control.

Palmisano, C, Todisco, M, Marotta, G, [...], Pezzoli, G, Isaias, I U, NeuroImage: Clinical, 2020, 28:102408 [75]

Giordano, R, Canesi, M, Isalberti, M, Marfia, G, Campanella, R, Vincenti, D, Cereda, V, Ranghetti, A, **Palmisano, C**, […], Pezzoli, G., Frontiers in Neuroscience, 2021, 15:723227 [353]

- **WP-4: What is the STN contribution to standing and walking?**

This study investigated the neural activity of the STN nucleus specific for static (i.e., standing) and dynamic (i.e., gait) activity.

Arnulfo, G*, Pozzi, N G*, **Palmisano, C**, [...], Isaias, I U, PLoS ONE, 2018, 13(6): e019869 [44]

Canessa, A, **Palmisano, C**, Isaias, I U*, Mazzoni, A*, Brain Stimulation, 2020, 13(6): 1743–1752 [286]

*these authors equally contributed to the study

6. Materials and Methods

My experimental work relied on a multimodal approach combining clinical, biomechanical, neuroimaging, and neurophysiological data. This methodological choice was fundamental in exploring the multifaceted pathophysiological mechanisms underlying motor control in patients with PD or parkinsonism.

First, clinical data allowed the identification of specific motor symptoms. Given the complex and diverse manifestations and symptoms in motor disorders, clinical data were essential for the selection of homogenous patient groups (e.g., *freezing of gait* in WP-2). Second, in all WP, movement analysis measurements granted the evaluation of the biomechanical resultants of (*feedforward*) motor control and the detailed quantification of symptom-specific alterations. Third, neuroimaging data opened an observational window on brain region dysfunctions, allowing for a connection to be made between the altered motor resultants and their primary cause (i.e., neurodegeneration of specific areas, WP-1 and WP-4). Last, in a set of DBS-implanted patients, I was able to perform neural recordings in the STN nucleus during gait (WP-4), thus exploring the online nucleus activity related to motor control.

The adoption of this multimodal approach was possible only in the context of a close collaboration between the Politecnico di Milano (POLIMI), the Julius-Maximilians-Universität Würzburg (JMU) and the University Hospital of Würzburg (UKW). Research lines were run in parallel at the two institutions, combining engineering, clinical, and neuroscience expertise. In particular, the recruitment and data acquisition of WP-1 and WP-4 were performed at the Neurology Department of the UKW, one of the few centers at the time of this study to have fully implantable devices capable of simultaneous stimulation and recording of the STN (i.e., Activa PC+S). The WP-2 and WP-3 were carried out in Milano thanks to the fruitful collaboration of the POLIMI with the Centro Parkinson, ASST G.Pini-CTO (CP) and the Laboratorio di Analisi del Movimento nel Bambino (LAMB) Fondazione Pierfranco e Luisa Mariani of the Department of Physiology and Transplantation of the Università degli Studi di Milano (UNIMI). Molecular imaging studies were carried out at the Nuclear Medicine Department of UKW for WP-1 and WP-4 and at the Fondazione IRCCS Ca' Granda Ospedale Maggiore Policlinico for WP-3.

The next paragraphs will explore in detail the materials and methods employed in this study. For further information specific for each WP, please refer to chapter 7.

6.1. Patient recruitment and clinical assessment

Patients with PD (WP-1,2,4) and with PSP (WP-3) were recruited at the UKW and at the CP. An expert in movement disorders (Dr. Ioannis Isaias) inspected the clinical records and identified patients eligible for the study. Recruitment was also performed among hospitalized patients at the time of the experiment. Patients' medical records were specifically checked for: (i) clinical diagnosis, (ii) neurological diseases other than PD or PSP, (iii) vestibular problems, (iv) diabetes, (v) cardiovascular pathologies or hypotension, (vi) orthopaedic issues or past major orthopaedic surgery, (vii) *freezing of gait*, (viii) dyskinesia. Based on the specific research purpose, different inclusion/exclusion criteria were defined for each WP. Please refer to chapter 7 for details on inclusion/exclusion criteria of each WP.
All eligible patients received a detailed description of the study they were recruited for. Patients gave their written informed consent prior to participation. All studies were approved by the local investigational review board and conformed to the declaration of Helsinki.
For each recruited patient, disease duration (the time in years from the clinically established diagnosis) and Levodopa Equivalent Daily Dose (LEDD) were collected. The levodopa equivalent dose (LEDD) was calculated using conversion factors for antiparkinsonian drugs that yield a total daily levodopa equivalent dose [363].
Age and gender were recorded, and groups were matched accordingly. Healthy subjects were recruited among patients' and investigators' relatives and friends. Please refer to chapter 7 for details on inclusion and exclusion criteria applied to healthy controls.
The next two paragraphs describe additional disease-specific clinical data collected for this study and patients' clinical condition at the time of the experiment.

6.1.1. Parkinson's Disease patients

Enrolled patients with PD were diagnosed according to the United Kingdom (UK) Parkinson Disease Brain Bank criteria [364].

PD patients performed the experimental protocols after overnight suspension of all dopaminergic drugs (Med-OFF). Stimulation of implanted patients (WP-4) was switched off for at least one hour before the experiment (Stim-OFF). Of note, all patients recruited for WP-4 were implanted at least six months before the recordings. Dopaminergic treatment and stimulation parameters were unchanged for at least two and one month, respectively, prior to the experiment. For one research project (WP-1) I also analyzed patients after the intake of a standard dose of levodopa (soluble levodopa+benserazide [Madopar®] 200+25 mg, Med-ON). The evaluation in Med-ON condition helped to assess the positive or detrimental influence of dopaminergic replacement therapy on APA and GI execution, thus deepening the understanding of the role of dopamine at GI. The standardized medication condition applied in my studies was of particular relevance since the vast majority of previous works on GI and gait evaluated PD patients only in their best motor condition, i.e., under the effect of their usual dopaminergic therapy, thus possibly monitoring drug action on GI rather than dopamine-related alterations.

Disease severity of patients was evaluated by means of the H&Y scale [187], which identifies five stages according to the level of disability of the subject. Severity of motor symptoms was assessed with the UPDRS-III [204]. The UPDRS-III of patients recruited for WP-1 was administered in Med-OFF and in Med-ON conditions at the time of the experiment. The UPDRS-III of implanted

patients (WP-4) was assessed in four different conditions within one week from the experiment: (i) Stim-OFF and Med-OFF; (ii) Stim-ON and Med-OFF; (iii) Stim-OFF and Med-ON and (iv) Stim-ON and Med-ON. For the clinical assessment in the Stim-OFF condition, the stimulator was switched off for at least two hours before the evaluation. For Stim-ON conditions, stimulation parameters were set as the clinically most effective (i.e., chronic stimulation settings). The UPDRS-III in Med-OFF condition was assessed after overnight suspension of all dopaminergic drugs. Motor status in Med-ON was evaluated after the intake of dopaminergic drugs according to the patient-specific pre-operative and post-operative therapeutic plans in Stim-OFF and -ON condition, respectively.

6.1.2. Progressive Supranuclear Palsy patients

Patients with PSP were enrolled for WP-3. PSP patients were diagnosed according to the Movement Disorder Society criteria [365]. All subjects with PSP were classified as Richardson's syndrome, which is predominantly characterized by early postural instability and oculomotor dysfunctions [366].

Despite the lack of efficacy of dopaminergic drugs on PSP symptoms, I asked for the suspension of all dopaminergic drugs for at least 12 hours prior to the experiment (Med-OFF) to avoid any eventual influence of dopaminergic drugs on task performance.

Patients with PSP were evaluated with the PSPRS within one month after the experiment [318]. The clinical assessment was performed in the morning in Med-OFF condition. Of note, given the association between PSP and cognitive impairment, all patients were accompanied by at least one relative or caregiver during both the clinical assessment and the experimental session. Caregivers provided additional information on patients' clinical status and supported them throughout the experimental session.

6.2. Neuroimaging

identification of brain areas related to the biomechanical resultants of GI (WP-1, WP3). Additionally, in WP-4 the quantification of the residual dopaminergic innervation of the two hemispheres, evaluated by a SPECT (see next paragraph) allowed identification of the least and most dopamine-depleted nuclei, thus possibly disentangling physiologic or adaptive from pathologic neural dynamics.

Hypokinetic movement disorders, and PD in particular, are traditionally identified by loss of function of a specific brain area (e.g., the nigro-striatal dopaminergic pathway). However, there are collateral and parallel brain alterations which may play a relevant role in the neurodegenerative processes and related symptoms [367]–[371]. The neuropathological picture of PD and motor disorders is indeed much more complex than a simple deficiency syndrome, and the interplay between the various brain circuits/area in determining the motor outcomes is still largely unknown. Additionally, altered biomechanical measurements may not be a direct effect of disease-related symptoms (e.g., bradykinesia, rigidity, etc.), but expression of compensatory mechanisms [1], [3], [13], [372].

In this context, neuroimaging findings together with biomechanical data may help in investigating the pathophysiological role of different brain regions, neurotransmitters, and circuits in motor control. A better distinction of pathological features from compensatory adaptations would pave the way towards a correct interpretation of motor alterations and the development of focused and effective therapies and treatments.

In my research, I took advantage of two neuroimaging evaluations performed during the patient clinical workup (WP-1 and -3) or specifically for research purposes (WP-4). In WP-1 and WP-4 the quantification of the residual dopaminergic innervation of the striatum in patients with PD was assessed with SPECT and FP-CIT. In WP-3 patients with PSP underwent a PET with FDG for a proper identification of disease-related brain metabolic alterations. The following paragraphs will explain in detail the neuroimaging data acquired in patients with PD (WP-1 and -4) and with PSP (WP-3).

6.2.1. Striatal dopamine transporter imaging

Patients with PD invariably show a loss of dopaminergic neurons in the SNc, and a consequent reduction of afferent fibers to the striatum [209]–[212]. The DAT, located at the dopaminergic nerve terminals, are also reduced [212], [373]–[376].

The FP-CIT is a radioligand that selectively binds to the DAT at the striatal level (both caudate and putamen nucleus), allowing an indirect measurement of the striatal dopaminergic innervation (**Figure 8**). SPECT with FP-CIT studies consistently showed a reduction of DAT density in PD patients [212], [218], [219], [224], [377] and a negative correlation between striatal DAT density and akinetic-rigid symptoms [218], [220]–[222]. The rate of decline of DAT binding fits a single exponential decline during early to moderate PD. Extrapolating the single exponential decline to the preclinical period leads to control values 2–3 years before the onset of symptoms [378]. This is in line with pathological studies estimating a 40–60% loss of dopaminergic cells and reduction

of synaptic function by up to 80% before the appearance of PD-related motor symptoms [379]. This supports the presence in PD of strong compensatory mechanisms over dopaminergic loss, possibly determining the clinical phenotype [380].

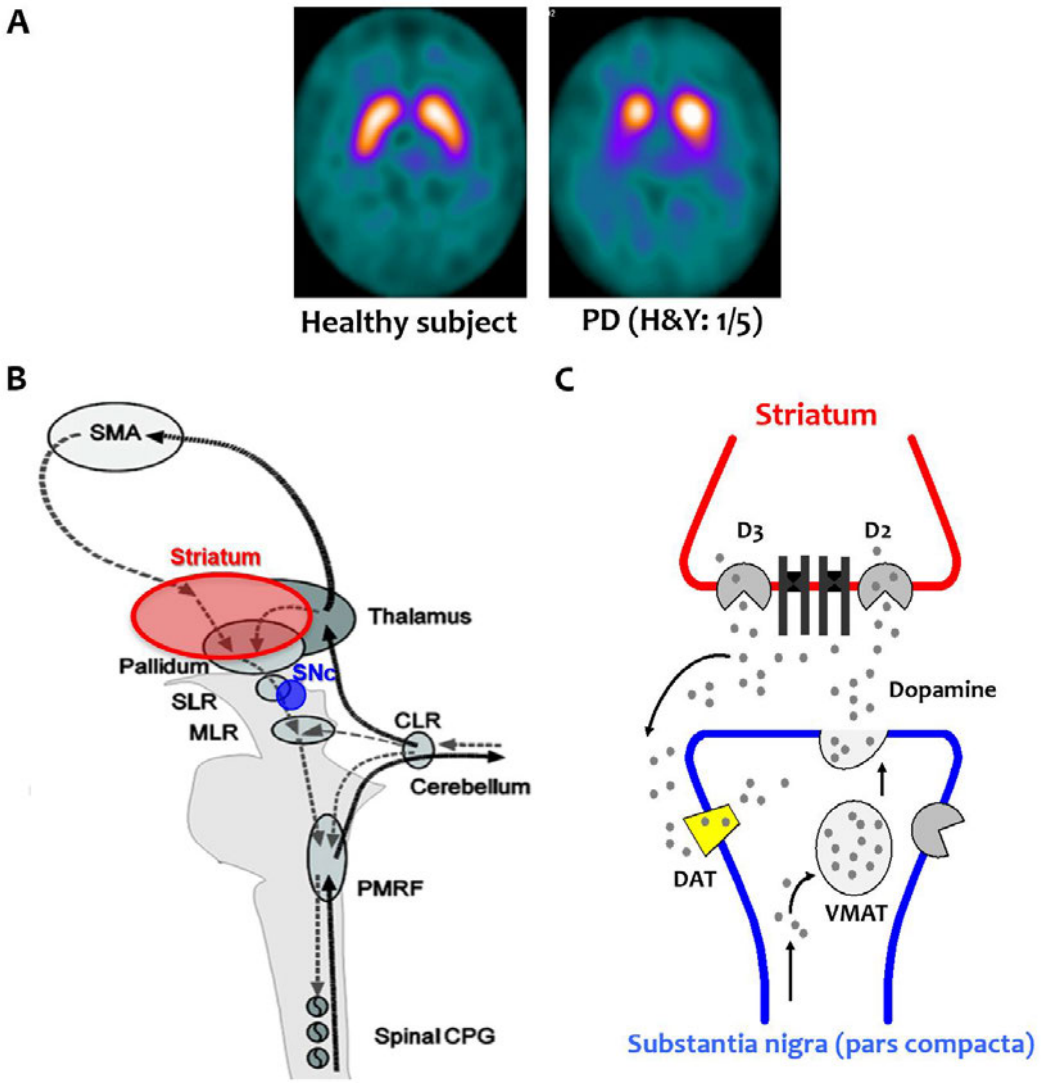

Figure 8: A) Example of a SPECT with FP-CIT image of a healthy subject and one patient with first-stage PD. The striatal nuclei, with a typical comma-shape, are clearly visible in the scan of the healthy subject (on the left). The DAT density is similar between the two hemispheres. The patient's image is instead characterized by a loss of DAT mostly involving the putamen (the tail of the comma) (on the right). The dopaminergic innervation is asymmetric among the two brain hemispheres, as expected for a patient at clinical stage 1 according to the H&Y staging system, with the left being more dopamine depleted. The colour code represents the estimation of the density of the DAT, with warmer colours indicating higher levels of FP-CIT binding. B) Sketch locating the Striatum and the Substantia Nigra pars compacta (in red and blue, respectively) in the supraspinal locomotor network. C) Schematic representation of the nigro-striatal dopaminergic pathway.
Abbreviations: CPG: Central Pattern Generators; CLR: cerebellar locomotor region; D2 and D3: dopamine receptors type 2 and 3; DAT: dopamine reuptake transporter; H&Y: Hoehn &Yahr scale; MLR: Mesencephalic Locomotor Region; SPECT: Single Photon Emission Computed Tomography; FP-CIT: [123I]-N-ω-fluoropropyl-2β-carbomethoxy-3β-(4-iodophenyl)nortropane; PD: Parkinson's Disease; PMRF: medullary and pontine reticular formations; SLR: subthalamic locomotor region; SNc: Substantia Nigra pars compacta; VMAT: vesicular monoamine transporter.

For WP-1 and WP-4, scans were performed at the UKW as described by Lapa and colleagues [381]. Briefly, data were acquired with a dual-headed integrated SPECT/CT system (Symbia T2; Siemens, Erlangen, Germany) equipped with a MELP (medium-energy low penetration) collimator. Scans were performed about 3 h after the injection of 150-180 MBq of FP-CIT (GE Healthcare, Munich, Germany). Brain reconstruction was performed using OSEM 3D (8 subsets and 8 iterations) with the application of 8 mm gaussian filtering. CT-based attenuation correction was also applied (Chang's correction technique). Subsequent analyses were performed using the PMOD software (Version 3.2; PMOD Technologies Ltd, Adliswil, Switzerland). In particular, the DAT non-displaceable binding potential (BP) was assessed for four regions of interest (ROI) in both hemispheres, i.e., caudate nucleus, putamen, striatum, and occipital cortex using the formula:

$$BP = \frac{count\ density\ target\ ROI - count\ density\ occipital\ ROI}{count\ density\ occipital\ ROI}$$

A normative data range was defined with a group of healthy controls, age- and gender-matched, previously acquired and analysed with the same methods. All PD patients recruited for this study showed pathological values of striatal dopaminergic uptake, further supporting the clinical diagnosis.

In WP-4, based on the residual dopaminergic innervation I identified the least (H+) and most (H-) affected hemispheres.

6.2.2. Imaging of metabolic brain activity

PET with FDG is a well-established molecular imaging exam for the evaluation of metabolic brain activity. FDG is a glucose analog with a phosphorylation (^{18}F) that prevents its release from the cell before radioactive decay. FDG is also missing the 2-hydroxyl group (-OH), which is needed for further glycolysis. Therefore, FDG cannot be metabolized in cells. As a result, the distribution of FDG is a good reflection of the distribution of glucose uptake, which closely correlates with tissue metabolism. Although mainly used for the clinical workup of metastatic cancers, in recent years FDG PET gained increasing value in the differential diagnosis of neurodegenerative parkinsonism and dementias [341]. In particular, atypical parkinsonism such as PSP, corticobasal syndrome (CBS) and multiple system atrophy (MSA) show distinctive patterns of metabolic brain alterations that can be well captured by FDG PET [341], [382]. The importance of FDG PET is further underlined by the fact that the correlation between the clinical diagnostic criteria and a neuropathological confirmation is still insufficient especially in suspected PSP and CBS cases [383], [384].

For WP-3, I recruited patients with PSP who underwent a FDG PET evaluation at the Fondazione IRCCS Ca' Granda Ospedale Maggiore Policlinico. Scans were performed with a PET/CT scanner Biograph Truepoint 64 (Siemens Healthineers, Erlangen, Germany) for 15 minutes in resting state condition. Patients were asked to sit quietly in a dimly lit room for approximately 30 minutes between the injection of 150-200 MBq of FDG and the scan. PET sections were reconstructed with an iterative algorithm (i.e., ordered subset expectation maximization [8 subsets and 6 iterations]). Twelve age and gender-matched healthy controls, acquired with the same methods, served as a control group. PET data were evaluated with the Statistical Parametric Mapping (SPM

12, Wellcome Department of Cognitive Neurology, London), with false discovery rate (FDR) correction for multiple testing ($p<0.01$) and age at PET scan as nuisance covariate. Significant differences between patients and healthy controls were investigated with a paired t-test applied to voxel-wise comparisons. Clusters with $k \geq 200$ voxels and threshold of $p<0.05$ family-wise corrected (FEW) were considered as significant. After whole brain analyses, spherical volume of interest (VOI) of 5 mmm radius were identified, centered in the peak voxel of significant clusters. The standardized uptake value ratio (SUVR) of FDG uptake was calculated as follows:

$$SUVR = \frac{mean\ count\ per\ voxel\ of\ the\ VOI}{mean\ count\ per\ voxel\ of\ the\ global\ brain}$$

6.3. Experimental sessions – data recording

6.3.1. Movement analysis

Movement analysis is the common thread through all WP of my research project. This technique allows the identification and evaluation of APA in healthy controls [4], [62], [81] and parkinsonian subjects [1], [14], [16], [18], [32], [56], as well as the effect of specific symptoms [2], [3], [13] and drugs and neurostimulation therapies [19], [33], [34], [76], [385] on the GI performance. Also, it was used to effectively explore pathophysiological mechanisms responsible for altered motor control at GI [38], [246], [386].

In the context of my research project, movement analysis allowed the recording of synchronized kinematic and dynamic measurements in a standardized environment, essential for the consistency of measurements across trials and patients. In particular, it provided biomechanical measurements directly related to *feedforward* motor control at GI and motor control during gait, which would not be accessible with a simple qualitative/clinical evaluation. It also granted a protected environment for the biomechanical assessment, essential for ensuring participants' safety, a fundamental concern when severe balance alterations are present (especially in WP-2 and 3).

I developed methods for the evaluation of the biomechanical resultants of APA in the context of WP-1 [38], then applied to WP-2 and WP-3 (see chapter 7). The biomechanical assessment also served to identify windows of interest for investigating brain activity related to the ongoing motor programs (WP-4). In this regard, the setup of data synchronization was a crucial step to allow for the combination of biomechanical and electrophysiological data (see paragraphs 6.3.3 and 6.4.2).

Optoelectronic systems and force plates

The kinematic analysis of GI was carried out in both laboratories thanks to optoelectronic systems. This equipment enabled an accurate and non-invasive evaluation of movement. Optoelectronic cameras are able to track the position of passive retroreflective markers placed on the subject. Each camera is provided with light emitters placed co-axially to the optics: the rays emitted by the camera are reflected by the markers, whose position is captured by the optics and recorded in the image plane of the camera. The system is then able to reconstruct the 3D position of the markers thanks to a triangulation procedure between the data collected by the various cameras.

The UKW and LAMB laboratories were equipped with motion capture systems based on visible and infra-red light, respectively, that provided similar results. At the beginning of my PhD course (2016– 2018), the UKW lab was equipped with an imaged-based movement reconstruction system (Simi Motion 3D 9.1.1, Munich, Germany). The system was composed of nine BASLER cameras (sampling frequency set at 100Hz) (**Figure 9**) placed around the walkway to define a calibration volume of approximately $10m^3$. This technology was based on visible light, and accordingly, has both advantages and disadvantages. On one hand, every camera provided the actual video recordings on which the 3D reconstruction algorithm acted to track the markers. This enabled the user to access the raw data, not only the resulting 3D reconstruction. In case of an error in

the reconstructed data, it was possible to manually correct the tracks operating on the original video. Additionally, this technique would allow for markerless recordings (not yet implemented at the time of the experiment), to track movement based on the shape of the subject rather than on marker displacement. This is of great relevance considering the long preparation time needed for a traditional gait analysis, especially when evaluating neurological patients under drug suspension. On the other hand, the system was quite sensitive to unwanted reflections of visible light, leading to frequent reconstruction errors (e.g., "ghost" and mis-labelled markers). Also, during data acquisition the light rays emitted by the cameras were visible to the patient and may have influenced his/her behavior during the motor performance.

For all these limitations, after preliminary recordings and testing my research group purchased in 2018 a new infrared motion capture system (SMART-DX 400, BTS, Milano, Italy) for the UKW laboratory, which was subsequently used for WP-1 and WP-4. I personally conducted the full installation of the new equipment. The system was composed of six optoelectronic cameras (sampling frequency set at 100Hz, **Figure 9**), placed in the gait laboratory around the walkway. The main difference, in regard to the old equipment, relied on the type of light rays used for the detection of the markers. The new system used infrared instead of visible light and the light rays were therefore invisible to the subject.

Figure 9: Motion capture cameras. On the left, a BASLER camera, used at UKW for WP-4; in the centre, a BTS SMART-DX camera, used at UKW for WP-1; on the right, a BTS SMART-D camera, used at the LAMB laboratory for WP-2 and WP-3
Abbreviations: LAMB: Laboratorio di Analisi del Movimento nel Bambino; UKW: University Hospital of Würzburg; WP: work package.

However, different from the previous system, the access to the raw data was not allowed. Indeed, in order to improve track quality, the user could act only on the reconstructed 3D marker trajectories to modify the parameters of the reconstruction algorithm. This prevented the recovery of missing samples in case of low data quality. Nevertheless, the device showed good performance in reconstructing marker trajectories without the need of relevant user corrections. The new device installed at UKW was similar to the one in use at the LAMB (six-cameras, SMART 1.10, BTS, Milano, Italy, **Figure 9**). At the LAMB, cameras were placed around the walkway to optimize marker detection during GI. The covered calibration volume was about 5 x 3 x 2 m and the sampling frequency was set at 60 Hz, the maximum available with this model. This system was used to carry out WP-2 and WP-3. Of relevance, both optoelectronic systems were provided

with syncrhonized videocamers (VIXTA, BTS, Milano, Italy), which allowed verification of correct task execution for each recording.

For all studies, I used the LAMB total body protocol for marker placement [387]. The protocol was composed of 29 markers placed on specific anatomical landmarks (**Figure 10**, red dots). To automatically compute the main anthropometric measurements (AM) of the subjects, I recorded the position of eight additional markers placed on medial positions and on the trochanters (**Figure 10**, blue dots) dur ing a short (~5 sec) standing acquisition (the anatomic calibration trial, **Figure 12**).

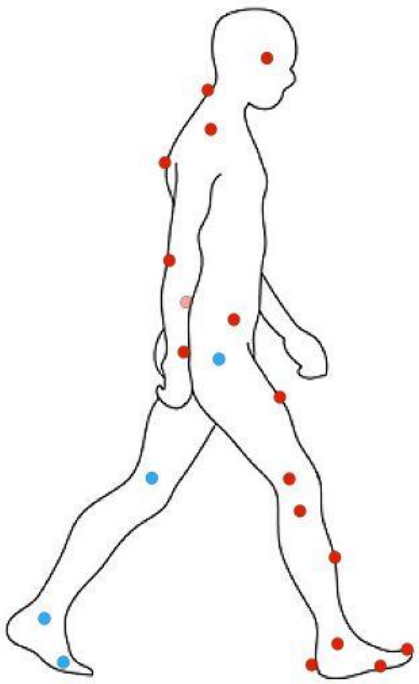

Figure 10: LAMB protocol for marker placement. Red dots: markers used for GI, standing and walking trials. Blue dots: markers added bilaterally for the anatomic calibration trial. During GI, markers were placed bilaterally in correspondence to (from the top to the bottom): the temple, the acromion, the lateral epicondyle, the ulnar styloid process, the anterior superior iliac spine (ASIS), the middle point of the thigh, the lateral condyle, the head of the fibula, the middle point of the shank, the lateral malleolus, the calcaneus, the fifth head of the metatarsus and the hallux. On the back, I placed one marker on the seventh cervical vertebra, the point of maximum kyphosis, the middle point of the posterior superior iliac spines (PSIS, red blurred dot in the figure). Only during the anatomic calibration trial, eight additional markers were placed on the trochanters, the medial condyles, the medial malleoli and the first metatarsal heads. The anatomic calibration allowed the computation of the main anthropometric parameters.
Abbreviations: GI: gait initiation; LAMB: Laboratorio di Analisi del Movimento nel Bambino.

During GI trials, the CoP pathway and the GRF exchanged with the floor by the subjects were monitored by means of two dynamometric force plates. The function of dynamometric force plates is based on the electrical properties of piezoelectric sensors, which produce electric signals in response to the applied load. Three piezoelectric transducers are placed under each corner of the platform to detect the force components applied in the three directions. The total force exchanged between the subject and the floor is obtained by the vector sum of all these components. The CoP, which is the point on the platform surface where the resultant force is applied, is computed through the static equilibrium equation of the moment. The two

laboratories were equipped with different models of KISTLER force plates (KISTLER 9260aa at UKW and KISTLER 9286a at LAMB, Winterhur, Switzerland). At UKW, I had two platforms available, placed side by side along the longer dimension (**Figure 11**). Sampling frequency was set at 800Hz. At LAMB, I used only one force plate, placed horizontally in respect to the walking direction (**Figure 11**), with a sampling frequency of 960Hz. Platforms were embedded in the walkway and hidden from the subject's view by a mat to avoid any possible motor behavior bias.

Figure 11: Dynamometric force plates placement. The left panel shows the configuration of the force plates at the UKW laboratory. On the right, the setup of the dynamometric force plates at the LAMB.
Abbreviations: LAMB: Laboratorio di Analisi del Movimento nel Bambino; UKW: University Hospital of Würzburg.

6.3.2. Subcortical recordings

The Activa PC+S

For WP-4, I had the unique opportunity to recruit eight parkinsonian patients who received an innovative device for DBS called Activa PC+S (Medtronic, PLC). The Activa PC+S is a prototype made available only to a few selected medical centers for research purposes. It was developed from the dual channels neurostimulator Activa PC (Medtronic, PLC) which has been in use for a long time for the treatment of PD and other neurological disorders. The Activa PC+S allowed, for the first time, to collect LFP in freely moving patients months/years after the surgery[285].

This device constituted a fundamental technical advance in the study of human locomotion and transient gait derangements (e.g., FoG) [44], [45], [286]. It also fostered the study of more specific task-related biomarkers [44] that could be used for aDBS paradigms in everyday life [52]. Specifically, the Activa PC+S provided, for the first time, deep brain recordings free from the "stunning effect". In previous studies, deep brain recordings were performed only at the time of the surgical procedure or shortly after surgery (3 – 7 days) with externalized electrodes [275]–[279] and thus, were possibly affected by the post-operative peri-electrode edema. For this reason, the recorded activity in pre- and post-operative sessions might differ from the real activity of the brain nucleus [44], [52], [283]. The relevance of such effect is clearly seen by the temporary improvement of motor symptoms immediately after the implantation even in absence of stimulation [280]–[282]. Conversely, being a fully implantable device, the Activa PC+S allowed the

recording of deep brain nuclei months and years after the implant, without any lesional effects and infection risks. Moreover, thanks to the healing of the surgical lesions on the scalp, the Activa PC+S allowed for the first time for the combining of STN LFP with high-density EEG recordings. This is of utmost relevance to explore network dynamics and their derangements by recording multiple hubs (i.e., STN and cortex) of the human locomotor network [45].

The surgical procedure

All subjects of WP-4 received quadripolar electrodes (model 3389, Medtronic, PLC), which consisted of four platinum-iridium cylindrical contacts of 1.5 mm each, spaced by 0.5 mm. Zero and 8 were the lowermost contacts and 3 and 11 were the uppermost contacts; contacts 0–3 refers to the right hemisphere and contacts 8–11 to the left hemisphere.

In all cases, the implanted target was the STN bilaterally. The target coordinates (i.e., 12 mm lateral, 2 mm posterior, 4 mm ventral to the mid-commissural point) were adjusted to patient's specific T2-weighted and susceptibility-weighted magnetic resonance images (Magnetom Trio, Siemens Healthcare, Erlangen, Germany). The proper electrode placement was checked by means of intraoperative microelectrode recordings and computed tomography scans and further confirmed after surgery by means of the SureTune™ software (Medtronic, PLC) [45], [273]. The surgical procedure has been extensively described in Steigerwald et al. 2008 [279]. All patients had an implantable pulse generator placed in the chest, under the clavicle, and connected to the leads implanted in the brain by means of cable extensions (see **Figure 7**).

LFP recordings

The Activa PC+S allowed recordings only with a single bipolar configuration. I chose the two contacts surrounding the one used for chronic stimulation (clinically most effective). LFP were collected from both STN simultaneously with a nominal sampling frequency of 422 Hz and amplified by 1000. Each recording session was limited to 15 minutes, the maximum time for on-board storage of the data. Each recording session was followed by approximately 15 minutes of data downloading. This greatly limited the duration of the experimental protocols as the patients were studied in Med-OFF and Stim-OFF condition, which could not be tolerated for long as PD-related symptoms were rapidly worsening. The recording sessions were kept as short as possible because the "sensing mode" of the device drained the battery faster than the conventional stimulation modality (one hour of recording shortened the life of the battery of about one day).

Of relevance, for safety reasons, the Activa PC+S was not provided with any output nor input for external signals/triggers. To overcome this limitation and allow the synchronization of the Activa PC+S recordings with the kinematic data, I used a programmable transcutaneous electrical nerve stimulator (TENS) to generate an electrical artifact to be fed into both the PC+S device and the kinematic data stream.

6.3.3. Experimental setup

Each experimental session started with an *anatomic calibration* trial for the automatic calculation of the main AM (see paragraph 6.4.1). This task consisted of a brief biomechanical recording (approximately 5 seconds) of the subject standing on the force plates with 37 markers (**Figure 12**). I asked the subjects to keep their arms apart and enlarge their BoS to ease the detection of

the medial points. The relative position of the markers recorded during this acquisition was used for the computation of the key AM, while the weight of the subject was calculated from the force plate recordings (see paragraph 6.4.1 and [38], [75]).

For WP-1,2,3, I analyzed the kinematic and dynamic data of at least 3 GI trials for each subject. The task was composed of a standing phase lasting 30 seconds and followed by walking till the end of the walkway (a pathway of approximately four meters in both laboratories). For the standing phase, at UKW subjects were asked to place each foot on a different platform, while at LAMB theyplaced both feet on the only available force plate. The feet position was self-selected by each subject as the most comfortable to stand still and start walking. Subjects were asked to stand quietly with their arms resting at the side of the body, looking straight in front of them, and to start walking after a verbal 'go' signal (**Figure 12**).

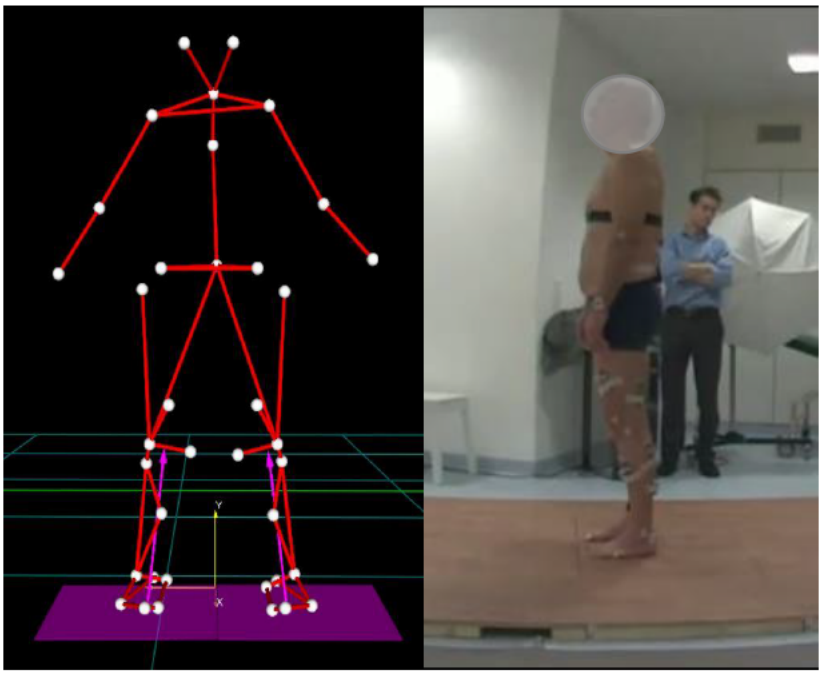

Figure 12: On the left, a frame of the 3D reconstruction of the marker tracks recorded during the anatomic calibration trial of a subject recruited for WP-2. Notice the additional markers on medial positions needed for the calculation of the main AM. On the right, a video frame of a GI trial performed by the same patient. Abbreviations: AM: anthropometric measurements; GI: gait initiation; PD: Parkinson's disease; WP: work package.

Subjects were instructed not to start walking promptly after the start signal but to wait a self-selected time afterwards, to avoid any possible influence/suppression of the APA due to fast reaction time [76], [372]. Feet position, swing foot and gait speed were also spontaneously decided by the subjects in order to prevent the alteration of their natural/preferred motor strategy.

Subjects enrolled for WP-4 underwent a specific experimental protocol designed for evaluating the STN activity during standing and gait (**Figure 13**). They were instructed to walk barefoot on the walkway of the lab at their preferred speed. At the beginning of each walking trial, subjects were asked to stand still for about 30 seconds before the walking period. Feet position and postural attitude during standing were not standardized across subjects. Each subject repeated

the task at least six times (range 6-10 trials; number of trials was limited due to patients' medical condition).

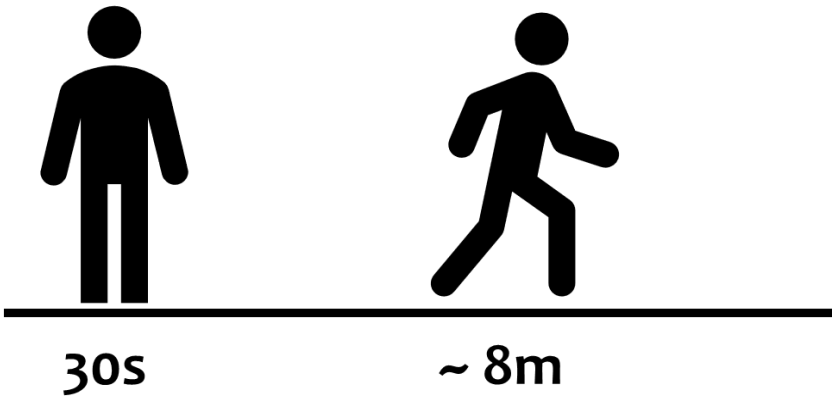

Figure 13: Scheme of the experimental protocol adopted for WP-4. Patients were asked to stand still for about 30 seconds before the walking trial. The walking trial was performed barefoot over the walkway of the lab (approximately eight meters long) at the preferred speed of the subjects. Postural attitude and starting foot were not standardized across trial and subjects.
Abbreviations: WP: work package.

For WP-4 I additionally used a bipolar EMG probe (FREEEMG 1000, BTS, Milano, Italy, sampling frequency set at 1000 Hz) to synchronize subcortical recordings and biomechanical data (**Figure 14**). For synchronization purposes, I used an electrical artifact produced by a TENS device (130 Hz, 250µs, amplitude as high as tolerated by the patient) recorded simultaneously by the Activa PC+S and the EMG probe. As the EMG probe was built in with the optoelectronic system, I could synchronize once EMG, kinematic, and dynamic data with the LFP recordings [285]. The TENS signal was delivered at the beginning and end of each acquisition. The stimulating electrodes of the TENS and the EMG probe were placed on the neck of the patients upon the cable connecting the IPG to the DBS electrodes. Each TENS artifact was manually delivered for about 5 seconds. Intensity of the TENS was rapidly increased, as much as could be tolerated by the patient, and then suddenly switched off. As a marker for synchronization, I used the sharp drop-off of the artifact corresponding to the end of the TENS stimulation, clearly visible in both data streams (**Figure 14** and paragraph 6.4.2). In the "Information for Prescribers" the company recommends to not place TENS electrodes so that the TENS current might spread over any part of the neurostimulation device. TENS currents are considered possible sources of Electromagnetic Interference (EMI) and as such their use in implanted patients is discouraged. However, no adverse effects/issues due to the combined use of DBS and TENS are so far known. Of note, the Activa PC+S did not provide the possibility of real-time data visualization. This prevented an online check for a proper detection of the TENS artifact, thus further increasing the complexity of data acquisition. Indeed, in some cases, the TENS was not captured by the Activa PC+S recordings and the data had to be discarded.

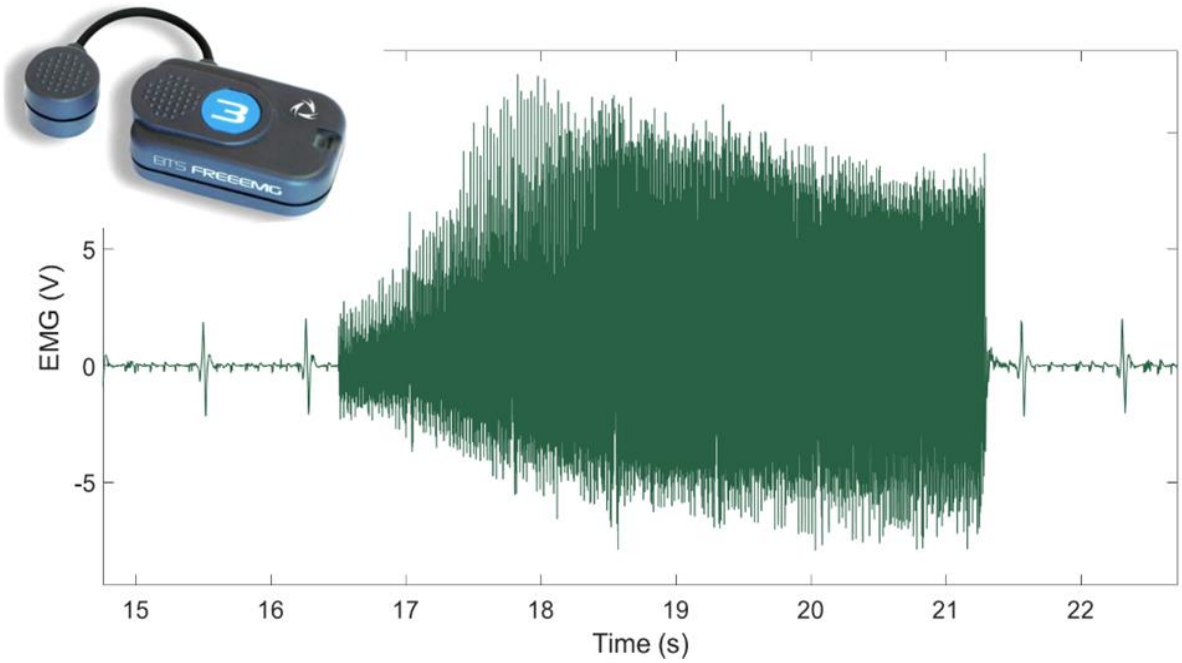

Figure 14: On the top left, a FREEMG bipolar probe. The sensor was placed on the neck in correspondence to the cable connecting the implantable pulse generator and the electrodes. TENS stimulator electrodes were placed near the EMG probe, to allow the electrical artifact to be fed into both EMG and subcortical recordings. The green track represents an example of a TENS artifact, as recorded by the EMG probe. The artifact lasted about 5 seconds and was clearly visible in the EMG data stream. The sharp drop-off of the artifact was used to synchronize biomechanical and subcortical signals. Please refer to paragraph "LFP preprocessing" for further information on the synchronization process.
Abbreviations: EMG: electromyographic; TENS: transcutaneous electrical nerve stimulator.

6.4. Experimental sessions – data analysis

6.4.1. Gait initiation: WP-1, WP-2, WP-3

Anticipatory Postural Adjustments

The kinematic resultants of APA at GI are easily detectable by means of dynamometric force plates. Specifically, stereotypical movements of the CoP, that can be evaluated as an indicator of effective APA, can be well captured by force plates. At UKW, to obtain the net CoP track from the signals recorded by the two force plates, I applied a weighted mean of the left and right CoP as follows:

$$CoP = \frac{CoP_L \times V_L + CoP_R \times V_R}{V_L + V_R}$$

where CoP_L and COP_R are the CoP pathways under the left and right foot, respectively, and V_R and V_L are the vertical components of left and right GRF, respectively [78].

I then continued the analysis to identify the Imbalance (IMB) and Unloading (UNL) (**Figure 15**). The IMB corresponds to the first backward and Medio-Lateral (ML) displacement of the CoP towards the swing (SW) foot and is the most relevant phase of APA as it is the only phase governed by *feedforward* motor control [38]. I defined the beginning of the IMB phase (APA onset, [AO]) as the first frame in which the CoP started travelling consistently backward and towards the SW foot [38], [56], [90]. The end of the IMB phase corresponded approximately to the heel off of the SW foot (HO_{SW}), and it was easily identifiable as the most ML displacement of the CoP towards the SW limb [38], [90]. The UNL phase was defined as the interval between the HO_{SW} and the subsequent toe off of the SW foot (TO_{SW}), i.e. the time when the CoP shifted from mainly lateral to principally anterior motion under the stance (ST) foot [38], [90].

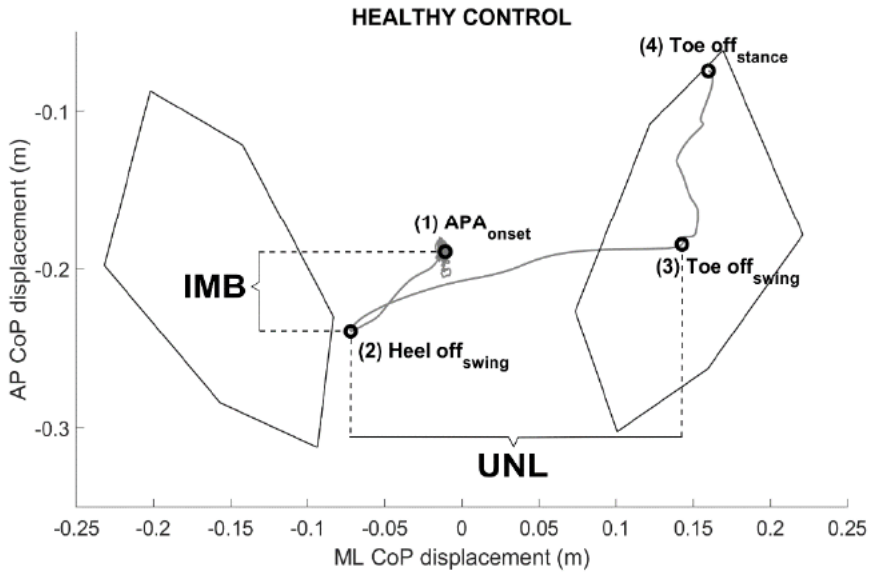

Figure 15: CoP pathway during a GI trial of a healthy subject. The trial was executed with the left foot as the swing limb. IMB and UNL phases were identified from the APA onset to the heel ff of the swing foot and from the heel off of the swing foot to the toe off of the swing foot, respectively. Numbers indicate the event sequence.
Abbreviations: AP: anterior-posterior; CoP: Centre of Pressure; GI: gait initiation; IMB: imbalance phase; ML: medio-lateral; UNL: unloading phase.

The identification of APA landmarks (AO, HO_{SW}, TO_{SW}) followed a mixed automatic/manual approach. The automatic approach showed satisfactory results with healthy controls and PD patients with mildly altered APA. It was less reliable when applied to severe parkinsonian patients (e.g., patients with FoG, WP-2) or patients with PSP (WP-3). The APA of these subjects were severely altered and variable across trials and patients (**Figure 16**), with respect to the expected pattern typical of healthy controls (**Figure 15**). In these cases, the algorithm for automatic identification was prone to frequent errors and the identification of APA was performed mainly by means of visual inspection of the CoP track.

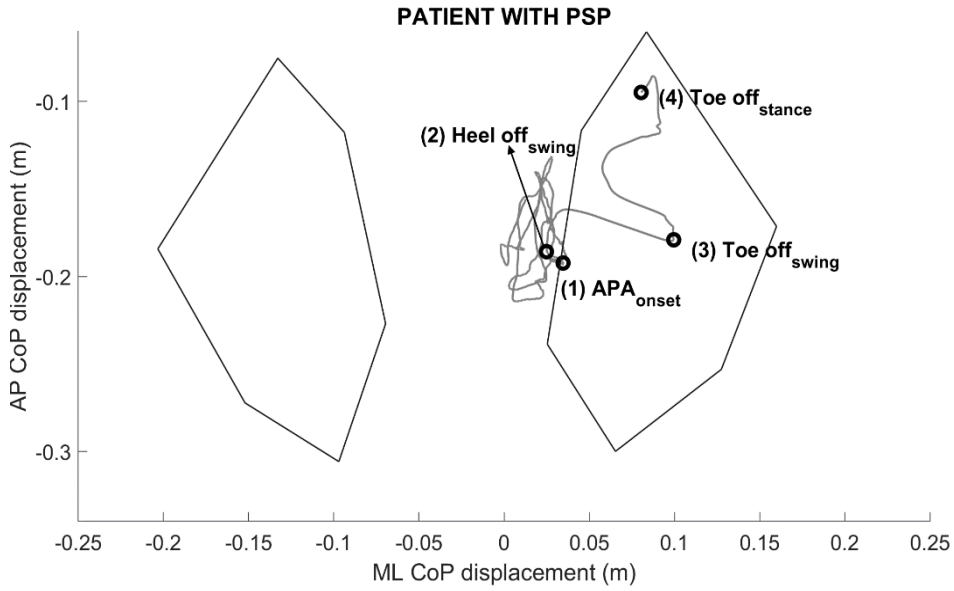

Figure 16: Representative CoP displacement (grey track) during APA at GI of a PSP patient. The trial was executed with the left foot as swing limb. APA showed severe alterations. In particular, IMB displacement is greatly reduced, and the CoP moves forward rather than backward during this phase. Numbers indicate the event sequence.
Abbreviations: AO: APA onset; AP: anterior-posterior; CoP: Centre of Pressure; GI: gait initiation; ML: medio-lateral.

For APA instant detection and phase evaluation, I developed a graphical user interface (GUI) in Matlab ambient (R2018b, The Mathworks Inc., USA) which allowed the visualization of CoP displacements in the ML and AP directions over time (stabilogram) and the CoP pathway in the transversal plane (statokinesigram, see **Figure 17**). The GUI was provided with functions for filtering the CoP tracks. To avoid any distortion in the phase of the signal, I opted for a zero-phase Butterworth low pass filter of the 3rd order. The GUI allowed visualization of the effect of two different filters with a cut-off frequency of 60 and 30Hz, respectively. The user could plot the filtered tracks together with the raw data and compare the action of the filters. After a preliminary analysis on the subjects recruited for WP-1, in agreement with previous works, I verified that the 30Hz cut-off was the best option to effectively remove the noise from the signal for APA phase detection, without introducing distortions in the original track [33], [38]. After the pre-processing phase, the user could opt for either the automatic or manual identification of each APA instant (i.e., AO, HO_{SW}, TO_{SW}). During the automatic detection procedure, the GUI suggested to the user candidate reference points to be checked, confirmed, or changed.

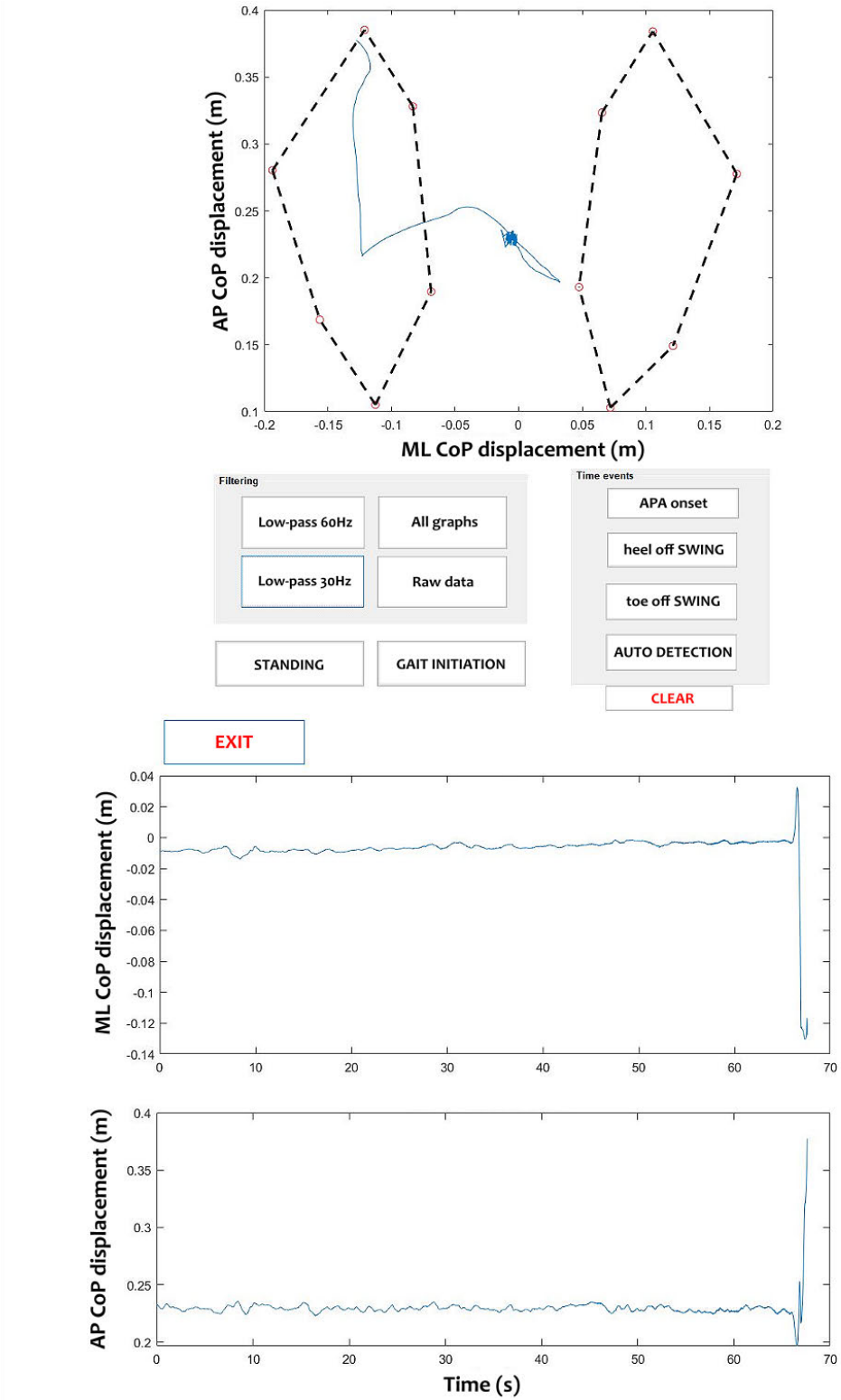

Figure 17: Graphical user interface for APA instants identification. The Filtering sections contains all the buttons needed to apply and visualize various filtering to the CoP tracks. The Time series section is dedicated to the identification of APA instants, providing for a manual or automatic detection procedure. When all instants are identified, it is possible to extract the main APA features (e.g., phases duration, CoP displacement and velocity etc) and also the main posturography measurements related to the standing (e.g., confidence ellipse) preceding the APA onset, thanks to the buttons GAITINI (i.e., abbreviation for "gait initiation") and STANDING, respectively.
Abbreviations: AP: anterior-posterior; CoP: Centre of Pressure; GAITINI: gait initiation; ML: medio-lateral.

The automatic selection of these points was based on an iterative procedure composed by the following steps:

- **Identification of a reference point related to the end of the standing phase (ST_{END}).** As the time of the vocal start signal was not recorded, ST_{END} was considered as the time corresponding to 0.5 s before the HO_{SW}. HO_{SW} was defined by means of kinematic variables (see below). I chose this specific interval as the average value of the IMB phase in the subjects recruited for project WP-1 was of 0.4 seconds. This value was estimated by means of a preliminary manual identification of the APA instants, and confirmed by the results of WP-1, Wp-2 and WP-3 [38], [75].
- **Definition of the confidence ellipse during the standing phase.** The confidence ellipse was drawn as the ellipse containing 95% of the points of the CoP track from the start of the recordings till the ST_{END} reference instant (**Figure 18**).
- **Identification of CoP points outside of the confidence ellipse.** In a half-second time window, starting from the ST_{END}, all points outside the reference ellipse were identified. As postural oscillations may cause the CoP to shortly exit the ellipse before the effective APA program, I considered only the portions of CoP track that never re-entered the ellipse until the HO_{SW}. The first point outside the confidence ellipse was used as a reference point to look for the AO in the preceding time-window (**Figure 18**).

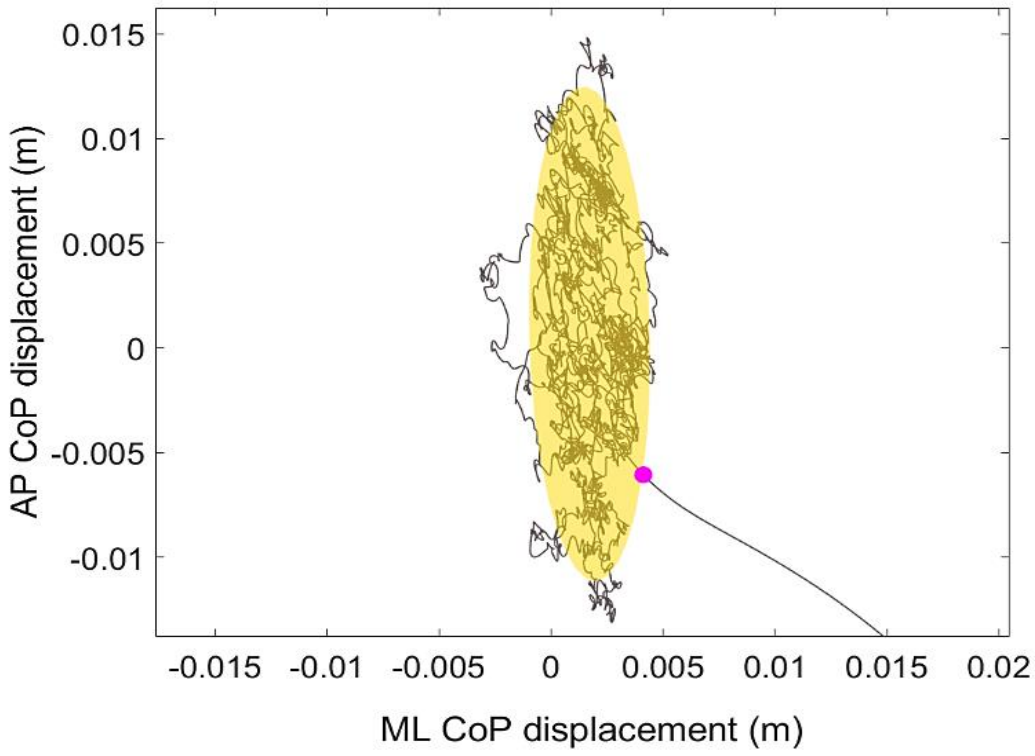

Figure 18: CoP trajectory (grey track) in the horizontal plane during the standing phase of a GI trial of a patient with PD. The yellow shape represents the confidence ellipse including the 95% of CoP points during the standing phase. The pink dot is the first point outside the confidence ellipse after the end of the standing phase, indicating that APA started shortly before.
Abbreviations: AP: anterior-posterior; APA: anticipatory postural adjustments; CoP: Centre of Pressure; GI: gait initiation; ML: medio-lateral; PD: Parkinson's disease.

- **CoP threshold velocity definition.** CoP velocity was calculated during the standing window, separately for the ML and AP directions. For each directional velocity, two thresholds were defined as the mean plus the standard deviation of the recorded velocity during the standing window. For ML direction, the threshold was considered as both positive and negative to account for trials executed with the left or the right foot.

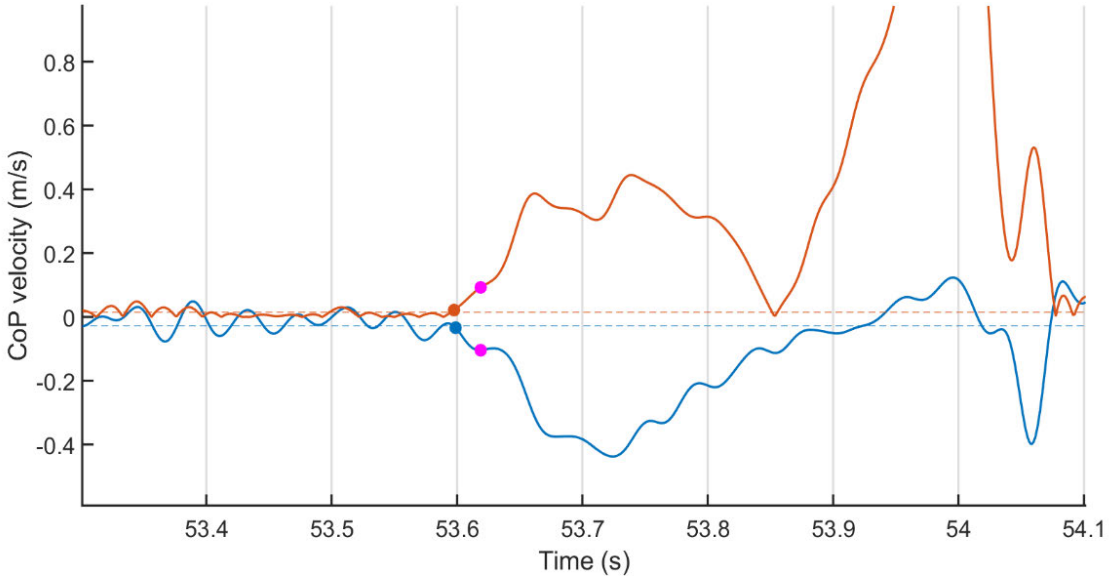

Figure 19: Anterior-posterior (blue solid line) and medio-lateral (red solid line) CoP velocity over time during APA performed by a PD patient. Two thresholds were defined during the standing phase separately for the anterior-posterior and medio-lateral velocity (dashed blue and red lines, respectively). Pink dots represent CoP velocity along the two directions at the time of exit of the CoP from the confidence ellipse (see Figure 18). Blue and red dots show the first points overcoming the pre-defined thresholds before the exit of the CoP from the confidence ellipse. AO was defined as the time instant corresponding to the first threshold passing (in this case, the red dot).
Abbreviations: AP: anterior-posterior; APA: anticipatory postural adjustments; CoP: Centre of Pressure; GI: gait initiation; ML: medio-lateral; PD: Parkinson's disease

- **AO identification**. The beginning of the APA was defined as the first observation before the point outside of the confidence ellipse (previously defined) in which the CoP velocity overcame the threshold in ML or AP direction (**Figure 19**).
- **HO_{SW} and TO_{SW} identification.** The end of IMB and UNL phase were identified as the first and second peaks of the absolute ML displacement of the CoP after the AO instant (**Figure 20**).

Also in the case of automatic detection, the GUI allowed the revision and change of the proposed instants. All tracks were visually inspected to correct eventual mistakes.

After the identification of the APA instants, the GUI allowed the calculation and saving of the main CoP features characterizing IMB and UNL phases in terms of duration, ML and AP displacement, and velocity. **Table 2** shows the formulas used for the calculation of the measurements of interest.

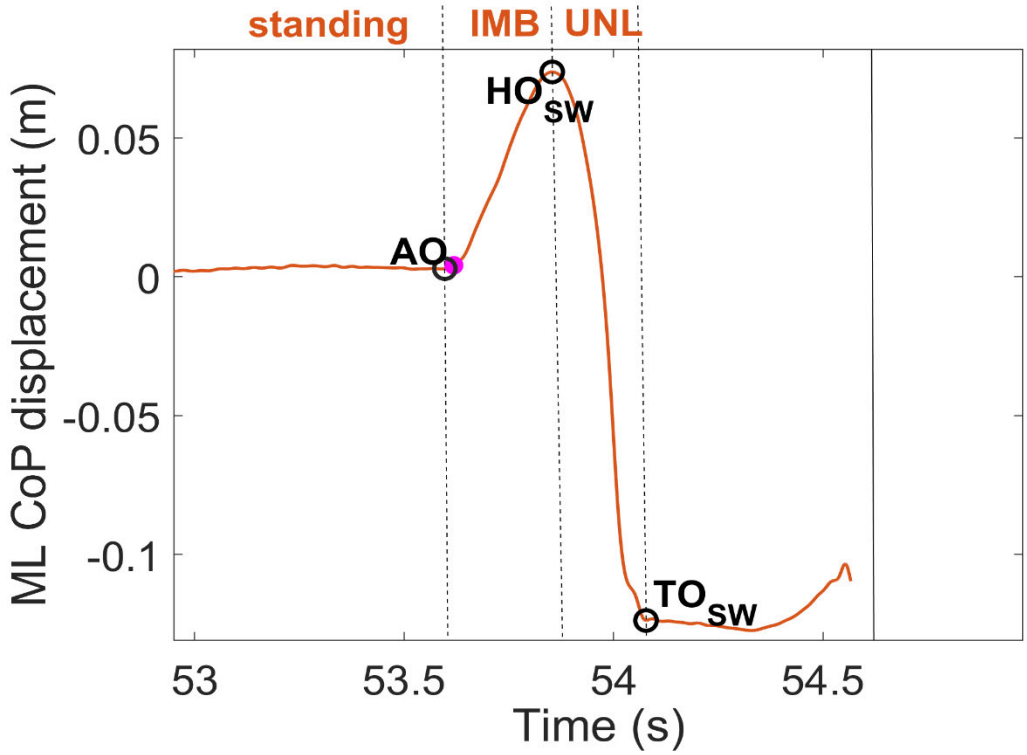

Figure 20: Example of ML CoP displacement over time during a GI trial of a patient with PD. After the identification of the AO instant, the HOsw and the TOsw were identified as the peaks of the absolute medio-lateral CoP displacement after AO. The pink dot represents the exit of the CoP from the confidence ellipse. The three instants of APA allowed the identification of the standing, IMB and UNL phases.
Abbreviations: AO: APA onset; AP: anterior-posterior; APA: anticipatory postural adjustments; CoP: Centre of Pressure; GI: gait initiation; HOSW: heel off of the swing heel; IMB: imbalance phase; ML: medio-lateral; PD: Parkinson's disease; TOSW: toe off of the swing foot; UNL: unloading phase.

Measurement	**Calculation in Matlab**	
	IMBALANCE	**UNLOADING**
Duration (s)	time (HO_{SW}) - time (AO)	time (TO_{SW}) - time (HO_{SW})
CoP displacement (mm)	CoP (HO_{SW}) - CoP (AO)	CoP (TO_{SW}) - CoP (HO_{SW})
CoP average velocity (mm/s)	abs (CoP (HO_{SW}) - CoP (AO)) / (time (HO_{SW}) - time (AO))	abs (CoP (TO_{SW}) - CoP (HO_{SW})) / (time (TO_{SW}) - time (HO_{SW}))
CoP maximal velocity (mm/s)	nanmax (abs (gradient (CoP (AO:HO_{SW}), 1/fs))	nanmax (abs (gradient (CoP (HO_{SW}:TO_{SW}), 1/fs))

Table 2: Formulas for the calculation of the main CoP measurements during APA at GI. All displacement and velocity measurements were calculated for both ML and AP directions.
Abbreviations: AO: APA onset; CoP: Centre of Pressure position; fs: sampling frequency; GI: gait initiation; HOSW: heel off of the swing limb; TOSW: toe off of the swing limb.

Kinematic measurements

The kinematics served to define the main features of the CoM at the relevant points of the APA dynamics. The final aim of APA is to accelerate the CoM forward while effectively controlling for balance and posture. The CoM displacement, velocity, and acceleration at the end of the various APA phases can be therefore, considered as indexes of the effectiveness of APA programming and execution, and postural control during the GI task [18], [38], [56], [200].

First, marker tracks were labelled according to the LAMB protocol and corrected for small reconstruction mistakes with the software SMART Tracker (BTS, Milano, Italy). The cleaned tracks were then interpolated with piecewise cubic spline interpolation and filtered with a 5th-order lowpass Butterworth filter (cut off frequency: 10 Hz) [38], [200] .

For the calculation of the CoM, the body was modelled with 16 body segments: the head, the arms, the forearms, the hands, the chest, the abdomen, the pelvis, the thighs, the shanks and the feet. The position of each segmental CoM as well as the mass of each body segment were obtained from the anthropometric tables and regression equations provided by Zatsiorsky and Seluyanov [388]. The position of body CoM was calculated as the weighted average of the position of each body segment, as follows:

$$CoM = \frac{\sum_j^{16} ScoM_j \times m_j}{M}$$

where *SCoM* and *m* are the displacement and mass of the j-th segmental Center of Mass, respectively, and *M* is the total body mass of the subject.

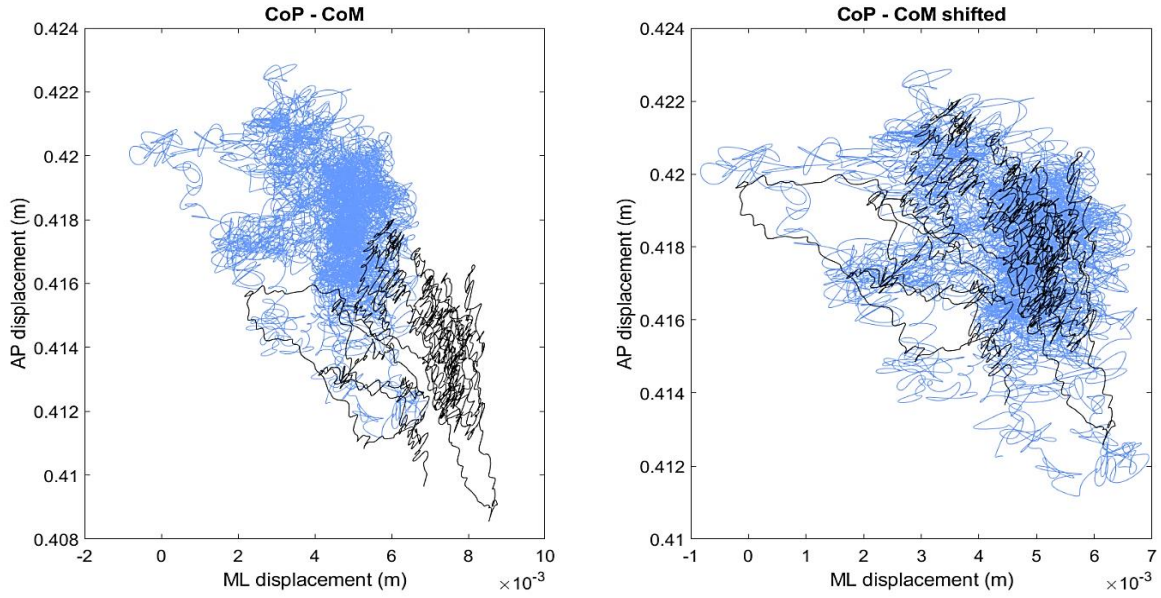

Figure 21: On the left, the raw trajectories of CoP (blue line) and CoM (black line) displacement in the transversal plane during the standing phase of a GI trial executed by one healthy subject. Of note, the average value of the two trajectories is different but the oscillation of the two tracks is similar. On the right, the difference between the average values of the two tracks was subtracted to the CoM displacement to obtain a superimposition of the two signals.
Abbreviations: AP: anterior-posterior; CoM: Centre of Mass; CoP: Centre of Pressure; GI: gait initiation; ML: medio-lateral.

The position of the CoM in respect to CoP and the CoM velocity and acceleration, were evaluated at the relevant points of APA (HO_{SW} and TO_{SW}) and at the toe off of the stance limb (TO_{ST}). For this step of the analysis only, CoP track was downsampled at the frequency of the kinematics, for sake of comparison between the two tracks. Of note, since the calculation of the position of the CoM is based on a model of the human body, its average value over time might be different from the real one, due to imprecise marker placement, mass distribution, and/or subject-specific features. In agreement with the inverted pendulum model for human posture [78], it can be assumed that during quiet standing the average value of the CoP and CoM position in the transversal plane are equal, since the subject is still. Based on this assumption, I calculated the average value of CoP and CoM displacement in the transversal plane during the standing phase before AO. The shift between the two signals was then subtracted from the CoM trajectory to superimpose the two tracks (**Figure 21**) and grant a correct estimation of the CoM position.

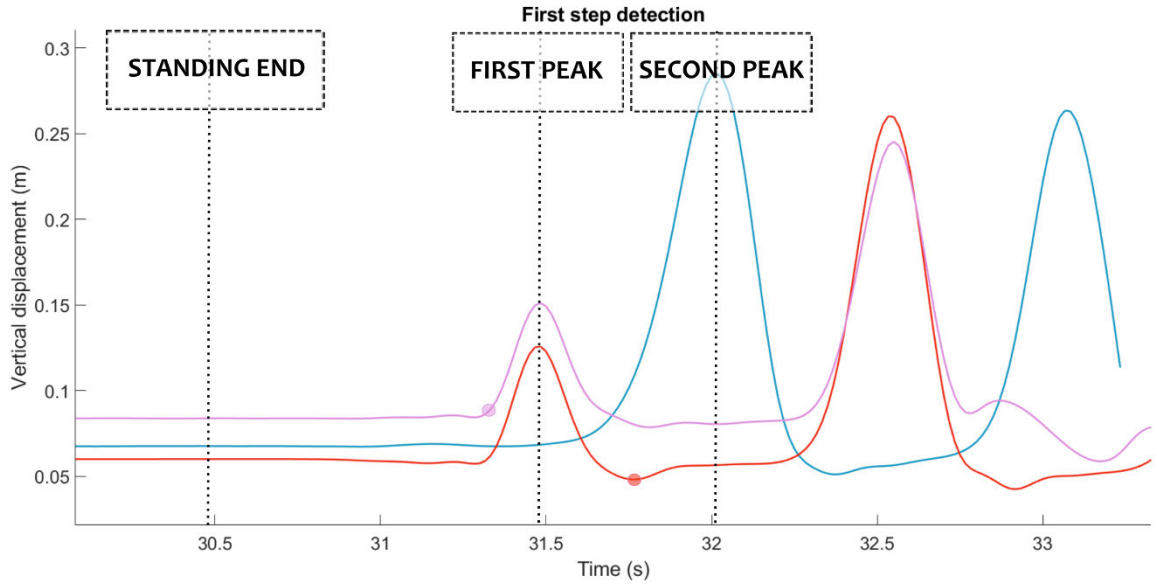

Figure 22: First step identification of a GI trial of a healthy subject. The figure shows the vertical displacement of the markers placed on the left lateral malleolus (pink line), left heel (red line) and right heel (blue line) during a GI trial (timeline cut from 30 seconds till the exit of the subject out of the calibration volume). The swing foot in the examined trial is the left. Pink dot: HOSW; red dot: heel contact of the first step (HCSW). Each step is characterized by the typical bell-shaped curve, which describes the swing phase of the considered step. Of note, foot clearance during the first step is considerably lower with respect to the subsequent steps.
Abbreviations: GI: gait initiation; HCSW: heel contact of the swing foot; HOSW: heel off of the swing foot.

I then identified the key features of the first step executed by the subject by means of the markers placed on the feet (**Figure 22**). Effective first step at GI is needed to counteract the imbalance caused by the voluntary CoP backwards displacement [78]. First, I detected all peaks above the 25% of the maximum value of the vertical displacement of the markers placed on the lateral malleoli. The first detected peak allowed the identification of the swing foot. Heel off of the swing foot was detected by imposing a threshold equal to the mean plus one standard deviation of the value recorded during the standing phase, from the beginning of the acquisition till one second before the first peak. The heel contact of the swing foot was detected on the track of the marker placed on the heel of the same foot. The heel contact was defined as the minimum between first

and second vertical peaks. First step was defined as the interval between the identified heel off and heel contact. It was characterized in terms of length and average and maximum velocity. The procedure for the identification of the first step was included in the previously described GUI. The user was asked to check and correct the identified instants if needed. Last, CoP position, in respect to the line connecting the markers placed on the heel, was extracted at HO_{SW} and TO_{SW}, to evaluate the position of the CoM in respect to the posterior margin of the BoS.

The second part of the kinematic analysis was dedicated to the definition and calculation of the BoS and AM parameters to assess their influence on the GI measurements. of note, the choice of the BoS was left to the subject to avoid any alterations of his/her preferred postural strategy. For each GI trial, I computed the main features of the BoS, similarly to what is shown by Rocchi and colleagues [32]. The BoS was characterized in terms of (**Figure 23**):

- **BoS width (BoSW, cm)**: the distance between the ankle articular centers, estimated as the middle points between the lateral and medial malleoli.
- **BoS area (BoSA, cm²)**: the area internal to the boundaries connecting the markers placed on the feet.
- **The opening angle of the BoS (β, deg)**: the sum of left and right extra-rotation angles (βL and βR, respectively), computed with respect to the horizontal line of the reference system of the laboratory.
- **The difference between feet extra-rotation angles (βΔ, deg):** the absolute value of the difference between βL and βR.
- **Foot alignment (FA, cm):** the AP distance between the markers placed on the heels.

The *anatomic calibration* trial preceding GI evaluation served for the calculation of the main AM. For all subjects I computed the following measurements:

- **Body height (BH, cm):** the distance between the marker placed on the seventh cervical vertebra and the floor increased by 20%.
- **Limb length (LL, cm):** the distance between the marker placed on the trochanters and on the lateral malleolus.
- **Foot length (FL, cm):** the distance between the markers placed on the heel and the hallux.
- **Inter-ASIS distance (IAD, cm):** the distance between the markers placed on the left and right ASIS.
- **Body mass (BM, Kg):** the average value of the vertical GRF during the *anatomic calibration*.
- **Body mass Index (BMI, Kg/cm²):** the ratio between the BM and the squared BH.

This set of parameters served for estimating and removing the influence of the AM on the outcome variables of GI. **Table 3** lists and describes the extracted AM, BoS and GI measurements and their abbreviations.

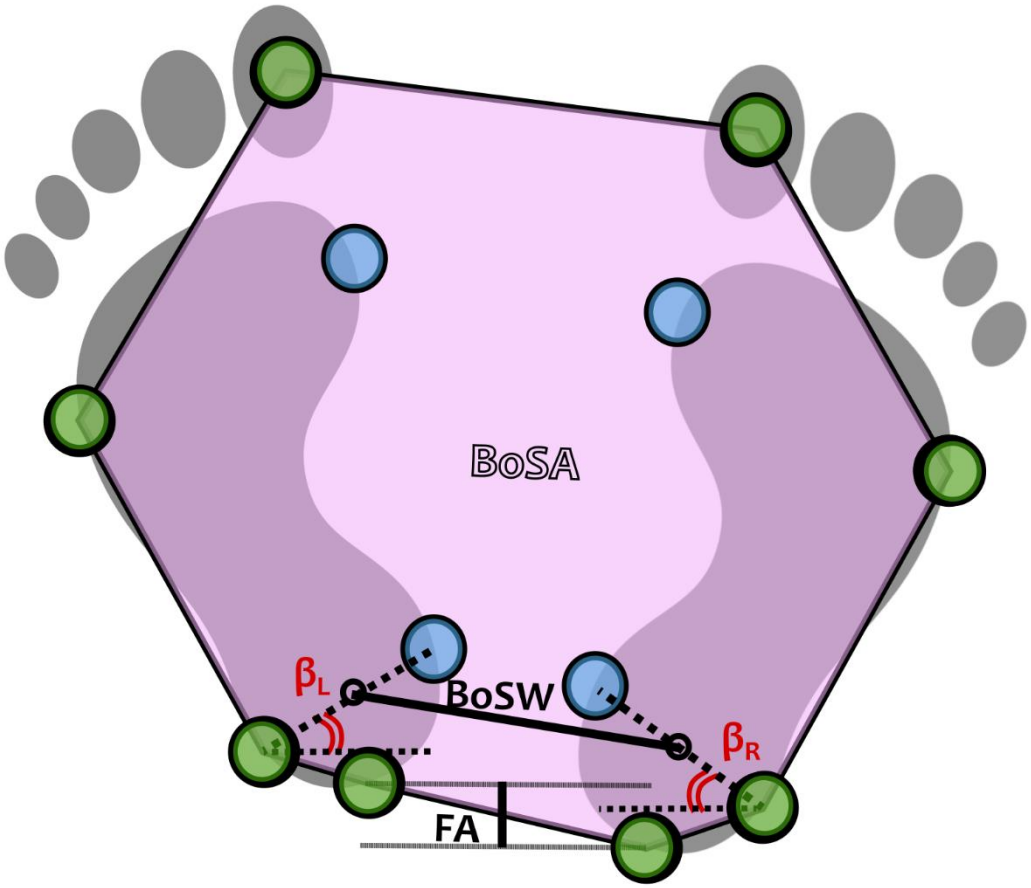

Figure 23: BoS parameters. Green dots represent the markers used during GI trials, blue dots are the additional markers placed only during the anatomic calibration trial and exploited to obtain BoS parameters and the anthropometric measurements (AM). BoSW was computed as the distance between the two ankle joint centres, considered for each foot as the middle points between the two malleoli. The BoSA was calculated as the pink area described by the line connecting the markers placed on the feet (black line). β_L and β_R are the left and right feet extra-rotation angles, respectively, computed for each foot as the angle between the axis passing through the malleoli and the horizontal axis of the reference system of the laboratory. The BoS opening angle (βΔ) was obtained as the sum of these two angles. To account for eventual asymmetric feet placement, the difference between the two extra-rotation angles (βΔ) as well as the anterior-posterior distance between the markers placed on the two heels (FA) were considered.
Abbreviations: BoS; Base of Support; BoSA; Base of Support Area; BoSW: Base of Support width; FA: foot alignment; GI: gait initiation; βL and βR: left and right foot extra-rotation angles.

	Abbreviation	Description	Decomposition
Anthropometric Measurements (AM)	BH	Body Height (cm)	
	IAD	Inter Anterior Superior Iliac Spine Distance (cm)	
	LL	Limb Length (cm)	
	FL	Foot Length (cm)	
	BM	Body Mass (kg)	
	BMI	Body Mass Index (kg/cm^2)	
Base of Support (BoS)	BA	Base of Support Area (cm^2)	
	BoSW	Base of Support Width (cm)	
	FA	Foot Alignment (cm)	
	β_Δ	Difference between feet extra-rotation angles (°)	
	β	BoS opening angle (°)	
Imbalance phase (IMB)	AOCoPD	CoP distance from the line passing through the markers on the heels at APA onset (%FL)	AP
	IMBT	Imbalance duration (s)	
	IMBD	Imbalance CoP displacement (mm)	AP, ML
	IMBAV	Imbalance CoP average velocity (mm/s)	AP, ML
	IMBMV	Imbalance CoP maximal velocity (mm/s)	AP, ML
	IMBCoMV	CoM velocity at imbalance end (m/s)	
	IMBCoMA	CoM acceleration at imbalance end (m/s^2)	
	IMBCoPCoM	CoP-CoM distance at imbalance end (m)	
	IMBSLOPE	Orientation of CoP-CoM vector with respect to the progression line at imbalance end (deg)	
	HOCoPD	CoP distance from the line passing through the markers on the heels at swing heel off (%FL)	AP
Unloading phase (UNL)	UNLT	Unloading duration (s)	
	UNLD	Unloading CoP displacement (mm)	AP, ML
	UNLAV	Unloading CoP average velocity (mm/s)	AP, ML
	UNLMV	Unloading CoP maximal velocity (mm/s)	AP, ML
	UNLCoMV	CoM velocity at unloading end (m/s)	
	UNLCoMA	CoM acceleration at unloading end (m/s^2)	
	UNLCoPCoM	CoP-CoM distance at unloading end (m)	
	UNLSLOPE	Slope of CoP-CoM vector at unloading end (deg)	
	TOCoPD	CoP distance from the line passing through the markers on the heels at the swing foot toe off (%FL)	AP
Stepping phase	TOCoMV	CoM velocity at stance foot toe off (m/s)	
	TOCoMA	CoM acceleration at stance foot toe off (m/s^2)	
	SL	First step length (m)	
	SAV	First step average velocity (m/s)	
	SMV	First step maximal velocity (m/s)	

Table 3: List of the extracted AM, BoS and GI measurements. GI measurements were subdivided into imbalance, unloading, and stepping phase.
Abbreviations: AM: anthropometric measurements; AP: anterior-posterior; BoS: Base of Support; CoP: Centre of Pressure; CoM: Centre of Mass; GI: gait initation; IMB: imbalance; ML: medio-lateral; UNL: unloading.

Partial correlation analysis

In each study, I considered the AM and the BoS specific to each subject. AM and BoS are of great interest when studying GI, since they may substantially affect the outcome variables of the performance, playing a confounding effect. It is important to notice that matching the recruited groups for AM is essential but not sufficient to avoid a possible influence of these parameters on the outcome measurements. In this regard, a normalization procedure is far more effective [389]. Surprisingly, despite BoS' proven role in affecting GI measurements, [32], its influence has been neglected in previous studies on the topic.

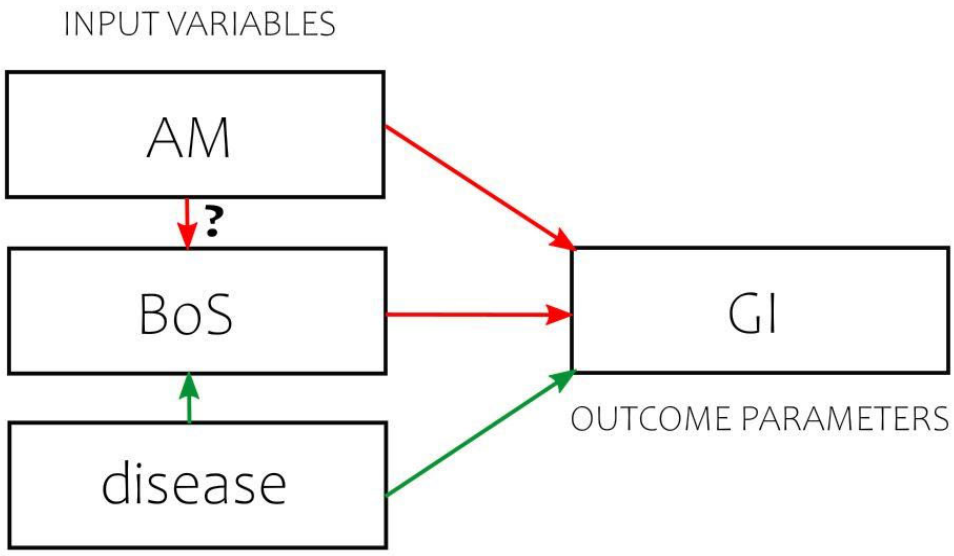

Figure 24: Relationship between the set of parameters taken into consideration in the assessment of GI. The aim of each WP was to characterize how the disease/symptoms affect the GI. AM and BoS might play as confounding factors on the outcome measurements. The relation between AM and BoS in physiological and pathological conditions are still unknown and, to some extend unforeseeable. Green arrows: connections of interest between parameters. Red arrows: confounding influences across measurements. Abbreviations: AM: Anthropometric Measurements; BoS: Base of Support; GI: Gait Initiation.

First essential step of all WP was to assess the relation between the AM and BoS variables and the GI measurements (**Figure 24**). To investigate the influence of AM and BoS on the GI measurements, I applied a partial correlation analysis able to disentangle the specific effect of the AM and BoS parameters on the set of variables of interest. Given three sets of variables X, Y, and Z, where Z is the outcome set of variables (i.e., the GI measurements) and X and Y are the two confounding sets of variables (i.e., the AM and BoS parameters), partial correlation allows computation of the correlation between X and Z, controlling for the influence of Y. More specifically, this data analysis technique calculates separately the linear regression between X and Z and between Y and Z. The residuals are compiled and the correlations between the residuals of the two models are computed. The following formula expresses the calculation of the sample partial correlation coefficient $\widehat{\rho_{XZ\cdot Y}}$ between X and Z, accounting for the influence of a third set of variables Y:

$$\widehat{\rho_{XZ\cdot Y}} = \frac{N \sum_{i=1}^{N} eX_i \, eZ_i}{\sqrt{N \sum_{i=1}^{N} eX_i} \sqrt{N \sum_{i=1}^{N} eZ_i}}$$

where eX_i and eZ_i are the residuals of the linear regression models between *X* and *Y* and between *Z* and *Y*, respectively. The procedure can be repeated to calculate the partial correlation coefficient between *Y* and *Z* accounting for the influence of *X*.

I calculated the partial correlation coefficient between the GI and BoS measurements, correcting for the AM, and between the GI measurements and AM, correcting for the BoS measurements. I used the function *partialcorr* of Matlab and considered a p-value of 0.01 and a partial correlation coefficient equal or higher to 0.5 as thresholds for significant correlation. For each WP, the analysis was applied separately for each recruited group. Of note, to allow the comparison across groups after the application of the partial correlation analysis and the further normalization procedure for the influence of the AM, I applied the partial correlation analysis on the z-score values. I calculated the z-score by subtracting from each observation the average value and dividing by the standard deviation of the variables computed internally for each group.

The partial correlation coefficient identified the GI variables affected by the BoS, which I excluded from further analyses. I opted for this conservative approach, as it is not possible to define what BoS parameters are affected by the disease *per se* (or by specific disease-related symptoms, e.g., rigidity) and voluntary (conscious or unconscious) compensatory attempts to increase postural stability and balance control. Indeed, PD patients were shown to adopt a (counterintuitive) narrow-based gait and were impaired in the modulation of their BoS [65], [382], [390]–[393]. Conversely, patients with PSP showed a broad BoS during standing [382].

All the GI measurements, solely dependent from the AM, were instead normalized. This procedure was possible as AM are not affected by patients' clinical condition, except for rare cases (e.g., camptocormia or weight loss due to severe dyskinesias) anyhow not present in the populations included in these studies. For the normalization, I adopted one of the approaches described by O'Malley [389], called by the author *decorrelation normalization* (**Figure 25**). Among the techniques presented in the paper, I chose the *decorrelation normalization* as it allows the removal of linear correlations between variables, the same type of relation identified with the partial correlation analysis. In particular this process allows each observation to be represented as its distance from the linear model fitting the data in the bidimensional space described by the two variables. This distance is, by definition, not correlated with both variables describing the space (**Figure 25**).

Given two variables x (i.e., AM measurement) and y (i.e., a GI measurement), resulted to be significantly correlated from the partial correlation analysis, the *decorrelation normalization* applies to each i-th observation as follows:

$$d_i = \frac{y_i - mx_i - c}{\sqrt{m^2 + 1}}$$

where x_i and y_i are the values of the variables *x* and *y* for the i-th observation, *m* and *c* are the angular coefficient and the intercept of the linear model (y=mx+c) fitting the data in the x-y plane, respectively, and d_i is the resulting distance between the i-th observation and the linear model fitting the data (**Figure 25**).

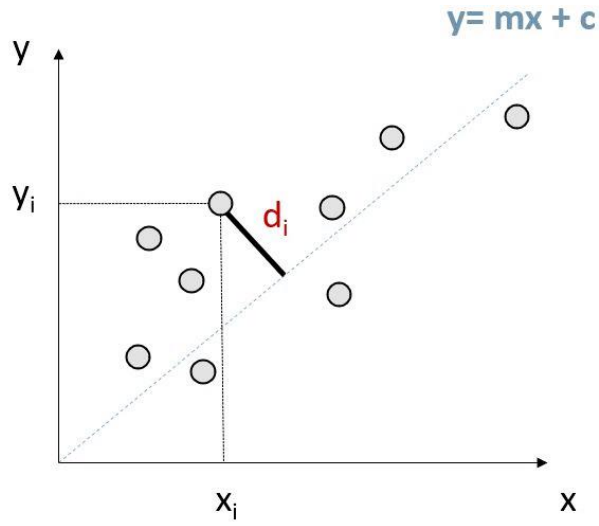

Figure 25: Example of the decorrelation normalization procedure. Gray points depict the observations in the plane described by two variables x and y, linearly correlated to each other. The dashed blue line represents the linear model fitting the data. In this case, the constant c of the model is equal to zero. To decorrelate the outcome variable y, each point can be described as its distance di from the line fitting the data. This distance is not correlated with the two variables generating the data distribution.

The decorrelation normalization has the great advantage of being a simple technique to apply and eliminate any linear correlations across the variables. On the other hand, the resulting variables have an unclear unit of measurement and data may be difficult to interpret. For this reason, the statistical analysis across groups was performed on the decorrelated data, but the biomechanical data in tables are presented as the mean and standard deviation of the original distribution.

6.4.2. Standing and walking: WP-4

Kinematic analysis

For WP-4, I first defined the standing and walking intervals. The standing was identified as the initial part of the trial, from 1 s after the synchronization artifact till 1 s before the first heel off. The video of each recording was checked to ensure the patient was standing still during this period. Trials in which patients were moving or talking were discarded from the analyses.

For the walking interval, I included only the portion at steady-state velocity to avoid any influence given by gait modulation (acceleration or deceleration phase). Specifically, after reconstructing and labeling the marker tracks for each trial, I interpolated with piecewise cubic spline interpolation and filtered with a 5th-order lowpass Butterworth filter (cut off frequency: 10 Hz) the data [38], [200]. I then computed the AP velocity of the marker placed on the middle point between the PSIS, which was previously shown to be a good approximation of the CoM [394]. The velocity was computed in the walking central portion, i.e., between one meter before and one after the middle point of the marker trajectory. I defined two thresholds as the average ± two times the standard deviation and excluded the parts in which the velocity exceeded these thresholds (i.e., acceleration and deceleration phase (**Figure 26**).

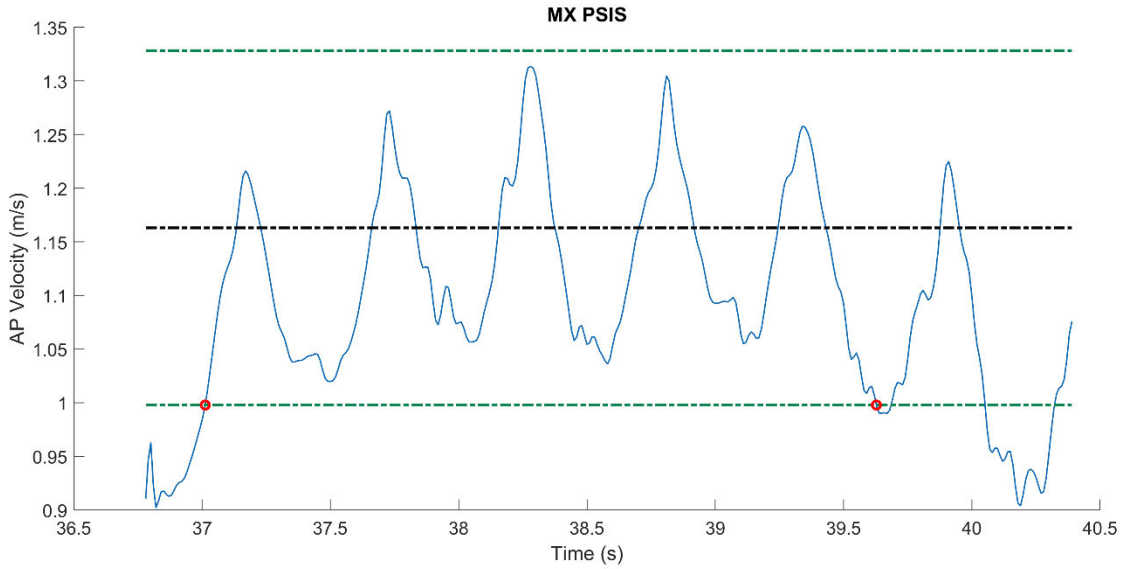

Figure 26: AP velocity of the marker placed on the middle point (MX) between the two PSIS of a patient (blue line) during a walking trial. The black line represents the average value computed in the central two meters of the walking pathway (in this specific trial covered by the patient between 38.15 and 39.01 s). I analysed the walking period at steady-state velocity, i.e., when the AP velocity was inside a range defined as the average value ± two times the standard deviation (green lines) computed in the central portion of the walking pathway. Red circles identify the beginning and end of gait at steady-state velocity.
Abbreviations: AP: anterior-posterior; PSIS: posterior superior iliac spines.

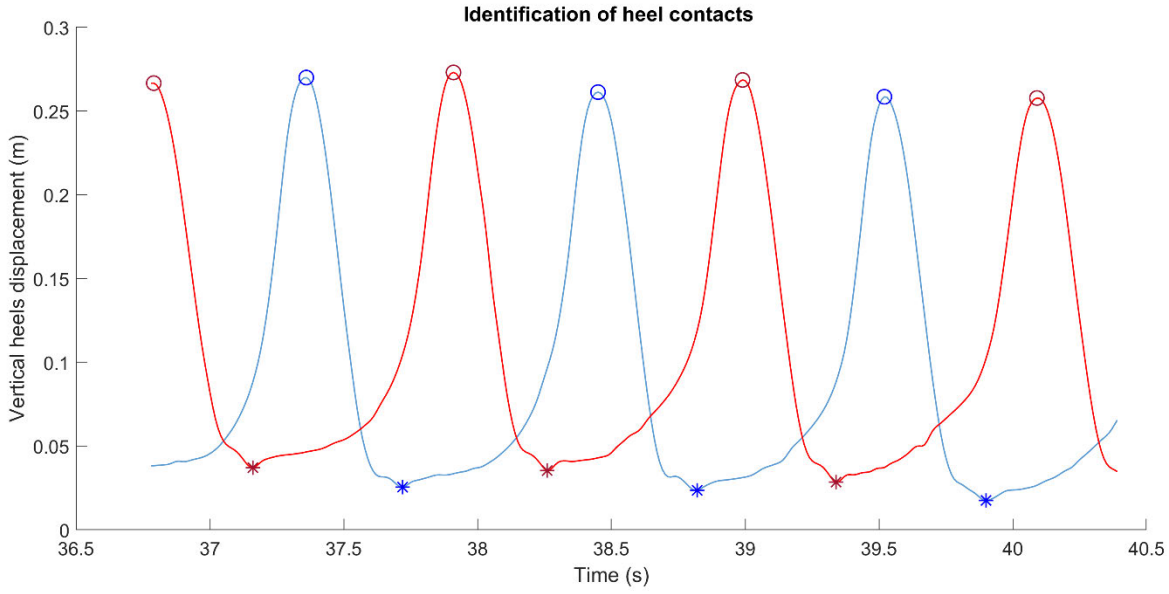

Figure 27: Trajectories of the markers placed on the left and right heels (red and blue lines, respectively). The peaks of the trajectories (red and blue circles) correspond to the maximum foot clearance during each swing phase and served to identify windows for the detection of left and right heel contacts (red and blue asterisks, respectively).

The main gait cycle events (i.e., heel contact and toe off instants) were identified by means of the markers placed bilaterally on the heel and the tip of the hallux. The heel contacts were detected as the local minima of the vertical trajectories of the markers on the heels in between subsequent peaks, correspondent to each swing phase (**Figure 27**). The toe off events were identified as the instant between two subsequent heel contacts in which the AP coordinate of the marker on the hallux advanced 1 cm with respect to the average value computed during the stance phase (**Figure 28**).

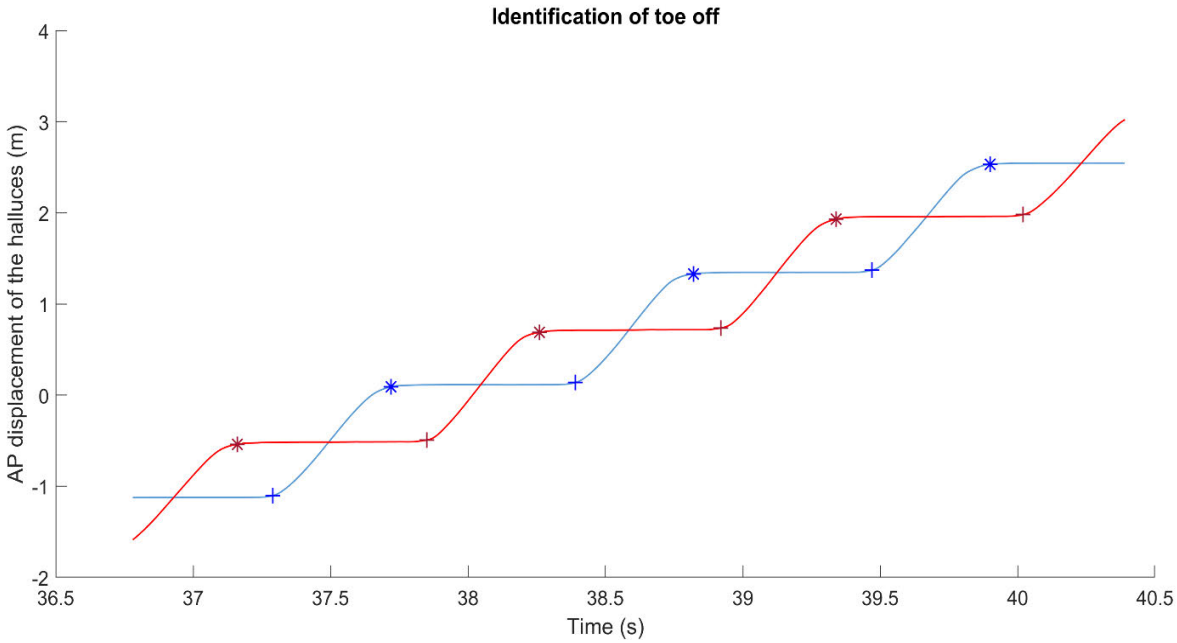

Figure 28: AP displacement of the markers placed on the left and right halluces (red and blue line, respectively). For each stance phase, the toe off of the left and right foot (red and clue crosses, respectively) was detected as the instant between two subsequent heel contacts (asterisks) in which the AP coordinate increased by 1 cm with respect to the average value computed over the preceding stance phase.
Abbreviations: AP: anterior-posterior.

LFP preprocessing

I implemented a pipeline for data synchronization in Matlab ambient (R2018b, The Mathworks Inc., USA) which included the following steps:

- **Automatic TENS artifacts identification**
  The pipeline defined the windows of interest in both the LFP and EMG recordings where the initial and final TENS artifacts were most likely to be present (**Figure 29**). The identification of the windows including the TENS artifact worked with a threshold-based criterion applied on the filtered signal around the TENS frequency (i.e., band-passed from 128 to 132Hz). The last peak of each detected TENS artifact was identified for further analyses and displayed to the user for a visual check. Only one LFP channel (the first) was considered for TENS identification. The pipeline allowed changing the LFP channel used for identification of the TENS artefacts and allowed for manual modification of the detected instants if necessary.

- **LFP sampling frequency calculation**
  After the definition of the TENS artefacts in LFP and EMG recordings, the inter-TENS distance was calculated for both data streams. The two TENS artifacts were fundamental for the computation of the correct sampling frequency of the Activa PC+S device, which could differ from the nominal value of 422Hz (mean: 421.94Hz, SD: 0.18Hz). I calculated the real sampling frequency as follows:

$$fs = \frac{\Delta TENS\ LFP}{\Delta TENS\ EMG} \times 422$$

where *ΔTENS LFP* and *ΔTENS EMG* were the distances in samples between the first and last TENS artifacts in the LFP and EMG data streams, respectively, and 422 is the nominal sampling frequency of the Activa PC+S.

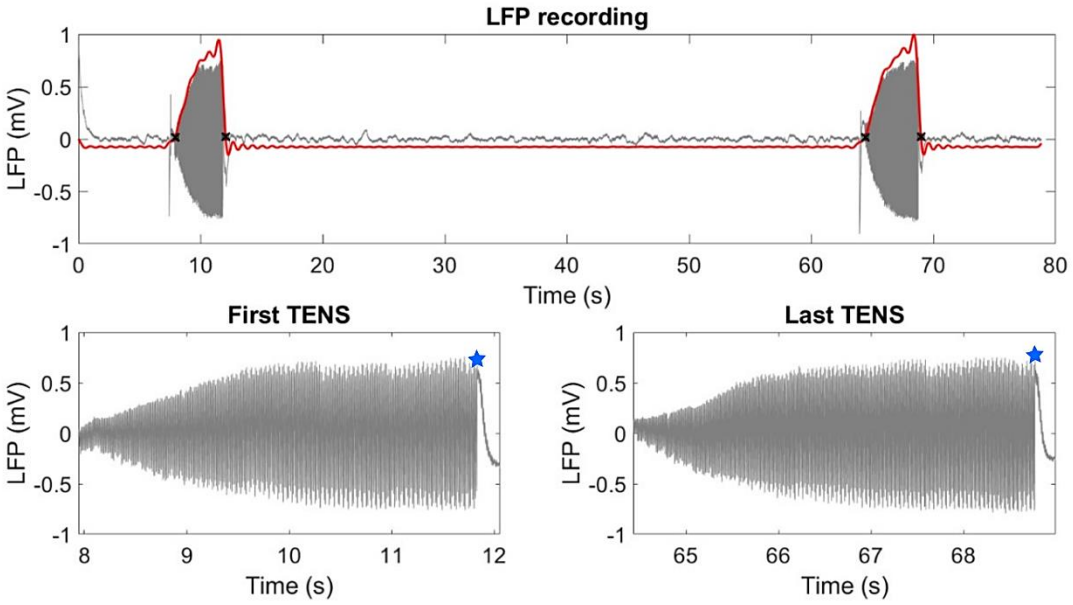

Figure 29: Automatic TENS artifact identification on an LFP recording. The grey line in the top panel shows the raw neural data recorded during a trial in the left STN of one PD patient. The red line displays the signal filtered around the frequency of the TENS (130 Hz) and the black crosses show the beginning and end points of the windows of interest, including each TENS artifact, identified with a threshold criterion. The bottom panels show a close-up of the first (on the left) and last (on the right) TENS artefact. For each identified TENS artifact, the pre-processing pipeline saved the last peak (blue stars) as reference point for further analysis (i.e., resampling and synchronization). Abbreviations: LFP: local field potentials; TENS: transcutaneous electrical nerve stimulator; PD: Parkinson's disease; STN: subthalamic nucleus.

- **Resampling at 400Hz**
  LFP recordings were resampled at 400Hz for further analyses as follows:

$$[p, q] = rat\left(\frac{400}{fs}\right)$$

$$LFP_{resampled} = resample(LFP, p, q)$$

where *rat* is a Matlab function computing the rational approximation of the ratio between the new sampling frequency (*400Hz*) and the actual LFP frequency (*fs*). The result was then used to sample down the *LFP* signal with the *resample* function by means of a linear approach.

- **LFP shift and alignment**

I kept the timeline of the biomechanical data as reference for the LFP timeline realignment, in order to easily analyze LFP signals based on kinematic events. For each trial I calculated the difference between the end of the first TENS artifact of LFP and EMG recordings and multiplied it for the new LFP sampling frequency (400Hz). LFP recordings were then shifted forward or backward for a number of samples equal to the inter-TENS distance. For shifting the signals forward, I added a vector of zeros, of length equal to the inter-TENS distance at the beginning of the signal. For the shift backwards, a number of samples equal to the inter-TENS distance was deleted from the beginning of the signal (**Figure 30**).

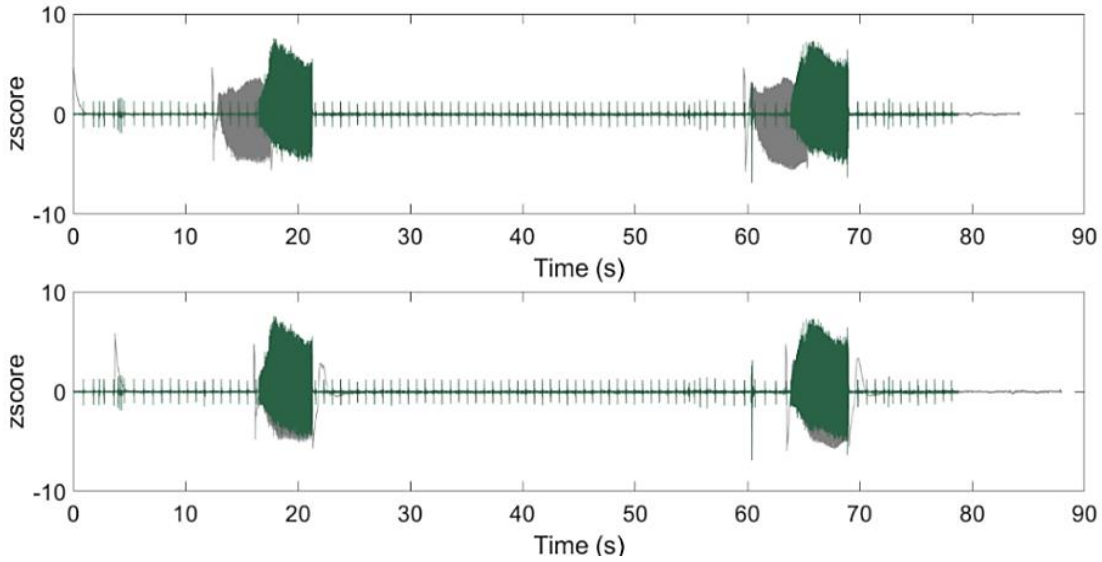

Figure 30: Synchronization process. In the top panel, the z-score of the EMG (green line) and resampled LFP (grey line) signals recorded during a trial of one PD patient are shown with their respective timelines. The TENS artifacts are not aligned across the two data streams, and they appear before in the timeline of the LFP data stream. The LFP signal was therefore shifted forward a number of samples equal to the inter-TENS distance across the two signals (bottom panel).
Abbreviations: EMG: electromyography; LFP: local field potentials; TENS: transcutaneous electrical nerve stimulator; PD: Parkinson's disease.

- **Signal cut**

To exclude any rebound of the LFP signals due to the TENS artifact from the analysis, I considered only the LFP portion between 2 s after the end of the first TENS till 2 s before the second TENS.

- **Artifact removal**
  After the synchronization and resample processes, I visually inspected the data. The LFP recordings were affected by three types of artifacts:

  - The first and most relevant artifact was related to the cardiac activity. This was present especially in the most ventral contacts [284], [285]. The main issue of the cardiac artifact was related to its frequency content, which extends from very low frequency to up to 40Hz [285], thus interfering with LFP recordings in alpha and beta bands. The signal to noise ratio of the heart activity was also quite variable, thus making the cardiac artifact either clearly visible or almost completely hidden by the neural activity across subjects and trials. To remove this artifact, for each trial and subject I identified the location of the QRS peaks, and the mean and standard deviation of heart rate based on the EMG recording of the probe positioned on the neck (**Figure 31**).

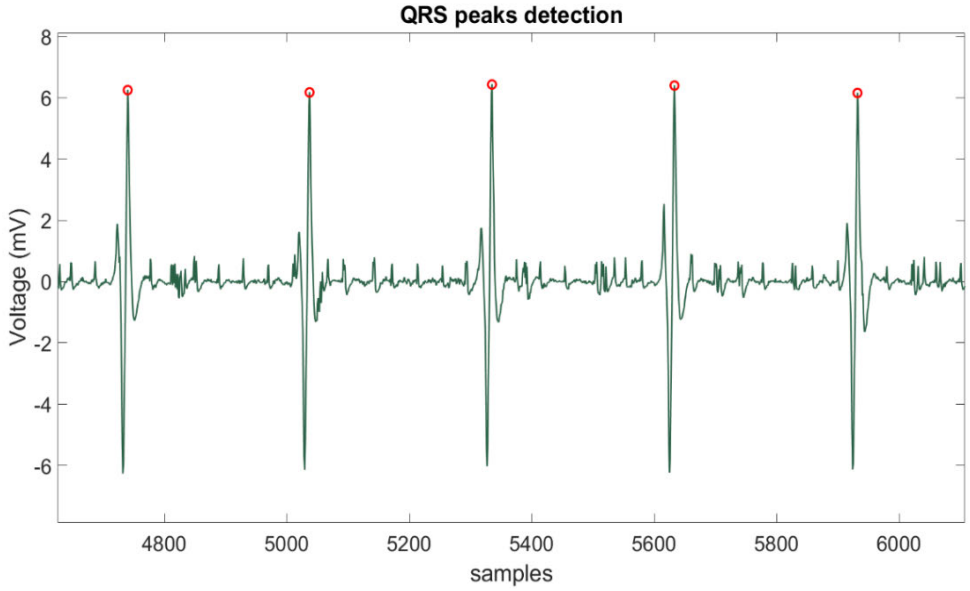

Figure 31: Exemplificative detection of QRS peaks (red dots) related to cardiac activity on the EMG signal (green line) of one PD patient recorded during a trial. Of note, EMG signal was resampled at 400Hz to allow the location of the peaks on the LFP timeline (in the figure 400 samples correspond to 1 s acquisition).
Abbreviations: EMG: electromyography; GI: gait initiation; LFP: local field potentials; PD: Parkinson's Disease.

This was possible as the probe used for TENS synchronization also recorded the mechanical artifacts of the carotid pulse. I then epoched the LFP signals with reference windows centered at the QRS peaks and equal to the mean plus two times the standard deviation of the heart rate. On the epoched data, I applied the singular value decomposition technique to identify the various components of the neural signals. Components were visually inspected to identify the ones related to the cardiac activity and then removed (**Figure 32**). The effect of the removal was visually checked and approved/discarded by the user.

- The second artifact encountered in the LFP recordings was related to a status interrogation of the PC+S device. The peculiar shape of this artifact, which consisted of a biphasic transition of about 500 ms, made it clearly recognizable. It rarely occurred and was easily removed by rejecting the time intervals in which the artifact appeared.

- The last artifact was due to the internal clock of the device and the multiplexer sampling circuitry. It was a rhythmical artifact with a frequency equal to one quarter of the chosen sampling frequency (i.e., 105Hz). The artifact did not affect my analyses since its frequency was far above the frequency band considered. Either way, it could have been removed by a Notch filter if necessary [285].

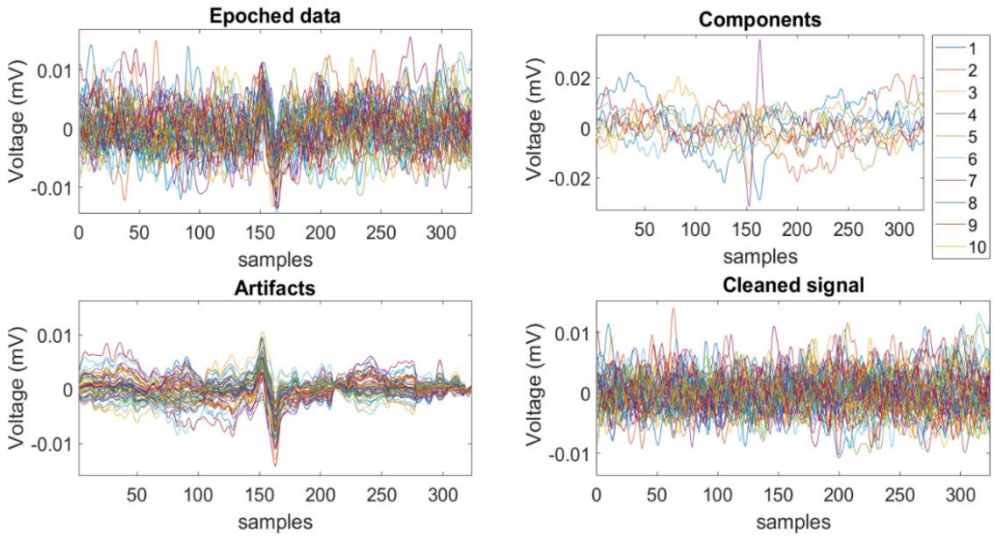

Figure 32: Processing for cardiac artifact removal. Top left: the LFP signal recorded in the left STN of one PD patient epoched on the QRS peaks as detected by the EMG recording. Top right: the ten components resulting from the singular value decomposition. I was able to select the components related to cardiac activity (in this case, components 1, 2 and 3) and visualize the signal reconstructed with only these three components ("artifacts", bottom left panel). The filtered version (band-passed 1÷80Hz) of the artifactual reconstruction was then subtracted from the signal (bottom right panel). Of relevance, the subtracted components do not solely model the cardiac artifact but include also neural content. The cleaning process might therefore affect neural components of the signal to some extent.
Abbreviations: ECG: electrocardiography; EMG: electromyography; GI: gait initiation; LFP: local field potentials; STN: Subthalamic nucleus; PD: Parkinson's disease.

LFP processing

After the cleaning process, I proceeded with a time-frequency analysis during the walking and standing periods, as identified by means of the kinematic data. Data of each hemisphere were analyzed separately and grouped across patients into more and less dopamine depleted hemispheres (i.e., STN- and STN+), according to the results of the FP-CIT SPECT. I epoched the neural data during walking into strides (i.e., from heel contact to the subsequent heel contact of the same foot) and applied a time-frequency decomposition with 46 Morlet wavelets between 5

and 40 Hz (central frequency set at 1 Hz, Full Width Half Maximum of 3 s, [395]. As stride duration varied across repetitions, the time-frequency representation was normalized by means of a time-warping algorithm with a third-order polynomial interpolation [396] to a 1.15 s window, equal to the mean stride duration across all recruited patients (see chapter 7). Time-warping was applied with a 1.5 s window to avoid border effects. I purposefully chose this window duration to be longer than the maximum stride duration recorded in the population of patients (see chapter 7). Similarly, for the standing period I identified subsequent non-overlapping epochs of 1.15 s each and computed the time-frequency representation for each window. In this case, the time-warping was not needed as no cyclic events related to standing were identified. For each epoch and condition (i.e., walking and standing) I estimated the power spectral density (PSD) by integrating the time-frequency representation over time. The mean PSD was computed for each condition as the average across epochs. The PSD were characterized by the co-presence of oscillatory components and a broadband pink noise, inversely proportional to the frequency ($\propto 1/f$). The 1/f component might hinder a proper detection of frequency peaks and frequency modulation across conditions, especially at low frequencies. To mitigate its influence, I modeled the average PSD of each condition into a sum of periodic oscillatory components and an aperiodic component described by a power law fit [397]. The aperiodic component was then removed from the PSD of each epoch with a parametrization procedure, thus allowing the analyses of the true oscillatory component only.

The PSD during walking and standing epochs obtained after the 1/f removal were then used for information analyses. Specifically, the mutual information [398] provides a quantitative evaluation of the reduction of uncertainty in determining the state of a system by knowing a neural activity feature [399], [400]. In this case, I used the information theory to quantify the information carried by a set of specific features (F) of the LFP activity over the state of the system (S, i.e., walking and standing). All information analyses were carried out with the Information Breakdown Toolbox [401].

The mutual information between the state of a system S and a neural feature F, is computed as:

$$I(S;F) = \sum_{s} P(s) \sum_{r} P(r|s) log_2 \frac{P(r|s)}{P(r)}$$

where P(s) is the probability of the system to be in the state s, $P(r)$ is the probability of the feature to assume the value r, and $P(r|s)$ is the probability of the feature to assume the value r in an epoch given a state s. I analyzed a set of six features:

i. the frequency showing the highest peak (f_{PEAK}) in the beta band (13-30Hz).

ii. the power over the entire beta band (P_{BETA}).

iii. the power in the range f_{STAND}±2Hz (P_{SF}), where f_{STAND} was defined as the frequency peak characterizing the average PSD during standing and identified as the frequency of the Gaussian component G with the highest amplitude in the parameterization process of the PSD.

iv. the power in the range f_{WALK}±2Hz (P_{WF}), where f_{WALK} was defined as the frequency peak characterizing the average PSD during walking and identified as the frequency of the

Gaussian component G with the highest amplitude in the parameterization process of the PSD.

v. the maximally informative frequency (f_{MIF}). This value was identified specifically for each patient by computing the spectral information [402], [403], that is, the information carried by the amplitude of the PSD at each frequency bin (5-40Hz). The f_{MIF} was defined as the frequency bin showing the highest significant peak.

vi. the power in the range f_{MIF}±2Hz (P_{MIF}), where f_{MIF} was defined as described in the previous point.

The information carried by each feature was computed separately for the two STN of the more and less dopamine depleted hemispheres (i.e., STN- and STN+). The information over the state of the system *S* carried by the joint knowledge of a feature bilaterally (*F1, F2*) was then computed as:

$$I(s; F_1, F_2) = \sum_{s} P(s) \sum_{r_{1,2}} P(r_1, r_2|s) log_2 \frac{P(r_1, r_2|s)}{P(r_1, r_2)}$$

where $P(s)$ is the probability of the system to be in the state *s*, $P(r_1, r_2|s)$ is the joint probability of the first feature to assume the value r_1 and the second feature to assume the value r_2 given a state *s*, $P(r_1, r_2)$ is the joint probability of the first feature to assume the value r1 and the second to assume the value r_2.

Additionally, the information redundancy was calculated as follows:

$$Red(s; F_1, F_2) = I(S; F_1) + I(S; F_2) - I(S; F_1, F_2)$$

This calculation allows estimation of the amount of information shared between the two features. In this way it is possible to optimize the number of monitored features to satisfactorily predict the state of the system. If the redundancy is inferior to the amount of the information carried by each single feature, each feature carries some independent information.

Due to the limited number of trials available, the estimated information was corrected with the Panzeri-Treves (PT) bias correction [404], available in the Information Breakdown Toolbox [401]. Mutual information was considered significant on the basis of a bootstrap test, i.e., when the information carried by a feature was higher than the 95th percentile of the information carried by randomized data in 100 repetitions.

The capacity of the defined features for discriminating the state of the system into two classes (i.e., standing and walking) was tested by means of a binary logistic regression classifier. A linear relationship between the different nth features *x* was defined as:

$$h_\alpha(x) = \alpha_0 + \alpha_1 x_1 + \alpha_2 x_2 + \cdots + \alpha_n x_n$$

The linear-based classification aimed at finding a family of parameters α, that optimally separated the two classes based on the selected features. The probability of belonging to one of the two classes (c_1 and c_2) was then determined as:

$$P(c_1|x, \alpha) = g(h_\alpha(x))$$

$$P(c_2|x, \alpha) = 1 - P(c_1|x, \alpha)$$

where $g(\cdot)$ is a sigmoid function to limit the probability between zero and one. The features included in the linear regression model were f_{PEAK}, P_{SF}, P_{WF}, P_{BETA}, and P_{MIF}, each one alone or specific combination pairs, separately for each hemisphere or combining the two sides together (see chapter 7). Models were validated with a leave-one-out cross validation approach. Since the number of epochs of standing and walking were different for each patient, I defined 100 subsamples of randomly selected epochs. Specifically, I randomly selected without replacement N standing epochs equal to the number of available walking epochs and merged the two datasets to build one subsample. For each patient, I evaluated the performance of the classifier on each subsample as the percentage of epochs correctly classified as standing or walking. The performance was then averaged across the 100 subsamples. I also evaluated the performance of the classifiers by means of the Receiver Operating Characteristic (ROC) curve, which plots the true positive rate (sensitivity) against the false positive rate (1-specificity) for different thresholds. By computing the area under the ROC curve (AUC), I was able to estimate the accuracy of the classifier in correctly identifying the state of the system. An AUC equal to 0.5 indicates a chance-level accuracy, while an AUC of 1 corresponds to no error in the classification.

7. Results

7.1. WP-1: Role of striatal dopamine at Gait Initiation in Parkinson's disease

Aim: to investigate the role of striatal dopamine in APA programming

7.1.1. Background

The contribution of the basal ganglia dopamine to GI execution is still largely unknown. Previous evidence suggests a fundamental role of dopamine [255], [405] and the cortico-basal ganglia circuitry [134], [406], [407] in the regulation and initiation of locomotion. Specifically, striatal dopamine might play a relevant role in APA programming at GI as involved in coding the movement-related energetic cost [408] and in learning and consolidating motor programs [409], [410]. Since PD is a predominantly dopamine deficiency syndrome [217], it embodies the ideal *in-vivo* model to study the contribution of dopamine to GI. In fact, in PD, locomotion can be severely affected particularly at movement initiation, thus supporting the involvement of the dopaminergic system in GI execution. *Start hesitation* is a major cause of falls for patients with PD [2], [3], [11], [25], [258], [411]–[413], which in turn leads to fractures and hospitalization [195], [202], [310], [414], [415], fear of falling [8], [416]–[418], diminished quality [25], [197], [412] and quantity of life [195], [197], [201], [415], [419].

Elucidating the contribution of striatal dopamine to GI is of great relevance to unveil and address the pathophysiological alterations underlying postural instability at GI in PD. In literature, several studies aimed at identifying the alterations of *feedforward* motor control at GI in PD [14]–[22] and the contribution of dopamine in the execution of the task [29]–[36]. However, results are controversial, and the role of striatal dopamine in *feedforward* motor control at GI still remains elusive [37]. The poor agreement in literature on the topic might be due to two confounding factors:

- **The BoS and AM**. Despite both BoS and AM might directly influence the biomechanical resultants of GI [32], [112], [420] the confounding effect of these variables on the performance of the task has been neglected in all previous studies investigating GI in parkinsonian patients [14]–[16], [18], [21], [29], [31], [33]. Of note, standardizing the BoS is a suboptimal solution [17], [20], [22], [30], [35], as this approach may prevent the subjects to adopt their natural strategy and hide disease related alterations of the BoS, which might be present in patients with PD [65], [382], [390]–[393].
- **The dopaminergic treatment**. Most of the previous studies on the topic analysed the patients without suspending the dopaminergic treatment [14]–[18], [21], [29]. This experimental choice might lead to evaluate the drug effect rather than the disease-related alterations of the motor pattern. Also, the effect of levodopa on motor symptoms might greatly vary across patients based on their clinical condition, possibly leading to uneven results. Last but not least, the acute effect of levodopa on APA might not reflect the only role of striatal dopamine, since the drug acts not only on the striatum but also on other brain areas such as the SMA [421], which is known to take part in the generation of APA at GI [20], [422], [423].

In this work, I aimed at identifying the alterations of *feedforward* motor control at GI in parkinsonian patients directly related to striatal dopaminergic loss. I analysed the biomechanical features of APA at GI in 26 unmedicated patients and in 27 healthy subjects. A subset of 13 patients underwent the evaluation also in Med-ON condition. I accounted for the influence of the BoS and the AM on GI measurements by applying the partial correlation technique as described in chapter 6, excluding all GI measurements dependent on the BoS and correcting the ones dependent on the AM. To directly investigate the role of striatal dopamine on GI, in a subset of 22 patients the biomechanical measurements of APA different from the normative range and ameliorated by levodopa were correlated with the results of a SPECT with FP-CIT, which provided an estimation of putaminal DAT and therefore dopaminergic innervation loss in each patient.
Thanks to these robust methods, I identified a reliable set of biomechanical features of APA altered in PD and directly related to striatal dopamine.

7.1.2. Materials and Methods

Subjects

Twenty-six subjects with idiopathic PD and 27 age-matched healthy controls (HC) were enrolled for this study. PD was diagnosed in accordance with the United Kingdom Brain Bank Clinical Diagnostic criteria. Patients were evaluated with the UPDRS-III scale by an expert neurologist (Prof. I.U. Isaias).

Table 4 shows the demographics and the clinical data of all subjects. I excluded subjects with vestibular problems, diabetes, cardiovascular pathologies or hypotension, neurological diseases other than PD, cognitive decline (Mini-Mental State Examination score lower than 27), orthopaedic issues or past major orthopaedic surgery. Among patients, I excluded those suffering from FoG, *start hesitation* or dyskinesia.

Ethical approval

The study was approved by the local ethical committee. All subjects gave written informed consent prior participation according to the Declaration of Helsinki. Of note, the neuroimaging evaluation was part of patients' clinical workup and not performed exclusively for this study.

Biomechanical experimental setup

The recordings took place at the Gait Laboratory of the UKW of Würzburg. All patients performed the experiment in Med-OFF condition (i.e., after overnight suspension of all dopaminergic drugs, PD-off). A cohort of 13 patients (PD"-off) additionally underwent the protocol in Med-ON condition (PD"-on, i.e., after the intake of a standard dose of levodopa). All subjects performed at least three GI trials. Participants were instructed to stand quietly with their arms at their sides on the two dynamometric force plates, with one foot placed on each platform. BoS was self-selected by each subject. After 30s, they were asked to start walking with their self-selected swing foot and at their preferred pace till the end of the walkway. Each subject performed also an *anatomic calibration* trial with eight additional markers, for the computation of the main AM (see paragraphs 6.3.3 and 6.4.1).

Biomechanical data analysis

The CoP key features of APA at GI were analysed thanks to the dynamic measurements, and the movement, velocity and acceleration of the CoM was monitored by means of the optoelectronic system at APA reference points. First step length, average and maximum velocity were also computed. The main AM and BoS measurements were extracted for each group. For a complete list of all extracted biomechanical measurements, please refer to **Table 3**. A partial correlation analysis was performed between the outcome GI measurements and the BoS, correcting for the AM, and between the GI measurements and the AM, correcting for the influence of the BoS. GI measurements dependent from the BoS were excluded from further analyses. GI measurements dependent from the AM were instead decorrelated as described in paragraph 6.4.1.

Molecular imaging

A subset of 22 patients underwent a SPECT with FP-CIT during their clinical workup. These data served to evaluate the residual striatal dopaminergic innervation of both brain hemispheres for the correlations with the GI measurements. Details on the neuroimaging data elaboration can be found in paragraph 6.2.1 . In particular, I took into account the values relative to the putamen nuclei, as the main motor structure in the striatum [424]. I grouped the putaminal values basing on the swing foot, defining as putamen-SWING the nucleus contralateral to the swing foot, putamen-STANCE the ipsilateral one.

Statistical analysis

For each subject, GI measurements were averaged across all available trials executed with the same swing foot. Each participant performed at least three GI trials with the same swing foot. For those subjects who executed the GI trials alternating the left and right as swing foot, I considered only the trials executed with the swing foot most frequently used during the experiment and then calculated the average values. Matching between the recruited groups was verified comparing demographic, clinical, AM and BoS measurements (HC vs. PD-off and PD"-off vs PD"-on, Wilcoxon test and Wilcoxon matched pairs test, respectively, p-value set at 0.05; gender distribution was compared across the two groups with the Pearson's chi-squared test, p-value set at 0.05). Partial correlation analysis was performed between the GI measurements and the AM and BoS parameters inside each group. Only partial correlation coefficient higher than 0.5 with a p-value lower than 0.01 were considered significant. GI measurements not dependent from the BoS measurements and decorrelated for the influence of the AM were then compared across groups. The GI measurements significantly different between healthy controls and patients (HC vs. PD-off, Wilcoxon test, p-value set at 0.05) were compared across drug conditions (PD"-off vs PD"-on, Wilcoxon matched pairs test, p-value set at 0.05). Only the ones ameliorated by levodopa intake were included in the correlation analysis with the neuroimaging findings. Data were correlated separately with the dopaminergic values of the putamen-SWING and putamen-STANCE, namely the putamen ipsilateral and contralateral to the swing and stance foot, respectively (Spearman's ρ correlation coefficient, p-value set at 0.05).

7.1.3. Results

Subjects

Groups did not differ for demographic, AM and BoS measurements. PD''-on derived significant benefit from levodopa intake, as shown by the significant change in the UPDRS-III score with respect to PD''- off (see **Table 4**).

	Data	HC	PD-off	PD''-off	PD''-on
DEM	Gender (M/N)	17/27 (~63%/)	18/26 (~69%)	8/13 (~61%)	8/13 (~61%)
	Age (yrs)	61.22 (5.15)	61.03 (7.94)	61.62 (9.13)	61.62 (9.13)
Clinical data	Disease duration (yrs)	(-)	10.85 (5.06)	10.84 (4.51)	10.84 (4.51)
	Hoen & Yahr (I–V stage)	(-)	2.62 (0.50)	2.62 (0.51)	2.62 (0.51)
	UPDRS-III (0–108 score)	(-)	28.87 (9.74)	26.36* (7.63)	9.54* (4.78)
	LEDD (mg)	(-)	893.04 (514.47)	985.25 (637.62)	985.25 (637.62)
AM	Body Height (BH, cm)	170.7 (9.8)	171.1 (10.8)	170.1 (11.5)	170.1 (11.5)
	Limb Length (LL, cm)	89.1 (4.8)	88.7 (6.9)	89.3 (8.4)	89.3 (8.4)
	Foot Length (FL, cm)	25.1 (1.6)	25.2 (1.6)	25.2 (1.9)	25.2 (1.9)
	Body Mass (BM, Kg)	75.25 (12.66)	75.57 (16.71)	69.93 (13.15)	69.93 (13.15)
	Body Mass Index (BMI, Kg/m^2)	25.51 (3.56)	25.63 (4.31)	24.07 (3.40)	24.07 (3.40)
	Inter ASIS distance (IAD, cm)	28.2 (2.9)	27.1 (2.6)	26.3 (2.2)	26.3 (2.2)
BoS	BoS Area (BA, cm^2)	713.21 (105.27)	672.89 (108.07)	667.56 (84.33)	680.27 (129.79)
	BoS Width (BoSW, cm)	18.14 (3.97)	16.46 (3.59)	16.72 (3.21)	17.68 (3.50)
	Foot Alignment (FA, cm)	0.68 (0.36)	0.79 (0.53)	0.89 (0.46)	0.94 (0.34)
	Difference between feet extra-rotation angles (β_Δ, deg)	6.94 (4.86)	5.34 (3.77)	5.89 (3.89)	5.41 (3.69)
	BoS opening angle (β, deg)	40.20 (14.58)	40.73 (11.45)	36.83 (11.67)	36.07 (13.90)

Table 4: Demographic data, clinical data, Anthropometric Measurements (AM) and Base of Support (BoS) measurements of the recruited subjects. Data are shown as mean (standard deviation). *: $p<0.05$, Wilcoxon matched pairs test.
Abbreviations: DEM: demographics; M: males; N: total number of subjects; UPDRS-III: Unified Parkinson's Disease Rating Scale motor part; LEDD: levodopa equivalent daily dose.

BoS influence

The partial correlation analysis revealed that IMB measurements were not influenced by the BoS, except for the velocity, acceleration, and position of the CoM at the end of the IMB. Conversely, most of UNL variables showed an interaction with the BoS, particularly along the ML direction. Since all GI measurements related to the BoS were excluded from further analyses, considerations on the UNL phase cann ot be considered definitive. **Table 5** shows the list and values of the measurements independent from the BoS in all groups. For a complete description of the variables, please refer to **Table 3**.

GI measurements	HC	PD-off	PD"-off	PD"-on
IMB duration (s)	0.40 (0.09)	0.41 (0.13)	0.41 (0.09)	0.42 (0.09)
IMB displacement (mm)	62.5 [a] (20.3)	45.8 [a] (22.3)	38.2 [b] (19.4)	49.5 [b] (19.5)
IMB displacement ML (mm)	44.2 [a] (15.0)	32.0 [a] (16.3)	27.6 [b] (14.4)	34.4 [b] (15.8)
IMB displacement AP (mm)	36.9 [a] (15.1)	27.5 [a] (16.1)	21.1 [b] (13.7)	31.8 [b] (13.4)
IMB average velocity (mm/s)	175.3 [a] (75.5)	130.6 [a] (73.4)	103.5 [b] (58.5)	129.4 [b] (75.5)
IMB average velocity ML (mm/s)	125.8 [a] (57.6)	91.5 [a] (53.1)	75.28 (44.2)	91.5 (56.0)
IMB average velocity AP (mm/s)	103.6 (50.5)	78.2 (49.4)	57.0 (38.5)	82.4 (51.3)
IMB maximal velocity (mm/s)	346.5 [a] (145.0)	260.3 [a] (156.7)	199.9 [b] (127.9)	266.6 [b] (135.1)
IMB maximal velocity ML (mm/s)	265.3 [a] (111.9)	207.1 [a] (136.3)	163.7 [b] (117.1)	203.1 [b] (117.4)
IMB maximal velocity AP (mm/s)	233.0 (107.3)	174.2 (100.3)	131.3 [b] (73.25)	179.6 [b] (91.1)
CoP distance at swing heel off (%FL)	30.48 (6.36)	32.21 (9.27)	35.11 (9.08)	37.51 (8.38)
UNL duration (s)	0.37 (0.08)	0.39 (0.10)	0.41 (0.08)	0.36 (0.09)
UNL displacement AP (mm)	- 13.4 [a] (18.3)	- 1.76 [a] (16.4)	- 2.22 (19.95)	6.5 (22.1)
UNL average velocity AP (mm/s)	64.3 [a] (35.7)	39.7 [a] (27.2)	44.8 (28.8)	54.7 (40.2)
UNL maximal velocity AP (mm/s)	347.5 (146.5)	311.1 (136.3)	306.6 (133.8)	348.6 (152.3)
CoM velocity at UNL end (m/s)	0.21 (0.06)	0.18 (0.05)	0.17 (0.06)	0.18 (0.07)
CoM acceleration at UNL end (m/s^2)	1.37 (0.40)	1.40 (0.45)	1.35 [b] (0.48)	1.71 [b, *] (0.70)
CoP-CoM distance at UNL end (m)	0.08 (0.03)	0.08 (0.02)	0.08 [b] (0.02)	0.09 [b, *] (0.02)
CoP distance at swing toe off (%FL)	36.05 (7.96)	33.04 (9.31)	36.25 (7.06)	34.89 (5.43)
CoM velocity at swing toe off (m/s)	0.86 [a] (0.13)	0.74 [a] (0.19)	0.67 [b] (0.19)	0.83 [b] (0.18)
CoM acceleration at swing toe off (m/s^2)	1.83 [a] (0.51)	1.42 [a] (0.39)	1.40 [b] (0.42)	1.93 [b] (0.46)
First step length (m)	0.60 [a] (0.21)	0.46 [a] (0.11)	0.43 [b] (0.11)	0.5 [b] 0 (0.12)
First step average velocity (m/s)	0.99 [a] (0.22)	0.85 [a] (0.23)	0.80 [b] (0.21)	0.96 [b] (0.24)

Table 5: List of GI measurements not dependent from the BoS in all groups. Data are shown as mean (standard deviation) before the decorrelation normalization process for sake of data intelligibility. ML

displacement was defined positive towards the swing foot and towards the stance foot for the IMB and UNL phase, respectively. For both IMB and UNL, the AP displacement was expressed as positive when oriented backwards. For a detailed description of all variables please refer to **Table 3**. [a] HC vs. PD-off, [b] PD"-off vs. PD"-on, Wilcoxon test and Wilcoxon matched pairs test, respectively, p-value<0.05, ***** detrimental effect of levodopa on the GI variables.
Abbreviations: AP: anterior-posterior; CoM: centre of mass; CoP: centre of pressure; FL: foot length; IMB: imbalance; ML: medio-lateral; UNL: unloading.

Role of putaminal dopamine on GI

I further investigated the correlations of putaminal DAT density with all measurements that differed between HC and PD-off and were significantly changed after levodopa intake. In particular, all IMB measurements except for the AP displacement (IMBD AP) correlated with the residual dopaminergic innervation level of both putamen nuclei, while the measurements of the stepping phase were mostly correlated with the values of the putamen contralateral to the swing foot (putamen-SWING, please refer to **Table 6**).

GI measurements	putamen-SWING	putamen-STANCE
IMB displacement	0.57	0.53
IMB displacement ML	0.44	0.53
IMB displacement AP	0.48	
IMB average velocity	0.44	0.46
IMB maximal velocity	0.46	0.50
IMB maximal velocity ML	0.44	0.50
CoM velocity at swing toe off	0.47	
CoM acceleration at swing toe off	0.54	0.45
First step length	0.46	
First step average velocity	0.42	

Table 6: Correlations between biomechanical and neuroimaging findings. In a subset of 22 PD patients, putaminal dopaminergic depletion was considered separately for the nucleus contralateral to the swing foot (putamen-SWING) and contralateral to the stance foot (putamen-STANCE) and correlated with GI variables different across groups. Correlations are shown as Spearman's ρ correlation coefficients. Only significant results (p<0.05) are shown.
Abbreviations: AP: anterior-posterior; CoM: centre of mass; GI: gait initiation; IMB: imbalance; ML: medio-lateral.

7.1.4. Discussion

With this work, I aimed to better elucidate the alterations of APA at GI and the role of putaminal dopamine in patients with PD. I first outlined the main PD-related alterations of this motor task, investigated the effect of levodopa intake and correlated the performance variables with the putaminal dopaminergic innervation of each single patient.

A preliminary, though fundamental part was to elucidate the impact of AM and BoS on kinematic APA resultants at GI. Indeed, despite it was shown that these two sets of variables can deeply impact GI biomechanical measurements [32], [112], [389], [420] their influence on the GI performance has been neglected in previous works [14]–[16], [18], [21], [29], [31], [33]. One of the most common approaches consisted in standardizing the BoS [17], [20], [22], [30] possibly

introducing a bias in the performance of the subjects. This methodological issue might be one of the main reasons for the different results present in literature on APA alterations at GI in PD patients. Only Rocchi and colleagues previously addressed this topic from a methodological point of view, investigating the GI of a group of parkinsonian patients adopting various BoS [32]. They provided useful evidence of a direct influence of the BoS measurements on the CoP variables during APA at GI. Nevertheless, they imposed on the patients a standardized BoS (feet parallel and 5 or 26 cm apart), thus possibly forcing them to an unnatural posture. In the present work, I assessed the correlation between BoS parameters and GI measurements allowing all the recruited subjects to adopt their own preferred BoS, thus without influencing their usual performance. Of note, while the impact of the AM on GI can be assumed to be equivalent in healthy and pathological subject, the BoS itself can change basing on the clinical condition [65], [382], [390]–[393]. The GI measurements affected by the BoS cannot therefore be decorrelated for BoS features as this procedure might imply a normalization for a disease-related variable. To ensure the robustness of the results, I excluded from the comparisons across groups all BoS-dependent variables. In regard to the AM, some of the previous work on GI in PD normalized the outcome measurements by dividing them for subjects' body height or foot length, without proving their relationship/correlation [18], [19]. Also, the division for the body height or a specific AM might lead to suboptimal results, as data might be affected by residual correlation [389]. To overcome this issue, I opted for a *decorrelation normalization* procedure, which allowed to remove any linear relation between AM and GI. This data transformation ensured a non-biased comparison across the recruited groups, without known confounding factors on the measured variables.

Of relevance, this is one of the few studies assessing patients in both Med-OFF and Med-ON condition. This is of fundamental importance when aiming at evaluating the role of dopamine in a dopamine-deficiency syndrome such as PD. First, the effect of levodopa might be highly variable across patients basing on their clinical conditions (e.g., development of dyskinesias), drug absorption in the intestine, time of the exam during the day etc., and can therefore lead to not homogeneous results across patients. Second, the dopaminergic treatment might restore only partially the physiological motor pattern. The Med-OFF condition allowed to evaluate the effect of the disease rather than the action of the drug and to have a reliable motor baseline to assess the effect of the dopaminergic replacement treatment.

CoP IMB measurements resulted to be a robust set of measurements for assessing GI performance in parkinsonian patients, as all of these variables were independent from the BoS. Except for the maximal first step velocity, the measurements of the stepping phase were also not dependent from the BoS measurements. Results showed instead that most of the UNL variables, particularly in the ML direction, were influenced by the BoS of the patient. All previous findings on this phase should be therefore carefully taken into considerations. Similarly, CoM measurements at the end of IMB phase were BoS-related and had to be excluded from further analyses.

The PD-off group showed reduced CoP displacement, average and maximal velocity during the IMB phase with respect to HC. The stepping phase was also strongly altered, both in terms of velocity and acceleration of the CoM at the swing toe off and first step length and average velocity. The UNL measurements considered in the analyses were instead similar to HC, except

for the AP displacement and velocity. Of note, while in the HC group the UNL AP displacement is in the majority of the cases forwards (negative values), several patients of the PD-off group displaced their CoP backwards. This may possibly reflect a compensatory mechanism adopted by parkinsonian patients to increase the poor moment arm generated during the previous IMB phase to propel the CoM forward. At the end of the UNL phase the velocity and acceleration of the CoM in the PD-off group reached indeed values similar to the normative data. On one hand, levodopa intake possibly enhanced the action of this compensatory mechanism, leading to a value of UNLCoMA above the normal range and possibly to postural instability and falls, if the first step is not promptly executed. On the other hand, step execution had a great benefit from the intake of levodopa, as first step length and velocity and also velocity and acceleration of CoM at swing toe off reached values within the normal range.

Alterations of the IMB phase in the unmedicated cohort of patients suggest an impaired *feedforward* motor control at GI in PD. The amelioration of IMB measurements in Med-ON condition and their correlation with putaminal dopamine strongly corroborates the hypothesis of a primary role of dopamine in *feedforward* motor control at GI in PD patients. Of note, both putamen nuclei resulted to be correlated with IMB measurements (see **Table 6**), thus suggesting a bilateral involvement in the pre-programming of the APA. Previously, several studies suggested a major role of the SMA in the sequencing and planning of the APA [20], [422]. In this context, it is important to notice that the putamen is a major target of the SMA [425] and the dopaminergic modulation of their connectivity is essential for coding motor programs [426], especially for their adaptation to environmental circumstances [44], [45], [427].

I hypothesize that striatal dopamine would play a relevant role in the choice of the most appropriate set of muscular synergies (i.e., APA) among the many available (pre-programmed) motor patterns, aiming at minimizing the expenditure of energy during movement execution.

Striatal dopamine also showed to contribute to the execution of the first step. The normalization of CoM velocity and acceleration at the swing toe off after levodopa intake may derive from the improvement of the IMB execution, which in turn can provide a proper forward momentum to the CoM. Levodopa intake also ameliorated first step length and average velocity, possibly because of a positive contribution on the PD-related muscular rigidity.

7.1.5. Conclusions and study limitations

In this work, I first elucidated the impact of AM and BoS on kinematic and dynamic APA resultants at GI. I then described for the first time correlations between GI biomechanical resultants and striatal DAT density in a group of parkinsonian patients as an *in vivo* model of striatal dopaminergic deficiency. Overall, my results suggest a relevant role of putaminal dopamine in the execution of the IMB phase and first step.

Despite the relevance and novelty of these findings, this study suffers from some limitations. First, even if the number of healthy and pathological participants recruited for the GI assessment is in line with previous studies [14], [16], [17], [19], [20], [29], [30], [32], [33], the subset of patients assessed in Med-ON condition and underwent to the neuroimaging exam was limited. Results should be further confirmed on larger cohorts. Second, even if the major neurodegeneration in PD is related to the dopaminergic circuitry, other neurotransmitters and circuits are involved both in the pathological process and compensatory activity [190], [407], [428], [429]. Further

neuroimaging studies should unveil the role of these neural circuits (e.g., noradrenergic, glutamatergic.) in APA programming and execution at GI.

7.1.6. Publications

Palmisano, C, Brandt, G, Vissani, M, [...], Frigo, C A, Isaias, I U, Frontiers in Bioengineering and Biotechnology, 2020, 8:137 [38]

7.2. WP-2: Alterations of GI related to Freezing of Gait in PD

Aim: to investigate the role of *Freezing of Gait* in APA programming

7.2.1. Background

FoG is a "brief, episodic absence or marked reduction of forward progression of the feet despite the intention to walk" [11], [25], [430]. It is a severe problem as it leads patients to falls, disability, decreased quality and quantity of life [11]. As pathophysiology of FoG is still poorly understood [23], [25], [259], [431], [432], its treatment is particularly challenging and still an unmet need. Despite the majority of FoG episodes are related to a hypodopaminergic state [258], [433] and generally responsive to levodopa at early stages of the disease [24], [191], [258], along disease progression they become more resistant to dopaminergic drugs [434] and also DBS [432] causing increase of dependency and numerous falls [11], [258], [432]. Also, there are cases of FoG related to the Med-ON state which challenge the therapeutic options available [25], [258], [435].

When investigating alterations of *feedforward* motor control at GI in PD, patients suffering from FoG constitute a particularly interesting case study. Indeed, FoG abruptly appears in most of the cases while turning or at GI (i.e. *start hesitation*) [23]–[25].

My research group was the first to directly record on-going FoG episodes and to demonstrate poor low-frequency cortical-STN connectivity in the most dopamine depleted brain hemisphere, in particular the SMA [45]. This cortical region is of major importance in controlling locomotion, especially in updating, sequencing, and switching between motor tasks, such as from standing to walking [45], [436], [437]. SMA was shown in particular to be involved in the generation of APA at GI [20], [422], [438] and in the forward propulsion of CoM during GI in patients with PSP (see WP-3, paragraph 7.3) [75]. Specifically, a poor engagement of the SMA during changes in the locomotor pattern or transitions (such as from standing to walking) might be at the basis of the difficulties at GI in PD patients with FoG [20].

Nevertheless, the pathological mechanisms underlying *start hesitation* are still elusive [25] and require further investigations. Specifically, the hypothesis of FoG-related alterations of *feedforward* motor control at GI in PD patients is still questionable. Indeed, the majority of the studies on GI in patients with PD failed to prove specific and consistent FoG-related biomechanical alterations of APA [26]–[28]. Two studies reported reduced medio-lateral displacement of the CoP during the APA in PD patients suffering from FoG [3], [13]. Since the CoP displacement was larger during ongoing FoG episodes [3], this finding was interpreted more as a compensatory mechanisms rather than an actual effect of disrupted *feedforward* motor control. Also, the work of Jacobs and coll. related the typical knee trembling accompanying FoG episodes to multiple APA, thus suggesting a difficulty in the stepping rather than in the execution of *feedforward* motor programs [13]. In general, all studies agreed in identifying a significant impairment of stepping at GI in PD subjects suffering from FoG [3], [13], [26]–[28].

Several confounding factors determined the poor agreement on this topic in the scientific literature. First, Huffmaster and coll. highlighted a different relationship between the initial stance condition, the APA, and the stepping performance in PD patients with and without FoG, despite no differences were found across the two groups in the initial feet position and APA measurements [28]. These results further support the influence of the BoS on GI execution [38],

[112], [420], aspect neglected in all other studies on GI in patients with PD and FoG [3], [13], [26], [27]. Second, in some of the previous works, light or sensory cues were used as start signals for the GI task [3], [13]. However, cueing helps patients overcoming FoG episodes and facilitate the initiation of walking [25], [76], [259], [372], [439], thus possibly masking specific FoG-related GI alterations. Last, the initial posture, and specifically the forward bending of the trunk, was proven to have a role in determining the subsequent GI performance in healthy controls [104], [107], [440]. This is of great importance in relation to FoG, as patient suffering from FoG usually show increased forward trunk flexion [382], [393], [441]–[445]. Outlining the influence of postural variables on the performance of GI in these patients might help in disentangling the actual alterations of *feedforward* motor control from changes related to an altered postural framework.

With this aim, I developed a robust methodological approach to characterize GI alterations specific for PD patients suffering from FoG. I also investigated the integrity of the movement timing by studying the movement onset of the various body segments [16]. Movement timing is primarily related to cerebellar activity [246], [446], [447] and I wanted to provide additional data supporting a compensatory, rather than detrimental, role of the cerebellum for postural maintenance in parkinsonian patients, as anticipated by a recent publication of mine [164]. I additionally addressed the impact of the postural asset on the GI task, to verify if APA alterations were related to actual *feedforward* motor control impairment or to alterations of the postural framework. I estimated the main postural angles (i.e., trunk, thigh, and shank) during standing preceding APA execution and correlated them with the GI outcome measurements. To avoid any confounding effects of the initial feet position and AM, I applied partial correlation analyses between these two sets variables and the outcome measurements as described in paragraph 6.4.1, similarly to WP-1 and WP-3. In addition, contrary to most published studies, I minimised the impact of dopaminergic drugs on the motor performance by studying all patients after 12h from withdrawal of all dopaminergic drugs (Med-OFF condition). To avoid the effect of cueing on the GI performance, I instructed the subjects to start walking at their preferred speed after a self-selected time from a verbal signal [25], [76], [259], [372], [439]. Last but not least, all subjects were free to adopt their preferred motor strategy in terms of feet position and stepping leg.

A better understanding of FoG-related biomechanical alterations at GI may offer an insight into the pathophysiological mechanism underlying this symptom, promoting the development of tailored and effective therapies.

7.2.2. Materials and Methods

Subjects

Twenty-three subjects with idiopathic PD and FoG (PDF) and 20 PD patients without FoG (PDNF) were recruited for the study. PD was diagnosed according to the United Kingdom Brain Bank Clinical Diagnostic criteria for PD, and history of FoG was clinically assessed by a neurologist expert in movement disorders (Prof. I.U. Isaias). Disease severity was evaluated with the UPDRS-III scale. Patients suffering from neurological disorders other than PD, cognitive decline as assessed by the Mini-Mental State Examination, vestibular problems, cardiovascular diseases, and orthopaedic pathologies affecting gait were excluded during the recruitment phase. We also excluded patients unable to perform at least three GI trials without help or assistance in Med-OFF condition. Data of 23 HC were selected from the HC cohort of WP-1 (see WP-1, paragraph 7.1) to match patients for demographic, AM and BoS features (**Table 7**).

Ethical approval

The experimental protocol was approved by the local Ethical Committee and the study conformed to the declaration of Helsinki. All subjects signed an informed consent for participating in the study.

Biomechanical experimental setup

The recordings took place at the Gait Laboratory of the LAMB of Milano. Patients performed the task in Med-OFF condition (i.e., in the morning after overnight withdrawal of all dopaminergic drugs). Subjects were instructed to stand quietly and with the arms at their sides for about 30 seconds on a dynamometric force plate and to start walking after a self-selected time interval from a verbal signal. Initial feet position and posture were self-selected by each subject. Stepping leg and walking speed were also not standardized. GI assessment was preceded by an *anatomic calibration* trial in which each subject was asked to stand on the force plate for about 5 seconds with eight additional markers to allow the calculation of the main AM (see paragraphs 6.3.1 and 6.3.3).

Biomechanical data analysis

Similar to WP-1 (paragraph 7.1)**,** I investigated key APA features by means of the signal recorded by the dynamometric force plate. Specifically, CoP pathway was analysed in terms of displacement, average and maximum velocity during the IMB and UNL phases. In addition, the position with respect to the CoP, the velocity and acceleration of the CoM were evaluated at APA reference points. First step length, average and maximal velocity were also calculated.

The movement onset of segmental CoM (SCoM) was evaluated to account for eventual alterations of movement timing [16]. In particular, I modelled the body with 16 rigid bodies: head, chest, abdomen, pelvis, arms, forearms, hands, thighs, shanks and feet. For each body segment, I identified the movement latency of each SCoM as the time interval from the APA onset to the segmental movement onset, identified with a threshold criterion. Specifically, the movement onset of each SCoM was defined as the time instant at which the AP displacement of the analysed segment overcame a threshold equal to the AP position of the segment at the APA onset plus two times the standard deviation of its AP position during the standing window preceding the GI (i.e., from the beginning of the recording till half a second before the APA onset, **Figure 33**). The movement latencies of each SCoM were then expressed as a percentage of the total GI duration, i.e., from APA onset to the HO_{SW}.

Additionally, I evaluated and related to the subsequent GI performance the postural asset preceding APA. Specifically, I calculated the main postural angles (i.e., trunk, thigh and shank) in the sagittal plane in a one-second time window before the APA onset, similarly to Crenna and coll. [19]. The trunk angle was defined as the angle between the line connecting the marker on the middle point between the posterior-superior iliac spines and on the 7^{th} cervical vertebra and the vertical axis of the laboratory. The thigh angle was computed as the angle described by the line connecting hip and knee centres of rotation and the vertical axis of the laboratory. Similarly, the shank angle was identified as the inclination in the sagittal plane of the vector passing through the ankle and knee centres of rotation. Of note, a positive trunk angle indicated forward bending,

while a positive thigh angle corresponded to a more anterior position of the hip centre with respect to the knee centre of rotation. Likewise, the shank angle was positive when the knee was more anterior with respect to the ankle centre of rotation (**Figure 34**).

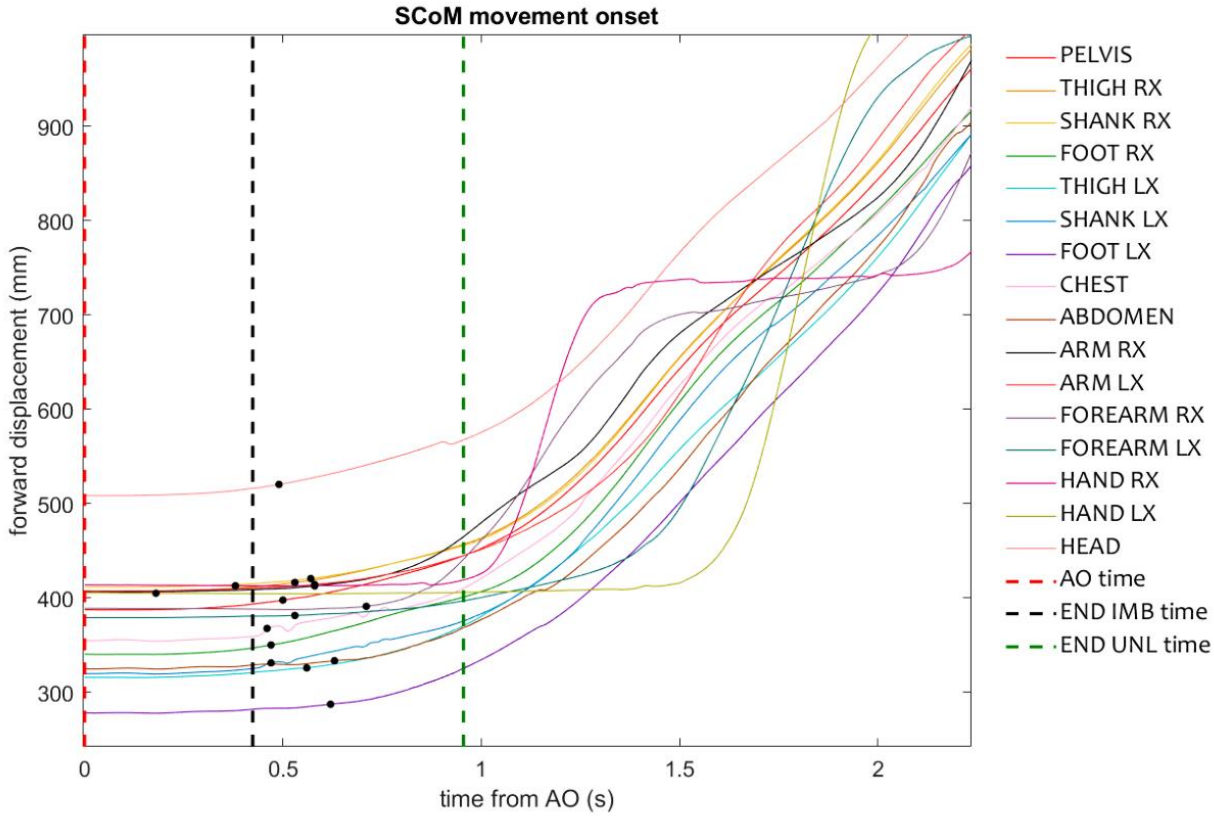

Figure 33: Exemplary identification of the movement onsets of the SCoM. For each segment, movement onset was defined as the instant when the segment overcame a threshold based on the standing window preceding GI. Movement onsets are displayed as black dots in the figure. Latencies of SCoM movement onsets from the AO (time zero in the figure, red dashed line) were normalized for the total GI duration (i.e., from the AO to the toe off of the swing foot, corresponding to the end of the UNL phase).
Abbreviations: AO: APA onset; GI: gait initiation; IMB: imbalance; LX: left; RX: right; UNL: unloading; SCoM: segmental Centre of Mass.

As for WP 1 and 3, the main AM and BoS measurements were computed for each subject. For a complete list of all GI, AM, and BoS parameters, please refer to **Table 3**. These variables served for a partial correlation analysis between the GI measurements of interest and the BoS, correcting for the influence of the AM, and between the GI measurements and the AM, correcting for the BoS. The same analysis was applied to the postural angles (i.e., correlation between the postural angles and the BoS, correcting for the influence of the AM, and between the postural angles and the AM, correcting for the BoS). To ensure the reliability of the results, GI measurements and postural angles, which showed any dependency from the BoS, were excluded from the subsequent analyses. I instead applied the *decorrelation normalization* procedure on the GI measurements and postural angles dependent from the AM, as described in paragraph 6.4.1.

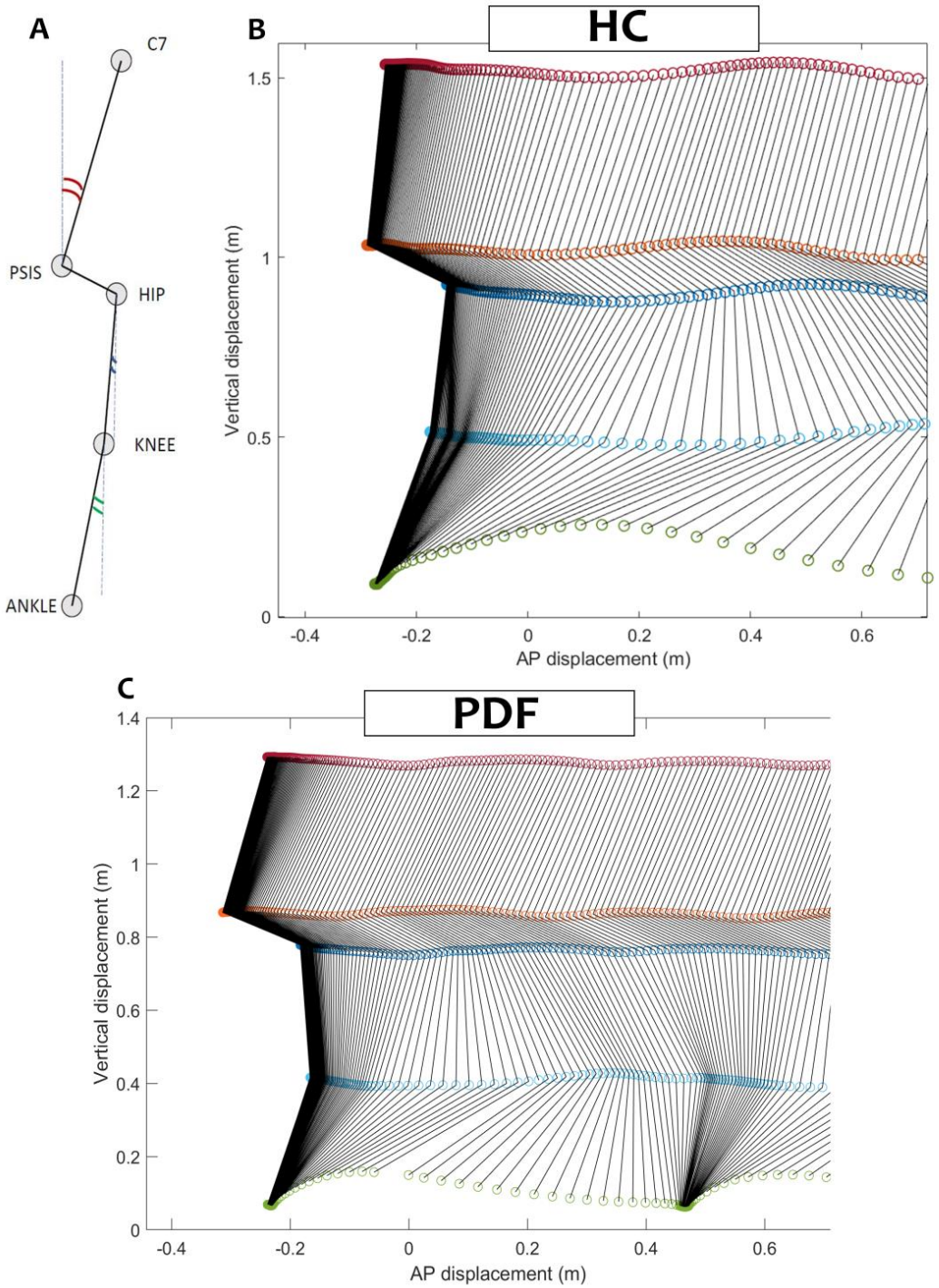

Figure 34: Postural angles during GI. The angles describing the postural attitude of the subjects were evaluated in the sagittal plane in a one-second window preceding the AO. A) Schematic representation of the postural angles. The trunk angle (in red) was defined as the inclination of the vector connecting the markers placed on the 7th cervical vertebra (C7) and the middle point between the posterior-superior iliac spines (PSIS). The thigh angle (in blue) corresponded to the angle between the line connecting the hip and knee joint centres and the vertical axis of the laboratory. Similarly, the shank angle (in green) was the inclination of the vector from the ankle to the knee joint centre. B) Movement along time in the sagittal plane of the points defining the postural angles during a GI trial on healthy subjects (C7 (red), PSIS (orange), the hip joint centre (blue), the knee joint centre (light blue), the ankle joint centre (green)). Black lines show the segments connecting these points over time. C) Same as B) but for a PD patient suffering from FoG (PDF). Initial posture is characterized by increased trunk and knee flexion. First step length is much shorter than in HC.
Abbreviations: AO: APA onset; AP: anterior-posterior; GI: gait initiation.

Statistical analysis

To avoid any confounding effect related to the adopted swing foot, GI measurements were averaged across trials (at least three for each subject) performed with the same swing foot. If both left and right feet were alternatively used by the subject, I considered only the trials executed with the swing foot most frequently used during the experimental session. I verified the matching across groups (HC, PDNF, PDF) for demographic, clinic, BoS and AM parameters with a Wilcoxon test (p-value=0.05). Gender distribution was compared with the Pearson's chi-squared test. Partial correlation analysis was applied separately inside each group (significant threshold set at Spearman's ρ=0.5 and p-value=0.01). GI measurements not influenced by the BoS and decorrelated for the AM, as well as the movement onset of the SCoM, were compared between the groups (Dunn's test, p-value set at 0.05 and adjusted with Bonferroni correction for multiple comparisons). In regard to the postural asset, the partial correlation analysis was applied separately inside each group (significant threshold set at Spearman's ρ=0.5 and p-value=0.01) and the postural angles not dependent from the BoS and decorrelated for the AM compared across groups (Dunn's test, p-value set at 0.05 and adjusted with Bonferroni correction for multiple comparisons). To account for the influence of the postural asset on the GI outcome measurements, I performed a partial correlation analysis between postural angles and GI measurements removing the influence of the group variable. A standing variable was considered significantly correlated to a GI measurement if Spearman's correlation coefficient ρ was higher than 0.5 and the p-value inferior to the threshold 0.05, adjusted with Bonferroni correction for multiple comparisons.

7.2.3. Results

Subjects

The groups involved in the study resulted to be matched for demographic, clinical, AM and BoS measurements (**Table 7**).

BoS influence

Results of the partial correlation analyses were in line with WP-1 (paragraph 7.1) [38]. Specifically, IMB and stepping phases were mildly affected by the chosen BoS, while several UNL measurements were dependent from the BoS.

Table 8 lists the GI measurements not affected by the BoS. The postural angles were not influenced by the BoS nor the AM in the analysed groups. For a complete description of all variables, please refer to **Table 3**.

Disease effect on GI

Both PDNF and PDF showed significant impairment in GI execution, with measurements more severely affected in the PDF group. CoP displacement, average and maximal velocity recorded during the IMB phase progressively reduced from HC to PDNF and PDF both in ML and AP directions. However, no statistically significant differences were found across the two pathological groups for IMB measurements. With regards to the UNL phase, it was mostly preserved in both patient groups, except for the AP displacement, which was in most of the cases forwards in the HC group and backwards in the PDF group, while PD patients showed intermediate values. The velocity of the CoM was reduced at the end of both the IMB and UNL phases in the PDF group only. Stepping ability was impaired in both PD groups, as shown by the

reduced value of step velocity. As a result, at the toe off of the stance foot the velocity of the CoM was decreased in both pathological groups with respect to HC. Of relevance, step length was reduced in both PD groups but significantly in the PDF cohort only.

Table 8 shows the analysed variables and the results of the statistical comparison across the three groups.

	Data	HC	PDNF	PDF
DEM	Gender (M/N)	14/23 (~61%)	10/20 (50%)	14/23 (~61%)
	Age (yrs)	61.17 (4.93)	63.32 (10.76)	63.83 (8.34)
Clinical data	Disease duration (yrs)	(-)	9.26 (3.89)	11.14 (3.47)
	Hoen & Yahr (I–V stage)	(-)	2.24 (0.42)	2.39 (0.50)
	UPDRS-III (0–108 score)	(-)	24.81 (9.43)	28.05 (9.96)
	LEDD (mg)	(-)	741.18 (221.26)	803.70 (358.33)
AM	Body Height (BH, cm)	169.94 (10.53)	167.79 (11.05)	168.09 (11.44)
	Limb Length (LL, cm)	88.81 (5.37)	88.23 (7.81)	87.21 (5.84)
	Foot Length (FL, cm)	24.93 (1.66)	25.17 (1.58)	24.59 (1.65)
	Body Mass (BM, Kg)	72.28 (11.11)	66.36 (13.01)	72.02 (14.83)
	Body Mass Index (BMI, Kg/m^2)	24.59 (3.02)	23.00 (3.99)	24.89 (5.18)
	Inter ASIS distance (IAD, cm)	27.76 (2.35)	27.89 (2.53)	27.42 (3.40)
BoS	BoS Area (BA, cm^2)	685.24 (91.56)	668.18 (75.19)	651.85 (114.90)
	BoS Width (BoSW, cm)	17.64 (4.10)	16.26 (2.78)	15.67 (2.59)
	Foot Alignment (FA, cm)	6.57 (3.36)	8.37 (4.54)	6.92 (3.76)
	Difference between feet extra-rotation angles (β_Δ, deg)	6.66 (3.29)	4.67 (2.58)	7.75 (4.98)
	BoS opening angle (β, deg)	40.67 (15.76)	37.25 (14.05)	43.56 (13.92)

Table 7: Demographic data, clinical data, AM and BoS measurements of the recruited subjects. Data are shown as mean (standard deviation). No statistically significant differences were found across groups (Wilcoxon each pair test, p-value<0.05).

Abbreviations: AM: anthropometric measurements; BoS: Base of Support; DEM: demographics; M: males; N: total number of subjects; UPDRS-III: Unified Parkinson's Disease Rating Scale motor part; LEDD: levodopa equivalent daily dose.

GI measurements	HC	PDNF	PDF
IMB duration (s)	0.39 (0.08)	0.38 (0.08)	0.33 (0.09)
IMB displacement (mm)	61.23[b] (20.32)	35.54 (19.71)	23.67[b] (9.94)
IMB displacement ML (mm)	42.07[a, b] (13.04)	24.04[a] (13.61)	17.76[b] (8.59)
IMB displacement AP (mm)	36.53[b] (16.17)	18.79 (14.75)	9.16[b] (5.93)
IMB average velocity (mm/s)	163.40[a, b] (62.29)	90.79[a] (47.29)	84.03[b] (46.81)
IMB average velocity ML (mm/s)	110.94[a] (34.90)	62.14[a] (34.80)	67.53 (41.47)
IMB average velocity AP (mm/s)	103.36[a, b] (53.78)	47.74[a] (34.39)	40.19[b] (30.45)
IMB maximal velocity (mm/s)	344.22[a, b] (149.41)	189.88[a] (113.54)	150.41[b] (64.26)
IMB maximal velocity ML (mm/s)	238.29[a, b] (77.82)	137.25[a] (72.76)	124.97[b] (56.96)
IMB maximal velocity AP (mm/s)	225.81[b] (110.67)	124.78 (65.52)	101.41[b] (55.74)
COM velocity at IMB end (m/s)	0.09[b] (0.03)	0.06 (0.03)	0.04[b] (0.02)
CoP-CoM distance at IMB end (m)	0.07[b] (0.02)	0.04 (0.02)	0.03[b] (0.01)
UNL duration (s)	0.36 (0.08)	0.40 (0.08)	0.45 (0.19)
UNL displacement AP (mm)	-9.67[b] (15.30)	-6.25[c] (18.22)	14.69[b, c] (14.70)
UNL average velocity (mm/s)	465.61 (162.21)	323.94 (131.02)	320.34 (150.20)
UNL average velocity ML (mm/s)	422.79 (148.96)	289.26 (121.24)	290.67 (140.81)
UNL average velocity AP (mm/s)	53.11 (20.97)	37.29 (17.16)	46.04 (34.21)
UNL maximal velocity AP (mm/s)	344.48 (154.35)	388.76 (169.88)	359.19 (178.76)
CoM velocity at UNL end (m/s)	0.21[b] (0.06)	0.16 (0.07)	0.11[b] (0.04)
CoM acceleration at UNL end (m/s2)	1.29 (0.33)	1.08 (0.41)	1.12 (0.25)
CoP-CoM distance at UNL end (m)	0.08 (0.03)	0.07 (0.03)	0.07 (0.02)
CoM velocity at swing toe off (m/s)	0.86[a, b] (0.13)	0.63[a] (0.24)	0.53[b] (0.18)
CoM acceleration at swing toe off (m/s²)	1.73[b] (0.38)	1.28 (0.42)	1.08[b] (0.33)
CoP-CoM distance at swing toe off (m)	0.48 (0.32)	0.51 (0.29)	0.34 (0.28)
First step length (m)	0.56[b] (0.07)	0.43 (0.14)	0.33[b] (0.13)
First step average velocity (m/s)	0.98[a, b] (0.14)	0.68[a] (0.27)	0.57[b] (0.27)
First step maximal velocity (m/s)	3.21 (0.52)	2.81 (0.72)	2.64 (0.80)

Table 8: List of GI measurements not dependent from the BoS in all groups. Data are shown as *mean (standard deviation)* before the *decorrelation normalization* process for sake of data intelligibility. ML displacement was defined positive towards the swing foot and towards the stance foot for the IMB and UNL phase, respectively. For both IMB and UNL, the AP displacement was expressed as positive when oriented backwards. For a detailed description of all variables please refer to **Table 3**. [a] HC vs. PDNF, [b] HC vs. PDF, [c] PDNF vs. PDF, Dunn's test, p-value<0.05 adjusted with Bonferroni correction for multiple comparisons.

Movement pattern during GI

Movement onset of the body segments analysed showed overall the same pattern in the three cohorts. The variability of segmental movement onset was quite significant in all the three groups, and particularly in the pathological ones, as shown by the high standard deviation values (**Table 9**).

	HC	PDNF	PDF
Pelvis (%)	60.62 (9.27)	62.47 (13.74)	62.66 (21.69)
Thigh ST (%)	65.76 (10.75)	71.72 (20.13)	63.39 (19.97)
Shank ST (%)	71.17 (14.36)	68.57 (19.98)	65.73 (21.95)
Foot ST (%)	68.37 (10.46)	77.24 (22.53)	65.02 (22.87)
Thigh SW (%)	62.67 (9.23)	64.75 (15.47)	55.85 (18.80)
Shank SW (%)	74.21 (13.85)	75.35 (24.26)	67.26 (19.36)
Foot SW (%)	69.15 (15.41)	64.63 (16.55)	59.20 (19.86)
Chest (%)	73.48 (14.29)	74.47 (26.12)	69.22 (19.85)
Abdomen (%)	79.50 (13.87)	81.57 (25.30)	57.88 (20.58)
Arm ST (%)	55.49 (18.27)	65.80 (26.63)	54.17 (19.98)
Arm SW (%)	62.71 (9.34)	65.08 (13.49)	56.57 (17.72)
Forearm ST (%)	38.98 (12.65)	53.73 (24.00)	39.40 (12.69)
Forearm SW (%)	51.34 (11.80)	62.57 (13.59)	47.26 (13.34)
Hand ST (%)	44.37 (19.82)	49.64 (21.32)	41.99 (30.95)
Hand SW (%)	34.36 (13.06)	46.93 (19.96)	47.71 (16.69)
Head (%)	54.33 (11.81)	58.15 (14.06)	60.06 (18.41)

Table 9: Movement onset of each SCoM from the AO expressed as percentage of the total GI duration. No significant differences across groups were found (Dunn's test, p-value<0.05 adjusted with Bonferroni correction for multiple comparisons).
Abbreviations: AO: APA onset; GI: gait initiation; SCoM: segmental centre of mass.

Postural asset and GI

Postural angles were not influence by both the AM and the BoS in the three cohorts. The analysis of the postural asset revealed significant alterations in both the pathological groups (**Table 10**). In particular, all PD patients showed increased trunk forward flexion and thigh angle with respect to HC. These alterations were more pronounced in the PDF group, even if there was no statistical difference between the two pathological cohorts. The postural asset did not show to have a significant impact on the GI outcome variables (**Table 11**). As expected, the shank angle was correlated to some IMB measurements, even if not significantly after correction for multiple comparisons.

	HC	PDNF	PDF
Trunk angle (°)	4.08 [a, b] (2.43)	9.06 [a] (4.37)	12.58 [b] (5.65)
Thigh angle (°)	6.31 [a, b] (2.69)	0.54 [a] (3.70)	-0.48 [b] (4.00)
Shank angle (°)	9.22 (2.93)	10.67 (2.77)	10.95 (2.47)

Table 10: Postural angles in the three recruited groups. Please refer to **Figure 34** for a description of the analysed angles. [a] HC vs. PDNF, [b] HC vs. PDF, [c] PDNF vs. PDF, Dunn's test, p-value<0.05 adjusted with Bonferroni correction for multiple comparisons.

	HC	Spearman's ρ	p-val
Shank angle (°)	IMB average velocity (mm/s)	0.32	0.014
	IMB average velocity AP (mm/s)	0.31	0.016
	IMB maximal velocity AP (mm/s)	0.38	0.003

Table 11: Only significant correlations between postural angles and GI measurements are shown (partial correlation analysis, Spearman's ρ, p-value<0.05). No prediction was significant after Bonferroni correction for multiple comparisons. Please refer to **Table 3** for a detailed description of all GI variables.

7.2.4. Discussion

In this work I aimed at characterizing alterations of GI preparation and execution in PD patients suffering from FoG. Both GI planning and performance were affected in patients with PD and FoG, as shown by the reduction of several measurements of the IMB, UNL, and stepping phase in the PDF group with respect to healthy controls. Specifically, the IMB and stepping measurements were progressively reduced from HC to PDNF and PDF, while the CoP displacement in the AP direction during the UNL phase was significantly altered in the PDF group only. Of relevance, the movement sequencing was preserved in both PDNF and PDF, thus confirming that the motor timing underlying GI is maintained in PD [16] regardless of the presence of FoG. Still, I found a relevant variability of segmental movement onset, especially in patients. This finding may be related to difficulties in putting into action the pre-programmed sequencing of GI. Further investigations on larger cohorts are warranted to better elucidate this aspect.

Of note, previous scientific works on the topic showed modest agreement in identifying alterations of GI specific for FoG, possibly because of the variable influence of several confounding factors. In this work, I developed a robust methodological approach designed to minimize and control this bias. First, I recruited groups of patients well-matched for both UPDRS-III and Hoen & Yahr (**Table 7**). In assessing the motor performance, I avoided "reaction-time" start signals, as they might alter *per se* the GI performance of patients with FoG [25], [64], [259], [372], [439]. Additionally, considering the variable effect of medication on FoG [25], [258], [435] and GI in patients with PD [38], all patients were examined after at least 12h from the last dose of dopaminergic drugs. Initial feet position was also shown to impact on the execution of GI [112], [420] specifically in PD patients suffering from FoG, despite the absence of FoG-related alterations of the BoS [28]. Therefore, the recruited groups were not only matched for the BoS and AM, but for the first time the influence of these two sets of variables was assessed and removed.

Alterations of the IMB measurements in both the PDNF and PDF groups suggest a PD-related impairment of *feedforward motor control* [38] at GI [10], [66], [69], [81], [85]–[90]. IMB phase during APA is modulated by top-down *feedforward* control in the context of the cortico-basal ganglia-thalamo-cortical network, with an important contribution of the SMA and the striatum [10], [20], [172], [419], [448]. Striatal dopamine deficiency might be at the basis of APA alterations in patients with PD [75]. Considering the prominent role of the SMA in the generation of the APA [20], [422], [436], [438], [449] and its impairment in patients with a positive history of FoG [45], I speculate that IMB measurements in PDF might be particularly affected because of a deficient or altered activity of this cortical area.

Consequently, PD patients may rely on bottom-up somatosensory signals to the cerebellum and the parietal cortex [246] as a compensatory mechanism to sustain poor *feedforward* motor control (premotor-cerebellar-parietal integration [246], [423], [450]–[454].

Conversely to IMB, the UNL indeed relies on proprioceptive *feedback* [455] and alterations of the CoP displacement in the AP direction during the UNL phase would additionally some difficulties of PD with FoG in the integration of somatosensory information, needed for the last adjustments prior to the step.

The activity of the cerebellum might have a regulatory role on the movement by modulating its rhythmic timing [246], [446], [447]. The correct temporal timing of the movement [16] would additionally suggest though a still preserved and compensating activity of the cerebellum in both PDNF and PDF. Such activity might have prevented the occurrence of FoG episodes during my recordings. Further neuroimaging studies (e.g., PET studies) are warranted to confirm these hypotheses.

Last but not least, in this work I explored the differences in the postural asset preceding GI between healthy controls and patients, and their influence on the subsequent motor performance. Both PD groups showed increased trunk and thigh flexion compared to HC. Stooped posture is a well-known feature of PD [456] and related to increased axial rigidity [457].

As expected [382], [393], [441]–[445], trunk was more flexed in the PDF group, despite the difference with the PDNF did not reach statistical significance. Thigh angle was instead decreased in both patient groups with respect to the normative data. As the trunk angle, the thigh angle was more compromised - even if not significantly - in the PDF group, which showed a negative average value. This result indicates that the hip centre of rotation in PDF patients was -in most of the cases- behind the knee centre of rotation, thus suggesting excessive hip/knee flexion [458]. It is important to notice that postural angles are all part of a unique kinematic chain, thus influencing each other for effective maintenance of postural control [459], [460]. In this context, increased thigh flexion might help counteracting the excessive bending of the trunk, as suggested by Aminiaghdam and coll. [461]. Indeed, increased trunk flexion would move forward the position of CoM, thus favouring forward propulsion, but also limiting the margin of stability and balance maintenance [462].

The representation of the body position can be affected by postural changes, thus inducing a re-scale of the APA properly adapted to the altered postural framework [10], [104], [108], [440], [460]. Surprisingly, in the studied cohort the postural asset did not show a relevant impact on the subsequent GI execution, possibly as postural angles may significantly influence the GI outcome variables only when greatly altered with respect to the physiological range [104], [107], [440]. Of

relevance, some IMB measurements were related to the shank angle (even if not significantly after correction for multiple comparisons). This result is in accordance with the inverted pendulum model, which points toward the "ankle strategy" as the main mechanism for regulating the position of the CoP during upright posture and postural transitions [4], [37], [61], [63], [81], [96], [125], [126], [463], [464]. Further evidence supporting the fundamental role of the muscles acting on the ankle joint at GI was shown by Delafontaine and coll., who induced a reduction of CoP displacement during APA in HC by reducing the range of motion of the ankles by means of a rigid orthosis [119]. In this framework, my results showed that even if stooped posture is an important destabilizing factor for PD patients, especially when positive history of FoG is present, it could not account for GI alterations.

7.2.5. Conclusions and study limitations

In this work, I studied the alterations of GI, posture, and their interplay in PD with and without a positive history of FoG. Of relevance, the influence of AM and BoS parameters on the biomechanical measurements was for the first time assessed and removed. Findings suggest that *feedforward* motor control is impaired in PD, especially if history of FoG is present. In addition, PDF patients show particularly altered *feedback* processing during the UNL phase causing poor weight transfer. The postural asset in PD is characterized by increased trunk flexion and decreased thigh flexion. However, postural abnormalities of PD are not directly related to impaired APA at GI.

Despite the relevance and novelty of these findings, this study suffers from some limitations. First, even if the number of healthy and pathological participants recruited for the GI assessment is in line with previous studies [14], [16], [17], [19], [20], [29], [30], [32], [33], results should be further confirmed on larger cohorts. Secondly, additional neuroimaging [134] and electrophysiological [465] studies should be performed to investigate the brain network derangements at the basis of the biomechanical alterations observed.

7.2.6. Publications

Palmisano, C, Beccaria, L, Haufe, S, Pezzoli, G, Isaias, I U, under review at Frontiers in Bioengineering and Biotechnology [362]

7.3. WP-3: GI in a model of risk of falling: Progressive Supranuclear Palsy

Aim: to define brain areas related to altered motor control at GI in patients with PSP

7.3.1. Background

PSP is a progressive atypical parkinsonism mainly characterized by early postural instability and falls [298], [310], [315]. For its peculiar clinical spectrum, this neurological disorder constitutes an *in-vivo* model of impaired postural control. Despite postural instability is the hallmark of PSP, our understanding of the brain alterations underlying this symptom is still surprisingly limited [315]. Investigating the anatomical correlates to impaired postural control in these patients might help not only to develop specific therapies, but also in unveiling the brain networks specifically responsible for balance maintenance.

Studies of postural control in patients with PSP are scarce [309], [349], [466], [467] and, besides this study of mine [75], only two investigated GI [308], [468]. Only Zwergal and coll. [349] and myself attempted imaging-kinematic correlations to deepen our understanding of the pathophysiological mechanisms behind PSP falls.

In general, patients with PSP show at GI poor braking capacity of the CoM during the stepping phase [468] and reduced moment CoP-CoM arm produced at the end of the IMB phase [308]. Despite the interest of these results, these studies suffered from major limitations. First, patients were examined without suspending [468] or standardizing [308] the intake of dopaminergic drugs. Second, the influence of AM and BoS on GI measurements was neglected. Additionally, these two studies failed to provide possible neural correlates to APA and GI alterations.

With regards to postural control, Ondo and coll. showed a very narrow coding of stability in patients with PSP as a result of marked alterations of CoP sway after concurrent alteration of visual and proprioceptive input. In this study, PSP patients also showed inadequate and incomplete muscular response (i.e., tibialis anterior and short- and medium-gastrocnemius) responsible for a delayed compensation of postural sways [466]. These results were further confirmed by Kammermeier and coll. who reported reduced resources and stability limits in PSP patients who actively keep the body segments close to vertical alignment. In this study, PSP patients maintained their upright stance with low velocities and frequencies, especially when deprived of visual flow. They also overreacted to small support surface perturbations with their whole body, which the authors comment as evocative of high centrally coding of tilt-related information scaling [309]. Posturography alone is however not able to precisely localise neuroanatomy of the central nervous system. A first attempt to relate the motor resultants of poor postural control in PSP with the underlying network pathophysiology was conducted by Zwergal and colleagues [349]. These authors correlated brain metabolic findings obtained with FDG PET with posturographic measurements, highlighting significant hypometabolism of the frontal and cingulate cortex, thalamus, caudate nucleus, and midbrain possibly responsible for altered postural control in PSP patients. Specifically, the thalamus and the caudate nucleus showed to have a prominent role in balance maintenance especially with somatosensory modulation.

In this work, I wanted to further explore the pathophysiology of postural control in PSP during GI, a motor task highly challenging for postural maintenance. By correlating the biomechanical

resultants of GI with brain metabolic alterations in patients with severe balance disorders, I aimed at capturing the brain areas chiefly involved in motor control at GI. For this study, I took advantage of previous results on the impact of AM and BoS, as described in paragraph 6.4.1. This is of great value, as PSP patients are expected to adopt enlarged BoS to prevent fall events.

7.3.2. Materials and Methods

Subjects

Twenty-six patients with PSP were recruited for the biomechanical assessment. Fourteen healthy controls matching patients for demographic and anthropometric data were selected from the healthy cohort of WP-1 for comparison. A second group of 12 age-matched HC, previously assessed with the same methods, was employed to define normative data for the brain metabolic assessment. We excluded subjects with vestibular problems, diabetes, cardiovascular pathologies or hypotension, neurological diseases other than PSP, orthopaedic issues or past major orthopaedic surgery. All patients were diagnosed according to the the Movement Disorder Society criteria [365] and classified as Richardson's syndrome because of the predominant early postural instability and oculomotor disfunctions [366]. Patients were evaluated with the PSPRS, composed by six areas: History, Mentation, Bulbar, Ocular motor, Limb motor, Gait and midline [317], [318]. The clinical assessment was performed in the morning after overnight suspension of all dopaminergic drugs.

Ethical approval

The study was approved by the local ethical committee. All subjects gave written informed consent prior participation according to the Declaration of Helsinki. Of note, the neuroimaging evaluation was part of patients' clinical workup and not performed exclusively for this study.

Biomechanical experimental setup

The recordings took place at the Gait Laboratory LAMB of the UNIMI of Milano. All patients performed the experiment in Med-OFF condition (i.e., after overnight suspension of all dopaminergic drugs). All subjects performed at least three GI trials (range: 3-7). Patients were allowed to rest between trials. The experimental protocol was designed similarly to the one of WP-1. Participants were instructed to stand quietly with their arms at their sides on the dynamometric force plate. Each subject self-selected the initial position of the feet. After 30s of quiet standing, they were asked to start walking at their preferred pace and with their self-selected swing foot, till the end of the walkway. Each subject performed also an *anatomic calibration* trial with eight additional markers, for the computation of the main AM (see paragraphs 6.3.1 and 6.3.3).

Biomechanical data analysis

Table 3 lists and describes all the calculated measurements. Briefly, I analysed the CoP displacement and velocity during the APA phases. Additionally, the movement, velocity and acceleration of the CoM were calculated at APA reference points. First step length, average and maximum velocity were also evaluated. The main AM and BoS measurements were computed for each subject. As previously described, I performed a partial correlation analysis between the GI variables and the BoS parameters, correcting for the AM, and between the GI measurements and

the AM, correcting for the influence of the BoS. To exclude any possible bias induced by the self-selected BoS, GI measurements dependent from any BoS parameter were excluded from further analyses. For GI measurements dependent from the AM, I applied the *decorrelation normalization* as described in paragraph 6.4.1.

Molecular imaging

A subset of 11 patients underwent PET with FDG within three months of the GI evaluation. These data served to investigate the brain metabolic alterations characterizing PSP. Details on neuroimaging data elaboration can be found in paragraph 6.2.2. FDG PET findings of an age-matched healthy group previously examined with the same methods were used as normative data.

Statistical analysis

The steps of the statistical analysis are similar to the ones adopted for WP-1 (see WP-1, paragraph 7.1). GI variables were averaged across the trials executed with the same swing foot. For the subjects who performed the task alternating the stepping foot, I included in the analysis only the trials executed with the swing foot most frequently used during the experiment. Outlier values were identified and removed by calculating the Mahalanobis distance. To verify the correct matching between the recruited cohorts, the demographic, clinical, AM and BoS measurements were compared with Student's t test or Wilcoxon test, p-value set at 0.05, basing on the data distribution of each variable (normality was tested with the Shapiro-Wilk test). Gender distribution was tested with Pearson's chi-squared test. For each group, I performed a partial correlation analysis between the GI measurements, AM and BoS parameters. The procedure is described in detail in the paragraph 6.4.1. Only partial correlation coefficients higher than 0.5 and with a p-value below 0.01 were considered significant. GI measurements not dependent from the BoS and decorrelated for the influence of the AM were compared across groups. I included in the subsequent correlation analysis with the clinical data and metabolic findings only the GI measurements significantly different between healthy controls and patients (Student's or Wilcoxon test as appropriate, threshold for significance adjusted with Bonferroni correction for multiple comparisons). Alterations of brain metabolic patterns in the PSP group were detected with a paired t test applied to voxel-wise comparison with respect to control subjects (analysis conducted with SPM, significance set at clusters with $k \geq 200$ voxels, p-value <0.05 FWE. Results were validated by means of a post hoc VOI analysis. The FDG uptake values of each VOI was computed and divided by the uptake of the whole cortex to reduce inter-subject variability. Clinical scores of the PSPRS scale and the uptake of hypometabolic brain areas were separately correlated to the altered GI biomechanical measurements (Spearman's ρ correlation coefficient, p-value <0.05).

7.3.3. Results

Subjects

Eight out of the 26 recruited patients were excluded from the analysis because of near fall episodes during the standing before the first step. Four additional patients were excluded because of the absence of the IMB phase. The group of the remaining 14 patients matched the HC group in terms of demographic, AM and BoS measurements (see **Table 12**).

	Data	HC	PSP
DEM	Gender (M/N)	9/14 (~64%)	6/14 (~43%)
	Age (yrs)	65.1 (3.4)	66.6 (4.7)
Clinical data	Disease duration (years)	(-)	5.3 (3.1)
	PSPRS History (0-24 score)	(-)	5.5 (2.1)
	PSPRS Mentation (0-16 score)	(-)	1.4 (1.1)
	PSPRS Bulbar (0-8 score)	(-)	2.9 (1.3)
	PSPRS Ocular motor (0-16 score)	(-)	8.3 (4.8)
	PSPRS Limb motor (0-16 score)	(-)	5.6 (1.9)
	PSPRS Gait and midline (0-20 score)	(-)	9.3 (2.7)
	PSPRS Total (0-100 score)	(-)	33.0 (9.7)
	LEDD (mg)	(-)	326.7 (304.0)
AM	Body Height (BH, cm)	169.4 (11.4)	163.7 (8.9)
	Limb Length (LL, cm)	88.9 (6.0)	84.0 (6.6)
	Foot Length (FL, cm)	25.0 (1.5)	24.3 (2.0)
	Body Mass (BM, Kg)	73.9 (13.2)	72.3 (11.6)
	Body Mass Index (BMI, Kg/m^2)	25.4 (3.7)	27.2 (5.3)
	Inter ASIS distance (IAD, cm)	28.6 (1.7)	30.6 (5.2)
BoS	BoS Area (BA, cm^2)	721.8 (126.5)	752.1 (113.4)
	BoS Width (BoSW, cm)	181.3 (51.1)	197.8 (40.9)
	Foot Alignment (FA, cm)	7.1 (4.1)	10.2 (6.0)
	Difference between feet extra-rotation angles (β_Δ, deg)	21.4 (9.3)	23.6 (6.8)
	BoS opening angle (β, deg)	20.1 (8.4)	21.3 (7.4)

Table 12: Demographic, clinical, AM and BoS data of the recruited subjects. Data are shown as mean (standard deviation). No statistical differences were found across the two groups ($p<0.05$, Wilcoxon test for all variables except for gender, compared with Pearson's chi-squared test).
Abbreviations: AM: anthropometric measurements; BoS: Base of Support; DEM: demographics; M: males; N: total number of subjects; PSPRS: Progressive Supranuclear Palsy Rating Scale; LEDD: levodopa equivalent daily dose.

BoS influence

Of relevance, no GI measurement was dependent from the BoS in the PSP group. Regarding the HC, the results of the partial correlation analysis were similar to the ones of WP-1 (paragraph 7.1) and WP-2 (paragraph 7.2). CoM velocity, acceleration and position with respect to the CoP calculated at the end of IMB were affected by the BoS. During the UNL phase the CoP displacement, average and maximum velocity towards the ML direction were also influenced by the BoS. In **Table 13**, all GI measurements independent from the BoS are listed for the two groups. For a complete description of all variables, please refer to **Table 3**.

Disease effect on GI

The biomechanical analysis of GI highlighted the complete disruption of APA programming in the PSP group (**Table 13**). In particular, the totality of the IMB measurements except for the phase duration (IMBT) was altered in the pathological cohort. The AP displacement and velocity of the CoP during UNL was instead preserved, but the resulting velocity and acceleration of the CoM at the end of this phase was decreased. Also, the time needed for shifting the weight to the stance foot (UNLT) was significantly prolonged with respect to the HC. The stepping phase showed alterations in both CoM velocity and distance from the CoP (TOCoMV and TOCoPCoM), first step length, maximal and average velocity (SL, SMV and SAV). Results of the statistical comparison between HC and PSP are shown in **Table 13**.

Clinical features and correlations with GI measurements

Table 14 shows the significant correlations between the clinical scores and the GI measurements. Only GI measurements different across groups were included in the correlation analyses with the clinical scores. Of relevance, while disease severity as evaluated by PSPRS scores correlated with GI outcome variables, disease duration was not related to the motor performance. In particular, the PSPRS categories regarding motor impairment (i.e., Limb motor and Gait and midline) were correlated with biomechanical variables of both the APA and stepping phase.

Metabolic features

In the PSP group six hypomethabolic areas were identified by the FDG PET: the right dorsolateral prefrontal cortex (cluster peak coordinates: x=46, y=14, z=50; k=381, pFWEcorr=0.005, Z-score=4.43), the left supplementary motor area (SMA, cluster peak coordinates: x=-8, y=18, z=62, k=221, pFWEcorr=0.039, Z-score=4.91), the middle cingulate cortex (cluster peak coordinates: x=12, y=4, z=38, k=493, pFWEcorr=0.01, Z-score=4.48), the left caudate nucleus (cluster peak coordinates: x=-14, y=6, z=12, k=366, pFWEcorr=0.006, Z-score=6.76) the medial thalamus and the midbrain (cluster peak coordinates: x=8, y=-20, z=12, k=2184, pFWEcorr<0.001, Z-score=6.31; subcluster peak coordinates: x=8, y=-20, z=-12, pFWEcorr<0.001, Zscore=6.22, respectively). The metabolic uptake values of these brain areas were correlated with the GI measurements which differed across the two groups. Significant correlations are shown in **Table 14**.

GI measurements	HC	PSP
IMB duration (s)	0.38 (0.09)	0.42 (0.20)
IMB displacement (mm)	66.7 (23.9) *	22.3 (10.3) *
IMB displacement ML (mm)	46.8 (18.5) *	18.2 (10.3) *
IMB displacement AP (mm)	41.1 (16.5) *	3.0 (7.7) *
IMB average velocity (mm/s)	193.8 (87.1) *	64.0 (43.2) *
IMB average velocity ML (mm/s)	137.4 (69.9) *	54.7 (40.1) *
IMB average velocity AP (mm/s)	118.4 (52.8) *	22.2 (19.4) *
IMB maximal velocity (mm/s)	379.1 (171.2) *	125.9 (77.4) *
IMB maximal velocity ML (mm/s)	287.6 (134.1) *	114.5 (73.6) *
IMB maximal velocity AP (mm/s)	264.4 (120.4) *	59.0 (37.8) *
UNL duration (s)	0.35 (0.08) *	0.76 (0.33) *
UNL displacement AP (mm)	-12.3 (17.9)	-1.3 (26.9)
UNL average velocity AP (mm/s)	57.3 (29.7)	37.9 (35.4)
UNL maximal velocity AP (mm/s)	366.4 (172.1)	187.7 (87.6)
CoM velocity at UNL end (m/s)	0.22 (0.07) *	0.12 (0.04) *
CoM acceleration at UNL end (m/s^2)	1.45 (0.45) *	0.76 (0.29) *
CoP-CoM distance at UNL end (m)	0.08 (0.03)	0.05 (0.02)
Slope CoP-CoM vector at UNL end (°)	39.9 (12.3) *	64.4 (15.9) *
CoM velocity at swing toe off (mm/s)	0.86 (0.18) *	0.32 (0.13) *
CoM acceleration at swing toe off (mm/s^2)	1.18 (0.38)	0.85 (0.33)
CoP-CoM distance at swing toe off (mm)	0.30 (0.06) *	0.16 (0.08) *
First step length (m)	0.55 (0.09) *	0.30 (0.09) *
First step average velocity (m/s)	1.01 (0.14) *	0.35 (0.14) *
First step maximal velocity (mm/s)	3.11 (0.52) *	1.97 (0.82) *

Table 13: List of GI measurements not dependent from the BoS in all groups. Data are shown as mean (standard deviation) before the decorrelation normalization process for sake of data intelligibility. ML displacement was defined positive towards the swing foot and towards the stance foot for the IMB and UNL phase, respectively. For both IMB and UNL, the AP displacement was expressed as positive when oriented backwards. For a detailed description of all variables please refer to **Table 3**. *: significant p values after Bonferroni correction for multiple comparisons, Student's or Wilcoxon test as appropriate.

		GI measurements	Spearman's ρ
PSPRS	History	UNL duration	0.53
	Limb motor	IMB average velocity ML	-0.58
		UNL duration	0.60
		CoP-CoM distance at UNL end	-0.59
	Gait and midline	UNL duration	0.59
		CoM velocity at swing toe off	-0.59
		First step maximal velocity	-0.57
FDG PET	Left caudate nucleus	IMB average velocity AP	0.66
		CoM velocity at UNL end	0.81
		CoP-CoM distance at swing toe off	0.74
	Left SMA	Slope CoP-CoM vector at UNL end	0.72
	Medial Thalamus	CoP-CoM distance at swing toe off	0.69
	Midbrain	CoP-CoM distance at swing toe off	0.70
	Middle Cingulate Cortex	CoM velocity at UNL end	0.64

Table 14: Clinical and biomechanical correlations with FDG PET findings. Only significant correlations are shown (Spearman's ρ correlation, $p<0.05$, uncorrected). For a detailed description of all GI variables, refer to **Table 3**.
Abbreviations: CoM: centre of mass; CoP: centre of pressure; FDG: 2-deoxy-2-[18F]fluoro-D-glucose; GI: gait initiation; IMB: imbalance; LEDD: levodopa equivalent daily dose; PET: positron emission tomography; PSPRS: Progressive Supranuclear Palsy Rating Scale; UNL: unloading.

7.3.4. Discussion

To my best knowledge, this is the first research work aiming to relate biomechanical performance at GI and brain metabolic alterations in these patients. Of relevance, I analysed patients with PSP in Med-OFF condition, also accounting for the influence of the AM and BoS in the evaluation of GI, two aspects overlooked in the previous works on the topic.

Biomechanical measurements showed a severe disruption of APA programming at GI in patients with PSP. Of relevance, four of the included patients did not present the IMB phase. IMB phase is the part of APA directly related to *feedforward* motor control. The absence of the IMB phase might suggest that these patients are not able anymore to put into action pre-programmed motor sequences to effectively accelerate forward the CoM while dynamically controlling balance [10], [20], [66]. PSP patients would rather move the CoP immediately toward the stance foot at the onset of GI, as previously suggested by Amano and coll. [308]. In the remaining patients, IMB phase was present but showed major alterations. Displacement and velocity of CoP during IMB phase were strongly reduced, particularly towards the AP direction, and not compensated during the subsequent UNL phase, as observed instead in patients with PD (WP-1,

paragraph 7.1). This led to a reduced CoP-CoM distance and vector slope at the end of the UNL. The inability to effectively modulate CoP position together with rigidity and bradykinesia [306], [307], which may prevent the prompt stepping forward as shown by reduced first step length and velocity, might expose these patients to high risk of falls during postural transitions. Of relevance, the categories *Limb motor* and *Gait and midline* of the PSPRS clinical scale correlated mostly with GI timing variables. These findings suggest that the PSPRS clinical scale might be particularly sensitive in capturing the bradykinetic aspects of the motor behaviour of these patients.

The neuroimaging findings highlighted which supraspinal areas are related to the disruption of *feedforward* motor control at GI observed in these patients. The caudate nucleus seems to have a predominant role in this process particularly for the production and control of the APA, as shown by the correlation of the metabolic uptake of this region with biomechanical variables of IMB, UNL and stepping phases in patients with PSP. This is in line with the findings of WP-1 (paragraph 7.1), where striatal dopamine was shown to be involved in GI execution in patients with PD [38]. Of relevance, patients with PSP were additionally characterized by hypometabolism of the SMA, a cortical area implicated in the production of the APA [20], [422], [438]. The uptake values of the SMA correlated positively with the slope of the vector connecting CoP and CoM at the end of the UNL phase, thus further supporting the role of this brain region in forward propelling the CoM during GI. Of note, postural instability in parkinsonian patients was shown to be related to caudate atrophy and poor connectivity between this nucleus and the SMA [469]. Also, the SMA was proven to be involved in the sequencing, online changing, and switching between motor programs [45], [436], [437]. Considering the multiple anatomical and functional connections of the basal ganglia with the cortex, thalamus and brainstem [406], [407], [425], [428], [470] my findings support the hypothesis of the importance of these structures, particularly the striatum [38] and their interplay with the SMA in *feedforward* motor control at GI and task execution, as in modulating locomotion in general [45], [471].

The results of the FDG uptake of the cingulate cortex were positively correlated to the CoM velocity at the end of the UNL (**Table 14**). The cingulate cortex is involved in several functions relevant for an effective motor control, such as executive and attentive functions, decision making, and performance monitoring [472]. It is not well-know its function in locomotion control, but some evidence points towards its possible role in handling feedback signals and information about the environment in order to adapt the gait pattern accordingly [9], [134], [139], [246], [473]. Also, together with the SMA it may favour the transition from linear walking to a more controlled gait [9]. The findings of my study fit well in this framework, suggesting a more cautious GI strategy, characterized by lower CoM velocity, in presence of altered feedback signals from the cingulate cortex.

The metabolic uptake values of thalamus and midbrain were decreased in PSP patients and correlated specifically with the final moment arm of the CoM. During locomotion, the thalamic nucleus was shown to play a relevant role in integrating information from the basal ganglia with cerebellar and somatosensory inputs, directly regulating the activity of the cortex during the various phases of the gait cycle [474]. The thalamus is particularly involved in gait modulation, e.g. during the adaptation of the gait pattern to a complex terrain or during transition from standing to walking [438], [474]. In PSP patients, previous works showed poor functional

connectivity between the thalamic region and other areas of the locomotor network, such as the SMA, the striatum, the cerebellum [475]. Of relevance, in PSP patients the thalamic and caudate hypometabolism were both related to increased CoP sway path during postural maintenance, but only the thalamus was engaged by the modulation of sensory inputs (i.e., eyes open/close and head straight/extended) [349]. These results suggest that if basal ganglia may be mainly responsible for APA programming, the activity of the thalamus may be instead dedicated to the optimization of the stepping phase by integrating the basal ganglia output with ascending somatosensory and cerebellar information.

The midbrain area includes the PPN and the cuneiform nucleus, both fundamental relay nodes in the supraspinal locomotor network, receiving inputs from the cortex, the basal ganglia and the cerebellum and projecting to the thalamocortical and reticulospinal pathways [476]. Our understanding of the role of different Midbrain nuclei in the control of human locomotion is very limited. Neuronal loss at the PPN level might contribute to gait disorders and postural instability in advanced PD patients [476]–[478]. A case study reported that an haemorrhage at the pontomesencephalic junction in the right pedunculopontine area caused inability to stand and stepping in an elderly woman [479]. DBS of the PPN provides additional information supporting this hypothesis. Low-frequency stimulation of the PPN can improve postural instability and gait in PD patients [480], [481], and promoted the normalization of the backward shift and velocity of the CoP during IMB and the velocity of the stepping at GI [481], but results are still controversial [478], [482].

PPN was also a target for DBS in patients with PSP [352] either alone [357]–[360] or in combination with the stimulation of the GPi [358]. Results in PSP were controversial and clinical efficacy not remarkable, but this might possibly be related to the difficulty of accurate targeting this multifaceted structure [478], to the lack of knowledge of the complex neurophysiological substrate of the locomotor network [315] and to the degeneration of the PPN in PSP patients [478], as suggested by my study. Indeed, my findings showed a correlation between the hypometabolism of the Midbrain and the final arm of the moment applied to the CoM (TOCoPCoM), supporting the hypothesis that the PPN might be the gateway node of the locomotor network, which would allow the appropriate forward propulsion at GI.

7.3.5. Conclusions and study limitations

In this work, I related for the first time brain metabolic alterations and GI biomechanics in patients with PSP, as a putative *in vivo* model of subjects with a distinctive deficit in postural maintenance. Findings suggested a different and selective involvement of the Caudate nucleus, Cingulate cortex, Thalamus, and Midbrain.

This study deepened our knowledge on the different nodes of the supraspinal locomotor network in APA programming at GI. Also, it corroborated the methodological pipeline developed in WP-1 (paragraph 7.1). to assess GI in healthy and pathological subjects accounting for the influence of AM and BoS for meaningful biomechanical-imaging correlations.

Despite the relevance and novelty of these findings, this study suffers from the small number of patients recruited, which derives mainly from the low prevalence of PSP. Only 14 patients were able to perform the biomechanical protocol and only 11 underwent the neuroimaging

assessment. Results should be further confirmed on larger cohorts. Considering the rarity of PSP [291], [293]–[295], [483], the number of patients recruited is still considerable and in line with previous studies [308], [349], [468]. Regarding the neuroimaging part, it is important to notice that the severe neuronal loss, which is present already at the time of the clinical diagnosis, might have masked significant correlations with the GI measurements [341]. Also, the low resolution of PET images might have prevented to identify the specific contribution to GI of small brain areas such as the PPN and CN.

7.3.6. Publications

Palmisano, C, Todisco, M, Marotta, G, [...], Pezzoli, G, Isaias, I U, NeuroImage: Clinical, 2020, 28:102408 [75]

Giordano, R, Canesi, M, Isalberti, M, Marfia, G, Campanella, R, Vincenti, D, Cereda, V, Ranghetti, A, **Palmisano, C**, […], Pezzoli, G., Frontiers in Neuroscience, 2021, 15:723227 [353]

7.4. WP-4: What is the STN contribution to standing and walking?

Aim: to investigate the neural activity changes of the STN between upright standing and linear walking

7.4.1. Background

High frequency (100-180Hz) STN DBS is a mainstay treatment for advanced stage PD, as greatly effective on the main motor symptoms (i.e., bradykinesia, rigidity and tremor) and able to reduce levodopa-related side effects (e.g., dyskinesia and motor fluctuations) [484], [485]. Still, its poor and sometimes even detrimental effect on gait disturbances [271], [273], [486], [487] represent a major limitation for a more widespread use of this treatment. In one study, about 42% of PD patients experienced a worsening of gait in the post-operative period while the global motor outcome improved [488]. STN DBS is particularly detrimental to gait rhythmicity and variability [489], FoG [490], and risk of falls [491], while it may improve stride length and lower limb range of motion [19], [492], [493]. The exact pathophysiological mechanism of this negative effect is still unclear, but one possible explanation could be related to the involuntary stimulation of the PPN nucleus, located just 5 mm away from the STN [432]. Indeed, high frequency stimulation of the PPN in patients with PD showed to deteriorate gait, while low-frequency stimulation lead to considerable gait improvement [480], [481]. In line, Moreau and coll. first demonstrated that lowering the frequency of stimulation from 130Hz to 60Hz can improve locomotion and FoG in PD patients [432], a finding further supported by other groups [494], [495].

Unfortunately, commercially available DBS devices allow only constant stimulation (continuous DBS, [cDBS]). The timely adjustment of the stimulation delivery (aDBS), would be an important improvement to optimize DBS efficacy, possibly allowing the reduction of the stimulation frequency during gait. Some attempts to modulate stimulation delivery are currently being investigated, and the first prototype devices for aDBS are forthcoming. The key factor for the successful design and application of aDBS paradigms remains the identification of the control variable to be used as an input signal to modulate stimulation changes [496].

The most studied biomarker are variations of the power of STN-LFP in the beta frequency band (13-30Hz) [52], [53], [288], [289], [496]. Unmedicated PD patients display an abnormal LFP synchronization and burst-like activity in the beta frequency range which is suppressed by levodopa intake [497]–[501] and cDBS [278] to an extent correlated with the improvement of akinetic-rigid symptoms [499], [502].

Consistent with these findings, aDBS devices under investigation aim to modulate stimulation delivery based on the detected beta power to ensure its suppression. However, identifying the beta band power exclusively as an expression of parkinsonian symptoms could be misleading in the development of aDBS protocols. Indeed, beta oscillations might carry relevant information in coding movements (and movement phases) [503], [504] and perceptual, cognitive processes [505]. Furthermore, beta power showed to be modulated by internally paced movement [497], [498] and motor programming and initiation [278], [504] and as such it could possibly be used as an input signal coding motor transitions (such as GI) and not a disease state.

The few studies reporting STN-LFP activity during human walking showed controversial results [42], [44], [47], [48], [284], [506], [507] with beta power being suppressed [47], [48], [506], [507]

or unchanged during gait [42], [44], [284]. Of relevance, all the studies showing a beta modulation during gait but one [47]were performed in the immediate post-operative period, thus being biased by the "stunning" effect (i.e., the peri-electrode edema due to leads placement).

The identification of robust biomarkers of gait is of fundamental importance for the successful application of aDBS paradigms and deserve further investigation [503]. In my most recent studies, I aimed at characterizing the neural activity of the STN nucleus during standing and walking in a group of implanted PD patients. I focused the analysis on the identification of power- and frequency-based neural features able to consistently distinguish in each patient standing and walking conditions. Besides power changes, I was mostly interested in exploring phase-resetting phenomena (e.g., frequency shifts) [508]–[512] as an alternative informational domain for understanding gait-related oscillatory electrical activity in the human basal ganglia and supraspinal locomotor network [513].

7.4.2. Materials and Methods

Subjects

I recruited eight patients with PD, diagnosed according to the United Kingdom Brain Bank Clinical Diagnostic criteria, implanted bilaterally with the DBS system Activa PC+S in the STN. For details on the DBS device and surgical procedure, please refer to paragraphs 4.3.5 and 6.3.2. Of relevance, all recruited patients were implanted at least six months before the experiment and had unchanged stimulation parameters and medication for at least the eight weeks prior to the recordings. Patients were not suffering from any neurological disorder other than PD, cognitive decline or mood disturbances as assessed by clinical scales (i.e., Parkinson neuropsychometric dementia assessment, Mattis dementia rating scale, Hamilton depression rating scale, and the non-motor symptoms scale). Psychometric tests were part of the clinical workup of the patients preparatory to the DBS implant. Before and after surgery, the motor state of the patients was evaluated with the UPDRS-III scale by a clinical expert in motor disorders (Prof. Isaias) in the following conditions (i) Stim-OFF and Med-OFF, (ii) Stim-ON and Med-OFF, (iii) Stim-OFF and Med-ON and (iv) Stim-ON and Med-ON. Please refer to paragraph 6.1 for further details on the medication condition during the assessments. Clinical and demographic data of the cohort are shown in **Table 15**. Eleven healthy subjects similar for demographic and anthropometric parameters (9 males, median age 60 years, range 50–66 years) were recruited for the biomechanical assessment. A second group of 15 healthy subjects (4 males, median age 67 years, range 44–74) underwent the neuroimaging assessment to define a normative set of data.

Ethical approval

The local ethical committee of the University Hospital of Würzburg approved the study. The Institutional Review Board of the Fondazione IRCCS Ca' Granda Ospedale Maggiore Policlinico di Milano approved the neuroimaging investigation on healthy controls. All subjects gave written informed consent, according to the Declaration of Helsinki.

Experimental setup

The experiment took place at the Gait Laboratory of the UKW of Würzburg. Patients were recorded in Stim-OFF (i.e., after two hours from the switching off of the stimulator) and Med-OFF condition (i.e., after overnight suspension of all dopaminergic drugs). Subjects were asked to

stand still for about 30s at the beginning of the walkway and at a verbal signal to start walking at their preferred speed and with their preferred stepping leg till its end. Initial stance position was not standardized to avoid any bias to the natural motor strategy of patients. The number of trials executed by each patient was limited by patients' clinical condition and ranged from six to ten. In addition to the assessment of standing and walking, each recording session started with an *anatomic calibration* which served for the computation of the main AM (see paragraphs 6.3.1 and 6.3.3).

Kinematic data analysis

First, I identified the standing and walking periods as the interval from the beginning of the trial till before the heel off of the swing foot and the interval at steady-state velocity, respectively. Please refer to 6.4.2 paragraph for further details. The standing was not biomechanically characterized as at the margin of the calibration volume of the optoelectronic system. During the walking period, I identified the strides by means of the markers placed on the feet. Thanks to the main gait cycle events (i.e., heel contacts and toe off) I was able to compute the stride duration, length, and velocity (normalized to subject's height), as well as the stance and double-support duration (time-normalized as a percentage of the stride duration). For each subject, variables were averaged over the trials. The analysis was performed on both patients and healthy controls. The identification of gait cycle events served also to identify windows of interest for the evaluation of the LFP activity in patients (see paragraph "LFP data analysis" later in the text).

Molecular imaging

Patients underwent a SPECT and FP-CIT to evaluate the residual density of the dopamine reuptake transporter (DAT) at the level of the striatum. Accordingly, the two analysed STN were classified as (+) and (-) when belonging to the less and most depleted hemisphere, respectively. A group of healthy control underwent the same protocol to define a normative set of data. Details on the neuroimaging data elaboration can be found in paragraph 6.2.

LFP data analysis

Recordings of LFP were performed with a bipolar derivation bridging the chronically active electrode [285] with a sampling frequency of 422 Hz and amplified by 1000. After the synchronization with the kinematic data and the pre-processing analyses (see paragraph 6.4.2 for further details), the LFP were decomposed in the time-frequency domain using 46 Morlet wavelets in the range 5-40Hz [395]. The time-frequency representation was epoched into strides, as identified by the kinematic events, and time-warped to a reference stride duration equal to the average stride duration of the patient cohort (1.15s). To avoid border effect introduced by the polynomial interpolation, the time-warping was applied with a window of 1.5s centred at each velocity peak of the swing foot. For the standing period, I identified windows of the same length (1.15s) with zero overlap and not related to any kinematic event. The PSD of walking and standing were computed as the average of the time-frequency representation by removing the 1/f component [397]. Separately for the two STN, classified as STN- and STN+, the PSD of walking and standing epochs were then analysed by means of mutual information techniques [398] with the Information Breakdown Toolbox [401]. I computed the information over the state of the system (i.e., walking or standing) carried by six features: i) the frequency showing the highest peak (f_{PEAK}) in the beta band (13-30Hz); ii) the power over the entire beta band (P_{BETA}); iii) the

power in the range f_{STAND}±2Hz (P_{SF}), where f_{STAND} was defined as the frequency peak during standing; iv) the power in the range f_{WALK}±2Hz (P_{WF}), where f_{WALK} was defined as the frequency peak during; v) the amplitude of the PSD at each frequency bin in the range (5-40)Hz; vi) the power in the range f_{MIF}±2Hz (P_{MIF}), where f_{MIF} was the maximally informative frequency, defined as the frequency bin showing the highest significant peak according to the spectral information [402], [403]. The information carried by the knowledge of a feature bilaterally and information redundancy were also computed [286]. For each single feature, I built a binary logistic regression classifier to test the ability of the feature in correctly classifying standing and walking epochs. An additional classifier using as input variables the P_{MIF} of both hemispheres was designed and tested (see "LFP preprocessing" for further details). The performance of each classifier was validated on 100 subsamples. Specifically, for each subject and subsample N standing and N walking epochs were randomly selected and merged, with N equal to the number of available walking epochs for the specific subject. The classifier was validated with a leave-one-out cross validation approach repeated on each subsample. The percentage of epochs correctly classified and the area under the ROC curve were computed to evaluate the performance of the classifier (see paragraph 6.4.2 for further details).

Statistical analysis

The Steel-Dwass all-pairs test (p-value set at 0.05) was used to compare the AM, the kinematic data and the neuroimaging findings between PD and HC. LFP features were compared across conditions (i.e, walking and standing) with a Wilcoxon signed rank test (p-value set at 0.05). Correlations between neuroimaging data and spectral features were also computed (Spearman's rho, p-value set at 0.05). All information analyses were performed with the Information Breakdown Toolbox [401]. Due to the limited number of observations, the information carried by the different features of the LFP signals were corrected with the Panzeri-Treves bias correction [404]. Significance was evaluated with a bootstrap test of 100 repetitions (threshold for significance equal to the 95% percentile of the information carried by randomized data). The information carried by each LFP feature over the state of the system was compared with a Wilcoxon signed rank test. The Clopper-Pearson test was used to evaluate the performance of the classifiers.

7.4.3. Results

Subjects and kinematic data

Clinical and demographic data of PD patients are shown in **Table 15**. Patients and HC did not differ for AM measurements (**Table 16**). PD patients showed decreased stride length, average and maximal velocity, but an overall preserved timing of the gait cycle (**Table 17**).

Molecular imaging data

All patients showed altered values of DAT density at a striatal level with respect to normative data. At a group level, DAT density in patients with PD was bilaterally decreased with respect to healthy controls for the Caudate and the Putamen nuclei and the Striatum (**Table 18**).

Subject	Age	Gender	Disease duration	LEDD		UPDRS					
				pre-DBS	post-DBS	pre-DBS		post-DBS			
						Med-OFF	Med-ON	Med-OFF		Med-ON	
								Stim-OFF	Stim-ON	Stim-OFF	Stim-ON
wue02	65	M	10	1100	800	40	23	39	19	17	16
wue03	61	M	18	2725	600	40	9	45	17	23	14
wue04	54	M	7	658	400	26	8	27	5	9	8
wue06	51	M	11	1133	180	46	11	48	12	11	6
wue07	61	M	10	650	220	43	24	29	15	8	9
wue09	55	M	19	1200	730	50	11	33	16	8	11
wue10	56	M	10	1200	550	69	14	65	25	20	5
wue11	53	F	11	1300	460	55	4	51	9	13	14

Table 15: Demographic and clinical data of the recruited patients. Each subject is indicated with an anonymization code. All patients benefited from the DBS implant as shown by the decrease of the LEDD and improvement of the UPDRS-III score in the post-operative evaluation.
Abbreviations: LEDD: Levodopa Equivalent Daily Dose; DBS: Deep Brain Stimulation; UPDRS: Unified Parkinson Disease Rating Scale.

ANTHROPOMETRIC MEASUREMENTS						
Subject	**Body height (cm)**	**Inter-ASIS distance (cm)**	**Foot length (cm)**	**Limb length (cm)**	**Weight (Kg)**	**BMI (Kg/m²)**
wue02	176.2	32.9	27.2	85.4	107.49	34.64
wue03	180.5	28.5	26.6	93.5	93.95	28.82
wue04	171.0	23.6	26.1	89.2	71.91	24.60
wue06	167.2	25.3	23.8	87.6	67.52	24.16
wue07	175.4	23.9	24.1	91.5	77.49	25.17
wue09	181.9	28.8	25.5	93.7	100.58	30.39
wue10	187.4	27.4	26.8	93.8	98.35	28.00
wue11	166.7	26.1	25.1	86.3	101.5	36.52
PD	175.1 (7.6)	26.8 (3.2)	25.5 (1.3)	89.6 (3.4)	89.26 (16.36)	29.07 (4.98)
HC	174.2 (6.5)	29.0 (3.5)	25.4 (1.5)	90.0 (3.0)	76.54 (10.74)	25.22 (3.58)

Table 16: AM parameters for each subject and the two groups (PD and HC). Data are shown as mean or mean (standard deviation) as appropriate. No significant differences were found ($p<0.05$, Steel-Dwass all pairs).
Abbreviations: BH: Body Height; BMI: Body Mass Index; FL: Foot Length; HC: Healthy Controls; PD: Parkinson's Disease.

GAIT CYCLE VARIABLES						
Subject	**Stride duration (s)**	**Stance duration (%stride)**	**Double support (%stride)**	**Stride length (%BH)**	**Stride average velocity (%BH/s)**	**Stride maximal velocity (%BH/s)**
wue02	1.18 (0.02)	65.11 (1.61)	30.55 (1.75)	72.38 (0.04)	65.80 (0.06)	195.01 (0.15)
wue03	1.18 (0.05)	62.38 (1.95	24.11 (1.97)	52.23 (0.04)	44.26 (0.05)	147.59 (0.25)
wue04	1.23 (0.03)	63.93 (1.16)	27.97 (1.69)	61.99 (0.03)	50.40 (0.04)	163.17 (0.13)
wue06	1.10 (0.04)	60.52 (1.37)	21.22 (1.94)	64.56 (0.09)	55.65 (0.07)	187.80 (0.20)
wue07	1.09 (0.04)	59.31 (2.07)	18.22 (3.41)	53.32 (0.06)	49.37 (0.07)	166.56 (0.20)
wue09	1.08 (0.03)	64.11 (1.65)	28.24 (2.59)	62.03 (0.06)	52.57 (0.05)	165.61 (0.70)
wue10	1.16 (0.04)	63.66 (1.57)	27.07 (2.22)	66.12 (0.07)	60.66 (0.05)	181.25 (0.19)
wue11	1.18 (0.04)	65.55 (1.57)	31.03 (2.48)	54.58 (0.05)	46.26 (0.05)	151.75 (0.13)
PD	1.15 (0.05)	63.07 (2.19)	26.05 (4.52)	60.94* (6.99)	53.12* (7.28)	169.84* (16.82)
HC	1.13 (0.09)	62.31 (1.62)	24.58 (3.32)	72.00* (6.41)	64.17* (9.37)	199.63* (21.44)

Table 17: Gait cycle variables for each subject and the two groups (PD and HC). Gait cycle variables were averaged across strides. Data are shown as mean (standard deviation). *****: p<0.05, Steel-Dwass all pairs.
Abbreviations: BH: Body Height; HC: Healthy Controls; PD: Parkinson's Disease.

Subject	**Caudate L**	**Putamen L**	**Striatum L**	**Caudate R**	**Putamen R**	**Striatum R**	**STN-**
wue02	0.88	0.57	0.72	1.43	0.91	1.17	L
wue03	0.49	0.31	0.40	0.31	0.28	0.30	R
wue04	1.15	0.7	0.93	0.58	0.44	0.5	R
wue06	1.31	0.59	0.95	1.56	0.91	1.2	L
wue07	0.92	0.64	0.76	1.22	0.79	1	L
wue09	0.72	0.48	0.61	0.62	0.37	0.49	R
wue10	0.97	0.5	0.75	1.2	0.74	0.96	L
wue11	1.15	0.79	0.96	1.41	0.74	1.05	L
PD	0.95* (0.26)	0.57* (0.15)	0.76* (0.19)	1.04* (0.47)	0.65* (0.25)	0.83* (0.35)	(-)
HC	2.57 (0.57)	2.30 (0.42)	2.33 (0.48)	2.62 (0.52)	2.23 (0.48)	2.30 (0.48)	(-)

Table 18: Neuroimaging findings. Values are shown as mean (standard deviation) and refer to the non-displaceable binding potential (BPND) of dopamine reuptake transporters (DAT) at the level of the caudate nucleus, putamen and striatum separately for the two hemispheres. Striatal values allowed to identify the STN belonging to the most (STN-) and less (STN+) depleted hemisphere for grouping LFP recordings across subjects. *****: p<0.05, Steel-Dwass all pairs.
Abbreviations: HC: Healthy Controls; L: Left hemisphere; PD: Parkinson's Disease; STN: subthalamic nucleus; R: Right hemisphere.

LFP features during standing and walking

The PSD during standing and walking showed distinct frequency peaks in the beta band (f_{PEAK}) for each patient and for both hemispheres. Specifically, the PSD of all STN- and in five out of eight STN+ shifted towards higher frequency from standing to walking. The frequency shift was statistically significant for the STN- only (STN-: 3.6 (0.68; 8.06) Hz and STN+: 2.45 (-4.16; 16.34) Hz; results in the text are shown as *median (range)* from now on). The power over the beta band (P_{BETA}) and around the frequency peak during standing (P_{SF}) was instead not different between conditions for both STN. On the contrary, the power computed around the frequency peak during walking (P_{WF}) differed for both STN- and STN+ (**Figure 35**). In regard to the mutual information, f_{PEAK} carried significant information for 16 of 18 hemispheres (STN-, 0.35 (0.002; 0.83) bits and STN+, 0.35 (0.03; 0.60) bits), while all other LFP features were poorly informative over the ongoing activity (P_{BETA} , STN-: 0.05 (0.003; 0.21) bits and STN+, 0.06 (0; 0.35) bits, significantly informative in 8/16 hemispheres; P_{SF}, STN-: 0.01 (0; 0.18) bits and STN+: 0.03 (0; 0.11) bits, significantly informative in 8/16 hemispheres; P_{WF}, STN-: 0.02 (0;0.40) bits and STN+: 0.05 (0;0.58) bits, significantly informative in 7/16 hemispheres). Of relevance, the information carried by the f_{PEAK} was significantly higher with respect to the information carried by the other features. Of relevance, no feature was significantly correlated with neuroimaging findings.

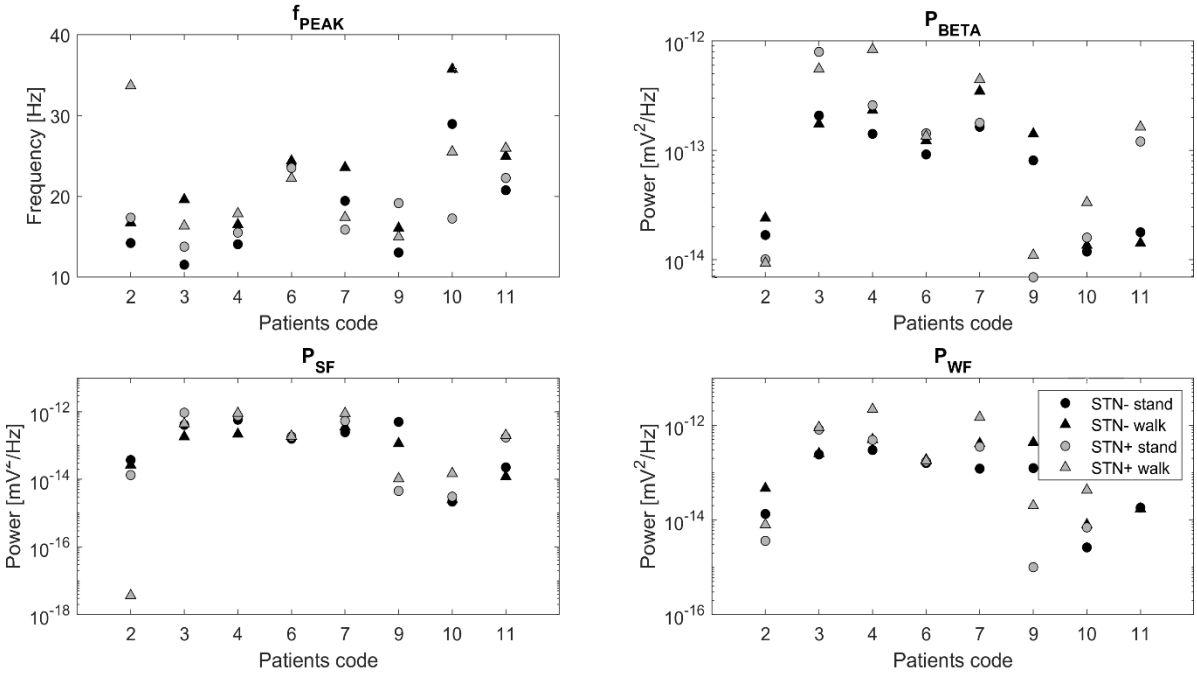

Figure 35: LFP features for the STN- (in black) and STN+ (in grey) during standing (circles) and walking (triangles) of each patient. P-values resulting from the comparison between the two conditions (i.e., stand and walk, Wilcoxon signed rank test) were significant only for the fPEAK of STN- and for PWF of both hemispheres.

Abbreviations: fPEAK: frequency with the highest beta peak (13-30Hz); fSTAND: frequency peak during standing; fWALK: frequency peak during walking; LFP: Local Field Potentials; PBETA: power over the entire beta band (13-30Hz); PSF: power in the range fSTAND±2Hz; PWF: power in the range fWALK ±2Hz; STN: Subthalamic Nucleus.

The maximally informative frequency

The maximally informative frequency (f_{MIF}) was defined for each STN as the frequency bin carrying the highest information over the state of the system. For all but one STN, it was located outside the range (f_{STAND}; f_{WALK}). The power computed over a four-Hertz range centered at the f_{MIF} (P_{MIF}) carried significant information for all but two STN (STN-: 0.16 (0.04; 0.41) bits and STN+: 0.25 (0.03; 0.58) bits). The joint knowledge of the P_{MIF} of both STN- and STN+ lead to an increase of information (both STN: 0.28 (0.14; 0.6) bits, significant for 16/18 STN) [286].

Performance of the classifiers

The classifiers based on P_{BETA}, P_{SF} and P_{WF} showed poor performance in identifying standing and walking epochs. On the contrary, the classifiers based on f_{PEAK} and P_{MIF} showed good ability in discriminating between the standing and walking conditions (performance with fPEAK, STN-: 0.87 (0.58; 1) and STN+: 0.90 (0.68; 1); performance with P_{MIF}, STN-: 0.78 (0.59; 0.92) and STN+: 0.84 (0. 71; 1)). Specifically, the first was significant for all patients and both STN and the latter for 7 out of 8 STN- and all STN+. By combining the P_{MIF} of the two hemispheres the performance of the classifier further improved (both STN, 0.90 (0.82; 1), significant for all patients [286].

7.4.4. Discussion

The results of this study showed a gait-related frequency shift in the STN activity of PD patients. This neural behaviour was exploited to identify a maximally informative frequency (f_{MIF}) whose power modulation (P_{MIF}) can reliably distinguish standing from walking condition at a single patient level. The P_{MIF} shows great potentialities as robust input signal for DBS protocols adaptive to the ongoing motor task.

In the past, intensive research has been conducted to develop aDBS devices with the idea of monitoring disease biomarkers, e.g., akinetic-rigid symptoms. While this approach might be optimal for monosymptomatic disorders (e.g., Essential tremor), it might be only partially effective in PD, where a combination of symptoms and compensatory mechanisms occurs depending on daily motor tasks and disease progression. In line, my work paves the way for a different approach to neuromodulation that aims at targeting changes in the motor state.

This study also expands our understanding of the role of the STN in human locomotion and the functioning of the supraspinal locomotor network. I envision a "clutch control" activity of the STN by conveying cortical (*feedforward*) and cerebellar (*feedback*) information by activating or inhibiting the MLR through direct glutamatergic projection or through the basal ganglia GABAergic output nuclei (i.e., the GPi and SNr). The frequency modulation recorded in the STN could then suggest the engaging of the "locomotor gear". Indeed, as suggested by Foffani and coll. [512], frequency modulation can be an effectively modality to convey the information flow across multiple, weakly connected circuits (autonomous oscillators [i.e., spinal central pattern generators], thalamocortical-basal ganglia, etc.) of a large-scale network such as the locomotor network [286].

Of note, frequency modulation during walking was observed in the absence of gait derangements (e.g., FoG) and did not correlate with dopaminergic striatal depletion. Kinematic data also showed that, despite the presence of akinetic-rigid symptoms, the timing of gait was in the

normal range for all recruited patients. These observations would support the notion that a gait-related subthalamic frequency shift in the beta range is a physiological rather than PD-related (pathological) neural behaviour. Network communication loss could directly result in gait derangements, as I showed with Pozzi and coll. [45] in FoG episodes. One can also envision that high frequency DBS might specifically interfere with frequency modulation mechanisms needed for effective postural transitions [286], [503].

This study also provides preliminary evidence that amplitude modulation might in some cases be only an epiphenomenon of other dynamics. Indeed, power changes over the beta band were not informative of the patient's motor state (i.e., walking). Their changes during standing and walking were most probably dependent on the frequency shift. This may incidentally well account for the large variability in previous studies regarding modulation in power of the signal recorded in STN during walking [42], [44], [47], [48], [284], [506], [507].

Because the devices currently available for aDBS are designed to monitor power rather than frequency modulation, I had to think of new metrics that would make the frequency shift a biomarker usable in terms of signal amplitude modulation. The P_{MIF} has this potential, as it can distinguish standing and walking only on the basis of a power modulation of a specific frequency range, centered at the maximally informative frequency. As such, it can be readily used in aDBS devices. Future studies are warranted to exploit its potential for gait-specific aDBS, for example as an input signal to reduce stimulation frequency during walking [432], [494], [495].

This study was among the first to apply information theory analysis on STN-LFP. The results provided preliminary evidence of the utility of such metrics for the identification of novel, disease-specific and task-related input signal for aDBS at a single patient level. Further confirmation of the general validity of such metrics for motor control comes from my more recent study on grasping movements in parkinsonian patients [504]. This approach opens new avenues for true patient-tailored delivery of neuromodulatory therapies.

Conclusions and study limitations

This study has greatly deepened our understanding of the functioning of the supraspinal locomotor network in PD. In this work, I identified a reliable input signal (P_{MIF}) to detect the walking state (from standing) in individual patients with PD and DBS. This work paves the way for new paradigms of aDBS, allowing proper adjustment of stimulation delivery based on the ongoing motor task and the optimization of the treatment of gait disturbances in patients with PD.

Despite the relevance and novelty of these findings, this study suffers from some limitations. First, although in line with previous studies [42], [44], [47], [48], [284], [506], [507], the number of patients recruited is limited to generalize the results obtained. Of note, at the time of the study the device used for subcortical recordings was a prototype and only available in a very limited number and in a few centers. New devices (e.g., the Percept®, Medtronic, see chapter 8) will allow these results to be validated.

The second important limitation is that the frequency shift was detected by analyzing walking periods of several seconds. Any modulation of stimulation for walking using this input signal would therefore be delayed with respect to the onset of walking. My next goal is to define the

minimum time window, possibly the APA phase of GI, for timely adjustment of stimulation parameters (see chapter 8).

Publications

Arnulfo, G*, Pozzi, N G*, **Palmisano, C**, [...], Isaias, I U, PLoS ONE, 2018, 13(6): e019869 [44]

Canessa, A, **Palmisano, C**, Isaias, I U*, Mazzoni, A*, Brain Stimulation, 2020, 13(6): 1743–1752 [286]

*these authors equally contributed to the work

8. Conclusions and future perspectives

8.1. Overview of the achievements of my thesis-related works

1. Influence of the BoS and AM on the kinematic resultants of APA at GI (WP-1)
2. Role of putaminal dopamine loss on APA production in PD (WP-1)
3. Effect of levodopa intake on GI in PD (WP-1)
4. Specific FoG-related APA alterations at GI in patients with PD (WP-2)
5. Impact of posture on GI (WP-2)
6. GI alterations in patients with PSP (WP-3)
7. Brain metabolic correlates with GI abnormalities in patients with PSP (WP-3)
8. Role of the STN in gait control in patients with PD (WP-4)
9. Identification of STN biomarkers for standing and walking in patients with PD (WP-4)

8.2. What's next

In my thesis work, I deepened the understanding of the locomotor network and its dysfunctions in patients with PD and parkinsonism.

Being PD mainly a dopamine-deficiency syndrome, I chose this neurological disorder as a model to study the role of dopamine and basal ganglia circuitry in locomotor control. In these patients, the lack of dopamine causes a profound alteration of the basal ganglia output leading to specific difficulties in motor planning and regulation, especially during transitions of motor states.

GI is one of the most common motor transitions (from quite standing to steady state gait) in daily life activities and characterized by a preparatory phase (APA) easy to detect and characterize in a gait laboratory environment. In the context of PD and parkinsonism, this motor task is also of great relevance as it relates to high risk of FoG and falls, possibly suggesting a failure in the preparatory phase of GI in these patients. Patients with PSP were involved as well in my research activities, as typically characterized by poor motor control and undergoing PET scans for diagnostic purposes. These patients suffer chiefly from postural imbalance and falls backward as a direct expression of neural networks failure to control equilibrium. Biomechanical correlations with FDG PET allowed me to precisely identify the regional cerebral glucose metabolism related to balance maintenance. The combination of neuroimaging and biomechanical studies was indeed a distinctive feature of my works, which I further expanded by adding direct recordings of deep brain structures (i.e., the STN nuclei) in patients with PD, for a better assessment of human supraspinal locomotor network.

My thesis work first focused on the methodological approach to the biomechanical assessment of GI. Indeed, despite the kinematic and dynamic aspects of GI had been previously extensively investigated, the role of experimental conditions and confounding variables had been neglected, thus leading to controversial results. In WP-1, I designed a robust approach to minimize the influence of confounding variables on the GI outcome variables. The experimental setup and pipeline for the data analyses designed in my PhD studies might provide useful guidelines for further studies on the GI assessment of both healthy subjects and patients.

The approach developed in WP-1 granted for reliable kinematic and dynamic measurements of GI, which paved the way for investigating locomotor control in PD and PSP (WP-1, WP-2 and WP-3). Specifically, I was able to better define the contribution of putaminal dopamine in GI execution and describe the impact of levodopa on GI in parkinsonian patients (WP1). Additionally, the findings of WP-3 provided further insights on the different brain regions involved in the control of GI.

I further expanded my research activity by specifically analyzing GI in PD patients suffering from FoG by studying the peculiar features of the biomechanical resultants in these patients (WP-2). Of relevance, this study showed for the first time that GI impairment in PD is not related to postural alterations typical of these patients (i.e., excessive trunk and knee flexion). This investigation provided valuable information for future works aimed at characterizing neural dynamics for the identification of symptom-specific derangements of the supraspinal locomotor network and thus biomarkers predictive of the onset of falls or FoG.

As highlighted in the "Introduction", the methods available for assessing the supraspinal locomotor network have limited either temporal (e.g., PET and SPECT) or spatial (e.g., EEG) resolution. The EEG additionally suffers from contamination by motion-related artifacts and the need for multiple repetitions of the motor task, which is often difficult to achieve in severely impaired patients. A very promising new experimental strategy is using DBS devices that allow recording the neural activity of the implanted brain region. I was among the first researchers to investigate the activity of the STN during gait by using prototypal DBS devices able not only to stimulate but also to record the activity of the implanted nucleus (WP-4). In this context, an important part of my PhD activities focused on the test and use of these novel devices (i.e., Activa PC+S, Percept™ PC, and Alpha DBS) facing technical issues and artefacts in the recordings. Because of the technical limitations of these cutting-edge devices (see chapter 6), I decided to start studying the activity of the STN during linear unperturbed gait and upright standing, which is still largely unknown, to move next to GI and gait modulation. Despite the technical difficulties, the simple fact that these devices are now commercially available will make their use widespread and bring closer the possibility of adaptive neuromodulation.

These new DBS sensing devices granted the opportunity to study patients in an ecological and domestic setting. Still, precise laboratory evaluations remain necessary and an essential part of neurophysiological studies of the supraspinal locomotor network. It is therefore critical to develop new and more reliable setups for objective multimodal recordings of gait disturbances. Only in this way we will be able to describe the exact and distinctive pathophysiological derangements of each symptom (e.g., FoG) in the context of a more general network disorder, and then use this information for proper restorative neuromodulatory therapies. With this aim, during my PhD years I supervised a student for a Master thesis at the Politecnico di Milano for the validation of a fully immersive experimental virtual reality (VR) setup developed to study gait modulation. In collaboration with the colleagues of the Department of the Human-Computer Interaction of the University of Würzburg, we created a VR environment with a virtual agent (VA) programmed to cross the trajectory of the patient. The direction, walking velocity, and onset of the VA were defined based on the movement of the patient as detected in real time. Specifically,

during each walking trial the VA started moving to cross the patient's trajectory at one-meter distance. This consistently induced a modulation of gait speed or its interruption and reprise, which are, together with GI, the most likely context for the occurrence of FoG and falls. Preliminary recordings were very promising: the VR setup was able to induce gait *freezing* episodes otherwise not present in the real-life gait.

The development of new and more performing sensing devices and recording leads (e.g., SenSight™, Medtronic PLC), and more reliable EEG systems (e.g., dual layer mobile EEG [515]), eventually combined with new VR setups, will allow an ecological but standardized gait assessment and open new research horizons for more effective neuromodulation strategies tailored to specific gait problems of each patient.

We are just at the beginning of a fantastic new journey in the field of neuroscience and neuromodulation that will lead to fundamental discoveries about the human brain and to improve the quality of life for many patients with motor disorders.

9. List of publications

1. M. Vissani*, **C. Palmisano***, J. Volkmann, G. Pezzoli, S. Micera, I. U. Isaias, A. Mazzoni, Impaired reach-to-grasp kinematics in parkinsonian patients relates to dopamine-dependent, subthalamic beta bursts, npj Parkinson's Disease, 2021, 7:53

2. Y. Thenaisie*, **C. Palmisano***, A. Canessa, B Keulen, P. Capetian, M.C. Jiménez, J. Bailly, E. Manferlotti, L. Beccaria, R. Zutt, G. Courtine, J. Bloch, N.A. van der Gaagh, C.F. Hoffmannh, E.M. Moraud, I.U. Isaias, M.F. Contarino, Towards adaptive deep brain stimulation: clinical and technical notes on a novel commercial device for chronic brain sensing, J. Neural Eng., 2021, 18, 042002

3. W.J. Neumann, M.M. Sorkhabi, M. Benjaber, L. K. Feldmann, A. Saryyeva, J. K. Krauss, M.F., Contarino, T. Sieger, R. Jech, G. Tinkhauser, C. Pollo, **C. Palmisano**, […] A.A. Kühn, T. Denison, The sensitivity of ECG contamination to surgical implantation site in adaptive neurostimulation, Brain Stimulation, 2021, 14(5): 1301-1306

4. R. Giordano, M. Canesi, M. Isalberti, G. Marfia, R. Campanella, D. Vincenti, V. Cereda, A. Ranghetti, **C. Palmisano**, […], A. Rivera-Ordaz, G. Pezzoli, Brief research report Safety and effectiveness of cell therapy in neurodegenerative diseases: Take-home messages from a phase I study of progressive supranuclear palsy, Frontiers in Neuroscience, 2021, 15: 723227

5. **C. Palmisano**, G. Brandt, M. Vissani, N.G. Pozzi, A. Canessa, J. Brumberg, G. Marotta, J. Volkmann, A. Mazzoni, G. Pezzoli, C.A. Frigo, I.U. Isaias, Gait initiation in Parkinson's disease: impact of dopamine depletion and initial stance condition, Frontiers in Bioengineering and Biotechnology, 2020, 8:137

6. **C. Palmisano**, M. Todisco, G. Marotta, J. Volkmann, C. Pacchetti, C.A. Frigo, G. Pezzoli, I.U. Isaias, Gait initiation in progressive supranuclear palsy: brain metabolic correlates, NeuroImage: Clinical, 2020, 28:102408

7. A. Canessa, **C. Palmisano**, I.U. Isaias, A. Mazzoni, Gait-related frequency modulation of beta oscillatory activity in the subthalamic nucleus of parkinsonian patients, Brain Stimulation, 2020, 13(6): 1743–1752

8. V. Farinelli, **C. Palmisano**, S.M. Marchese, C.M.M Strano, S. D'Arrigo, C. Pantaleoni, A. Ardissone, N. Nardocci, R. Esposti, P. Cavallari, Postural control in children with Congenital Cerebellar Ataxia, Applied Science, 2020, 10:1606

9. I.U Isaias, J. Brumberg, N.G. Pozzi, **C. Palmisano**, A. Canessa, G. Marotta, J. Volkmann, G. Pezzoli, Brain metabolic alterations herald falls in patients with Parkinson's disease, Ann Clin Transl Neurol., 2020, doi: 10.1002/acn3.51013

10. **C. Palmisano**, G. Brandt, N.G. Pozzi, A. Leporini, V. Maltese, A. Canessa, J. Volkmann, G. Pezzoli, C.A. Frigo, I.U. Isaias, Sit-to-walk performance in Parkinson's disease: A comparison between faller and non-faller patients, Clin Biomech., 2019, 63:140-146

11. M. Arlotti, **C. Palmisano**, B. Minafra, M. Todisco, C. Pacchetti, A. Canessa, N.G. Pozzi, R. Cilia, M. Prenassi, S. Marceglia, A. Priori, P. Rampini, S. Barbieri, D. Servello, J. Volkmann, G. Pezzoli, I.U. Isaias, Monitoring subthalamic oscillations for 24 hours in a freely moving Parkinson's disease patient, Mov Disord., 2019, doi: 10.1002/mds.27657

12. N.G. Pozzi, A. Canessa, **C. Palmisano**, J. Brumberg, F. Steigerwald, M.M. Reich, B. Minafra, C. Pacchetti, G. Pezzoli, J. Volkmann, I.U. Isaias, Freezing of gait in Parkinson's disease reflects a sudden derangement of locomotor network dynamics, Brain, 2019, 142; 2037–2050

13. V. Farinelli, L. Hosseinzadeh, **C. Palmisano**, C. A. Frigo, An easily applicable method to analyse the ankle-foot power absorption and production during walking, Gait & Posture, 2019, 71:56-61

14. G. Arnulfo*, N.G. Pozzi*, **C. Palmisano**, A. Leporini, A. Canessa, J. Brumberg, G. Pezzoli, C. Matthies, J. Volkmann, I.U. Isaias, Phase matters: A role for the subthalamic network during gait, PLoS One, 2018, 13(6): e0198691

15. F. Turco, A. Canessa, C. Olivieri, N.G. Pozzi, **C. Palmisano**, G. Arnulfo, G. Marotta, J. Volkmann, G. Pezzoli, I.U. Isaias, Cortical response to levodopa in Parkinson's disease patients with dyskinesias, Eur J Neurosci., 2018, 48(6):2362-2373

Under review

16. **C. Palmisano**, L. Beccaria, S. Haufe, J. Volkmann, G. Pezzoli, I.U. Isaias, Gait initiation impairment in patients with Parkinson's disease and freezing of gait, under review at Frontiers in Bioengineering and Biotechnology

17. **C. Palmisano**, P. Kullmann, I. Hanafi, M. Verrecchia, M.E. Latoschik, A. Canessa, M. Fischbach, I.U. Isaias, Real-time avoidance of an obstacle dynamically adjusted to patient behavior: a study on gait modulation in fully immersive virtual reality, under review at Frontiers in Human Neuroscience

18. S. Haufe, **C. Palmisano**, F. Pellegrini, I.U. Isaias, Gait event prediction from surface electromyography in parkinsonian patients, under review at Frontiers in Human Neuroscience

*these authors contributed equally to the work

10. Bibliography

[1] R. J. Elble, R. Cousins, K. Leffler, and L. Hughes, 'Gait initiation by patients with lower-half parkinsonism', *Brain*, vol. 119, no. 5, pp. 1705–1716, 1996, doi: 10.1093/brain/119.5.1705.

[2] R. G. Cohen, J. G. Nutt, and F. B. Horak, 'Recovery from Multiple APAs Delays Gait Initiation in Parkinson's Disease.', *Front. Hum. Neurosci.*, vol. 11, p. 60, 2017, doi: 10.3389/fnhum.2017.00060.

[3] C. Schlenstedt *et al.*, 'Are hypometric anticipatory postural adjustments contributing to freezing of gait in Parkinson's disease?', *Front. Aging Neurosci.*, vol. 10, no. FEB, pp. 1–9, 2018, doi: 10.3389/fnagi.2018.00036.

[4] A. E. Patla, J. S. Frank, D. A. Winter, S. Rietdyk, S. Prentice, and S. Prasad, 'Age-related changes in balance control system: initiation of stepping', *Clin. Biomech.*, vol. 8, no. 4, pp. 179–184, 1993, doi: 10.1016/0268-0033(93)90012-7.

[5] N. Chastan *et al.*, 'Gait and balance disorders in Parkinson's disease: Impaired active braking of the fall of centre of gravity', *Mov. Disord.*, vol. 24, no. 2, pp. 188–195, 2009, doi: 10.1002/mds.22269.

[6] H. Stolze, S. Klebe, C. Zechlin, C. Baecker, L. Friege, and G. Deuschl, 'Falls in frequent neurological diseases: Prevalence, risk factors and aetiology', *J. Neurol.*, vol. 251, no. 1, pp. 79–84, 2004, doi: 10.1007/s00415-004-0276-8.

[7] S. N. Robinovitch *et al.*, 'Video capture of the circumstances of falls in elderly people residing in long-term care: An observational study', *Lancet*, vol. 381, no. 9860, pp. 47–54, 2013, doi: 10.1016/S0140-6736(12)61263-X.

[8] R. Tisserand, T. Robert, P. Chabaud, M. Bonnefoy, and L. Chèze, 'Elderly fallers enhance dynamic stability through anticipatory postural adjustments during a choice stepping reaction time', *Front. Hum. Neurosci.*, vol. 10, no. NOV2016, pp. 1–15, 2016, doi: 10.3389/fnhum.2016.00613.

[9] D. C. Hinton, A. Thiel, J. P. Soucy, L. Bouyer, and C. Paquette, 'Adjusting gait step-by-step: Brain activation during split-belt treadmill walking', *Neuroimage*, vol. 202, no. August, 2019, doi: 10.1016/j.neuroimage.2019.116095.

[10] E. Yiou, T. Caderby, A. Delafontaine, P. Fourcade, and J.-L. L. Honeine, 'Balance control during gait initiation: State-of-the-art and research perspectives.', *World J. Orthop.*, vol. 8, no. 11, pp. 815–828, 2017, doi: 10.5312/wjo.v8.i11.815.

[11] B. R. Bloem, J. M. Hausdorff, J. E. Visser, and N. Giladi, 'Falls and freezing of Gait in Parkinson's disease: A review of two interconnected, episodic phenomena', *Mov. Disord.*, vol. 19, no. 8, pp. 871–884, 2004, doi: 10.1002/mds.20115.

[12] B. R. Bloem, Y. A. M. Grimbergen, M. Cramer, M. Willemsen, and A. H. Zwinderman, 'Prospective assessment of falls in Parkinson's disease', *J. Neurol.*, vol. 248, pp. 950–958, 2001, doi: 10.1016/S0890-5401(03)00059-2.

[13] J. V. Jacobs, J. G. Nutt, P. Carlson-Kuhta, M. Stephens, and F. B. Horak, 'Knee trembling during freezing of gait represents multiple anticipatory postural adjustments', *Exp. Neurol.*, vol. 215, no. 2, pp. 334–341, 2009, doi: 10.1016/j.expneurol.2008.10.019.

[14] P. Crenna, C. Frigo, P. Giovannini, and I. Piccolo, *The initiation of gait in Parkinson's disease*, no. 5. Academic Press Limited, 1990.

[15] N. Gantchev, F. Viallet, R. Aurenty, and J. Massion, 'Impairment of posturo-kinetic co-

ordination during initiation of forward oriented stepping movements in parkinsonian patients', *Electroencephalogr. Clin. Neurophysiol.*, vol. 101, no. 2, pp. 110–120, 1996, doi: 10.1016/0924-980X(95)00253-H.

[16] R. Rosin, H. Topka, and J. Dichgans, 'Gait initiation in Parkinson's disease', *Mov. Disord.*, vol. 12, no. 5, pp. 682–690, 1997, doi: 10.1002/mds.870120509.

[17] S. E. Halliday, D. A. Winter, J. S. Frank, A. E. Patla, and N. L. G. Ontario, 'The initiation of gait in young, elderly, and Parkinson's disease subjects', *Gait Posture*, vol. 8, no. 1, pp. 8–14, 1998, [Online]. Available: https://journals-scholarsportal-info.myaccess.library.utoronto.ca/pdf/09666362/v08i0001/8_tiogiyeapds.xml%0Apapers3://publication/uuid/F1644F59-2A2C-4291-8889-5308B68014C3.

[18] C. J. Hass, D. E. Waddell, R. P. Fleming, J. L. Juncos, and R. J. Gregor, 'Gait initiation and dynamic balance control in Parkinson's disease', *Arch. Phys. Med. Rehabil.*, vol. 86, no. 11, pp. 2172–2176, 2005, doi: 10.1016/j.apmr.2005.05.013.

[19] P. Crenna *et al.*, 'Impact of subthalamic nucleus stimulation on the initiation of gait in Parkinson's disease', *Exp. Brain Res.*, vol. 172, no. 4, pp. 519–532, 2006, doi: 10.1007/s00221-006-0360-7.

[20] J. V. Jacobs, J. S. Lou, J. A. Kraakevik, and F. B. Horak, 'The supplementary motor area contributes to the timing of the anticipatory postural adjustment during step initiation in participants with and without Parkinson's disease', *Neuroscience*, vol. 164, no. 2, pp. 877–885, 2009, doi: 10.1016/j.neuroscience.2009.08.002.

[21] R. T. Roemmich *et al.*, 'Spatiotemporal variability during gait initiation in Parkinson's disease', *Gait Posture*, vol. 36, no. 3, pp. 340–343, 2012, doi: 10.1016/j.gaitpost.2012.01.018.

[22] G. Bonora, M. Mancini, I. Carpinella, L. Chiari, F. B. Horak, and M. Ferrarin, 'Gait initiation is impaired in subjects with Parkinson's disease in the OFF state: Evidence from the analysis of the anticipatory postural adjustments through wearable inertial sensors', *Gait Posture*, vol. 51, pp. 218–221, 2017, doi: 10.1016/j.gaitpost.2016.10.017.

[23] N. Giladi, J. Balash, and J. M. Hausdorff, 'Gait disturbances in Parkinson's disease', in *Mapping the Progress of Alzheimer's and Parkinson's Disease*, K. Academic/Plenum, Ed. New York, 2002, pp. 329–335.

[24] J. D. Schaafsma, Y. Balash, T. Gurevich, A. L. Bartels, J. M. Hausdorff, and N. Giladi, 'Characterization of freezing of gait subtypes and the response of each to levodopa in Parkinson's disease', *Eur. J. Neurol.*, vol. 10, no. 4, pp. 391–398, 2003, doi: 10.1046/j.1468-1331.2003.00611.x.

[25] J. G. Nutt, B. R. Bloem, N. Giladi, M. Hallett, F. B. Horak, and A. Nieuwboer, 'Freezing of gait: Moving forward on a mysterious clinical phenomenon', *Lancet Neurol.*, vol. 10, no. 8, pp. 734–744, 2011, doi: 10.1016/S1474-4422(11)70143-0.

[26] S. H. G. Mensink *et al.*, 'Additional weight load increases freezing of gait episodes in Parkinson's disease; an experimental study', *J. Neurol.*, vol. 261, no. 5, pp. 999–1008, 2014, doi: 10.1007/s00415-014-7274-2.

[27] A. C. de Souza Fortaleza *et al.*, 'Dual task interference on postural sway, postural transitions and gait in people with Parkinson's disease and freezing of gait', *Gait Posture*, vol. 56, pp. 76–81, 2017, doi: 10.1016/j.gaitpost.2017.05.006.

[28] S. L. A. Huffmaster, C. Lu, P. J. Tuite, and C. D. MacKinnon, 'The Transition from Standing to Walking Is Affected in People with Parkinson's Disease and Freezing of Gait', *J. Parkinsons. Dis.*, vol. 10, no. 1, pp. 233–243, 2020, doi: 10.3233/JPD-191649.

[29] A. Burleigh-Jacobs, F. B. Horak, J. G. Nutt, and J. A. Obeso, 'Step initiation in Parkinson's disease: Influence of levodopa and external sensory triggers', *Mov. Disord.*, vol. 12, no. 2, pp. 206–215, 1997, doi: 10.1002/mds.870120211.

[30] J. S. Frank, F. B. Horak, and J. Nutt, 'Centrally initiated postural adjustments in parkinsonian patients on and off levodopa', *J. Neurophysiol.*, vol. 84, no. 5, pp. 2440–2448, 2000, doi: 10.1152/jn.2000.84.5.2440.

[31] J. V. Jacobs and F. B. Horak, 'Abnormal proprioceptive-motor integration contributes to hypometric postural responses of subjects with parkinson's disease', *Neuroscience*, vol. 141, no. 2, pp. 999–1009, 2006, doi: 10.1016/j.neuroscience.2006.04.014.

[32] L. Rocchi, L. Chiari, M. Mancini, P. Carlson-Kuhta, A. Gross, and F. B. Horak, 'Step initiation in Parkinson's disease: Influence of initial stance conditions', *Neurosci. Lett.*, vol. 406, pp. 128–132, 2006, doi: 10.1016/j.neulet.2006.07.027.

[33] A. M. S. Muniz, J. Nadal, K. E. Lyons, R. Pahwa, and W. Liu, 'Long-term evaluation of gait initiation in six Parkinson's disease patients with bilateral subthalamic stimulation', *Gait Posture*, vol. 35, no. 3, pp. 452–457, 2012, doi: 10.1016/j.gaitpost.2011.11.006.

[34] L. Rocchi, P. Carlson-Kuhta, L. Chiari, K. J. Burchiel, P. Hogarth, and F. B. Horak, 'Effects of deep brain stimulation in the subthalamic nucleus or globus pallidus internus on step initiation in Parkinson disease: Laboratory investigation', *J. Neurosurg.*, vol. 117, no. 6, pp. 1141–1149, 2012, doi: 10.3171/2012.8.JNS112006.

[35] L. M. Hall, S. G. Brauer, F. Horak, and P. W. Hodges, 'The effect of Parkinson's disease and levodopa on adaptation of anticipatory postural adjustments', *Neuroscience*, vol. 250, pp. 483–492, 2013, doi: 10.1016/j.neuroscience.2013.07.006.

[36] E. V. Papa, O. Addison, K. B. Foreman, and L. E. Dibble, 'Reproducibility and responsiveness of gait initiation in Parkinson's disease', *J. Biomech.*, vol. 87, pp. 197–201, 2019, doi: 10.1016/j.jbiomech.2019.03.009.

[37] J. Massion, 'Movement, posture and equilibrium: Interaction and coordination', *Prog. Neurobiol.*, vol. 38, no. 1, pp. 35–56, 1992, doi: 10.1016/0301-0082(92)90034-C.

[38] C. Palmisano *et al.*, 'Gait initiation in Parkinson's disease: impact of dopamine depletion and initial stance condition', *Front. Bioeng. Biotechnol.*, vol. 8, no. 137, 2020, doi: 10.3389/fbioe.2020.00137.

[39] R. D. Seidler, D. C. Noll, and G. Thiers, 'Feedforward and feedback processes in motor control', *Neuroimage*, vol. 22, pp. 1775–1783, 2004.

[40] P. A. Guertin, 'Preclinical evidence supporting the clinical development of central pattern generator-modulating therapies for chronic spinal cord-injured patients', *Front. Hum. Neurosci.*, vol. 8, no. MAY, pp. 1–17, 2014, doi: 10.3389/fnhum.2014.00272.

[41] I. Pisotta and M. Molinari, 'Cerebellar contribution to feedforward control of locomotion', *Front. Hum. Neurosci.*, vol. 8, no. JUNE, pp. 1–5, 2014, doi: 10.3389/fnhum.2014.00475.

[42] J. Syrkin-Nikolau *et al.*, 'Subthalamic neural entropy is a feature of freezing of gait in freely moving people with Parkinson's disease', *Neurobiol. Dis.*, vol. 108, pp. 288–297, 2017, doi: 10.1016/j.nbd.2017.09.002.

[43] C. Anidi *et al.*, 'Neuromodulation targets pathological not physiological beta bursts during gait in Parkinson's disease', *Neurobiol. Dis.*, vol. 120, pp. 107–117, Dec. 2018, doi: 10.1016/j.nbd.2018.09.004.

[44] G. Arnulfo *et al.*, 'Phase matters: A role for the subthalamic network during gait', *PLoS*

One, vol. 13, no. 6, pp. 1–19, 2018, doi: 10.1371/journal.pone.0198691.

[45] N. G. Pozzi *et al.*, 'Freezing of gait in Parkinson's disease reflects a sudden derangement of locomotor network dynamics', *Brain*, vol. 142, no. 7, pp. 2037–2050, 2019, doi: 10.1093/brain/awz141.

[46] C. C. Chen *et al.*, 'Subthalamic nucleus oscillations correlate with vulnerability to freezing of gait in patients with Parkinson's disease', *Neurobiol. Dis.*, vol. 132, 2019, doi: 10.1016/j.nbd.2019.104605.

[47] F. Hell, A. Plate, J. H. Mehrkens, and K. Bötzel, 'Subthalamic oscillatory activity and connectivity during gait in Parkinson's disease', *NeuroImage Clin.*, vol. 19, no. February, pp. 396–405, 2018, doi: 10.1016/j.nicl.2018.05.001.

[48] A. Singh, A. Plate, S. Kammermeier, J. H. Mehrkens, J. Ilmberger, and K. Bötzel, 'Freezing of gait-related oscillatory activity in the human subthalamic nucleus', *Basal Ganglia*, vol. 3, no. 1, pp. 25–32, 2013, doi: 10.1016/j.baga.2012.10.002.

[49] J. B. Toledo *et al.*, 'High beta activity in the subthalamic nucleus and freezing of gait in Parkinson's disease', *Neurobiol. Dis.*, vol. 64, pp. 60–65, 2014, doi: 10.1016/j.nbd.2013.12.005.

[50] J. Wagner, S. Makeig, M. Gola, C. Neuper, and G. Müller-Putz, 'Distinct β band oscillatory networks subserving motor and cognitive control during gait adaptation', *J. Neurosci.*, vol. 36, no. 7, pp. 2212–2226, 2016, doi: 10.1523/JNEUROSCI.3543-15.2016.

[51] Y. Thenaisie *et al.*, 'Towards adaptive deep brain stimulation: clinical and technical notes on a novel commercial device for chronic brain sensing', *medRxiv*, p. 2021.03.10.21251638, 2021.

[52] M. Arlotti *et al.*, 'Monitoring subthalamic oscillations for 24 hours in a freely moving Parkinson's disease patient', *Mov. Disord.*, vol. 34, no. 5, pp. 757–759, 2019, doi: 10.1002/mds.27657.

[53] M. Arlotti *et al.*, 'Eight-hours adaptive deep brain stimulation in patients with Parkinson disease', *Neurology*, vol. 90, no. 11, pp. e971–e976, 2018, doi: 10.1212/WNL.0000000000005121.

[54] C. J. Hass *et al.*, 'The influence of Tai Chi training on the center of pressure trajectory during gait initiation in older adults', *Arch. Phys. Med. Rehabil.*, vol. 85, no. 10, pp. 1593–1598, 2004, doi: 10.1016/j.apmr.2004.01.020.

[55] O. Kiehn, 'Decoding the organization of spinal circuits that control locomotion', *Nat. Rev. Neurosci.*, vol. 17, no. 4, pp. 224–238, 2016, doi: 10.1038/nrn.2016.9.

[56] M. Martin, M. Shinberg, M. Kuchibhatla, L. Ray, J. J. Carollo, and M. L. Schenkman, 'Gait initiation in community-dwelling adults with Parkinson disease.', *Phys. Ther.*, vol. 82, pp. 566–577, 2002, doi: 10.1093/ptj/82.12.1264.

[57] C. J. Hass, D. E. Waddell, S. L. Wolf, J. L. Juncos, and R. J. Gregor, 'Gait initiation in older adults with postural instability', *Clin. Biomech.*, vol. 23, no. 6, pp. 743–753, 2008, doi: 10.1016/j.clinbiomech.2008.02.012.

[58] Y. Gahéry and J. Massion, 'Co-ordination between posture and movement', *Trends Neurosci.*, vol. 4, pp. 199–202, 1981, doi: 10.1016/0166-2236(81)90064-3.

[59] J. Massion, 'Postural changes accompanying voluntary movements. Normal and pathological aspects', *Hum. Neurobiol.*, vol. 2, no. 4, pp. 261–267, 1984.

[60] Y. Brenière, M. Cuong Do, and S. Bouisset, 'Are dynamic phenomena prior to stepping essential to walking?', *J. Mot. Behav.*, vol. 19, no. 1, pp. 62–76, 1987, doi:

10.1080/00222895.1987.10735400.
[61] Y. Brenière and M. C. Do, 'Control of Gait initiation', *J. Mot. Behav.*, vol. 23, no. 4, pp. 235–240, 1991, doi: 10.1080/00222895.1991.9942034.
[62] P. Crenna and C. Frigo, 'A motor programme for the initiation of foroward-oriented movements in humans', *J. Physiol.*, vol. 437, pp. 635–653, 1991.
[63] R. Lepers and Y. Brenière, 'The role of anticipatory postural adjustments and gravity in gait initiation', *Exp. Brain Res.*, vol. 107, pp. 118–124, 1995.
[64] A. Delval, C. Tard, and L. Defebvre, 'Why we should study gait initiation in Parkinson' s disease', *Clin. Neurophysiol.*, vol. 44, no. 1, pp. 69–76, 2014, doi: 10.1016/j.neucli.2013.10.127.
[65] A. Charlett, C. Weller, A. G. Purkiss, S. M. Dobbs, and R. J. Dobbs, 'Breadth of base whilst walking: Effect of ageing and parkinsonism', *Age Ageing*, vol. 27, no. 1, pp. 49–54, 1998, doi: 10.1093/ageing/27.1.49.
[66] A. E. Polcyn, D. C. Kerrigan, and J. J. Collins, 'Age-Related Changes in the Initiation of Gait: Degradation of Central Mechanisms for Momentum Generation', *Arch. Phys. Med. Rehabil.*, vol. 79, no. December, pp. 1582–1589, 1998.
[67] S. Patchay, Y. Gahéry, and G. Serratrice, 'Early postural adjustments associated with gait initiation and age-related walking difficulties', *Mov. Disord.*, vol. 17, no. 2, pp. 317–326, 2002, doi: 10.1002/mds.10074.
[68] G. A. Mbourou, Y. Lajoie, and N. Teasdale, 'Step length variability at gait initiation in elderly fallers and non-fallers, and young adults', *Gerontology*, vol. 49, no. 1, pp. 21–26, 2003, doi: 10.1159/000066506.
[69] J. Mickelborough, M. L. Van Der Linden, R. C. Tallis, and A. R. Ennos, 'Muscle activity during gait initiation in normal elderly people', *Gait Posture*, vol. 19, no. 1, pp. 50–57, 2004, doi: 10.1016/S0966-6362(03)00016-X.
[70] S. Vallabhajosula, T. A. Buckley, M. D. Tillman, and C. J. Hass, 'Age and Parkinson's disease related kinematic alterations during multi-directional gait initiation', *Gait Posture*, vol. 37, no. 2, pp. 280–286, 2013, doi: 10.1016/j.gaitpost.2012.07.018.
[71] S. Hesse, F. Reiter, M. Jahnke, M. Dawson, T. Sarkodie-Gyan, and K. H. Mauritz, 'Asymmetry of gait initiation in hemiparetic stroke subjects', *Arch. Phys. Med. Rehabil.*, vol. 78, no. 7, pp. 719–724, 1997, doi: 10.1016/S0003-9993(97)90079-4.
[72] C. Stackhouse, P. A. Shewokis, S. R. Pierce, B. Smith, J. McCarthy, and C. Tucker, 'Gait initiation in children with cerebral palsy', *Gait Posture*, vol. 26, no. 2, pp. 301–308, 2007, doi: 10.1016/j.gaitpost.2006.09.076.
[73] J. G. Remelius, J. Hamill, J. Kent-Braun, and R. E. A. Van Emmerik, 'Gait initiation in multiple sclerosis', *Motor Control*, vol. 12, no. 2, pp. 93–108, 2008, doi: 10.1123/mcj.12.2.93.
[74] V. Farinelli *et al.*, 'Postural control in children with cerebellar ataxia', *Appl. Sci.*, vol. 10, no. 5, pp. 1–13, 2020, doi: 10.3390/app10051606.
[75] C. Palmisano *et al.*, 'Gait initiation in progressive supranuclear palsy : brain metabolic correlates', *NeuroImage Clin.*, vol. 28, p. 102408, 2020, doi: 10.1016/j.nicl.2020.102408.
[76] A. Delval *et al.*, 'Auditory cueing of gait initiation in Parkinson's disease patients with freezing of gait', *Clin. Neurophysiol.*, vol. 125, pp. 1675–1681, 2014, doi: 10.1016/j.clinph.2013.12.101.
[77] S. Bouisset and M. Zattara, 'Biomechanical study of the programming of anticipatory postural adjustments associated with voluntary movement', *J. Biomech.*, vol. 20, no. 8,

pp. 735–742, 1987, doi: 10.1016/0021-9290(87)90052-2.
[78] D. A. Winter, 'Human balance and posture control during standing and walking', *Gait Posture*, vol. 3, no. 4, pp. 193–214, 1995, doi: 10.1016/0966-6362(96)82849-9.
[79] C. A. Frigo, *Bioingegneria del sistema motorio*. Aracne Editrice, 2018.
[80] P. Gatev, S. Thomas, T. Kepple, and M. Hallett, 'Feedforward ankle strategy of balance during quiet stance in adults', *J. Physiol.*, vol. 514, no. 3, pp. 915–928, 1999, doi: 10.1111/j.1469-7793.1999.915ad.x.
[81] R. J. Elble, C. Moody, K. Leffler, and R. Sinha, 'The initiation of normal walking', *Mov. Disord.*, vol. 9, no. 2, pp. 139–146, 1994, doi: 10.1002/mds.870090203.
[82] E. G. Walsh, 'Possible factors in postural sway', in *Cerebellum, Posture and Cerebral Palsy*, London: Heinemann, 1963, pp. 31–37.
[83] L. Baratto, P. G. Morasso, C. Re, and G. Spada, 'A new look at posturographic analysis in the clinical context: sway-density versus other parameterization techniques.', *Motor Control*, vol. 6, no. 3, pp. 246–270, 2002, doi: 10.1123/mcj.6.3.246.
[84] R. Fitzpatrick, D. Burke, and S. C. Gandevia, 'Loop gain of reflexes controlling human standing measured with the use of postural and vestibular disturbances', *J. Neurophysiol.*, vol. 76, no. 6, pp. 3994–4008, 1996, doi: 10.1152/jn.1996.76.6.3994.
[85] S. Carlsöö, 'The initiation of walking', *Acta anat.*, vol. 65, pp. 1–9, 1966.
[86] R. Herman, T. Cook, B. Cozzens, and W. Freedman, 'Control of postural reactions in man: the initiation of gait', in *Control of Posture and Locomotion*, R. Stein, K. Pearson, and J. Redford, Eds. New York: Plenum Press, 1973, pp. 363–388.
[87] T. Cook and B. Cozzens, 'Human solutions for locomotion: the initiation of gait', in *Neural Control of Locomotion*, R. Herman, S. Grillner, P. Stein, and D. Stuart, Eds. New York: Plenum Press, 1976, pp. 65–76.
[88] R. Mann, J. Hagy, V. White, and D. Liddell, 'The initiation of gait', *J Bone Jt. Surg*, vol. 61a, pp. 232–9, 1979.
[89] Y. Brenière, M. Do, and J. Sanchez, 'A biomechanical study of the gait initiation process', *J Biophys Méd Nucléaire*, vol. 5, pp. 197–205, 1981.
[90] I. U. Isaias *et al.*, 'Gait initiation in children with rett syndrome', *PLoS One*, vol. 9, no. 4, p. e92736, 2014, doi: 10.1371/journal.pone.0092736.
[91] J. Gormley, D. Barr, A. Bell, J. Ravey, and R. Mollan, 'Examination of the duration of gait initiation by use of an electrogoniometer', *Gait Posture*, vol. 1, no. 2, pp. 85–91, 1993, doi: 10.1016/0966-6362(93)90019-W.
[92] K. Hiraoka and K. Abe, 'Cortical and spinal control of ankle joint muscles before and during gait initiation', *Somatosens. Mot. Res.*, vol. 24, no. 3, pp. 127–133, 2007, doi: 10.1080/10425170701550615.
[93] Y. Brenière, G. Dietrich, and M. Do, 'Analytical expression of anticipatory movements in gait initiation', in *Biomechanics XI-A*, G. de Groot, P. Hollander, P. Huijing, and G. Van Ingen Schenau, Eds. Amsterdam, The Netherlands: Free University Press, 1988, pp. 371–376.
[94] Y. Brenière and G. Dietrich, 'Heel-off perturbation during gait initiation: Biomechanical analysis using triaxial accelerometry and a force plate', *J. Biomech.*, vol. 25, no. 2, pp. 121–127, 1992, [Online]. Available: http://www.embase.com/search/results?subaction=viewrecord&from=export&id=L22046778%5Cnhttp://dx.doi.org/10.1016/0021-9290(92)90269-

7%5Cnhttp://resolver.lib.washington.edu/resserv?sid=EMBASE&issn=00219290&id=doi:10.1016/0021-9290(92)90269-7&atitle=Heel-off.

[95] D. Brunt, M. J. Lafferty, A. Mckeon, B. Goode, C. Mulhausen, and P. Polk, 'Invariant characteristic of gait initiation', *Am. J. Phys. Med. Rehabil.*, vol. 70, no. 4, pp. 206–212, 1991.

[96] Y. Jian, D. A. Winter, M. G. Ishac, and L. Gilchrist, 'Trajectory of the body COG and COP during initiation and termination of gait', *Gait Posture*, vol. 1, pp. 9–22, 1993, doi: 10.1103/PhysRevLett.70.2649.

[97] C. A. Miller and M. C. Verstraete, 'Determination of the step duration of gait initiation using a mechanical energy analysis', *J. Biomech.*, vol. 29, no. 9, pp. 1195–1199, 1996, doi: 10.1016/0021-9290(96)00033-4.

[98] S. Patchay and Y. Gahéry, 'Effect of asymmetrical limb loading on early postural adjustments associated with gait initiation in young healthy adults', *Gait Posture*, vol. 18, no. 1, pp. 85–94, 2003, doi: 10.1016/S0966-6362(02)00167-4.

[99] M. Henriksson and H. Hirschfeld, 'Physically active older adults display alterations in gait initiation', *Gait Posture*, vol. 21, no. 3, pp. 289–296, 2005, doi: 10.1016/j.gaitpost.2004.03.001.

[100] S. Park, H. Choi, K. Ryu, S. Kim, and Y. Kim, 'Kinematics, kinetics and muscle activities of the lower extremity during the first four steps from gait initiation to the steady-state walking', *J. Mech. Sci. Technol.*, vol. 23, no. 1, pp. 204–211, 2009, doi: 10.1007/s12206-008-0812-z.

[101] M. Nissan and M. W. Whittle, 'Initiation of gait in normal subjects: a preliminary study', *J. Biomed. Eng.*, vol. 12, no. 2, pp. 165–171, 1990, doi: 10.1016/0141-5425(90)90139-E.

[102] Y. Dessery, F. Barbier, C. Gillet, and P. Corbeil, 'Does lower limb preference influence gait initiation?', *Gait Posture*, vol. 33, no. 4, pp. 550–555, 2011, doi: 10.1016/j.gaitpost.2011.01.008.

[103] A. Delval *et al.*, 'Anticipatory postural adjustments during step initiation: Elicitation by auditory stimulation of differing intensities', *Neuroscience*, vol. 219, pp. 166–174, 2012, doi: 10.1016/j.neuroscience.2012.05.032.

[104] S. Leteneur, E. Simoneau, C. Gillet, Y. Dessery, and F. Barbier, 'Trunk's Natural Inclination Influences Stance Limb Kinetics, but Not Body Kinematics, during Gait Initiation in Able Men', *PLoS One*, vol. 8, no. 1, p. e55256, 2013, doi: 10.1371/journal.pone.0055256.

[105] M. L. Mille, M. Simoneau, and M. W. Rogers, 'Postural dependence of human locomotion during gait initiation', *J. Neurophysiol.*, vol. 112, no. 12, pp. 3095–3103, 2014, doi: 10.1152/jn.00436.2014.

[106] B. C. Muir, S. Rietdyk, and J. M. Haddad, 'Gait initiation: The first four steps in adults aged 20-25 years, 65-79 years, and 80-91 years', *Gait Posture*, vol. 39, no. 1, pp. 490–494, 2014, doi: 10.1016/j.gaitpost.2013.08.037.

[107] B. Fawver, J. A. Roper, C. Sarmento, and C. J. Hass, 'Forward leaning alters gait initiation only at extreme anterior postural positions', *Hum. Mov. Sci.*, vol. 59, pp. 1–11, 2018, doi: 10.1016/j.humov.2018.03.006.

[108] B. Stansfield, K. Hawkins, S. Adams, and D. Church, 'Spatiotemporal and kinematic characteristics of gait initiation across a wide speed range', *Gait Posture*, vol. 61, pp. 331–338, 2018, doi: 10.1016/j.gaitpost.2018.02.003.

[109] L. Laudani, L. Rum, M. S. Valle, A. Macaluso, G. Vannozzi, and A. Casabona, 'Age

differences in anticipatory and executory mechanisms of gait initiation following unexpected balance perturbations', *Eur. J. Appl. Physiol.*, vol. 121, no. 2, pp. 465–478, 2021, doi: 10.1007/s00421-020-04531-1.

[110] L. Rum, G. Vannozzi, A. Macaluso, and L. Laudani, 'Neuromechanical response of the upper body to unexpected perturbations during gait initiation in young and older adults', *Aging Clin. Exp. Res.*, vol. 33, no. 4, pp. 909–919, 2020, doi: 10.1007/s40520-020-01592-2.

[111] Y. Brenière and M. C. Do, 'When and How Does Steady State Gait Movement From Upright Posture Begin?', *J. Biomech.*, vol. 19, no. 12, pp. 1035–1040, 1986.

[112] A. Couillandre, Y. Brenière, and B. Maton, 'Is human gait initiation program affected by a reduction of the postural basis?', *Neurosci. Lett.*, vol. 285, no. 2, pp. 150–154, 2000, doi: 10.1016/S0304-3940(00)01015-6.

[113] T. Gélat, A. Le Pellec, and Y. Brenière, 'Evidence for a common process in gait initiation and stepping on to a new level to reach gait velocity', *Exp. Brain Res.*, vol. 170, pp. 336–344, 2006, doi: 10.1007/s00221-005-0214-8.

[114] N. Chastan *et al.*, 'Influence of sensory inputs and motor demands on the control of the centre of mass velocity during gait initiation in humans', *Neurosci. Lett.*, vol. 469, pp. 400–404, 2010, doi: 10.1016/j.neulet.2009.12.038.

[115] T. Gélat, L. Coudrat, and A. Le Pellec, 'Gait initiation is affected during emotional conflict', *Neurosci. Lett.*, vol. 497, no. 1, pp. 64–67, 2011, doi: 10.1016/j.neulet.2011.04.030.

[116] T. Caderby, G. Dalleau, P. Leroyer, B. Bonazzi, D. Chane-Teng, and M. C. Do, 'Does an additional load modify the Anticipatory Postural Adjustments in gait initiation?', *Gait Posture*, vol. 37, no. 1, pp. 144–146, 2013, doi: 10.1016/j.gaitpost.2012.06.012.

[117] T. Caderby, E. Yiou, N. Peyrot, M. Begon, and G. Dalleau, 'Influence of gait speed on the control of mediolateral dynamic stability during gait initiation', *J. Biomech.*, vol. 47, no. 2, pp. 417–423, 2014, doi: 10.1016/j.jbiomech.2013.11.011.

[118] T. Caderby, E. Yiou, N. Peyrot, X. de Viviés, B. Bonazzi, and G. Dalleau, 'Effects of changing body weight distribution on mediolateral stability control during gait initiation', *Front. Hum. Neurosci.*, vol. 11, p. 127, 2017, doi: 10.3389/fnhum.2017.00127.

[119] A. Delafontaine, O. Gagey, S. Colnaghi, M. C. Do, and J. L. Honeine, 'Rigid ankle foot orthosis deteriorates mediolateral balance control and vertical braking during gait initiation', *Front. Hum. Neurosci.*, vol. 11, p. 214, 2017, doi: 10.3389/fnhum.2017.00214.

[120] R. Artico, P. Fourcade, C. Teyssèdre, T. Caderby, A. Delafontaine, and E. Yiou, 'Influence of swing-foot strike pattern on balance control mechanisms during gait initiation over an obstacle to be cleared', *Appl. Sci.*, vol. 10, no. 1, p. 244, 2020, doi: 10.3390/app10010244.

[121] M. F. Vieira *et al.*, 'Effects of additional load at different heights on gait initiation: A statistical parametric mapping of center of pressure and center of mass behavior', *PLoS One*, vol. 16, no. 6, p. e0242892, 2021, doi: 10.1371/journal.pone.0242892.

[122] S. J. Phillips, E. M. Roberts, and T. C. Huang, 'Quantification of intersegmental reactions during rapid swing motion', *J. Biomech.*, vol. 16, no. 6, pp. 411–417, 1983, doi: 10.1016/0021-9290(83)90073-8.

[123] A. L. Hof, M. G. J. Gazendam, and W. E. Sinke, 'The condition for dynamic stability', *J. Biomech.*, vol. 38, pp. 1–8, 2005, doi: 10.1016/j.jbiomech.2004.03.025.

[124] T. Yamashita and R. Katoh, 'Moving pattern of point of application of vertical resultant force during level walking', *J. Biomech.*, vol. 9, no. 2, pp. 93–99, 1976, doi: 10.1016/0021-9290(76)90128-7.

[125] D. Brunt, S. M. Liu, M. Trimble, J. Bauer, and M. Short, 'Principles underlying the organization of movement initiation from quiet stance', *Gait Posture*, vol. 10, no. 2, pp. 121–128, 1999, doi: 10.1016/S0966-6362(99)00020-X.

[126] D. Brunt, M. Short, M. Trimble, and S. M. Liu, 'Control strategies for initiation of human gait are influenced by accuracy constraints', *Neurosci. Lett.*, vol. 285, no. 3, pp. 228–230, 2000, doi: 10.1016/S0304-3940(00)01063-6.

[127] A. Queralt, J. Valls-Solé, and J. M. Castellote, 'Speeding up gait initiation and gait-pattern with a startling stimulus', *Gait Posture*, vol. 31, no. 2, pp. 185–190, 2010, doi: 10.1016/j.gaitpost.2009.10.003.

[128] M. L. Mille *et al.*, 'Posture and locomotion coupling: A target for rehabilitation interventions in persons with Parkinson's disease', *Parkinsons. Dis.*, no. May 2014, p. 54186, 2012, doi: 10.1155/2012/754186.

[129] K. Hiraoka, H. Kunimura, H. Oda, T. Kawasaki, and Y. Sawaguchi, 'Rhythmic movement and rhythmic auditory cues enhance anticipatory postural adjustment of gait initiation', *Somatosens. Mot. Res.*, vol. 37, no. 3, pp. 213–221, 2020, doi: 10.1080/08990220.2020.1777959.

[130] C. M. Michel and D. Brunet, 'EEG source imaging: A practical review of the analysis steps', *Front. Neurol.*, vol. 10, p. 325, 2019, doi: 10.3389/fneur.2019.00325.

[131] M. Fahimi Hnazaee *et al.*, 'Localization of deep brain activity with scalp and subdural EEG', *Neuroimage*, vol. 223, p. 117344, 2020, doi: 10.1016/j.neuroimage.2020.117344.

[132] C. M. McCrimmon *et al.*, 'Electrocorticographic encoding of human gait in the leg primary motor cortex', *Cereb. Cortex*, vol. 28, no. 8, pp. 2752–2762, 2018, doi: 10.1093/cercor/bhx155.

[133] Y. Ouchi *et al.*, 'Changes in dopamine availability in the nigrostriatal and mesocortical dopaminergic systems by gait in Parkinson's disease', *Brain*, vol. 124, pp. 784–792, 2001.

[134] C. la Fougère *et al.*, 'Real versus imagined locomotion: A [18F]-FDG PET-fMRI comparison', *Neuroimage*, vol. 50, no. 4, pp. 1589–1598, 2010, doi: 10.1016/j.neuroimage.2009.12.060.

[135] C. Udina *et al.*, 'Functional Near-Infrared Spectroscopy to Study Cerebral Hemodynamics in Older Adults During Cognitive and Motor Tasks: A Review', *Front. Aging Neurosci.*, vol. 11, p. 367, 2020, doi: 10.3389/fnagi.2019.00367.

[136] K. Takakusaki, 'Neurophysiology of gait: From the spinal cord to the frontal lobe', *Mov. Disord.*, vol. 28, no. 11, pp. 1483–1491, 2013, doi: 10.1002/mds.25669.

[137] S. Grillner, 'Biological Pattern Generation: The Cellular and Computational Logic of Networks in Motion', *Neuron*, vol. 52, no. 5, pp. 751–766, 2006, doi: 10.1016/j.neuron.2006.11.008.

[138] S. M. Danner *et al.*, 'Human spinal locomotor control is based on flexibly organized burst generators', *Brain*, vol. 138, no. 3, pp. 577–588, 2015, doi: 10.1093/brain/awu372.

[139] J. T. Gwin, K. Gramann, S. Makeig, and D. P. Ferris, 'Electrocortical activity is coupled to gait cycle phase during treadmill walking', *Neuroimage*, vol. 54, no. 2, pp. 1289–1296, 2011, doi: 10.1016/j.neuroimage.2010.08.066.

[140] M. Seeber, R. Scherer, J. Wagner, T. Solis-Escalante, and G. R. Müller-Putz, 'High and low gamma EEG oscillations in central sensorimotor areas are conversely modulated during the human gait cycle', *Neuroimage*, vol. 112, pp. 318–326, 2015, doi: 10.1016/j.neuroimage.2015.03.045.

[141] T. H. Petersen, M. Willerslev-Olsen, B. A. Conway, and J. B. Nielsen, 'The motor cortex drives the muscles during walking in human subjects', *J. Physiol.*, vol. 590, no. 10, pp. 2443–2452, 2012, doi: 10.1113/jphysiol.2012.227397.

[142] L. Roeder, T. W. Boonstra, S. S. Smith, and G. K. Kerr, 'Dynamics of corticospinal motor control during overground and treadmill walking in humans', *J. Neurophysiol.*, vol. 120, no. 3, pp. 1017–1031, 2018, doi: 10.1152/jn.00613.2017.

[143] P. Jensen *et al.*, 'Using Corticomuscular and Intermuscular Coherence to Assess Cortical Contribution to Ankle Plantar Flexor Activity During Gait', *J. Mot. Behav.*, vol. 51, no. 6, pp. 668–680, 2019, doi: 10.1080/00222895.2018.1563762.

[144] M. Rambour, A. Caux-Dedeystère, H. Devanne, L. Defebvre, P. Derambure, and A. Delval, 'Influence of repetitive transcranial magnetic stimulation on tibialis anterior activity during walking in humans', *Neurosci. Lett.*, vol. 616, pp. 49–56, 2016, doi: 10.1016/j.neulet.2016.01.027.

[145] M. Wieser, J. Haefeli, L. Bütler, L. Jäncke, R. Riener, and S. Koeneke, 'Temporal and spatial patterns of cortical activation during assisted lower limb movement', *Exp. Brain Res.*, vol. 203, no. 1, pp. 181–191, 2010, doi: 10.1007/s00221-010-2223-5.

[146] J. Wagner, T. Solis-Escalante, P. Grieshofer, C. Neuper, G. Müller-Putz, and R. Scherer, 'Level of participation in robotic-assisted treadmill walking modulates midline sensorimotor EEG rhythms in able-bodied subjects', *Neuroimage*, vol. 63, no. 3, pp. 1203–1211, 2012, doi: 10.1016/j.neuroimage.2012.08.019.

[147] M. Severens, B. Nienhuis, P. Desain, and J. Duysens, 'Feasibility of measuring event Related Desynchronization with electroencephalography during walking', *Proc. Annu. Int. Conf. IEEE Eng. Med. Biol. Soc. EMBS*, vol. 8, pp. 2764–2767, 2012, doi: 10.1109/EMBC.2012.6346537.

[148] M. Seeber, R. Scherer, J. Wagner, T. Solis-Escalante, and G. R. Müller-Putz, 'EEG beta suppression and low gamma modulation are different elements of human upright walking', *Front. Hum. Neurosci.*, vol. 8, p. 485, 2014, doi: 10.3389/fnhum.2014.00485.

[149] F. Artoni *et al.*, 'Unidirectional brain to muscle connectivity reveals motor cortex control of leg muscles during stereotyped walking', *Neuroimage*, vol. 159, pp. 403–416, 2017, doi: 10.1016/j.neuroimage.2017.07.013.

[150] B. J. Farrell, M. A. Bulgakova, I. N. Beloozerova, M. G. Sirota, and B. I. Prilutsky, 'Body stability and muscle and motor cortex activity during walking with wide stance', *J. Neurophysiol.*, vol. 112, no. 3, pp. 504–524, 2014, doi: 10.1152/jn.00064.2014.

[151] C. Iglesias, G. Lourenco, and V. Marchand-pauvert, 'Weak motor cortex contribution to the quadriceps activity during human walking', *Gait Posture*, vol. 35, no. 3, pp. 360–366, 2012, doi: 10.1016/j.gaitpost.2011.10.006.

[152] N. L. Hansen, S. Hansen, L. O. D. Christensen, N. T. Petersen, and J. B. Nielsen, 'Synchronization of lower limb motor unit activity during walking in human subjects', *J. Neurophysiol.*, vol. 86, no. 3, pp. 1266–1276, 2001, doi: 10.1152/jn.2001.86.3.1266.

[153] C. Capaday, B. A. Lavoie, H. Barbeau, C. Schneider, and M. Bonnard, 'Studies on the corticospinal control of human walking. I. Responses to focal transcranial magnetic stimulation of the motor cortex', *J. Neurophysiol.*, vol. 81, no. 1, pp. 129–139, 1999, doi: 10.1152/jn.1999.81.1.129.

[154] M. Mihara, I. Miyai, M. Hatakenaka, K. Kubota, and S. Sakoda, 'Role of the prefrontal cortex in human balance control', *Neuroimage*, vol. 43, no. 2, pp. 329–336, 2008, doi:

10.1016/j.neuroimage.2008.07.029.
[155] A. Mierau, B. Pester, T. Hülsdünker, K. Schiecke, H. K. Strüder, and H. Witte, 'Cortical Correlates of Human Balance Control', *Brain Topogr.*, vol. 30, no. 4, pp. 434–446, 2017, doi: 10.1007/s10548-017-0567-x.
[156] T. Solis-Escalante, J. van der Cruijsen, D. de Kam, J. van Kordelaar, V. Weerdesteyn, and A. C. Schouten, 'Cortical dynamics during preparation and execution of reactive balance responses with distinct postural demands', *Neuroimage*, vol. 188, pp. 557–571, 2019, doi: 10.1016/j.neuroimage.2018.12.045.
[157] J. B. Weersink, N. M. Maurits, and B. M. de Jong, 'EEG time-frequency analysis provides arguments for arm swing support in human gait control', *Gait Posture*, vol. 70, pp. 71–78, 2019, doi: 10.1016/j.gaitpost.2019.02.017.
[158] A. P. Georgopoulos and S. Grillner, 'Visuomotor coordination in reaching and locomotion', *Science (80-.).*, vol. 245, no. 4923, pp. 1209–1210, 1989, doi: 10.1126/science.2675307.
[159] K. Lajoie, J. É. Andujar, K. Pearson, and T. Drew, 'Neurons in area 5 of the posterior parietal cortex in the cat contribute to interlimb coordination during visually guided locomotion: A role in working memory', *J. Neurophysiol.*, vol. 103, no. 4, pp. 2234–2254, 2010, doi: 10.1152/jn.01100.2009.
[160] D. S. Marigold and T. Drew, 'Contribution of cells in the posterior parietal cortex to the planning of visually guided locomotion in the cat: Effects of temporary visual interruption', *J. Neurophysiol.*, vol. 105, no. 5, pp. 2457–2470, 2011, doi: 10.1152/jn.00992.2010.
[161] C. Corradi-Dell'Acqua, M. D. Hesse, R. I. Rumiati, and G. R. Fink, 'Where is a nose with respect to a foot? The left posterior parietal cortex processes spatial relationships among body parts', *Cereb. Cortex*, vol. 18, no. 12, pp. 2879–2890, 2008, doi: 10.1093/cercor/bhn046.
[162] A. Pellijeff, L. Bonilha, P. S. Morgan, K. McKenzie, and S. R. Jackson, 'Parietal updating of limb posture: An event-related fMRI study', *Neuropsychologia*, vol. 44, no. 13, pp. 2685–2690, 2006, doi: 10.1016/j.neuropsychologia.2006.01.009.
[163] A. Parkinson, L. Condon, and S. R. Jackson, 'Parietal cortex coding of limb posture: In search of the body-schema', *Neuropsychologia*, vol. 48, no. 11, pp. 3228–3234, 2010, doi: 10.1016/j.neuropsychologia.2010.06.039.
[164] I. U. Isaias *et al.*, 'Brain metabolic alterations herald falls in patients with Parkinson's disease', *Ann. Clin. Transl. Neurol.*, pp. 579–583, 2020, doi: 10.1002/acn3.51013.
[165] O. Felician *et al.*, 'The Role of Human Left Superior Parietal Lobule in Body Part Localization', *Ann. Neurol.*, vol. 55, no. 5, pp. 749–751, 2004, doi: 10.1002/ana.20109.
[166] G. I. Allen and N. Tsukahara, 'Cerebrocerebellar Communication Systems', *Physiol. Rev.*, vol. 54, no. 4, pp. 957–1006, 1974.
[167] Y. Shimansky, J. J. Wang, R. A. Bauer, V. Bracha, and J. R. Bloedel, 'On-line compensation for perturbations of a reaching movement is cerebellar dependent: Support for the task dependency hypothesis', *Exp. Brain Res.*, vol. 155, no. 2, pp. 156–172, 2004, doi: 10.1007/s00221-003-1713-0.
[168] W. T. Thach, H. P. Goodkin, and J. G. Keating, 'The cerebellum and the adaptive coordination of movement', *Annu. Rev. Neurosci.*, vol. 15, pp. 403–442, 1992, doi: 10.1146/annurev.ne.15.030192.002155.

[169] M. L. Shik, F. V Severin, and G. N. Orlovsky, 'Control of walking and running by means of electrical stimulation of the mesencephalon.', *Electroencephalogr. Clin. Neurophysiol.*, vol. 26, no. 5, p. 549, May 1969.
[170] V. Caggiano *et al.*, 'Midbrain circuits that set locomotor speed and gait selection', *Nature*, vol. 553, no. 7689, pp. 455–460, 2018, doi: 10.1038/nature25448.
[171] A. Parent and L. N. Hazrati, 'Functional anatomy of the basal ganglia. II. The place of subthalamic nucleus and external pallidium in basal ganglia circuitry', *Brain Res. Rev.*, vol. 20, no. 1, pp. 128–154, 1995, doi: 10.1016/0165-0173(94)00008-D.
[172] J. P. Varghese, D. M. Merino, K. B. Beyer, and W. E. McIlroy, 'Cortical control of anticipatory postural adjustments prior to stepping', *Neuroscience*, vol. 313, pp. 99–109, 2016, doi: 10.1016/j.neuroscience.2015.11.032.
[173] A. Delval *et al.*, 'Motor Preparation of Step Initiation: Error-related Cortical Oscillations', *Neuroscience*, vol. 393, pp. 12–23, 2018, doi: 10.1016/j.neuroscience.2018.09.046.
[174] D. B. Coelho *et al.*, 'Frontal hemodynamic response during step initiation under cognitive conflict in elderly and young healthy people', *Journals Gerontol. Ser. A*, vol. 76, no. 2, pp. 216–223, 2021.
[175] S. Von Campenhausen *et al.*, 'Prevalence and incidence of Parkinson's disease in Europe', *Eur. Neuropsychopharmacol.*, vol. 15, no. 4, pp. 473–490, 2005, doi: 10.1016/j.euroneuro.2005.04.007.
[176] S. K. Van Den Eeden *et al.*, 'Incidence of Parkinson's disease: Variation by age, gender, and race/ethnicity', *Am. J. Epidemiol.*, vol. 157, no. 11, pp. 1015–1022, 2003, doi: 10.1093/aje/kwg068.
[177] E. R. Dorsey and B. R. Bloem, 'The Parkinson pandemic - A call to action', *JAMA Neurol.*, vol. 75, no. 1, pp. 9–10, 2018, doi: 10.1001/jamaneurol.2017.3299.
[178] W. Poewe *et al.*, 'Parkinson disease', *Nat. Rev. Dis. Prim.*, vol. 23, no. 3, p. 17013, 2017, doi: 10.1038/nrdp.2017.13.
[179] G. Pezzoli and E. Cereda, 'Exposure to pesticides or solvents and risk of Parkinson disease', *Neurology*, vol. 80, no. 22, pp. 2035–2041, 2013, doi: 10.1212/WNL.0b013e318294b3c8.
[180] S. Fahn and D. Sulzer, 'Neurodegeneration and Neuroprotection in Parkinson Disease', *NeuroRx*, vol. 1, no. 1, pp. 139–154, 2004, doi: 10.1602/neurorx.1.1.139.
[181] H. T. S. Benamer *et al.*, 'Accurate differentiation of parkinsonism and essential tremor using visual assessment of [123I]-FP-CIT SPECT imaging: The [123I]-FP-CIT study group', *Mov. Disord.*, vol. 15, no. 3, pp. 503–510, 2000, doi: 10.1002/1531-8257(200005)15:3<503::AID-MDS1013>3.0.CO;2-V.
[182] H. Braak, K. Del Tredici, U. Rüb, R. A. I. De Vos, E. N. H. Jansen Steur, and E. Braak, 'Staging of brain pathology related to sporadic Parkinson's disease', *Neurobiol. Aging*, vol. 24, no. 2, pp. 197–211, 2003, doi: 10.1016/S0197-4580(02)00065-9.
[183] M. Hodaie, J. S. Neimat, and A. M. Lozano, 'The dopaminergic nigrostriatal system and Parkinson's disease: Molecular events in development, disease, and cell death, and new therapeutic strategies', *Neurosurgery*, vol. 60, no. 1, pp. 17–30, 2007, doi: 10.1227/01.NEU.0000249209.11967.CB.
[184] C. H. Adler and T. G. Beach, 'Neuropathological basis of nonmotor manifestations of Parkinson's disease', *Mov. Disord.*, vol. 31, no. 8, pp. 1114–1119, 2016, doi: 10.1002/mds.26605.

[185] P. Barone *et al.*, 'The PRIAMO study: A multicenter assessment of nonmotor symptoms and their impact on quality of life in Parkinson's disease', *Mov. Disord.*, vol. 24, no. 11, pp. 1641–1649, 2009, doi: 10.1002/mds.22643.
[186] R. B. Postuma *et al.*, 'MDS clinical diagnostic criteria for Parkinson's disease', *Mov. Disord.*, vol. 30, no. 12, pp. 1591–1599, 2015, doi: 10.1002/mds.26424.
[187] M. M. Hoehn and M. D. Yahr, 'Parkinsonism: onset, progression, and mortality', *Neurology*, vol. 17, no. 5, pp. 427–442, 1967.
[188] D. J. Gelb, E. Oliver, and S. Gilman, 'Diagnostic Criteria for Parkinson Disease', *Arch Neurol.*, vol. 56, no. 1, pp. 33–39, 1999, [Online]. Available: http://www.ncbi.nlm.nih.gov/pubmed/10916036.
[189] N. Giladi and Y. Balash, 'The clinical approach to gait disturbances in Parkinson's disease; maintaining independent mobility', *J Neural Transm Suppl.*, vol. 70, pp. 327–332, 2006, doi: doi: 10.1007/978-3-211-45295-0_49. PMID: 17017548.
[190] N. Yanagisawa, 'Natural history of Parkinson's disease: From dopamine to multiple system involvement', *Park. Relat. Disord.*, vol. 12, no. SUPPL. 2, pp. S40–S46, 2006, doi: 10.1016/j.parkreldis.2006.05.011.
[191] S. Perez-Lloret *et al.*, 'Prevalence, determinants, and effect on quality of life of freezing of gait in Parkinson disease', *JAMA Neurol.*, vol. 71, no. 7, pp. 884–890, 2014, doi: 10.1001/jamaneurol.2014.753.
[192] N. Giladi, R. Kao, and S. Fahn, 'Freezing phenomenon in patients with parkinsonian syndromes', *Mov. Disord.*, vol. 12, no. 3, pp. 302–305, 1997, doi: 10.1002/mds.870120307.
[193] C. G. Canning, S. S. Paul, and A. Nieuwboer, 'Prevention of falls in Parkinson's disease: a review of fall risk factors and the role of physical interventions', *Neurodegener. Dis. Manag.*, vol. 4, no. 3, pp. 203–221, 2014, doi: 10.2217/nmt.14.22.
[194] B. H. Wood, J. A. Bilclough, A. Bowron, and R. W. Walker, 'Incidence and prediction of falls in Parkinson's disease: a prospective multidisciplinary study', *j Neurol Neurosurg Psychiatry*, vol. 72, pp. 721–725, 2002, doi: 10.1007/s10654-015-0019-4.
[195] M. K. Y. Mak and M. Y. C. Pang, 'Parkinsonian single fallers versus recurrent fallers: Different fall characteristics and clinical features', *J. Neurol.*, vol. 257, no. 9, pp. 1543–1551, 2010, doi: 10.1007/s00415-010-5573-9.
[196] R. Camicioli and S. R. Majumdar, 'Relationship between mild cognitive impairment and falls in older people with and without Parkinson's disease: 1-Year Prospective Cohort Study', *Gait Posture*, vol. 32, no. 1, pp. 87–91, 2010, doi: 10.1016/j.gaitpost.2010.03.013.
[197] G. K. Kerr, C. J. Worringham, M. H. Cole, P. F. Lacherez, J. M. Wood, and P. A. Silburn, 'Predictors of future falls in Parkinson disease', *Neurology*, vol. 75, no. 2, pp. 116–124, 2010, doi: 10.1212/WNL.0b013e3181e7b688.
[198] R. M. Pickering *et al.*, 'A meta-analysis of six prospective studies of falling in Parkinson's disease', *Mov. Disord.*, vol. 22, no. 13, pp. 1892–1900, 2007, doi: 10.1002/mds.21598.
[199] M. Matinolli, J. T. Korpelainen, K. A. Sotaniemi, V. V. Myllylä, and R. Korpelainen, 'Recurrent falls and mortality in Parkinson's disease: A prospective two-year follow-up study', *Acta Neurol. Scand.*, vol. 123, no. 3, pp. 193–200, 2011, doi: 10.1111/j.1600-0404.2010.01386.x.
[200] C. Palmisano *et al.*, 'Sit-to-walk performance in Parkinson's disease: a comparison between faller and non-faller patients', *Clin. Biomech.*, vol. 63, pp. 140–146, 2019, doi: 10.1016/j.clinbiomech.2019.03.002.

[201] J.-H. Park, Y.-J. Kang, and F. B. Horak, 'What Is Wrong with Balance in Parkinson's Disease?', *J. Mov. Disord.*, vol. 8, no. 3, pp. 109–114, 2015, doi: 10.14802/jmd.15018.
[202] J. C. Pressley *et al.*, 'The impact of comorbid disease and injuries on resource use and expenditures in parkinsonism', *Neurology*, vol. 60, no. 1, pp. 87–93, 2003, doi: 10.1212/01.wnl.0000082160.30833.50.
[203] R. W. Walker, A. Chaplin, R. L. Hancock, R. Rutherford, and W. K. Gray, 'Hip fractures in people with idiopathic Parkinson's disease: Incidence and outcomes', *Mov. Disord.*, vol. 28, no. 3, pp. 334–340, 2013, doi: 10.1002/mds.25297.
[204] C. G. Goetz *et al.*, 'Movement Disorder Society-Sponsored Revision of the Unified Parkinson's Disease Rating Scale (MDS-UPDRS): Scale presentation and clinimetric testing results', *Mov. Disord.*, vol. 23, no. 15, pp. 2129–2170, 2008, doi: 10.1002/mds.22340.
[205] C. Ramaker, J. Marinus, A. M. Stiggelbout, and B. J. van Hilten, 'Systematic evaluation of rating scales for impairment and disability in Parkinson's disease', *Mov. Disord.*, vol. 17, no. 5, pp. 867–876, 2002, doi: 10.1002/mds.10248.
[206] A. Ginanneschi *et al.*, 'Evaluation of Parkinson's Disease: Reliability of Three Rating Scales', *Neuroepidemiology*, vol. 7, no. 1, pp. 38–41, 1988, doi: 10.1159/000110159.
[207] G. Geminiani *et al.*, 'Interobserver reliability between neurologists in training of Parkinson's disease rating scales. A multicenter study', *Mov. Disord.*, vol. 6, no. 4, pp. 330–335, 1991, doi: 10.1002/mds.870060411.
[208] M. Richards, K. Marder, L. Cote, and R. Mayeux, 'Interrater reliability of the unified Parkinson's disease rating scale motor examination', *Mov. Disord.*, vol. 9, no. 1, pp. 89–91, 1994, doi: 10.1002/mds.870090114.
[209] R. Duvoisin and L. I. Golbe, 'Towards a definition of Parkinson's disease', *Neurology*, vol. 39, p. 746, 1989.
[210] D. C. German, K. Manaye, W. K. Smith, D. J. Woodward, and C. B. Saper, 'Midbrain dopaminergic cell loss in parkinson's disease: Computer visualization', *Ann. Neurol.*, vol. 26, no. 4, pp. 507–514, 1989, doi: 10.1002/ana.410260403.
[211] S. Goto, A. Hirano, and S. Matsumoto, 'Subdivisional involvement of nigrostriatal loop in idiopathic parkinson's disease and striatonigral degeneration', *Ann. Neurol.*, vol. 26, no. 6, pp. 766–770, 1989, doi: 10.1002/ana.410260613.
[212] S. Asenbaum, W. Pirker, P. Angelberger, and G. Bencsits, '[123 I] -CIT and SPECT in essential tremor and Parkinson's disease', *J. Neural Transm.*, vol. 105, pp. 1213–1228, 1998.
[213] D. Sulzer *et al.*, 'Neuromelanin detection by magnetic resonance imaging (MRI) and its promise as a biomarker for Parkinson's disease', *npj Park. Dis.*, vol. 4, no. 11, 2018, doi: 10.1038/s41531-018-0047-3.
[214] D. E. Huddleston *et al.*, 'Imaging Parkinsonian Pathology in Substantia Nigra with MRI', *Curr. Radiol. Rep.*, vol. 6, no. 15, 2018, doi: 10.1007/s40134-018-0272-x.
[215] N. Pyatigorskaya, C. Gallea, D. Garcia-Lorenzo, M. Vidailhet, and S. Lehericy, 'A review of the use of magnetic resonance imaging in Parkinson's disease', *Ther. Adv. Neurol. Disord.*, vol. 7, no. 4, pp. 206–220, 2014, doi: 10.1177/1756285613511507.
[216] A. P. Strafella *et al.*, 'Molecular imaging to track Parkinson's disease and atypical parkinsonisms: New imaging frontiers', *Mov. Disord.*, vol. 32, no. 2, pp. 181–192, 2017, doi: 10.1002/mds.26907.
[217] I. U. Isaias *et al.*, 'Striatal dopamine transporter binding in Parkinson's disease associated with the LRRK2 Gly2019Ser mutation', *Mov. Disord.*, vol. 21, no. 8, pp. 1144–1147, 2006, doi:

10.1002/mds.20909.
[218] I. U. Isaias *et al.*, '[123I]FP-CIT striatal binding in early Parkinson's disease patients with tremor vs. akinetic-rigid onset', *Neuroreport*, vol. 18, no. 14, pp. 1499–1502, 2007, doi: 10.1097/WNR.0b013e3282ef69f9.
[219] G. Gerasimou *et al.*, 'SPECT study with I-123-Ioflupane (DaTSCAN) in patients with essential tremor. Is there any correlation with Parkinson's disease?', *Ann. Nucl. Med.*, vol. 26, no. 4, pp. 337–344, 2012, doi: 10.1007/s12149-012-0577-4.
[220] J. O. Rinne, J. T. Kuikka, K. A. Bergström, and U. K. Rinne, 'Striatal dopamine transporter in different disability stages of Parkinson's disease studied with [123I]β-CIT SPECT', *Park. Relat. Disord.*, vol. 1, no. 1, pp. 47–51, 1995, doi: 10.1016/1353-8020(95)00012-U.
[221] J. Booij *et al.*, '[123I]FP-CIT SPECT shows a pronounced decline of striatal dopamine transporter labelling in early and advanced Parkinson's disease', *J. Neurol. Neurosurg. Psychiatry*, vol. 62, pp. 133–140, 1997, doi: 10.1136/jnnp.62.2.133.
[222] W. Staffen, A. Mair, J. Unterrainer, E. Trinka, and G. Ladurner, 'Measuring the progression of idiopathic Parkinson's disease with [123I] β-CIT SPECT', *J. Neural Transm.*, vol. 107, pp. 543–552, 2000, doi: 10.1007/s007020070077.
[223] A. R. Kupsch *et al.*, 'Impact of DaTscan SPECT imaging on clinical management, diagnosis, confidence of diagnosis, quality of life, health resource use and safety in patients with clinically uncertain parkinsonian syndromes: a prospective 1-year follow-up of an open-label contr', *J. Neurol. Neurosurg. & Psychiatry*, vol. 83, no. 6, pp. 620 LP – 628, Jun. 2012, doi: 10.1136/jnnp-2011-301695.
[224] I. U. Isaias and A. Antonini, 'Single-photon emission computed tomography in diagnosis and differential diagnosis of Parkinson's disease', *Neurodegener. Dis.*, vol. 7, pp. 319–329, 2010, doi: 10.1159/000314498.
[225] I. Gayed *et al.*, 'The impact of DaTscan in the diagnosis of Parkinson disease', *Clin. Nucl. Med.*, vol. 40, no. 5, pp. 390–393, 2015, doi: 10.1097/RLU.0000000000000766.
[226] T. Xie, P. Warnke, and U. J. Kang, 'Role of datscan and clinical diagnosis in parkinson disease', *Neurology*, vol. 79, no. 16, p. 1744, 2012, doi: 10.1212/01.wnl.0000422079.28545.80.
[227] J. P. Hubble, 'Essential Tremor', *Clin. Neurophysiol.*, vol. 12, no. 6, pp. 453–482, 1989.
[228] E. D. Louis and J. J. Ferreira, 'How common is the most common adult movement disorder? Update on the worldwide prevalence of essential tremor', *Mov. Disord.*, vol. 25, no. 5, pp. 534–541, 2010, doi: 10.1002/mds.22838.
[229] R. J. Elble, 'What is essential tremor?', *Curr Neurol Neurosci Rep.*, vol. 13, no. 6, p. 353, 2013, doi: 10.1038/jid.2014.371.
[230] W. C. Koller, B. Vetere-Overfield, and R. Barter, 'Tremors in Early Parkinson's Disease', *Clin. Neuropharmacol.*, vol. 4, pp. 293–297, 1989.
[231] M. A. Thenganatt and E. D. Louis, 'Distinguishing essential tremor from Parkinson's disease: Bedside tests and laboratory evaluations', *Expert Rev. Neurother.*, vol. 12, no. 6, pp. 687–696, 2012, doi: 10.1586/ern.12.49.
[232] S. Sadasivan and J. H. Friedman, 'Experience with DaTscan at a tertiary referral center', *Park. Relat. Disord.*, vol. 21, no. 1, pp. 42–45, 2015, doi: 10.1016/j.parkreldis.2014.10.022.
[233] J. Brumberg and I. U. Isaias, *SPECT Molecular Imaging in Atypical Parkinsonism*, 1st ed., vol. 142. Elsevier Inc., 2018.
[234] I. T. Hsiao *et al.*, 'Correlation of parkinson disease severity and 18F-DTBZ positron

emission tomography', *JAMA Neurol.*, vol. 71, no. 6, pp. 758–766, 2014, doi: 10.1001/jamaneurol.2014.290.

[235] A. Kumar, '[11C]DTBZ-PET correlates of levodopa responses in asymmetric Parkinson's disease', *Brain*, vol. 126, no. 12, pp. 2648–2655, Sep. 2003, doi: 10.1093/brain/awg270.

[236] K. L. Leenders *et al.*, 'The Nigrostriatal Dopaminergic System Assessed in Vivo by Positron Emission Tomography in Healthy Volunteer Subjects and Patients With Parkinson's Disease', *Arch. Neurol.*, vol. 47, no. 12, pp. 1290–1298, 1990, doi: 10.1001/archneur.1990.00530120034007.

[237] K. L. Leenders *et al.*, 'Brain dopamine metabolism in patients with Parkinson's disease measured with positron emission tomography', *J. Neurol. Neurosurg. Psychiatry*, vol. 49, no. 8, pp. 853–860, 1986, doi: 10.1136/jnnp.49.8.853.

[238] S. A. Eshuis, R. P. Maguire, K. L. Leenders, S. Jonkman, and P. L. Jager, 'Comparison of FP-CIT SPECT with F-DOPA PET in patients with de novo and advanced Parkinson's disease', *Eur. J. Nucl. Med. Mol. Imaging*, vol. 33, no. 2, pp. 200–209, 2006, doi: 10.1007/s00259-005-1904-y.

[239] N. Ibrahim *et al.*, 'The sensitivity and specificity of F-DOPA PET in a movement disorder clinic.', *Am. J. Nucl. Med. Mol. Imaging*, vol. 6, no. 1, pp. 102–9, 2016, [Online]. Available: http://www.ncbi.nlm.nih.gov/pubmed/27069770%0Ahttp://www.pubmedcentral.nih.gov/articlerender.fcgi?artid=PMC4749509.

[240] E. F. J. De Vries, G. Luurtsema, M. Brüssermann, P. H. Elsinga, and W. Vaalburg, 'Fully automated synthesis module for the high yield one-pot preparation of 6-[18F]fluoro-L-DOPA', *Appl. Radiat. Isot.*, vol. 51, no. 4, pp. 389–394, 1999, doi: 10.1016/S0969-8043(99)00057-3.

[241] S. Cervenka, 'PET radioligands for the dopamine D1-receptor: Application in psychiatric disorders', *Neurosci. Lett.*, vol. 691, pp. 26–34, 2019, doi: 10.1016/j.neulet.2018.03.007.

[242] D. Vallone, R. Picetti, and E. Borrelli, 'Structure and function of dopamine receptors', *Neurosci. Biobehav. Rev.*, vol. 24, no. 1, pp. 125–132, 2000, doi: 10.1016/S0149-7634(99)00063-9.

[243] C. R. Gerfen and D. J. Surmeier, 'Modulation of striatal projection systems by dopamine', *Annu. Rev. Neurosci.*, vol. 34, pp. 441–466, 2011, doi: 10.1146/annurev-neuro-061010-113641.

[244] C. Hamani, J. Neimat, and A. M. Lozano, 'Deep brain stimulation for the treatment of Parkinson's disease', *J. Neural Transm. Suppl.*, no. 70, p. 393—399, 2006, doi: 10.1007/978-3-211-45295-0_59.

[245] A. M. Lozano and N. Lipsman, 'Probing and Regulating Dysfunctional Circuits Using Deep Brain Stimulation', *Neuron*, vol. 77, no. 3, pp. 406–424, 2013, doi: 10.1016/j.neuron.2013.01.020.

[246] C. Tard *et al.*, 'Brain metabolic abnormalities during gait with freezing in Parkinson's disease', *Neuroscience*, vol. 307, pp. 281–301, 2015, doi: 10.1016/j.neuroscience.2015.08.063.

[247] N. Asch *et al.*, 'Independently together: subthalamic theta and beta opposite roles in predicting Parkinson's tremor', *Brain Commun.*, vol. 136, no. (Pt 12), pp. 3659–70, 2020, doi: 10.1093/braincomms/fcaa074.

[248] J. Hirschmann *et al.*, 'A direct relationship between oscillatory subthalamic nucleus-cortex coupling and rest tremor in Parkinson's disease', *Brain*, vol. 136, no. 12, pp. 3659–3670, 2013, doi: 10.1093/brain/awt271.

[249] W. J. Neumann *et al.*, 'Subthalamic synchronized oscillatory activity correlates with motor impairment in patients with Parkinson's disease', *Mov. Disord.*, vol. 31, no. 11, pp. 1748–1751, 2016, doi: 10.1002/mds.26759.
[250] A. J. Lees, E. Tolosa, and C. W. Olanow, 'Four pioneers of L-dopa treatment: Arvid Carlsson, Oleh Hornykiewicz, George Cotzias, and Melvin Yahr', *Mov. Disord.*, vol. 30, no. 1, pp. 19–36, Jan. 2015, doi: 10.1002/mds.26120.
[251] A. M. Bonnet, Y. Loria, M.-H. Saint-Hilaire, F. Lhermitte, and Y. Agid, 'Motor Score', *Neurology*, vol. 37, pp. 1539–1542, 1987.
[252] B. P. Bejjani *et al.*, 'Axial parkinsonian symptoms can be improved: The role of levodopa and bilateral subthalamic stimulation', *J. Neurol. Neurosurg. Psychiatry*, vol. 68, pp. 595–600, 2000, doi: 10.1136/jnnp.68.5.595.
[253] H. Zach, M. Dirkx, D. Roth, J. Pasman, B. Bloem, and R. Helmich, 'Dopamine-responsive and dopamine-resistant resting tremor in Parkinson disease', *Neurology*, vol. 95, no. 11, pp. e1461–e1470, 2020, doi: 10.1212/WNL.0000000000010316.
[254] O. Blin, A. M. Ferrandez, J. Pailhous, and G. Serratrice, 'Dopa-sensitive and Dopa-resistant gait parameters in Parkinson's disease', *J. Neurol. Sci.*, vol. 103, no. 1, pp. 51–54, 1991, doi: 10.1016/0022-510X(91)90283-D.
[255] N. I. Bohnen and R. Cham, 'Postural Control, Gait, and Dopamine Functions in Parkinsonian Movement Disorders', *Clin. Geriatr. Med.*, vol. 22, no. 4, pp. 797–812, 2006, doi: 10.1016/j.cger.2006.06.009.
[256] C. Curtze, J. G. Nutt, P. Carlson-Kuhta, M. Mancini, and F. B. Horak, 'Levodopa Is a Double-Edged Sword for Balance and Gait in People With Parkinson's Disease', *Mov. Disord.*, vol. 30, no. 10, pp. 1361–1370, Sep. 2015, doi: 10.1002/mds.26269.
[257] M. Speechley and M. Tinetti, 'Falls and Injuries in Frail and Vigorous Community Elderly Persons', *J. Am. Geriatr. Soc.*, vol. 39, no. 1, pp. 46–52, 1991, doi: 10.1111/j.1532-5415.1991.tb05905.x.
[258] N. Giladi, 'Medical treatment of freezing of gait', *Mov. Disord.*, vol. 23, no. SUPPL. 2, pp. S482–S488, 2008, doi: 10.1002/mds.21914.
[259] J. M. Shine, S. L. Naismith, and S. J. G. Lewis, 'The pathophysiological mechanisms underlying freezing of gait in Parkinson's Disease', *J. Clin. Neurosci.*, vol. 18, no. 9, pp. 1154–1157, 2011, doi: 10.1016/j.jocn.2011.02.007.
[260] A. R. Crossman, 'A hypothesis on the pathophysiological mechanisms that underlie levodopa- or dopamine agonist-induced dyskinesia in Parkinson's disease: Implications for future strategies in treatment', *Mov. Disord.*, vol. 5, no. 2, pp. 100–108, 1990, doi: 10.1002/mds.870050203.
[261] M. Fabbri *et al.*, 'Do patients with late-stage Parkinson's disease still respond to levodopa?', *Park. Relat. Disord.*, vol. 26, pp. 10–16, 2016, doi: 10.1016/j.parkreldis.2016.02.021.
[262] B. S. Connolly and A. E. Lang, 'Pharmacological treatment of Parkinson disease: A review', *JAMA - J. Am. Med. Assoc.*, vol. 311, no. 16, pp. 1670–1683, 2014, doi: 10.1001/jama.2014.3654.
[263] J. Volkmann, 'Deep Brain Stimulation for the Treatment of Parkinson's Disease', *J. Clin. Neurophysiol.*, vol. 21, no. 1, pp. 6–17, 2004, doi: 10.1097/00004691-200401000-00003.
[264] L. Vercueil, 'Fifty years of brain surgery for dystonia: revisiting the Irving S. Cooper's legacy, and looking forward.', *Acta Neurol. Belg.*, vol. 103, no. 3, pp. 125–128, Sep. 2003.

[265] J. Guridi, J. A. Obeso, M. C. Rodriguez-Oroz, A. M. Lozano, and M. Manrique, 'L-DOPA-INDUCED DYSKINESIA AND STEREOTACTIC SURGERY FOR PARKINSON'S DISEASE', *Neurosurgery*, vol. 62, no. 2, pp. 311–325, 2006, doi: 10.1227/01.NEU.0000297052.97282.CF.

[266] S. J. Groiss, L. Wojtecki, M. Sudmeyer, and A. Schnitzler, 'Deep brain stimulation in Parkinson-s disease', *Ther. Adv. Neurol. Disord.*, vol. 2, no. 6, pp. 379–391, 2009, doi: 10.1177/1756285609339382.

[267] J. Gardner, 'A history of deep brain stimulation: Technological innovation and the role of clinical assessment tools', *Soc. Stud. Sci.*, vol. 43, no. 5, pp. 707–728, 2013, doi: 10.1177/0306312713483678.

[268] O. S. Cooper, A. R. M. Upton, and I. Amin, 'Reversibility of chronic neurologic deficits. Some effects of electrical stimulation of the thalamus and Internal Capsule in man', *Appl. Neurophysiol.*, vol. 43, pp. 244–258, 1980, [Online]. Available: https://www.m-culture.go.th/mculture_th/download/king9/Glossary_about_HM_King_Bhumibol_Adulyadej's_Funeral.pdf.

[269] A. L. Benabid, P. Pollak, A. Louveau, S. Henry, and J. de Rougemont, 'Combined (Thalamotomy and Stimlation) Stereotactic Surgery of the VIM Thalamic Nucleus for Bilateral Parkinson DIsease', *Appl. Neurophysiol.*, vol. 50, pp. 344–346, 1987, [Online]. Available: https://www.m-culture.go.th/mculture_th/download/king9/Glossary_about_HM_King_Bhumibol_Adulyadej's_Funeral.pdf.

[270] E. B. Montgomery, *Deep Brain Stimulation Programming*. 2017.

[271] M. C. Rodriguez-Oroz *et al.*, 'Bilateral deep brain stimulation in Parkinson's disease: A multicentre study with 4 years follow-up', *Brain*, vol. 128, no. 10, pp. 2240–2249, 2005, doi: 10.1093/brain/awh571.

[272] D. Tarsy, J. L. Vitek, P. A. Starr, and M. Okun, *Deep Brain Stimulation in Neurological and Psychiatric Disorders*. Springer Science & Business Media, 2008.

[273] M. M. Reich *et al.*, 'Progressive gait ataxia following deep brain stimulation for essential tremor: adverse effect or lack of efficacy?', *Brain*, vol. 139, no. 11, pp. 2948–2956, 2016, doi: 10.1093/brain/aww223.

[274] A. H. Snijders *et al.*, 'Physiology of freezing of gait', *Ann. Neurol.*, vol. 80, no. 5, pp. 644–659, 2016, doi: 10.1002/ana.24778.

[275] P. Brown, A. Oliviero, P. Mazzone, A. Insola, P. Tonali, and V. Di Lazzaro, 'Dopamine dependency of oscillations between subthalamic nucleus and pallidum in Parkinson's disease', *J. Neurosci.*, vol. 21, no. 3, pp. 1033–1038, 2001, doi: 10.1523/jneurosci.21-03-01033.2001.

[276] A. Priori *et al.*, 'Rhythm-specific pharmacological modulation of subthalamic activity in Parkinson's disease', *Exp. Neurol.*, vol. 189, no. 2, pp. 369–379, 2004, doi: 10.1016/j.expneurol.2004.06.001.

[277] P. Brown and D. Williams, 'Basal ganglia local field potential activity: Character and functional significance in the human', *Clin. Neurophysiol.*, vol. 116, no. 11, pp. 2510–2519, 2005, doi: 10.1016/j.clinph.2005.05.009.

[278] A. A. Kühn *et al.*, 'High-frequency stimulation of the subthalamic nucleus suppresses oscillatory β activity in patients with Parkinson's disease in parallel with improvement in motor performance', *J. Neurosci.*, vol. 28, no. 24, pp. 6165–6173, 2008, doi: 10.1523/JNEUROSCI.0282-08.2008.

[279] F. Steigerwald *et al.*, 'Neuronal activity of the human subthalamic nucleus in the parkinsonian and nonparkinsonian state', *J. Neurophysiol.*, vol. 100, no. 5, pp. 2515–2524, 2008, doi: 10.1152/jn.90574.2008.
[280] J. Volkmann, J. Herzog, F. Kopper, and G. Geuschl, 'Introduction to the programming of deep brain stimulators', *Mov. Disord.*, vol. 17, no. 3, pp. S181–S187, 2002, doi: 10.1002/mds.10162.
[281] D. Kondziolka and J. Y. K. Lee, 'Long-lasting microthalamotomy effect after temporary placement of a thalamic stimulating electrode', *Stereotact. Funct. Neurosurg.*, vol. 82, pp. 127–130, 2004, doi: 10.1159/000079844.
[282] D. Maltête *et al.*, 'Microsubthalamotomy: An immediate predictor of long-term subthalamic stimulation efficacy in Parkinson disease', *Mov. Disord.*, vol. 23, no. 7, pp. 1047–1050, 2008, doi: 10.1002/mds.22054.
[283] E. Lalo *et al.*, 'Patterns of bidirectional communication between cortex and basal ganglia during movement in patients with Parkinson disease', *J. Neurosci.*, vol. 28, no. 12, pp. 3008–3016, 2008, doi: 10.1523/JNEUROSCI.5295-07.2008.
[284] E. J. Quinn *et al.*, 'Beta oscillations in freely moving Parkinson's subjects are attenuated during deep brain stimulation', *Mov. Disord.*, vol. 30, no. 13, pp. 1750–1758, 2015, doi: 10.1002/mds.26376.
[285] A. Canessa *et al.*, 'Striatal dopaminergic innervation regulates subthalamic beta-oscillations and cortical-subcortical coupling during movements: Preliminary evidence in subjects with Parkinson's disease', *Front. Hum. Neurosci.*, vol. 10, no. DEC2016, pp. 1–12, 2016, doi: 10.3389/fnhum.2016.00611.
[286] A. Canessa, C. Palmisano, I. U. Isaias, and A. Mazzoni, 'Gait-related frequency modulation of beta oscillatory activity in the subthalamic nucleus of parkinsonian patients', *Brain Stimul.*, vol. 13, pp. 1743–1752, 2020, doi: 10.1016/j.brs.2020.09.006.
[287] S. Little *et al.*, 'Adaptive deep brain stimulation in advanced Parkinson disease.', *Ann. Neurol.*, vol. 74, no. 3, pp. 449–457, 2013, doi: 10.1002/ana.23951.
[288] M. Rosa *et al.*, 'Adaptive deep brain stimulation in a freely moving parkinsonian patient', *Mov. Disord.*, vol. 30, no. 7, pp. 1003–1005, 2015, doi: 10.1002/mds.26241.
[289] S. Little *et al.*, 'Bilateral adaptive deep brain stimulation is effective in Parkinson's disease', *J. Neurol. Neurosurg. Psychiatry*, vol. 87, no. 7, pp. 717–721, 2016, doi: 10.1136/jnnp-2015-310972.
[290] J. C. Steele, 'Progressive Supranuclear Palsy', *Arch. Neurol.*, vol. 10, no. 4, p. 333, 1964.
[291] L. I. Golbe, P. H. Davis, B. S. Schoenberg, and R. C. Duvoisin, 'Prevalence and natural history of progressive supranuclear palsy', *Neurology*, vol. 38, pp. 1031–1034, 1988.
[292] J. H. Bower, D. M. Maraganore, S. K. McDonnell, and W. A. Rocca, 'Incidence of progressive supranuclear palsy and multiple system atrophy in Olmsted County, Minnesota, 1976 to 1990', *Neurology*, vol. 49, no. 5, pp. 1284–1288, 1997, doi: 10.1212/WNL.49.5.1284.
[293] A. Schrag, Y. Ben-Shlomo, and N. P. Quinn, 'Prevalence of progressive supranuclear palsy and multiple system atrophy: A cross-sectional study', *Lancet*, vol. 354, pp. 1771–1775, 1999, doi: 10.1016/S0140-6736(99)04137-9.
[294] U. Nath *et al.*, 'The prevalence of progressive supranuclear palsy (Steele-Richardson-Olszewski syndrome) in the UK', *Brain*, vol. 124, no. 7, pp. 1438–1449, 2001, doi: 10.1093/brain/124.7.1438.

[295] M. Kawashima, M. Miyake, M. Kusumi, Y. Adachi, and K. Nakashima, 'Prevalence of progressive supranuclear palsy in Yonago, Japan', *Mov. Disord.*, vol. 19, no. 10, pp. 1239–1240, 2004, doi: 10.1002/mds.20149.

[296] E. R. Maher and A. J. Lees, 'The clinical features and natural history of the Steele-Richardson-Olszewski syndrome (progressive supranuclear palsy)', *Neurology*, vol. 36, no. 7, pp. 1005–1008, 1986.

[297] B. Bluett and I. Litvan, 'Pathophysiology, genetics, clinical features, diagnosis and therapeutic trials in progressive supranuclear palsy', *Expert Opin. Orphan Drugs*, vol. 3, no. 3, pp. 253–265, 2015, [Online]. Available: http://www.embase.com/search/results?subaction=viewrecord&from=export&id=L602567115%5Cnhttp://dx.doi.org/10.1517/21678707.2015.1018180.

[298] I. Litvan *et al.*, 'Natural history of progressive supranuclear palsy (Steele-Richardson-Olszewski syndrome) and clinical predictors of survival: A clinicopathological study', *J. Neurol. Neurosurg. Psychiatry*, vol. 61, no. 6, pp. 615–620, 1996, doi: 10.1136/jnnp.60.6.615.

[299] L. I. Golbe *et al.*, 'Follow-up study of risk factors in progressive supranuclear palsy', *Neurology*, vol. 47, no. 1, pp. 148–154, 1996, doi: 10.1212/WNL.47.1.148.

[300] J. S. Vidal, M. Vidailhet, P. Derkinderen, T. Dubard De Gaillarbois, C. Tzourio, and A. Alpérovitch, 'Risk factors for progressive supranuclear palsy: A case-control study in France', *J. Neurol. Neurosurg. Psychiatry*, vol. 80, no. 11, pp. 1271–1274, 2009, doi: 10.1136/jnnp.2008.149849.

[301] I. Litvan *et al.*, 'Environmental and occupational risk factors for progressive supranuclear palsy: Case-control study', *Mov. Disord.*, vol. 31, no. 5, pp. 644–652, 2016, doi: 10.1002/mds.26512.

[302] C. L. Joachim, J. H. Morris, K. S. Kosik, and D. J. Selkoe, 'Tau antisera recognize neurofibrillary tangles in a range of neurodegenerative disorders', *Ann. Neurol.*, vol. 22, no. 4, pp. 514–520, 1987, doi: 10.1002/ana.410220411.

[303] D. R. Williams and A. J. Lees, 'Progressive supranuclear palsy: clinicopathological concepts and diagnostic challenges', *Lancet Neurol.*, vol. 8, no. 3, pp. 270–279, 2009, doi: 10.1016/S1474-4422(09)70042-0.

[304] J. J. Hauw *et al.*, 'Preliminary NINDS neuropathologic criteria for Steele-Richardson-Olszewski syndrome (progressive supranuclear palsy).', *Neurology*, vol. 44, no. 11, pp. 2015–2019, Nov. 1994, doi: 10.1212/wnl.44.11.2015.

[305] A. L. Boxer, J. Yu, L. I. Golbe, I. Litvan, A. E. Lang, and G. U. Höglinger, 'New diagnostic and therapeutics for progressive supranuclear palsy', *Lancet Neurol.*, vol. 16, no. 7, pp. 552–563, 2017, doi: 10.1016/S1474-4422(17)30157-6.New.

[306] A. C. Ludolph *et al.*, 'Tauopathies with parkinsonism: Clinical spectrum, neuropathologic basis, biological markers, and treatment options', *Eur. J. Neurol.*, vol. 16, no. 3, pp. 297–309, 2009, doi: 10.1111/j.1468-1331.2008.02513.x.

[307] D. R. Williams *et al.*, 'Characteristics of two distinct clinical phenotypes in pathologically proven progressive supranuclear palsy: Richardson's syndrome and PSP-parkinsonism', *Brain*, vol. 128, no. 6, pp. 1247–1258, 2005, doi: 10.1093/brain/awh488.

[308] S. Amano *et al.*, 'Parkinsonism and Related Disorders Discriminating features of gait performance in progressive supranuclear palsy', *Park. Relat. Disord.*, vol. 21, no. 8, pp. 888–893, 2015.

[309] S. Kammermeier *et al.*, 'Postural stabilization differences in idiopathic Parkinson's disease

and progressive supranuclear palsy during self-triggered fast forward weight lifting', *Front. Neurol.*, vol. 8, p. 743, 2018, doi: 10.3389/fneur.2017.00743.

[310] D. R. Williams, H. C. Watt, and A. J. Lees, 'Predictors of falls and fractures in bradykinetic rigid syndromes: A retrospective study', *J. Neurol. Neurosurg. Psychiatry*, vol. 77, no. 4, pp. 468–473, 2006, doi: 10.1136/jnnp.2005.074070.

[311] G. Saranza and A. E. Lang, 'Levodopa challenge test: indications, protocol, and guide', *J. Neurol.*, 2020, doi: 10.1007/s00415-020-09810-7.

[312] R. M. Liscic, K. Srulijes, A. Gröger, W. Maetzler, and D. Berg, 'Differentiation of Progressive Supranuclear Palsy: Clinical, imaging and laboratory tools', *Acta Neurol. Scand.*, vol. 127, no. 5, pp. 362–370, 2013, doi: 10.1111/ane.12067.

[313] J. Youn, Y. Okuma, M. Hwang, D. Kim, and J. W. Cho, 'Falling Direction can Predict the Mechanism of Recurrent Falls in Advanced Parkinson's Disease', *Sci. Rep.*, vol. 7, no. 1, p. 3921, 2017, doi: 10.1038/s41598-017-04302-7.

[314] C. L. Wielinski, C. Erickson-Davis, R. Wichmann, M. Walde-Douglas, and S. A. Parashos, 'Falls and injuries resulting from falls among patients with Parkinson's disease and other Parkinsonian syndromes', *Mov. Disord.*, vol. 20, no. 4, pp. 410–415, 2005, doi: 10.1002/mds.20347.

[315] F. S. Brown, J. B. Rowe, L. Passamonti, and T. Rittman, 'Falls in Progressive Supranuclear Palsy', *Mov. Disord. Clin. Pract.*, vol. 7, no. 1, pp. 16–24, 2020, doi: 10.1002/mdc3.12879.

[316] A. Schrag *et al.*, 'Measuring quality of life in PSP: The PSP-QoL', *Neurology*, vol. 67, no. 1, pp. 39–44, 2006, doi: 10.1212/01.wnl.0000223826.84080.97.

[317] I. Piot *et al.*, 'The Progressive Supranuclear Palsy Clinical Deficits Scale', *Mov. Disord.*, vol. 35, no. 4, pp. 650–661, 2020, doi: 10.1002/mds.27964.

[318] L. I. Golbe and P. A. Ohman-Strickland, 'A clinical rating scale for progressive supranuclear palsy', *Brain*, vol. 130, no. 6, pp. 1552–1565, 2007, doi: 10.1093/brain/awm032.

[319] J. C. Hobart, S. J. Cano, J. P. Zajicek, and A. J. Thompson, 'Rating scales as outcome measures for clinical trials in neurology: problems, solutions, and recommendations', *Lancet Neurol.*, vol. 6, no. 12, pp. 1094–1105, 2007, doi: 10.1016/S1474-4422(07)70290-9.

[320] G. Respondek *et al.*, 'Validation of the movement disorder society criteria for the diagnosis of 4-repeat tauopathies', *Mov. Disord.*, vol. 35, no. 1, pp. 171–176, 2020, doi: 10.1002/mds.27872.

[321] G. Longoni *et al.*, 'MRI measurements of brainstem structures in patients with Richardson's syndrome, progressive supranuclear palsy-parkinsonism, and Parkinson's disease', *Mov. Disord.*, vol. 26, no. 2, pp. 247–255, 2011, doi: 10.1002/mds.23293.

[322] S. Zanigni *et al.*, 'Accuracy of MR markers for differentiating Progressive Supranuclear Palsy from Parkinson's disease', *NeuroImage Clin.*, vol. 11, pp. 736–742, 2016, doi: 10.1016/j.nicl.2016.05.016.

[323] S. Nigro *et al.*, 'Magnetic Resonance Parkinsonism Index and midbrain to pons ratio: Which index better distinguishes Progressive Supranuclear Palsy patients with a low degree of diagnostic certainty from patients with Parkinson Disease?', *Park. Relat. Disord.*, vol. 41, pp. 31–36, 2017, doi: 10.1016/j.parkreldis.2017.05.002.

[324] A. Varrone, K. L. Marek, D. Jennings, R. B. Innis, and J. P. Seibyl, '[123I]β-CIT SPECT imaging demonstrates reduced density of striatal dopamine transporters in Parkinson's disease and multiple system atrophy', *Mov. Disord.*, vol. 16, no. 6, pp. 1023–1032, 2001, doi: 10.1002/mds.1256.

[325] L. Filippi *et al.*, '[123]I-FP-CIT in progressive supranuclear palsy and in parkinson's disease: a spect semiquantitative study', *Nucl. Med. Commun.*, vol. 27, no. 4, pp. 381–386, 2006, doi: 10.1097/01.mnm.0000202858.45522.df.

[326] L. D. Perju-Dumbrava *et al.*, 'Dopamine transporter imaging in autopsy-confirmed Parkinson's disease and multiple system atrophy', *Mov. Disord.*, vol. 27, no. 1, pp. 65–71, 2012, doi: 10.1002/mds.24000.

[327] V. Kaasinen, T. Kankare, J. Joutsa, and T. Vahlberg, 'Presynaptic striatal dopaminergic function in atypical parkinsonism: A metaanalysis of imaging studies', *J. Nucl. Med.*, vol. 60, no. 12, pp. 1757–1763, 2019, doi: 10.2967/jnumed.119.227140.

[328] T. Shigekiyo and S. Arawaka, 'Laterality of specific binding ratios on DAT-SPECT for differential diagnosis of degenerative parkinsonian syndromes', *Sci. Rep.*, vol. 10, p. 15761, 2020, doi: 10.1038/s41598-020-72321-y.

[329] S. Jin *et al.*, 'Differential Diagnosis of Parkinsonism Using Dual-Phase F-18 FP-CIT PET Imaging', *Nucl. Med. Mol. Imaging (2010).*, vol. 47, no. 1, pp. 44–51, 2013, doi: 10.1007/s13139-012-0182-4.

[330] D. J. Brooks *et al.*, 'Differing patterns of striatal 18F-dopa uptake in Parkinson's disease, multiple system atrophy, and progressive supranuclear palsy', *Ann. Neurol.*, vol. 28, no. 4, pp. 547–555, 1990, doi: 10.1002/ana.410280412.

[331] M. Otsuka *et al.*, 'Striatal blood flow, glucose metabolism and 18F-Dopa uptake: Difference in Parkinson's disease and atypical Parkinsonism', *J. Neurol. Neurosurg. Psychiatry*, vol. 54, no. 10, pp. 898–904, 1991, doi: 10.1136/jnnp.54.10.898.

[332] M. Suzuki, T. J. Desmond, R. L. Albin, and K. A. Frey, 'Cholinergic vesicular transporters in progressive supranuclear palsy', *Neurology*, vol. 58, no. 7, pp. 1013–1018, 2002, doi: 10.1212/WNL.58.7.1013.

[333] D. J. Brooks *et al.*, 'Striatal D2 receptor status in patients with Parkinson's disease, striatonigral degeneration, and progressive supranuclear palsy, measured with11C-raclopride and positron emission tomography', *Ann. Neurol.*, vol. 31, no. 2, pp. 184–192, Feb. 1992, doi: 10.1002/ana.410310209.

[334] A. Antonini, J. Schwarz, W. H. Oertel, H. F. Beer, U. D. Madeja, and K. L. Leenders, '[11C]raclopride and positron emission tomography in previously untreated patients with Parkinson's disease: Influence of L-dopa and lisuride therapy on striatal dopamine D2-receptors.', *Neurology*, vol. 44, no. 7, pp. 1325–1329, Jul. 1994, doi: 10.1212/wnl.44.7.1325.

[335] U. K. Rinne, A. Laihinen, J. O. Rinne, K. Naågren, J. Bergman, and U. Ruotsalainen, 'Positron emission tomography demonstrates dopamine D2 receptor supersensitivity in the striatum of patients with early Parkinson's disease', *Mov. Disord.*, vol. 5, no. 1, pp. 55–59, 1990, doi: 10.1002/mds.870050114.

[336] M. Maruyama *et al.*, 'Imaging of Tau Pathology in a Tauopathy Mouse Model and in Alzheimer Patients Compared to Normal Controls', *Neuron*, vol. 79, no. 6, pp. 1094–1108, Sep. 2013, doi: 10.1016/j.neuron.2013.07.037.

[337] C.-F. Xia *et al.*, '[18F]T807, a novel tau positron emission tomography imaging agent for Alzheimer's disease', *Alzheimer's Dement.*, vol. 9, no. 6, pp. 666–676, Nov. 2013, doi: 10.1016/j.jalz.2012.11.008.

[338] M. Marquié *et al.*, 'Validating novel tau positron emission tomography tracer [F-18]-AV-1451 (T807) on postmortem brain tissue', *Ann. Neurol.*, vol. 78, no. 5, pp. 787–800, Nov. 2015, doi: 10.1002/ana.24517.

[339] M. Song *et al.*, 'Feasibility of short imaging protocols for [18F]PI-2620 tau-PET in progressive supranuclear palsy', *Eur. J. Nucl. Med. Mol. Imaging*, May 2021, doi: 10.1007/s00259-021-05391-3.
[340] R. Smith, M. Schöll, M. Honer, C. F. Nilsson, E. Englund, and O. Hansson, 'Tau neuropathology correlates with FDG-PET, but not AV-1451-PET, in progressive supranuclear palsy', *Acta Neuropathol.*, vol. 133, no. 1, pp. 149–151, Jan. 2017, doi: 10.1007/s00401-016-1650-1.
[341] T. Eckert *et al.*, 'FDG PET in the differential diagnosis of parkinsonian disorders', *Neuroimage*, vol. 26, pp. 912–921, 2005, doi: 10.1016/j.neuroimage.2005.03.012.
[342] D. Eidelberg *et al.*, 'The Metabolic Topography of Parkinsonism', *J. Cereb. Blood Flow Metab.*, vol. 14, no. 5, pp. 783–801, Sep. 1994, doi: 10.1038/jcbfm.1994.99.
[343] A. Feigin *et al.*, 'Modulation of metabolic brain networks after subthalamic gene therapy for Parkinson's disease', *Proc. Natl. Acad. Sci. U. S. A.*, vol. 104, no. 49, pp. 19559–19564, 2007, doi: 10.1073/pnas.0706006104.
[344] M. Trošt *et al.*, 'Network modulation by the subthalamic nucleus in the treatment of Parkinson's disease', *Neuroimage*, vol. 31, no. 1, pp. 301–307, May 2006, doi: 10.1016/j.neuroimage.2005.12.024.
[345] J. Wang, Y. Ma, Z. Huang, B. Sun, Y. Guan, and C. Zuo, 'Modulation of metabolic brain function by bilateral subthalamic nucleus stimulation in the treatment of Parkinson's disease', *J. Neurol.*, vol. 257, no. 1, pp. 72–78, Jan. 2010, doi: 10.1007/s00415-009-5267-3.
[346] H. Mure *et al.*, 'Parkinson's disease tremor-related metabolic network: Characterization, progression, and treatment effects', *Neuroimage*, vol. 54, no. 2, pp. 1244–1253, Jan. 2011, doi: 10.1016/j.neuroimage.2010.09.028.
[347] C. C. Tang, K. L. Poston, V. Dhawan, and D. Eidelberg, 'Abnormalities in Metabolic Network Activity Precede the Onset of Motor Symptoms in Parkinson's Disease', *J. Neurosci.*, vol. 30, no. 3, pp. 1049–1056, Jan. 2010, doi: 10.1523/JNEUROSCI.4188-09.2010.
[348] A. Zwergal *et al.*, 'Functional disturbance of the locomotor network in progressive supranuclear palsy', *Neurology*, vol. 80, no. 7, pp. 634–641, Feb. 2013, doi: 10.1212/WNL.0b013e318281cc43.
[349] A. Zwergal *et al.*, 'Postural imbalance and falls in PSP correlate with functional pathology of the thalamus', *Neurology*, vol. 77, no. 2, pp. 101–109, 2011, doi: 10.1212/WNL.0b013e318223c79d.
[350] R. Lamb, J. D. Rohrer, A. J. Lees, and H. R. Morris, 'Progressive Supranuclear Palsy and Corticobasal Degeneration: Pathophysiology and Treatment Options', *Curr. Treat. Options Neurol.*, vol. 18, p. 42, 2016, doi: 10.1007/s11940-016-0422-5.
[351] M. R. Khanna, J. Kovalevich, V. M. Y. Lee, J. Q. Trojanowski, and K. R. Brunden, 'Therapeutic strategies for the treatment of tauopathies: Hopes and challenges', *Alzheimer's Dement.*, vol. 12, no. 10, pp. 1051–1065, 2016, doi: 10.1016/j.jalz.2016.06.006.
[352] D. V. Moretti, 'Available and future treatments for atypical parkinsonism. A systematic review', *CNS Neurosci. Ther.*, vol. 25, no. 2, pp. 159–174, 2019, doi: 10.1111/cns.13068.
[353] R. Giordano *et al.*, 'Brief research report Safety and effectiveness of cell therapy in neurodegenerative diseases: Take-home messages from a phase I study of progressive supranuclear palsy', *Front. Neurosci. Neurodegener. Neurodegener.*, vol. under revi, no. October, pp. 1–11, 2021, doi: 10.3389/fnins.2021.723227.
[354] I. Clerici *et al.*, 'Rehabilitation in progressive supranuclear palsy: Effectiveness of two

multidisciplinary treatments', *PLoS One*, vol. 12, no. 2, p. e0170927, 2017, doi: 10.1371/journal.pone.0170927.

[355] M. Suteerawattananon, B. MacNeill, and E. J. Protas, 'Supported treadmill training for gait and balance in a patient with progressive supranuclear palsy', *Phys. Ther.*, vol. 82, no. 5, pp. 485–495, 2002, doi: 10.1093/ptj/82.5.485.

[356] S. Nicolai *et al.*, 'A 6-week intervention study in patients with progressive supranuclear palsy', *Z. Gerontol. Geriatr.*, vol. 43, no. 4, pp. 224–228, 2010, doi: 10.1007/s00391-010-0125-6.

[357] L. Brusa *et al.*, 'Implantation of the nucleus tegmenti pedunculopontini in a PSP-P patient: Safe procedure, modest benefits', *Mov. Disord.*, vol. 24, no. 13, pp. 2020–2032, 2009, doi: 10.1002/mds.22706.

[358] D. Servello, E. Zekaj, C. Saleh, C. Menghetti, and M. Porta, 'Long-term follow-up of deep brain stimulation of peduncolopontine nucleus in progressive supranuclear palsy: Report of three cases', *Surg. Neurol. Int.*, vol. 5, pp. S416–S420, 2014, doi: 10.4103/2152-7806.140208.

[359] E. Scelzo *et al.*, 'Peduncolopontine nucleus stimulation in progressive supranuclear palsy: A randomised trial', *J. Neurol. Neurosurg. Psychiatry*, vol. 88, no. 7, pp. 613–614, 2017, doi: 10.1136/jnnp-2016-315192.

[360] I. Galazky *et al.*, 'Deep brain stimulation of the pedunculopontine nucleus for treatment of gait and balance disorder in progressive supranuclear palsy: Effects of frequency modulations and clinical outcome', *Park. Relat. Disord.*, vol. 50, pp. 81–86, 2018, doi: 10.1016/j.parkreldis.2018.02.027.

[361] Y. Wen, B. Jiao, Y. Zhou, and L. Shen, 'A systematic review and meta-analysis of Deep Brain Stimulation for Progressive Supranuclear Palsy', *Res. Sq.*, vol. [Preprint], May 2020, doi: 10.21203/rs.3.rs-122655/v1.

[362] C. Palmisano, L. Beccaria, S. Haufe, J. Volkmann, G. Pezzoli, and I. U. Isaias, 'Gait initiation impairment in patients with Parkinson's disease and freezing of gait', *Front. Bioeng. Biotechnol.*, vol. under revi, 2021.

[363] C. L. Tomlinson, R. Stowe, S. Patel, C. Rick, R. Gray, and C. E. Clarke, 'Systematic review of levodopa dose equivalency reporting in Parkinson's disease', *Mov. Disord.*, vol. 25, no. 15, pp. 2649–2653, 2010, doi: 10.1002/mds.23429.

[364] A. . Hughes, S. E. Daniel, Y. Ben-Shlomo, and A. . Lees, 'The accuracy of diagnosis of parkinsonian syndromes in a specialist movement disorder service', *Brain*, vol. 125, pp. 861–870, 2002, [Online]. Available: http://www.embase.com/search/results?subaction=viewrecord&from=export&id=L34279780.

[365] G. U. Höglinger *et al.*, 'Clinical diagnosis of progressive supranuclear palsy: The movement disorder society criteria', *Mov. Disord.*, vol. 32, no. 6, pp. 853–864, 2017, doi: 10.1002/mds.26987.

[366] G. Respondek *et al.*, 'The phenotypic spectrum of progressive supranuclear palsy: A retrospective multicenter study of 100 definite cases', *Mov. Disord.*, vol. 29, no. 14, pp. 1758–1766, 2014, doi: 10.1002/mds.26054.

[367] B. Scatton, F. Javoy-Agid, L. Rouquier, B. Dubois, and Y. Agid, 'Reduction of cortical dopamine, noradrenaline, serotonin and their metabolites in Parkinson's disease', *Brain Res.*, vol. 275, pp. 321–328, 1983, doi: 10.1016/0006-8993(83)90993-9.

[368] P. Gaspar, C. Duyckaerts, C. Alvarez, F. Javoy-Agid, and B. Berger, 'Alterations of dopaminergic and noradrenergic innervations in motor cortex in parkinson's disease', *Ann. Neurol.*, vol. 30, no. 3, pp. 365–374, 1991, doi: 10.1002/ana.410300308.
[369] C. Buddhala *et al.*, 'Dopaminergic, serotonergic, and noradrenergic deficits in Parkinson disease', *Ann. Clin. Transl. Neurol.*, vol. 2, no. 10, pp. 949–959, 2015, doi: 10.1002/acn3.246.
[370] M. Sommerauer *et al.*, 'Evaluation of the noradrenergic system in Parkinson's disease: An 11 C-MeNER PET and neuromelanin MRI study', *Brain*, vol. 141, no. 2, pp. 496–504, 2017, doi: 10.1093/brain/awx348.
[371] I. U. Isaias, J. Brumberg, G. Marotta, J. Volkmann, and G. Pezzoli, 'Brain metabolic alterations herald falls in patients with Parkinson' s disease', *Ann. Clin. Transl. Neurol.*, vol. 7, no. 4, pp. 579–583, 2020, doi: 10.1002/acn3.51013.
[372] C. Tard *et al.*, 'Attention modulates step initiation postural adjustments in Parkinson freezers', *Park. Relat. Disord.*, vol. 20, pp. 284–289, 2014, doi: 10.1016/j.parkreldis.2013.11.016.
[373] C. Pimoule, F. Schoemaker, F. Javoy-Agid, B. Scatton, F. Agid, and S. Z. Langer, 'Decrease in [3H]Cocaine Binding to the Dopamine Transporter in Parkinson's Disease', *Eur. J. Pharmacol.*, vol. 95, no. 1–2, pp. 145–146, 1983.
[374] J. M. Maloteaux, M. A. Vanisberg, C. Laterre, F. Javoy-Agid, Y. Agid, and P. M. Laduron, '[3H]GBR 12935 binding to dopamine uptake sites: subcellular localizatio and reduction in Parkinson's disease and progressive supranuclear palsy', *Eur. J. Pharmacol.*, vol. 156, no. 3, pp. 331–340, 1988, doi: 10.1016/0014-2999(88)90278-6.
[375] M. J. Kaufman and B. K. Madras, 'Severe depletion of cocaine recognition sites associated with the dopamine transporter in Parkinson's-diseased striatum', *Synapse*, vol. 9, no. 1, pp. 43–49, 1991, doi: 10.1002/syn.890090107.
[376] H. B. Niznik, E. F. Fogel, F. F. Fassos, and P. Seeman, 'The Dopamine Transporter Is Absent in Parkinsonian Putamen and Reduced in the Caudate Nucleus', *J. Neurochem.*, vol. 56, no. 1, pp. 192–198, 1991, doi: 10.1111/j.1471-4159.1991.tb02580.x.
[377] K. Marek, J. Seibyl, R. Holloway, K. Kieburtz, D. Oakes, and A. Lang, 'A multicenter assessment of dopamine transporter imaging with DOPASCAN/SPECT in parkinsonism', *Neurology*, vol. 55, no. 10, pp. 1540–1547, Nov. 2000, doi: 10.1212/WNL.55.10.1540.
[378] J. Schwarz, A. Storch, W. Koch, O. Pogarell, P. E. Radau, and K. Tatsch, 'Loss of dopamine transporter binding in Parkinson's disease follows a single exponential rather than linear decline', *J. Nucl. Med.*, vol. 45, no. 10, pp. 1694–1697, 2004.
[379] P. Mahlknecht, K. Seppi, and W. Poewe, 'The concept of prodromal Parkinson's disease', *J. Parkinsons. Dis.*, vol. 5, no. 4, pp. 681–697, 2015, doi: 10.3233/JPD-150685.
[380] I. U. Isaias *et al.*, 'A role for locus coeruleus in Parkinson tremor', *Front. Hum. Neurosci.*, vol. 5, p. 179, 2012, doi: 10.3389/fnhum.2011.00179.
[381] C. Lapa *et al.*, 'Influence of CT-based attenuation correction on dopamine transporter SPECT with [(123)I]FP-CIT.', *Am. J. Nucl. Med. Mol. Imaging*, vol. 5, no. 3, pp. 278–86, 2015, [Online]. Available: http://www.ncbi.nlm.nih.gov/pubmed/26069861%0Ahttp://www.pubmedcentral.nih.gov/articlerender.fcgi?artid=PMC4446396.
[382] C. Raccagni *et al.*, 'Gait and postural disorders in parkinsonism: a clinical approach', *J. Neurol.*, vol. 267, pp. 3169–3176, 2020, doi: 10.1007/s00415-019-09382-1.
[383] G. Respondek, S. Roeber, H. Kretzschmar, and C. Troakes, 'Accuracy of the National

Institute for Neurological Disorders and Stroke/Society for Progressive Supranuclear Palsy and Neuroprotection and Natural History in Parkinson Plus Syndromes Criteria for the Diagnosis of Progressive Supranuclear Palsy', *Mov. Disord.*, vol. 28, no. 4, pp. 504–509, 2013, doi: 10.1002/mds.25327.

[384] S. K. Alexander, T. Rittman, J. H. Xuereb, T. H. Bak, J. R. Hodges, and J. B. Rowe, 'Validation of the new consensus criteria for the diagnosis of corticobasal degeneration', *J. Neurol. Neurosurg. Psychiatry*, vol. 85, no. 8, pp. 923–927, 2014, doi: 10.1136/jnnp-2013-307035.

[385] M. Heilbron *et al.*, 'Anticipatory postural adjustmens are modulated by substantia nigra stimulation in people with Parkinson's disease and freezing of gait', *Park. Relat. Disord.*, vol. 66, pp. 34–39, 2019.

[386] G. Lagravinese, E. Pelosin, G. Bonassi, F. Carbone, G. Abbruzzese, and L. Avanzino, 'Gait initiation is influenced by emotion processing in Parkinson's disease patients with freezing', *Mov. Disord.*, vol. 33, no. 4, pp. 609–617, 2018, doi: 10.1002/mds.27312.

[387] A. Ferrari *et al.*, 'Quantitative comparison of five current protocols in gait analysis', *Gait Posture*, vol. 28, no. 2, pp. 207–216, 2008, doi: 10.1016/j.gaitpost.2007.11.009.

[388] V. M. Zatsiorsky, *Kinetics of Human Motion*. Human Kinetics, 2002.

[389] M. J. O'Malley, 'Normalization of temporal-distance parameters in pediatric gait', *J. Biomech.*, vol. 29, no. 5, pp. 619–625, 1996, doi: 10.1016/0021-9290(95)00088-7.

[390] D. Ferrazzoli *et al.*, 'Balance dysfunction in Parkinson's disease: The role of posturography in developing a rehabilitation program', *Parkinsons. Dis.*, vol. 520128, 2015, doi: 10.1155/2015/520128.

[391] A. Mirelman *et al.*, 'Arm swing as a potential new prodromal marker of Parkinson's disease', *Mov. Disord.*, vol. 31, no. 10, pp. 1527–1534, 2016, doi: 10.1002/mds.26720.

[392] M. Pistacchi *et al.*, 'Gait analysis and clinical correlations in early Parkinson's disease', *Funct. Neurol.*, vol. 32, no. 1, pp. 28–34, 2017, doi: 10.11138/FNeur/2017.32.1.028.

[393] J. Nonnekes, R. J. M. Goselink, E. Růzicka, A. Fasano, J. G. Nutt, and B. R. Bloem, 'Neurological disorders of gait, balance and posture: A sign-based approach', *Nat. Rev. Neurol.*, vol. 14, no. 3, pp. 183–189, 2018, doi: 10.1038/nrneurol.2017.178.

[394] C. Napier, X. Jiang, C. L. MacLean, C. Menon, and M. A. Hunt, 'The use of a single sacral marker method to approximate the centre of mass trajectory during treadmill running', *J. Biomech.*, vol. 108, p. 109886, 2020, doi: 10.1016/j.jbiomech.2020.109886.

[395] C. Torrence and G. P. Compo, 'A Practical Guide to Wavelet Analysis', *Bull. Am. Meteorol. Soc.*, vol. 79, no. 1, pp. 61–78, 1998, doi: 10.1175/1520-0477(1998)079<0061:APGTWA>2.0.CO;2.

[396] H. Sadeghi *et al.*, 'Reduction of gait data variability using curve registration', *Gait Posture*, vol. 12, pp. 257–264, 2000.

[397] M. Haller *et al.*, 'Parameterizing neural power spectra', *Neuroscience*, 2018, doi: 10.1101/299859.

[398] C. Shannon, 'A mathematical theory of communication.', *Bell Sys Tech J*, vol. 27, pp. 379–423, 1948, doi: 10.1016/s0016-0032(23)90506-5.

[399] S. Panzeri, F. Petroni, R. S. Petersen, and M. E. Diamond, 'Decoding neuronal population activity in rat somatosensory cortex: Role of columnar organization', *Cereb. Cortex*, vol. 13, no. 1, pp. 45–52, 2003, doi: 10.1093/cercor/13.1.45.

[400] A. Mazzoni, N. Brunel, S. Cavallari, N. K. Logothetis, and S. Panzeri, 'Cortical dynamics

during naturalistic sensory stimulations: Experiments and models', *J. Physiol. Paris*, vol. 105, pp. 2–15, 2011, doi: 10.1016/j.jphysparis.2011.07.014.

[401] C. Magri, K. Whittingstall, V. Singh, N. K. Logothetis, and S. Panzeri, 'A toolbox for the fast information analysis of multiple-site LFP, EEG and spike train recordings', *BMC Neurosci.*, vol. 10, no. 81, 2009, doi: 10.1186/1471-2202-10-81.

[402] A. Belitski *et al.*, 'Low-frequency local field potentials and spikes in primary visual cortex convey independent visual information', *J. Neurosci.*, vol. 28, no. 22, pp. 5696–5709, 2008, doi: 10.1523/JNEUROSCI.0009-08.2008.

[403] A. Mazzoni, S. Panzeri, N. K. Logothetis, and N. Brunel, 'Encoding of naturalistic stimuli by local field potential spectra in networks of excitatory and inhibitory neurons', *PLoS Comput. Biol.*, vol. 4, no. 12, p. e1000239, 2008, doi: 10.1371/journal.pcbi.1000239.

[404] S. Panzeri and A. Treves, 'Network : Computation in Neural Systems Analytical estimates of limited sampling biases in different information measures', *Netw. Comput. Neural Syst.*, vol. 7, no. 1, pp. 87–107, 1996, doi: 10.1080/0954898X.1996.11978656.

[405] P. Zangger, 'The effect of 4-aminopyridine on the spinal locomotor rhythm induced by l-DOPA', *Brain Res.*, vol. 215, no. 1–2, pp. 211–223, 1981, doi: 10.1016/0006-8993(81)90503-5.

[406] J. A. Obeso *et al.*, 'The basal ganglia in Parkinson's disease: Current concepts and unexplained observations', *Ann. Neurol.*, vol. 64, no. SUPPL. 2, 2008, doi: 10.1002/ana.21481.

[407] D. Devos, L. Defebvre, and R. Bordet, 'Dopaminergic and non-dopaminergic pharmacological hypotheses for gait disorders in Parkinson's disease', *Fundam. Clin. Pharmacol.*, vol. 24, no. 4, pp. 407–421, 2010, doi: 10.1111/j.1472-8206.2009.00798.x.

[408] P. Mazzoni, A. Hristova, and J. W. Krakauer, 'Why don't we move faster? Parkinson's disease, movement vigor, and implicit motivation', *J. Neurosci.*, vol. 27, no. 27, pp. 7105–7116, 2007, doi: 10.1523/JNEUROSCI.0264-07.2007.

[409] L. Marinelli *et al.*, 'Learning and consolidation of visuo-motor adaptation in Parkinson's disease', *Park. Relat. Disord.*, vol. 15, no. 1, pp. 6–11, 2009, doi: 10.1016/j.parkreldis.2008.02.012.

[410] I. U. Isaias *et al.*, 'Dopaminergic striatal innervation predicts interlimb transfer of a visuomotor skill', *J. Neurosci.*, vol. 31, no. 41, pp. 14458–14462, 2011, doi: 10.1523/JNEUROSCI.3583-11.2011.

[411] N. Fabre *et al.*, 'Normal frontal perfusion in patients with frozen gait', *Mov. Disord.*, vol. 13, no. 4, pp. 677–683, 1998, doi: 10.1002/mds.870130412.

[412] M. D. Latt, S. R. Lord, J. G. L. Morris, and V. S. C. Fung, 'Clinical and physiological assessments for elucidating falls risk in Parkinson's disease', *Mov. Disord.*, vol. 24, no. 9, pp. 1280–1289, 2009, doi: 10.1002/mds.22561.

[413] M. Djurić-Jovičić, N. S. Jovičić, I. Milovanović, S. Radovanović, N. Kresojević, and M. B. Popović, 'Classification of walking patterns in Parkinson's disease patients based on inertial sensor data', *10th Symp. Neural Netw. Appl. Electr. Eng. NEUREL-2010 - Proc.*, pp. 3–6, 2010, doi: 10.1109/NEUREL.2010.5644040.

[414] R. W. Genever, T. W. Downes, and P. Medcalf, 'Fracture rates in Parkinson's disease compared with age- and gender-matched controls: A retrospective cohort study', *Age Ageing*, vol. 34, no. 1, pp. 21–24, 2005, doi: 10.1093/ageing/afh203.

[415] J. Idjadi *et al.*, 'Hip fracture outcomes in patients with Parkinson's disease.', *Am J Orthop (Belle Mead NJ)*, vol. 34, no. 7, pp. 341–6, 2005.

[416] J. Murphy and B. Isaacs, 'The Post-Fall Syndrome', *Gerontology*, vol. 28, pp. 265–270, 1982.
[417] B. Vellas, F. Cayla, H. Bocquet, F. De Pemille, and J. L. Albarede, 'Prospective study of restriction of acitivty in old people after falls', *Age Ageing*, vol. 16, no. 3, pp. 189–193, 1987, doi: 10.1093/ageing/16.3.189.
[418] B. E. Maki, P. J. Holliday, and A. K. Topper, 'Fear of falling and postural performance in the elderly', *Journals Gerontol.*, vol. 46, no. 4, pp. M123-131, 1991, doi: 10.1093/geronj/46.4.M123.
[419] D. S. Peterson and F. B. Horak, 'Neural control of walking in people with parkinsonism', *Physiology*, vol. 31, no. 2, pp. 95–107, 2016, doi: 10.1152/physiol.00034.2015.
[420] E. Dalton, M. Bishop, M. D. Tillman, and C. J. Hass, 'Simple change in initial standing position enhances the initiation of gait', *Med. Sci. Sports Exerc.*, vol. 43, no. 12, pp. 2352–2358, 2011, doi: 10.1249/MSS.0b013e318222bc82.
[421] F. Turco *et al.*, 'Cortical response to levodopa in Parkinson's disease patients with dyskinesias', *Eur. J. Neurosci.*, vol. 48, no. 6, pp. 2362–2373, 2018, doi: 10.1111/ejn.14114.
[422] C. D. MacKinnon *et al.*, 'Preparation of anticipatory postural adjustments prior to stepping', *J. Neurophysiol.*, vol. 97, no. 6, pp. 4368–4379, 2007, doi: 10.1152/jn.01136.2006.
[423] L. Mouchnino *et al.*, 'Facilitation of cutaneous inputs during the planning phase of gait initiation', *J. Neurophysiol.*, vol. 114, no. 1, pp. 301–308, 2015, doi: 10.1152/jn.00668.2014.
[424] F. Cheruel, J. F. Dormont, M. Amalric, A. Schmied, and D. Farin, 'The role of putamen and pallidum in motor initiation in the cat', *Exp. Brain Res.*, vol. 100, no. 2, pp. 250–266, 1994, doi: 10.1007/BF00227195.
[425] R. B. Postuma and A. Dagher, 'Basal ganglia functional connectivity based on a meta-analysis of 126 positron emission tomography and functional magnetic resonance imaging publications', *Cereb. Cortex*, vol. 16, no. 10, pp. 1508–1521, 2006, doi: 10.1093/cercor/bhj088.
[426] J. T. Coull, H. J. Hwang, M. Leyton, and A. Dagher, 'Dopamine precursor depletion impairs timing in healthy volunteers by attenuating activity in putamen and supplementary motor area', *J. Neurosci.*, vol. 32, no. 47, pp. 16704–16715, 2012, doi: 10.1523/JNEUROSCI.1258-12.2012.
[427] J. W. Barter, S. Li, T. Sukharnikova, M. A. Rossi, R. A. Bartholomew, and H. H. Yin, 'Basal ganglia outputs map instantaneous position coordinates during behavior', *J. Neurosci.*, vol. 35, no. 6, pp. 2703–2716, 2015, doi: 10.1523/JNEUROSCI.3245-14.2015.
[428] J. A. Obeso *et al.*, 'Functional organization of the basal ganglia: Therapeutic implications for Parkinson's disease', *Mov. Disord.*, vol. 23, no. SUPPL. 3, pp. 548–559, 2008, doi: 10.1002/mds.22062.
[429] J. B. Koprich, T. H. Johnston, P. Huot, S. H. Fox, and J. M. Brotchie, 'New insights into the organization of the basal ganglia', *Curr. Neurol. Neurosci. Rep.*, vol. 9, no. 4, pp. 298–304, 2009, doi: 10.1007/s11910-009-0045-2.
[430] N. Giladi and A. Nieuwboer, 'Understanding and treating freezing of gait in Parkinsonism, proposed working definition, and setting the stage', *Mov. Disord.*, vol. 23, no. SUPPL. 2, pp. 423–425, 2008, doi: 10.1002/mds.21927.
[431] S. J. G. Lewis and R. A. Barker, 'A pathophysiological model of freezing of gait in Parkinson's disease', *Park. Relat. Disord.*, vol. 15, no. 5, pp. 333–338, 2009, doi: 10.1016/j.parkreldis.2008.08.006.

[432] C. Moreau *et al.*, 'STN-DBS Frequency effects on freezing of gait in advanced parkinson disease', *Neurology*, vol. 71, no. 2, pp. 80–84, 2009, doi: doi:10.1212/01.wnl.0000303972.16279.46.

[433] N. Giladi *et al.*, 'Validation of the Freezing of Gait Questionnaire in patients with Parkinson's disease', *Mov. Disord.*, vol. 24, no. 5, pp. 655–661, 2009, doi: 10.1002/mds.21745.

[434] A. L. Bartels, Y. Balash, T. Gurevich, J. D. Schaafsma, J. M. Hausdorff, and N. Giladi, 'Relationship between freezing of gait (FOG) and other features of Parkinson's: FOG is not correlated with bradykinesia', *J. Clin. Neurosci.*, vol. 10, no. 5, pp. 584–588, 2003, doi: 10.1016/S0967-5868(03)00192-9.

[435] L. M. Ambani and M. H. Van Woert, 'Start hesitation - A side efect of long-term Levodopa terapy', *N. Engl. J. Med.*, vol. 288, no. 21, pp. 1113–1115, 1973.

[436] S. Della Sala, A. Francescani, and H. Spinnler, 'Gait apraxia after bilateral supplementary motor area lesion', *j Neurol Neurosurg Psychiatry*, vol. 72, pp. 77–85, 2002.

[437] P. Nachev, C. Kennard, and M. Husain, 'Functional role of the supplementary and pre-supplementary motor areas', *Nat. Rev. Neurosci.*, vol. 9, pp. 856–869, 2008, doi: 10.1038/nrn2478.

[438] K. Takakusaki, 'Functional Neuroanatomy for Posture and Gait Control', *J. Mov. Disord.*, vol. 10, no. 1, pp. 1–17, 2017, doi: 10.14802/jmd.16062.

[439] A. Nieuwboer *et al.*, 'Cueing training in the home improves gait-related mobility in Parkinson's disease: The RESCUE trial', *J. Neurol. Neurosurg. Psychiatry*, vol. 78, no. 2, pp. 134–140, 2007, doi: 10.1136/jnnp.200X.097923.

[440] A. P. Fortin, Y. Dessery, S. Leteneur, F. Barbier, and P. Corbeil, 'Effect of natural trunk inclination on variability in soleus inhibition and tibialis anterior activation during gait initiation in young adults', *Gait Posture*, vol. 41, no. 2, pp. 378–383, 2015, doi: 10.1016/j.gaitpost.2014.09.019.

[441] N. Giladi, H. Shabtai, E. Rozenberg, and E. Shabtai, 'Gait festination in Parkinson's disease', *Park. Relat. Disord.*, vol. 7, no. 2, pp. 135–138, 2001, doi: 10.1016/S1353-8020(00)00030-4.

[442] M. E. Morris, R. Iansek, and B. Galna, 'Gait festination and freezing in Parkinson's disease: Pathogenesis and rehabilitation', *Mov. Disord.*, vol. 23, no. SUPPL. 2, pp. S451–S460, 2008, doi: 10.1002/mds.21974.

[443] P. Lorenzi, R. Rao, G. Romano, A. Kita, and F. Irrera, 'Mobile Devices for the Real-Time Detection of Specific Human Motion Disorders', *IEEE Sens. J.*, vol. 16, no. 23, pp. 8220–8227, 2016, doi: 10.1109/JSEN.2016.2530944.

[444] A. Kita, P. Lorenzi, R. Rao, and F. Irrera, 'Reliable and robust detection of freezing of gait episodes with wearable electronic devices', *IEEE Sens. J.*, vol. 17, no. 6, pp. 1899–1908, 2017, doi: 10.1109/JSEN.2017.2659780.

[445] E. M. J. Bekkers *et al.*, 'Adaptations to postural perturbations in patients with freezing of gait', *Front. Neurol.*, vol. 9, p. 540, 2018, doi: 10.3389/fneur.2018.00540.

[446] L. Avanzino, E. Pelosin, C. M. Vicario, G. Lagravinese, G. Abbruzzese, and D. Martino, 'Time processing and motor control in movement disorders', *Front. Hum. Neurosci.*, vol. 10, p. 631, 2016, doi: 10.3389/fnhum.2016.00631.

[447] J. H. Drucker *et al.*, 'Internally guided lower limb movement recruits compensatory cerebellar activity in people with Parkinson's disease', *Front. Neurol.*, vol. 10, p. 573, 2019,

doi: 10.3389/fneur.2019.00537.
[448] K. Hiraoka, Y. Matuo, A. Iwata, T. Onishi, and K. Abe, 'The effects of external cues on ankle control during gait initiation in Parkinson's disease', *Park. Relat. Disord.*, vol. 12, no. 2, pp. 97–102, 2006, doi: 10.1016/j.parkreldis.2005.07.006.
[449] A. Richard, A. Van Hamme, X. Drevelle, J. L. Golmard, S. Meunier, and M. L. Welter, 'Contribution of the supplementary motor area and the cerebellum to the anticipatory postural adjustments and execution phases of human gait initiation', *Neuroscience*, vol. 358, pp. 181–189, 2017, doi: 10.1016/j.neuroscience.2017.06.047.
[450] T. Hanakawa, H. Fukuyama, Y. Katsumi, M. Honda, and H. Shibasaki, 'Enhanced lateral premotor activity during paradoxical gait in parkinson's disease', *Ann. Neurol.*, vol. 45, no. 3, pp. 329–336, 1999, doi: 10.1002/1531-8249(199903)45:3<329::AID-ANA8>3.0.CO;2-S.
[451] N. Picard and P. L. Strick, 'Imaging the premotor areas', *Curr. Opin. Neurobiol.*, vol. 11, no. 6, pp. 663–672, 2001, doi: 10.1016/S0959-4388(01)00266-5.
[452] M. Voss, J. N. Ingram, D. M. Wolpert, and P. Haggard, 'Mere expectation to move causes attenuation of sensory signals', *PLoS One*, vol. 3, no. 8, p. e2866, 2008, doi: 10.1371/journal.pone.0002866.
[453] F. Bolzoni, C. Bruttini, R. Esposti, C. Castellani, and P. Cavallari, 'Transcranial direct current stimulation of SMA modulates anticipatory postural adjustments without affecting the primary movement', *Behav. Brain Res.*, vol. 291, pp. 407–413, 2015, doi: 10.1016/j.bbr.2015.05.044.
[454] T. Wolbers, M. Hegarty, C. Büchel, and J. M. Loomis, 'Spatial updating: How the brain keeps track of changing object locations during observer motion', *Nat. Neurosci.*, vol. 11, no. 10, pp. 1223–1230, 2008, doi: 10.1038/nn.2189.
[455] H. Ruget, J. Blouin, N. Teasdale, and L. Mouchnino, 'Can prepared anticipatory postural adjustments be updated by proprioception?', *Neuroscience*, vol. 155, no. 3, pp. 640–648, 2008, doi: 10.1016/j.neuroscience.2008.06.021.
[456] M. Gandolfi *et al.*, 'Four-week trunk-specific exercise program decreases forward trunk flexion in Parkinson's disease: A single-blinded, randomized controlled trial', *Park. Relat. Disord.*, vol. 64, pp. 268–274, 2019, doi: 10.1016/j.parkreldis.2019.05.006.
[457] W. G. Wright, V. S. Gurfinkel, J. Nutt, F. B. Horak, and P. J. Cordo, 'Axial hypertonicity in Parkinson's disease: Direct measurements of trunk and hip torque', *Exp Neurol.*, vol. 208, no. 1, pp. 38–46, 2007, [Online]. Available: https://www.ncbi.nlm.nih.gov/pmc/articles/PMC3624763/pdf/nihms412728.pdf.
[458] G. Albani, V. Cimolin, A. Fasano, C. Trotti, M. Galli, and A. Mauro, '"Masters and servants" in parkinsonian gait: a three-dimensional analysis of biomechanical changes sensitive to disease progression.', *Funct Neurol*, vol. 29, no. 2, pp. 99–105, 2014.
[459] T. Blackburn and D. Padua, 'Sagittal-Plane Trunk Position, Landing Forces, and Quadriceps Electromyographic Activity', *J. Athl. Train.*, vol. 44, no. 2, pp. 174–179, 2009, doi: 10.4085/1062-6050-44.2.174.
[460] F. Yoshii, Y. Moriya, T. Ohnuki, M. Ryo, and W. Takahashi, 'Postural deformities in Parkinson ' s disease – Mutual relationships among neck flexion , fore-bent , knee-bent and lateral-bent angles and correlations with clinical predictors', *J. Clin. Mov. Disord.*, vol. 3, no. 1, pp. 3–9, 2016, doi: 10.1186/s40734-016-0029-8.
[461] S. Aminiaghdam, C. Rode, R. Müller, and R. Blickhan, 'Increasing trunk flexion transforms human leg function into that of birds despite different leg morphology', *J. Exp. Biol.*, vol.

220, no. 3, pp. 478–486, 2017, doi: 10.1242/jeb.148312.
[462] J. V. Jacobs, D. M. Dimitrova, J. G. Nutt, and F. B. Horak, 'Can stooped posture explain multidirectional postural instability in patients with Parkinson's disease?', *Exp. Brain Res.*, vol. 166, no. 1, pp. 78–88, 2005, doi: 10.1007/s00221-005-2346-2.
[463] H. A. Chang and D. E. Krebs, 'Dynamic balance control in elders: Gait initiation assessment as a screening tool', *Arch. Phys. Med. Rehabil.*, vol. 80, no. 5, pp. 490–494, 1999, doi: 10.1016/S0003-9993(99)90187-9.
[464] M. E. Hernandez, J. A. Ashton-Miller, and N. B. Alexander, 'The effect of age, movement direction, and target size on the maximum speed of targeted COP movements in healthy women', *Hum. Mov. Sci.*, vol. 31, no. 5, pp. 1213–1223, 2012, doi: 10.1016/j.humov.2011.11.002.
[465] A. D. Nordin, W. D. Hairston, and D. P. Ferris, 'Human electrocortical dynamics while stepping over obstacles', *Sci. Rep.*, vol. 9, p. 4693, 2019, doi: 10.1038/s41598-019-41131-2.
[466] W. Ondo *et al.*, 'Computerized Posturography Analysis of Progressive Supranuclear Palsy', *Arch. Neurol.*, vol. 57, no. 10, pp. 1464–1469, Oct. 2000, doi: 10.1001/archneur.57.10.1464.
[467] K. Liao *et al.*, 'Why do patients with PSP fall?: Evidence for abnormal otolith responses', *Neurology*, vol. 70, no. 10, pp. 802–809, Mar. 2008, doi: 10.1212/01.wnl.0000304134.33380.1e.
[468] M. L. Welter *et al.*, 'Control of vertical components of gait during initiation of walking in normal adults and patients with progressive supranuclear palsy', *Gait Posture*, vol. 26, no. 3, pp. 393–399, 2007, doi: 10.1016/j.gaitpost.2006.10.005.
[469] K. Rosenberg-Katz, T. Herman, Y. Jacob, N. Giladi, T. Hendler, and J. M. Hausdorff, 'Gray matter atrophy distinguishes between Parkinson disease motor subtypes', *Neurology*, vol. 80, no. 16, pp. 1476–1484, 2013, doi: 10.1212/WNL.0b013e31828cfaa4.
[470] J. W. Mink, 'THE BASAL GANGLIA: FOCUSED SELECTION AND INHIBITION OF COMPETING MOTOR PROGRAMS JONATHAN', *Prog. Neurobiol.*, vol. 50, pp. 381–425, 1996, doi: 10.1016/S0301-0082(96)00042-1.
[471] I. U. Isaias, J. Volkmann, A. Marzegan, G. Marotta, P. Cavallari, and G. Pezzoli, 'The Influence of Dopaminergic Striatal Innervation on Upper Limb Locomotor Synergies', *PLoS One*, vol. 7, no. 12, p. e51464, 2012, doi: 10.1371/journal.pone.0051464.
[472] E. J. Bubb, C. Metzler-Baddeley, and J. P. Aggleton, 'The cingulum bundle: Anatomy, function, and dysfunction', *Neurosci. Biobehav. Rev.*, vol. 92, pp. 104–127, 2018, doi: 10.1016/j.neubiorev.2018.05.008.
[473] A. L. Rosso *et al.*, 'Higher step length variability indicates lower gray matter integrity of selected regions in older adults', *Gait Posture*, vol. 40, no. 1, pp. 225–230, 2014, doi: 10.1016/j.gaitpost.2014.03.192.
[474] V. Marlinski, W. U. Nilaweera, P. V Zelenin, M. G. Sirota, and I. N. Beloozerova, 'Signals from the ventrolateral thalamus to the motor cortex during locomotion', *J. Neurophysiol.*, vol. 107, no. 1, pp. 455–472, Jan. 2012, doi: 10.1152/jn.01113.2010.
[475] J. L. Whitwell, J. Xu, J. Mandrekar, J. L. Gunter, C. R. Jack, and K. A. Josephs, 'Imaging measures predict progression in progressive supranuclear palsy', *Mov. Disord.*, vol. 27, no. 14, pp. 1801–1804, 2012, doi: 10.1002/mds.24970.
[476] P. A. Pahapill and A. M. Lozano, 'The pedunclopontine nucleus and Parkinson's disease', *Brain*, vol. 123, pp. 1767–1783, 2000, doi: 10.1016/j.nbd.2018.08.017.

[477] P. Winn, 'How best to consider the structure and function of the pedunculopontine tegmental nucleus: Evidence from animal studies', *J. Neurol. Sci.*, vol. 248, no. 1–2, pp. 234–250, 2006, doi: 10.1016/j.jns.2006.05.036.
[478] D. Devos, L. Defebvre, and R. Bordet, 'Dopaminergic and non-dopaminergic pharmacological hypotheses for gait disorders in Parkinson's disease', *Fundam. Clin. Pharmacol.*, vol. 24, pp. 407–421, 2010, doi: 10.1111/j.1472-8206.2009.00798.x.
[479] J. C. Masdeu, U. Alampur, R. Cavaliere, and G. Tavoulareas, 'Astasia and gait failure with damage of the pontomesencephalic locomotor region', *Ann. Neurol.*, vol. 35, no. 5, pp. 619–621, 1994, doi: 10.1002/ana.410350517.
[480] P. Plaha and S. S. Gill, 'Deep Brain Stimulation of the Pedunculopontine Nucleus for Parkinson's Disease', *Neuroreport*, vol. 16, no. 17, pp. 1883–1887, 2005, doi: 10.1002/9781118346396.ch5.
[481] P. Mazzone *et al.*, 'Implantation of human pedunculopontine nucleus: A safe and clinically relevant target in Parkinson's disease', *Neuroreport*, vol. 16, no. 17, pp. 1877–1881, 2005, doi: 10.1097/01.wnr.0000187629.38010.12.
[482] A. Stefani *et al.*, 'Bilateral deep brain stimulation of the pedunculopontine and subthalamic nuclei in severe Parkinson's disease', *Brain*, vol. 130, no. 6, pp. 1596–1607, 2007, doi: 10.1093/brain/awl346.
[483] L. I. Golbe, 'The epidemiology of PSP', *J. Neural Transm. Suppl.*, no. 42, pp. 263–273, 1994, doi: 10.1007/978-3-7091-6641-3_20.
[484] F. J. G. Vingerhoets, J. G. Villemure, P. Temperli, C. Pollo, E. Pralong, and J. Ghika, 'Subthalamic DBS replaces levodopa in Parkinson's disease', *Neurology*, vol. 58, no. 3, pp. 396–401, 2002, doi: doi:10.1212/wnl.58.3.396.
[485] S. Fahn, 'The history of dopamine and levodopa in the treatment of Parkinson's disease', *Mov. Disord.*, vol. 23, no. SUPPL. 3, pp. S497–S508, 2008, doi: 10.1002/mds.22028.
[486] L. Defebvre, J. Blatt, S. Blond, J. L. Bourriez, J.-D. Guieu, and A. Destée, 'Effect of Thalamic Stimulation on Gait in Parkinson Disease', *Arch Neurol.*, vol. 53, no. 9, pp. 898–903, 1996.
[487] C. Schrader *et al.*, 'GPi-DBS may induce a hypokinetic gait disorder with freezing of gait in patients with dystonia', *Neurology*, vol. 77, no. 5, pp. 483–488, 2011, doi: 10.1212/WNL.0b013e318227b19e.
[488] B. F. L. van Nuenen, R. A. J. Esselink, M. Munneke, J. D. Speelman, T. van Laar, and B. R. Bloem, 'Postoperative gait deterioration after bilateral subthalamic nucleus stimulation in Parkinson's disease', *Mov. Disord.*, vol. 23, no. 16, pp. 2404–2419, 2008, doi: 10.1002/mds.21986.
[489] M. Pötter-Nerger and J. Volkmann, 'Deep brain stimulation for gait and postural symptoms in Parkinson's disease', *Mov. Disord.*, vol. 28, no. 11, pp. 1609–1615, 2013, doi: 10.1002/mds.25677.
[490] H. Stolze *et al.*, 'Effects of Bilateral Subthalamic Nucleus Stimulation and Medication on Parkinsonian Speech Impairment', *Neurology*, vol. 57, no. 1, pp. 144–146, 2001, doi: 10.1016/j.jvoice.2006.10.010.
[491] J. M. Hausdorff, L. Gruendlinger, L. Scollins, S. O'Herron, and D. Tarsy, 'Deep brain stimulation effects on gait variability in Parkinson's disease', *Mov. Disord.*, vol. 24, no. 11, pp. 1688–1692, 2009, doi: 10.1002/mds.22554.
[492] M. Ferrarin *et al.*, 'Quantitative analysis of gait in Parkinson's disease: A pilot study on the

effects of bilateral sub-thalamic stimulation', *Gait Posture*, vol. 16, no. 2, pp. 135–148, 2002, doi: 10.1016/S0966-6362(01)00204-1.

[493] M. Rizzone *et al.*, 'High-frequency electrical stimulation of the subthalamic nucleus in Parkinson's disease: Kinetic and kinematic gait analysis', *Neurol. Sci.*, vol. 23, no. SUPPL. 2, pp. 103–104, 2002, doi: 10.1007/s100720200090.

[494] M. Tagliati, 'Fine-tuning gait in Parkinson disease', *Neurology*, vol. 71, no. 2, pp. 76–77, 2008, doi: 10.1212/01.wnl.0000316807.94657.e0.

[495] H. Brozova, C. Republic, I. Barnaure, R. L. Alterman, and M. Tagliati, 'STN-DBS frequency effects on freezing of gait in advanced Parkinson Disease', *Neurology*, vol. 72, pp. 770–771, 2009.

[496] A. Priori, G. Foffani, L. Rossi, and S. Marceglia, 'Adaptive deep brain stimulation (aDBS) controlled by local field potential oscillations', *Exp. Neurol.*, vol. 245, pp. 77–86, 2013, doi: 10.1016/j.expneurol.2012.09.013.

[497] M. Cassidy *et al.*, 'Movement-related changes in synchronization in the human basal ganglia', *Brain*, vol. 125, no. 6, pp. 1235–1246, 2002, doi: 10.1093/brain/awf135.

[498] A. Priori *et al.*, 'Movement-related modulation of neural activity in human basal ganglia and its L-DOPA dependency: Recordings from deep brain stimulation electrodes in patients with Parkinson's disease', *Neurol. Sci.*, vol. 23, no. SUPPL. 2, pp. 101–102, 2002, doi: 10.1007/s100720200089.

[499] A. A. Kühn, A. Kupsch, G. H. Schneider, and P. Brown, 'Reduction in subthalamic 8-35 Hz oscillatory activity correlates with clinical improvement in Parkinson's disease', *Eur. J. Neurosci.*, vol. 23, no. 7, pp. 1956–1960, 2006, doi: 10.1111/j.1460-9568.2006.04717.x.

[500] F. Torrecillos *et al.*, 'Modulation of beta bursts in the subthalamic nucleus predicts motor performance', *J. Neurosci.*, vol. 38, no. 41, pp. 8905–8917, 2018, doi: 10.1523/JNEUROSCI.1314-18.2018.

[501] G. Tinkhauser, A. Pogosyan, H. Tan, D. M. Herz, A. A. Kühn, and P. Brown, 'Beta burst dynamics in Parkinson's disease off and on dopaminergic medication', *Brain*, vol. 140, no. 11, pp. 2968–2981, 2017, doi: 10.1093/brain/awx252.

[502] W. J. Neumann *et al.*, 'Long term correlation of subthalamic beta band activity with motor impairment in patients with Parkinson's disease', *Clin. Neurophysiol.*, vol. 128, no. 11, pp. 2286–2291, 2017, doi: 10.1016/j.clinph.2017.08.028.

[503] I. Iturrate *et al.*, 'Beta-driven closed-loop deep brain stimulation can compromise human motor behavior in Parkinson's Disease', *bioRxiv Prepr.*, 2019, doi: 10.1101/696385.

[504] M. Vissani *et al.*, 'Impaired reach-to-grasp kinematics in parkinsonian patients relates to dopamine-dependent, subthalamic beta bursts', *npj Park. Dis.*, vol. 7, p. 53, 2021, doi: 10.1038/s41531-021-00187-6.

[505] R. Schmidt, M. H. Ruiz, B. E. Kilavik, M. Lundqvist, P. A. Starr, and A. R. Aron, 'Beta oscillations in working memory, executive control of movement and thought, and sensorimotor function', *J. Neurosci.*, vol. 39, no. 42, pp. 8231–8238, 2019, doi: 10.1523/JNEUROSCI.1163-19.2019.

[506] L. Storzer *et al.*, 'Bicycling suppresses abnormal beta synchrony in the Parkinsonian basal ganglia', *Ann. Neurol.*, vol. 82, no. 4, pp. 592–601, 2017, doi: 10.1002/ana.25047.

[507] P. Fischer *et al.*, 'Alternating modulation of subthalamic nucleus beta oscillations during stepping', *J. Neurosci.*, vol. 38, no. 22, pp. 5111–5121, 2018, doi: 10.1523/JNEUROSCI.3596-17.2018.

[508] S. Makeig *et al.*, 'Dynamic brain sources of visual evoked responses', *Science (80-.).*, vol. 295, no. 5555, pp. 690–694, 2002, doi: 10.1126/science.1066168.
[509] S. Makeig, S. Debener, J. Onton, and A. Delorme, 'Mining event-related brain dynamics', *Trends Cogn. Sci.*, vol. 8, no. 5, pp. 204–210, 2004, doi: 10.1016/j.tics.2004.03.008.
[510] B. H. Jansen, G. Agarwal, A. Hegde, and N. N. Boutros, 'Phase synchronization of the ongoing EEG and auditory EP generation', *Clin. Neurophysiol.*, vol. 114, no. 1, pp. 79–85, 2003, doi: 10.1016/S1388-2457(02)00327-9.
[511] T. Gruber and M. M. Müller, 'Oscillatory brain activity dissociates between associative stimulus content in a repetition priming task in the human EEG', *Cereb. Cortex*, vol. 15, no. 1, pp. 109–116, 2005, doi: 10.1093/cercor/bhh113.
[512] G. Foffani, A. M. Bianchi, G. Baselli, and A. Priori, 'Movement-related frequency modulation of beta oscillatory activity in the human subthalamic nucleus', *J. Physiol.*, vol. 568, no. 2, pp. 699–711, 2005, doi: 10.1113/jphysiol.2005.089722.
[513] E. B. Montgomery Jr., 'Basal ganglia physiology and pathophysiology: A reappraisal', *Park. Relat. Disord.*, vol. 13, no. 8, pp. 455–465, 2007, doi: 10.1016/j.parkreldis.2007.07.020.
[514] W. Neumann *et al.*, 'The sensitivity of ECG contamination to surgical implantation site in adaptive neurostimulation', *medRxiv*, 2021, doi: 10.1101/2021.01.15.426827.
[515] N. Richer, R. J. Downey, W. D. Hairston, D. P. Ferris, and A. D. Nordin, 'Motion and Muscle Artifact Removal Validation Using an Electrical Head Phantom, Robotic Motion Platform, and Dual Layer Mobile EEG', *IEEE Trans. Neural Syst. Rehabil. Eng.*, vol. 28, no. 8, pp. 1825–1835, 2020, doi: 10.1109/TNSRE.2020.3000971.

11. Acknowledgments

12. Appendix

12.1. List of figures

12.2.List of tables

12.3.List of abbreviations

aDBS	adaptive DBS
AM	anthropometric measurements
AO	APA onset
AOCoPD	distance between CoP and heels at AO
AP	anterior-posterior
APA	anticipatory postural adjustments
ASIS	anterior superior iliac spine
AUC	area under the ROC curve
BM	body mass
BMI	body mass index
BoS	base of support
BoSA	BoS area
BoSW	BoS width
BP	DAT non-displaceable binding potential
BW	body weight
CLR	cerebellar locomotor region
CN	cuneiform nucleus
CoM	centre of mass
CoP	centre of pressure
CP	Centro Parkinson, ASST G.Pini-CTO
CPGs	central pattern generators
D1-R	D1-receptor
D2-R	D2-receptor
D3-R	D3-receptor
DAT	dopamine reuptake transporters
DBS	deep brain stimulation
DLPFC	dorso-lateral prefrontal cortex
DTBZ	[11C]dihydrotetrabenazine
ECoG	electrocorticography
EEG	electroencephalography
EG	electrogoniometers
EMG	electromyography
ERD	extended event-related desynchronization
ERS	extended event-related synchronization
FA	foot alignment
FDG	18F-labelled fluorodeoxyglucose
F-Dopa	6-[18F]-fluoro-L-dopa
FDR	false discovery rate
FEW	family-wise corrected
FL	foot length
fMIF	maximally informative frequency
fNIRS	functional near-infrared spectroscopy
FoG	freezing of gait
FP-CIT	[123I]-N-ω-fluoropropyl-2β-carbomethoxy-3-(4-iodophenyl)nortropane

fPEAK	frequency peak
GI	gait initiation
GPe	globus pallidus externum
GPi	globus pallidus internus
GRF	ground reaction force
GUI	graphical user interface
H	hemisphere
H&Y	Hoehn & Yahr
HC	healthy controls
HO	heel off
HOCoPD	distance between CoP and heels at HO
IAD	inter-ASIS distance
IMB	imbalance
IMBAV	IMB average velocity
IMBCoMA	CoM acceleration at the end of IMB/UNL/TO
IMBCoMV	CoM velocity at the end of IMB/UNL/TO
IMBCoPCoM	distance between CoP and CoM at the end of IMB/UNL
IMBD	IMB displacement
IMBMV	IMB maximal velocity
IMBSLOPE	slope of the vector connecting CoP and CoM at the end of IMB
IMBT	IMB duration
IPG	internal pulse generator
JMU	Julius-Maximilians-Universität Würzburg
LAMB	laboratorio di analisi del movimento nel bambino
LEDD	Levodopa equivalent daily dose
LFP	local field potentials
LL	limb length
M1	primary motor cortex
ML	medio-lateral
MLR	mesencephalic locomotor region
MRN	mesencephalic reticular nucleus
PBETA	power over the beta band
PD	Parkinson's disease
PET	positron emission tomography
PMRF	medullary and pontine reticular formations
POLIMI	Politecnico di Milano
PPN	pedunculopontine nucleus
PSD	power spectral density
PSF	power around the standing frequency peak
PSIS	posterior superior iliac spine
PSP	progressive supranuclear palsy
PSP-C	PSP with predominant cerebellar ataxia
PSP-CBS	corticobasal syndrome
PSPCDS	PSP clinical deficits scale
PSP-F	PSP with predominant frontal presentation
PSP-P	predominant parkinsonism
PSP-PGF	PSP with progressive gait freezing
PSP-QoL	PSP-quality of life scale

PSPRS	PSP rating scale
PSP-RS	Steele-Richardson-Olszewski PSP syndrome
PSP-SL	PSP with predominant speech or language disorder
PT	Panzeri-Treves bias correction
PWF	power around the walking frequency peak
ROC	receiver operating characteristic
ROI	region of interest
SAV	first step average velocity
SCoM	segmental CoM
SL	first step length
SLR	subthalamic locomotor region
SMA	supplementary motor area
SMV	first step maximal velocity
SNc	substantia nigra pars compacta
SNr	substantia nigra pars reticulata
SPECT	single-photon emission computed tomography
ST	stance
STEND	end of the standing phase
STN	subthalamic nucleus
SUVR	standardized uptake value ratio
SW	swing
TENS	transcutaneous electrical nerve stimulator
TO	toe off
UK	United Kingdom
UKW	University Hospital of Würzburg
UNIMI	Università degli Studi di Milano
UNL	unloading
UNLAV	UNL average velocity
UNLCoMA	CoM acceleration at the end of UNL
UNLCoMV	CoM velocity at the end of UNL
UNLCoPCoM	distance between CoP and CoM at the end of UNL
UNLD	UNL displacement
UNLMV	UNL maximal velocity
UNLSLOPE	slope of the vector connecting CoP and CoM at the end of UNL
UNLT	UNL duration
UPDRS-III	unified Parkinson's disease rating scale
VA	virtual agent

12.4.Curriculum Vitae